National Library
of Canada

Acquisitions and
Bibliographic Services Branch

395 Wellington Street
Ottawa, Ontario
K1A 0N4

Bibliothèque nationale
du Canada

Direction des acquisitions et
des services bibliographiques

395, rue Wellington
Ottawa (Ontario)
K1A 0N4

Your file Votre référence

Our file Notre référence

NOTICE

The quality of this microform is heavily dependent upon the quality of the original thesis submitted for microfilming. Every effort has been made to ensure the highest quality of reproduction possible.

If pages are missing, contact the university which granted the degree.

Some pages may have indistinct print especially if the original pages were typed with a poor typewriter ribbon or if the university sent us an inferior photocopy.

Reproduction in full or in part of this microform is governed by the Canadian Copyright Act, R.S.C. 1970, c. C-30, and subsequent amendments.

AVIS

La qualité de cette microforme dépend grandement de la qualité de la thèse soumise au microfilmage. Nous avons tout fait pour assurer une qualité supérieure de reproduction.

S'il manque des pages, veuillez communiquer avec l'université qui a conféré le grade.

La qualité d'impression de certaines pages peut laisser à désirer, surtout si les pages originales ont été dactylographiées à l'aide d'un ruban usé ou si l'université nous a fait parvenir une photocopie de qualité inférieure.

La reproduction, même partielle, de cette microforme est soumise à la Loi canadienne sur le droit d'auteur, SRC 1970, c. C-30, et ses amendements subséquents.

Canada

UNIVERSITY OF ALBERTA

PYRITIC SULPHUR REMOVAL FROM BITUMINOUS COAL USING A COMBINED COAL/OIL AGGLOMERATION AND FLOTATION PROCESS

BY ©

James Bradley Marr, P. Eng.

A thesis submitted to the Faculty of Graduate Studies and Research in partial fulfillment of the requirements for the degree of **Master of Science**

IN

Environmental Engineering.

Department of Civil Engineering

EDMONTON, ALBERTA
Fall 1992

National Library
of Canada

Bibliothèque nationale
du Canada

Canadian Theses Service

Service des thèses canadiennes

Ottawa, Canada
K1A 0N4

The author has granted an irrevocable non-exclusive licence allowing the National Library of Canada to reproduce, loan, distribute or sell copies of his/her thesis by any means and in any form or format, making this thesis available to interested persons.

The author retains ownership of the copyright in his/her thesis. Neither the thesis nor substantial extracts from it may be printed or otherwise reproduced without his/her permission.

L'auteur a accordé une licence irrévocable et non exclusive permettant à la Bibliothèque nationale du Canada de reproduire, prêter, distribuer ou vendre des copies de sa thèse de quelque manière et sous quelque forme que ce soit pour mettre des exemplaires de cette thèse à la disposition des personnes intéressées.

L'auteur conserve la propriété du droit d'auteur qui protège sa thèse. Ni la thèse ni des extraits substantiels de celle-ci ne doivent être imprimés ou autrement reproduits sans son autorisation.

ISBN 0-315-77104-6

Canada

UNIVERSITY OF ALBERTA

RELEASE FORM

NAME OF AUTHOR: James Bradley Marr, P. Eng.

TITLE OF THESIS: Pyritic Sulphur Removal from Bituminous Coal Using a Combined Coal/Oil Agglomeration and Flotation Process.

DEGREE: Master of Science in Environmental Engineering

YEAR THIS DEGREE GRANTED: 1992

Permission is hereby granted to the UNIVERSITY OF ALBERTA Library to lend or sell such copies for private, scholarly or scientific research purposes only.

The author reserves all other publication and other rights in association with the copyright in the thesis, and except as herein before provided neither the thesis nor any substantial portion thereof may be printed or otherwise reproduced in any material form whatever without the author's prior written permission.

James Bradley Marr, P. Eng.

10440-80 Street,
Edmonton, Alberta
Canada
T6A 3J6

Date: Oct. 9, 1992

UNIVERSITY OF ALBERTA

FACULTY OF GRADUATE STUDIES AND RESEARCH

The undersigned certify that they have read, and recommend to the Faculty of Graduate Studies and Research for acceptance, a thesis entitled Pyritic Sulphur Removal From a Bituminous Coal Using a Combined Coal/Oil Agglomeration and Flotation Process submitted by James Bradley Marr, P. Eng. in partial fulfillment of the requirements for the degree of Master of Science in Environmental Engineering.

Daniel W. Smith
Daniel W. Smith

Steve E. Hrudey

Nosa O. Egiebor

October 1, 1992

Disclaimer

The information in this study is intended for general use only. The use of any part of this study with respect to any specific application must be done so based upon an independent examination and verification of the data to determine if the application of the information is suitable. Any use or reliance upon the material contained in this study is done so with the understanding that the full liability and risks arising from the application rests with the person or persons using the information.

Dedication

To my Dear Sweetheart,
Miss Andrea Kim Prendergast,
and for my loving Parents and Family.

Abstract

The study investigated the removal of pyrite and ash from a Bituminous coal using a coal/oil agglomeration and flotation process. The test coal is classified as High Volatile A Bituminous, (Illinois No 6), containing a calorific value of about 33,000 kJ/kg, and 6.6 total sulphur % dry ash free basis (TS (% daf)) and 33.0 ash % dry basis (ash (% db)).

The washability analysis, which defines the theoretical cleaning potential of the test coal, indicates the TS (% daf) can be reduced to 3.5 % at a combustible matter recovery (CMR (%)) of 90 %. The washability results indicate a theoretical ash (% db) of 11.0 % at a CMR(%) of 90 % can be achieved.

The process performed from poor to fair with respect to TS (% daf) removal, providing product at 4.6 % TS (% daf) for a range of CMR (%) of 75 to 90 %. The process performed very good in terms of ash (% db) removal, reducing ash to 14 % (% db) at a CMR (%) of 90 %.

The experiment used a 2^5 factorial design:

x1 oil (% daf),
x2 frother (% daf),
x3 energy (J/L),
x4 temperature (°C), and
x5 size (d_{50} in microns).

Two other factors varied during testing:

x6 % solids in the product (%), and
x7 sample age after preparation (days).

The CMR (%) regression indicated oil, frother, and temperature are predominant factors. Energy input and sample age have less impact, and the CMR (%) tested independent of size and % solids at a probability of 0.01. The interaction between oil and frother indicates that a single pathway for CMR (%) exists. Recovery by hydraulic entrainment and natural flotation appears non-existent.

The TS (% daf) regression indicated that oil, frother, and temperature are predominant factors. Energy input had minimal impact, and variations in size and age had more substantial impact. Per cent solids tested insignificant at a probability of 0.01.

The interaction between temperature and frother indicated a different regression equation exists when compared to CMR (%). The interaction indicated that the liberated pyrite reports to the product by capture within agglomerates, or via natural flotation.

Acknowledgment

The author wishes to extend his gratitude to the following persons for their generous support in the completion of this thesis:

- Dr. Daniel W. Smith
- Mr. Peter Mohammed
- Dr. Leszek Ignasiak
- Dr. Kaz Symocha

Special thanks to Dr. Smith for his valuable guidance and support. Special thanks to Mr. Peter Mohammed for his outstanding dedication in participating in the completion of the experimental program. Special thanks to Dr. Symocha and Dr. Ignasiak for their and technical support and guidance, and the Alberta Research Council for their financial support.

TABLE OF CONTENTS

page

Disclaimer iv

Abstract vi

Acknowledgments viii

List of Tables xii

List of Figures xvi

List of Abbreviations xxi

1.0 Introduction 1
- 1.1 Purpose and Scope of Work 9

2.0 Sulphur Reduction 10
- 2.1 Strategies 10
- 2.2 Coal and Oil Agglomeration Process Description 16
- 2.3 Agglomeration 18
  - 2.3.1 Fundamentals 18
    - 2.3.1.1 Transport Mechanisms 20
    - 2.3.1.2 Attachment Mechanisms 25
  - 2.3.2 Process Variables 35
    - 2.3.2.1 Feed Variations 35
    - 2.3.2.2 Chemical Parameters 39
    - 2.3.2.3 Physical Parameters 42
    - 2.3.2.4 Mixing Designs and Configurations 49
- 2.4 Flotation 56
  - 2.4.1 Fundamentals 56
    - 2.6.2.1 Transport Mechanisms 59
    - 2.6.2.2 Attachment Mechanisms 60
  - 2.4.2 Process Variables 63
    - 2.4.2.1 Feed Variations 63
    - 2.4.2.2 Chemical Parameters 67
    - 2.4.2.3 Physical Parameters 69
    - 2.4.2.4 Equipment Components 73

3.0 Design Specifications 77
- 3.1 Flow Schemes 80
  - 3.1.1 Flow scheme 1 80
  - 3.1.2 Flow scheme 2 80
- 3.2 Coal Grinding and Feeding Systems 84
- 3.3 Slurry Conditioning 86
- 3.4 High Shear Mixing 86
- 3.5 Separation System 88
  - 3.5.1 Flotation Cell 88

3.5.2 Pyrite Separator 91
3.6 Water Flowrate Controls 92
3.7 Frother Addition Systems 94
3.8 Oil Addition 96

4.0 Experimental Method 99
4.1 Phase 1 Commission Testing 99
4.2 Phase 2 Development of Experimental Method 99
4.2.1 Series 1 Sample Preparation and Collection 100
4.2.1.1 Feed Coal Preparation 100
4.2.1.2 Feed Coal Sample Collection 100
4.2.1.3 Feed Sample Preparation for Assay Analysis 101
4.2.1.4 Product and Tailings Stream Sample Preparation 101
4.2.2 Series 2 Steady State Analysis and Repeatability 102
4.2.3 Series 3 Apparatus Modifications 124
4.3 Phase 3 Experimental Investigation 127
4.3.1 System Performance 127
4.3.2 Detailed Mass Balance Experimental Procedure 127
4.3.3 Washability Tests 127
4.4 Experimental Design 129

5.0 Analytical Procedures 132

6.0 Method of Calculations 134

6.1 Assay Calculations 134
6.2 Performance Calculations 136

7.0 Feed Coal Characterization 139

8.0 Results 147
8.1 Process Performance 147
8.2 Regression Analysis 152
8.3 Graphical Evaluation 158
8.4 Raw Data 160

9.0 Discussion 167
9.1 Process Performance 169
9.2 Regression Analysis 171
9.2.1 Group 1 Data 172
9.2.2 Group 2 Data 179
9.2.3 Group 3 Data 182
9.2.4 Group 4 Data 185
9.2.5 Group 5 Data 187
9.3 Graphic Analysis 189
9.3.1 Oil Concentration 189
9.3.2 Frother Concentration 190
9.3.3 Energy Input 190
9.3.4 Temperature Input 191
9.3.5 Particle Size 192
9.3.6 Per cent Solids in Product Phase 192
9.3.7 Sample Age 193
9.4 Apparatus 193
9.5 Experimental Methodology 195

9.6 Data Analysis 195

10.0 Conclusions 197
10.1 Process Performance 197
10.1.1 TS (% daf) 197
10.1.2 Ash Content (% db) 197
10.2 Process Fundamentals 197
10.3 Main and Interactive Factors 199
10.3.1 CMR (%) 199
10.3.2 TS (% daf) 200
10.3.3 Ash (% db) 201

11.0 Recommendations 203

Cited References 204

Bibliography 208

Appendix 1 Probability Models 213

A1.1 Combustible Matter Recovery 217
A1.2 Total Sulphur Reduction 226
A1.3 Ash Rejection 234

Appendix 2 Regression Work For Test E10 241

Appendix 3 Regression Work For Test E11 252

Appendix 4 Regression Work For Tests E10 and E11 Combined 264

Appendix 5 Regression Work for Tests E10, E11, E12 Combined 268

Appendix 6 Regression Work for Tests E10, E11, E12 and E13 Combined 275

Appendix 7 Computer Data used in Regression Work for Appendices 1-6 282

Appendix 8 Summary of Graphic Evaluations for Tests E10 through E12 292

List of Tables **Page**

Table 3.1	Summary of Operating Test Conditions	83
Table 3.2	High Shear Mixer Vessel Volume versus RPM	88
Table 3.3	Air Input (L/min.) versus RPM	91
Table 3.4	Water Flow Rates (g/min.) versus Rotameter Setting	94
Table 3.5	Frother Mass Flow (g/min.) Solution and % Relative Error vs. Experimental Level	96
Table 3.6	Oil Mass Flow (g/min.) & % Relative Error vs. % Capacity	98
Table 4.1	Steady State Results for Test D5 (1 min. Sample Interval)	115
Table 4.2	Steady State Results for Test D6 (1 min. Sample Interval)	115
Table 4.3	Steady State Results for Test D7 (1 min. Sample Interval)	116
Table 4.4	Steady State and Repeatability Analysis - Tests D6 & D7 (30 min. Sample Intervals)	119
Table 4.5	Detailed Mass Balance for Tests D6 & D7 (Flow Scheme 1)	123
Table 4.6	Detailed Mass Balance for Tests E 12 & E13	124
Table 4.7	Steady State Analysis and Test Repeatability for Flow Scheme 2	125
Table 4.8	Main Factors of the Experimental Design	130
Table 4.9	Experimental Set Points	131
Table 5.1	Summary of Analytical Instruments and Methods	132
Table 6.1	Algorithms Describing the Main Factors Dimensional Analysis	135
Table 6.2	Algorithms Describing the Process Performance Calculations	137
Table 6.3	Rejection and Reduction Algorithms	138
Table 7.1	Proximate Analysis of Test Coal	139
Table 7.2	Ultimate Analysis[a] of Test Coal	140
Table 7.3	Ash and Sulphur Contents of Test Coal	140
Table 7.4	Calorific Value versus Sample Ash Content	141
Table 7.5	Size Analysis Data for Test Coals E10, E11 and E12	143
Table 8.1	Raw Results from Washability Analysis for Test E10 and E11	150

Table 8.2 Washability Analysis for Test Coals E10 and E11 151
Table 8.3 Summary of Regression Work 153
Table 8.4 Regression Analysis of CMR (%) for Main Factors for Test E10 157
Table 8.5 Summary of Main Factors for Test E10 161
Table 8.6 Summary of Main Factors for Test E11 162
Table 8.7 Summary of Main Factors for Tests E12 and E13 163
Table 8.8 Summary of Main Responses for Test E10 164
Table 8.9 Summary of Main Responses for Test E11 165
Table 8.10 Summary of Main Responses for Tests E12 and E13 166
Table A2.1 Regression Analysis of CMR (%) for Main Factors for Test E10 242
Table A2.2 Regression Analysis for CMR (%) for Main Factors and Interactions for Test E10 243
Table A2.3 Regression Analysis for CMR (%) for Main Factors and Interactions for Test E10 244
Table A2.4 Regression Analysis for CMR (%) for Main Factors and Interactions for Test E10 245
Table A2.5 Regression Analysis for CMR (%) for Main Factors and Interactions for Test E10 246
Table A2.6 Regression Analysis for TS (% daf) for Main Factors and Interactions for Test E10 247
Table A2.7 Regression Analysis for TS (% daf) for Main Factors and Interactions for Test E10 248
Table A2.8 Regression Analysis for TS (% daf) for Main Factors and Interactions for Test E10 249
Table A2.9 Regression Analysis for TS (% daf) for Main Factors and Interactions for Test E10 250
Table A2.10 Regression Analysis for Ash (% db) for Main Factors and Interactions for Test E10 251
Table A3.1 Regression Analysis for CMR (%) for Main Factors for Test E11 253
Table A3.2 Regression Analysis for CMR (%) for Main Factors and Interactions for Test E11 254

Table A3.3	Regression Analysis for CMR (%) for Main Factors and Interactions for Test E11	255
Table A3.4	Regression Analysis for CMR (%) for Main Factors and Interactions for Test E11	256
Table A3.5	Regression Analysis for TS (% daf) for Main Factors and Interactions for Test E11	257
Table A3.6	Regression Analysis for TS (% daf) for Main Factors and Interactions for Test E11	258
Table A3.7	Regression Analysis for TS (% daf) for Main Factors and Interactions for Test E11	259
Table A3.8	Regression Analysis for TS (% daf) for Main Factors and Interactions for Test E11	260
Table A3.9	Regression Analysis for TS (% daf) for Main Factors and Interactions for Test E11	261
Table A3.10	Regression Analysis for Ash (% db) for Main Factors and Interactions for Test E11	262
Table A3.11	Regression Analysis for Ash (% db) for Main Factors and Interactions for Test E11	263
Table A4.1	Regression Analysis for CMR (%) for Main Factors and Interactions for Tests E10 and E11	265
Table A4.2	Regression Analysis for TS (% daf) for Main Factors and Interactions for Tests E10 and E11	266
Table A4.3	Regression Analysis for Ash (% db) for Main Factors and Interactions for Tests E10 & E11	267
Table A5.1	Regression Analysis for CMR (%) for Main Factors and Interactions for Tests E10, E11 & E12	269
Table A5.2	Regression Analysis for CMR (%) for Main Factors and Interactions for Tests E10, E11, & E12	270
Table A5.3	Regression Analysis for TS (% daf) for Main Factors and Interactions for Tests E10, E11, & E12	271
Table A5.4	Regression Analysis for TS (% daf) for Main Factors and Interactions for Tests E10, E11, & E12	272
Table A5.5	Regression Analysis for Ash (% db) for Main Factors and Interactions for Tests E10, E11, & E12	273
Table A5.6	Regression Analysis for Ash (% db) for Main Factors and Interactions for Tests E10, E11, & E12	274

Table A6.1 Regression Analysis for CMR (%) for Main Factors and Interactions for Tests E10, E11 & E12 276

Table A6.2 Regression Analysis for CMR (%) for Main Factors and Interactions for Tests E10, E11, & E12 277

Table A6.3 Regression Analysis for TS (% daf) for Main Factors and Interactions for Tests E10, E11, & E12 278

Table A6.4 Regression Analysis for TS (% daf) for Main Factors and Interactions for Tests E10, E11, & E12 279

Table A6.5 Regression Analysis for Ash (% db) for Main Factors and Interactions for Tests E10, E11, & E12 280

Table A6.6 Regression Analysis for Ash (% db) for Main Factors and Interactions for Tests E10, E11, & E12 281

Table A7.1 Coded Regression Data for Test E10 283

Table A7.2 Raw Regression Data for Test E10 284

Table A7.3 Coded Regression Data for Test E11 285

Table A7.4 Raw Regression Data for Test E11 286

Table A7.5 Raw Regression Data for Test E10 & E11 287

Table A7.6 Raw Regression Data for Test E10, E11 and E12 288

Table A7.7 Raw Regression Data for Tests E10, E11, E12 and E13 290

List of Figures **Page**

Figure 1.1	Selective Coal and Oil Agglomeration Process	6
Figure 1.2	Pyrite and Ash Rich Matter Liberation	5
Figure 1.3	Primary, Secondary, and Tertiary Agglomeration	8
Figure 2.1	Process Configuration for Sulphur Free Power Generation	15
Figure 2.2	Structure Formation During Agglomeration (After Botsariz and Glazman)	21
Figure 2.3	Transport Mechanisms	22
Figure 2.4	Attachment Mechanisms	26
Figure 2.5	Surface Tension Phenomena	28
Figure 3.1	Bench Scale Primary Flotation Cell No. 1	78
Figure 3.2	Bench Scale Pyrite Separator	79
Figure 3.3	Bench Scale (5 kg/hr) Continuous Coal and Oil Agglomeration and Flotation Pilot Plant for Ash and Pyrite Removal - Flow Scheme 1	81
Figure 3.4	Bench Scale (5 kg/hr) Continuous Coal and Oil Agglomeration and Flotation Pilot Plant for Ash and Pyrite Removal - Flow Scheme 2	82
Figure 3.5	Coal Mass Feed Rate (g/min.) and % Relative Error versus % Coal Feeder Capacity	85
Figure 3.6	High Shear Mixer 1 and 2 Volume (mL) versus Speed (RPM)	87
Figure 3.7	Air Input (L/min and L/min*m^2) versus RPM	90
Figure 3.8	Conditioner, Flotation Cell 1, and the Pyrite Separator Water Mass Flow Rates Versus Rotameter Setting	93
Figure 3.9	Frother Loading in grams/min of a 1 % Stock Solution of MIBC versus Pump Capacity Level (e.g.. -1 representing low level capacity, and +1 representing high level capacity)	95
Figure 3.10	Oil Mass Flow Rate (grams/min.) and % Relative Error versus % Oil Feeder Capacity	97
Figure 4.1	Step Input Salt Tracer (KCl) Concentration at the High Shear Vessel versus Time (minutes)	103

Figure 4.2 Normalized (C/Cmax) Step Input Salt Tracer (KCl) Concentration at the High Shear Vessel versus Normalized Time (t/tr) 105

Figure 4.3 Step Input Salt Tracer (KCl) Concentration at the Flotation Vessel versus Time (minutes) 106

Figure 4.4 Normalized (C/Cmax) Step Input Salt Tracer (KCl) Concentration at the Flotation Vessel versus Normalized Time (minutes) 107

Figure 4.5 Interval Solids Recovery (g) versus Mean Interval Time (minutes) 108

Figure 4.6 Normalized Interval Solids Recovery (S/St) versus Normalized Time (t/tr) 109

Figure 4.7 Batch Flotation Kinetic Test on Prewashed Illinois No. 6 Coal 111

Figure 4.8 Repeat Test Intervals for Total Sulphur (% daf), and Ash Contents (% db), versus Run Time (minutes) for One Minute Sample Intervals during Test D5 (Flow Scheme 1) 112

Figure 4.9 Repeat Test Intervals for Total Sulphur (% daf), and Ash Contents (% db), versus Run Time (minutes) for One Minute Sample Intervals during Test D6 (Flow Scheme 1) 113

Figure 4.10 Repeat Test Intervals for Total Sulphur (% daf), and Ash Contents (% db), versus Run Time (minutes) for One Minute Sample Intervals during Test D7 (Flow Scheme 1) 114

Figure 4.11 Repeat Test Intervals for Total Sulphur (% daf), Pyrite (% daf), and Ash (% db) Contents versus Run Time for Thirty Minute Composite Sampling Experiment for Test D6 (Flow Scheme 1) 117

Figure 4.12 Repeat Test Intervals for Total Sulphur (% daf), Pyrite (% daf), and Ash (% db) Contents versus Run Time for Thirty Minute Composite Sampling Experiment for Test D7 (Flow Scheme 1) 118

Figure 4.13 Combustible Matter Recovery (%), Total Sulphur Rejection (%), Total Sulphur Reduction (%), and Ash Rejection (%) versus Run Time (hours) for Test D6 120

Figure 4.14 Combustible Matter Recovery (%), Total Sulphur Rejection (%), Total Sulphur Reduction (%), and Ash Rejection (%) versus Run Time (hours) for Test D7 121

Figure 4.15 Repeat Runs for Total Sulphur (% daf) and Ash Content (% db) versus Run Time (minutes) for the 126

Ten Minute Sample Intervals For Experiments E9, E10, E11, E12, and E13

Figure 4.16 Sample Locations for Flowsheet 2 128

Figure 7.1 Heat Content of Illinois No. 6 ROM Coal (BTU/LB and kJ/kg) versus Ash Content (% db) 142

Figure 7.2 Cumulative % Passing and Retained vs. Screen Size for Tests E10 and E13 144

Figure 7.3 Cumulative % Passing and Retained vs. Screen Size for Tests E12 145

Figure 7.4 Cumulative % Passing and Retained vs. Screen Size for Tests E11 146

Figure 8.1 % Combustible Matter Recovery vs. Total Sulphur Content (% daf) for Tests E10, E11, E12 and E13 148

Figure 8.2 % Combustible Matter Recovery vs. Total Ash Content (% db) for Tests E10, E11, E12 and E13 149

Figure 8.3 Example Tables A8.1 and A8.2 159

Figure A1 Combustible Matter Recovery Model 215

Figure A2 Schematic Representation of Probabilistic Models 216

Figure A3 Total Sulphur Reduction Model 227

Figure A4 Total Ash Rejection Model 235

Figure A8.1 % Combustible Matter Recovery versus Coded Oil Concentration for Test E 10 293

Figure A8.2 Total Sulphur Content (% daf) versus Coded Oil Concentration for Test E 10 293

Figure A8.3 Total Ash Content (% db) versus Coded Frother Concentration for Test E 10 294

Figure A8.4 % Combustible Matter Recovery versus Coded Frother Concentration for Test E 10 294

Figure A8.5 Total Sulphur Content (% daf) versus Coded Frother Concentration for Test E 10 295

Figure A8.6 Total Ash Content (% db) versus Coded Frother Concentration for Test E 10 295

Figure A8.7 % Combustible Matter Recovery versus Coded Energy Level for Test E 10 296

Figure A8.8 Total Sulphur Content (% daf) versus Coded Energy Input for Test E 10 296

Figure A8.9 Total Ash Content (% db) versus Coded Energy Input for Test E 10 297

Figure A8.10 % Combustible Matter Recovery versus Coded Temperature for Test E 10 297

Figure A8.11 Total Sulphur Content (% daf) versus Coded Temperature for Test E 10 298

Figure A8.12 Total Ash Content (% db) versus Coded Temperature for Test E 10 298

Figure A8.13 % Combustible Matter Recovery versus Coded Oil Concentration for Test E 11 299

Figure A8.14 Total Sulphur Content (% daf) versus Coded Oil Concentration for Test E 11 299

Figure A8.15 Total Ash Content (% db) versus Coded Oil Concentration for Test E 11 300

Figure A8.16 % Combustible Matter Recovery versus Coded Frother Concentration for Test E 11 300

Figure A8.17 Total Sulphur Content (% daf) versus Coded Frother Concentration for Test E 11 301

Figure A8.18 Total Ash Content (% db) versus Coded Frother Concentration for Test E 11 301

Figure A8.19 % Combustible Matter Recovery versus Coded Energy Input for Test E 11 302

Figure A8.20 Total Sulphur Content (% daf) versus Coded Energy Input for Test E 11 302

Figure A8.21 Total Ash Content (% db) versus Coded Energy Input for Test E 11 303

Figure A8.22 % Combustible Matter Recovery versus Coded Temperature for Test E 11 303

Figure A8.23 Total Sulphur Content (% daf) versus Coded Temperature for Test E 11 304

Figure A8.24 Total Ash Content (% db) versus Coded Temperature for Test E 11 304

Figure A8.25 % Combustible Matter Recovery versus Coded Size for Tests E 10 and E 11 305

Figure A8.26 Total Sulphur Content (% daf) versus Coded Size for Tests E 10 and E 11 305

Figure A8.27 Total Ash Content (% db) versus Coded Size for Tests E 10 and E 11 306

Figure A8.28 % Combustible Matter Recovery versus Coded Oil Concentration for Test E 12 306

Figure A8.29 Total Sulphur Content (% daf) versus Coded Oil Concentration for Test E 12 307

Figure A8.30 Total Ash Content (% db) versus Coded Oil Concentration for Test E 12 307

Figure A8.31 % Combustible Matter Recovery versus Coded Frother Concentration for Test E 12 308

Figure A8.32 Total Sulphur Content (% daf) versus Coded Frother Concentration for Test E 12 308

Figure A8.33 Total Ash Content (% db) versus Coded Frother Concentration for Test E 12 309

Figure A8.34 % Combustible Matter Recovery versus Coded Energy Input for Test E 12 309

Figure A8.35 Total Sulphur Content (% daf) versus Coded Energy Input for Test E 12 310

Figure A8.36 Total Ash Content (% db) versus Coded Energy Input for Test E12 310

Figure A8.37 Total Sulphur Content (% daf) versus % Solids Concentration in the Froth Phase for Tests E10, E11, E12 and E13 311

Figure A8.38 Total Ash Content (% db) versus % Solids Concentration in the Froth Phase for Tests E10, E11, E12 and E13 312

Figure A8.39 % Combustible Matter Recovery versus % Solids Concentration in the Froth Phase for Tests E10, E11, E12 and E13 313

List of Abbreviations

ASTM	American Society for Testing and Materials
% daf	Per cent dry ash free basis
% db	Per cent dry basis
% dmmf	Percent mineral matter free
AR	Total Ash Rejection (%)
Ash (% db)	Total Ash Content on a per cent dry basis
CMR (%)	Per cent Combustible Matter Recovery
pH	$-\text{Log}\,[H^+]$
RPM	Revolutions per Minute
SO_2	Sulphur Dioxide
TS (% daf)	Total Sulphur Content (% daf)
TSR	Total Sulphur Rejection (%)
TSRed	Total Sulphur Reduction (% daf)
US	United States
USA	United States of America
USSR	Previously known as the Union of Soviet Socialist Republic

1.0. Introduction

The combustion of high sulphur coals creates specific forms of air and water pollution. Air pollution can be in the form of carbon, sulphur and nitrogen dioxides as well as volatile metals and organics, and some radioactive emissions. Sulphur and nitrogen dioxides are identified as precursors of acid rain, and many countries are experiencing serious problems associated with air, water, and soil pollution as a result of the deposition of their acidic forms. (Effer, 1981; Likens et al., 1979; Males, 1981; Gorham, 1981; Leaf, 1990)

It is generally agreed among scientists about the world, that the atmospheric concentration of carbon dioxide is increasing (Moses and Dahlman, 1981). An increase in the carbon dioxide concentration has been proposed to have adverse long term effects on the overall environment of the earth, such as global warming. The release of volatile metals and organics, and the emission of some radioactive materials have also been attributed to the combustion of coal and may bioaccumulate in the environment over time (Gorham, 1981; Freedman, 1981).

Acid mine drainage associated with coal utilization creates both chemical and physical water pollution which is capable of adversely influencing both soil and aquatic environments. Heavy metals and some soluble organics are also released with acid mine drainage waters, increasing the severity of the pollution. The tailings stream from any process designed to selectively remove pyrite from bituminous coals will have potential management problems associated with acid mine drainage.

Coal utilization has been identified as a major cause for the increase in acidity of both rain and snow. The combustion of high sulphur coals creates large quantities of both sulphur and nitrogen oxides. When these oxides equilibrate in the atmosphere, they form sulphuric and nitric acids which lowers the acidity of precipitation. In a natural atmosphere, the acidity is largely influenced by the concentration and pressure of carbon dioxide, and at standard conditions, carbon dioxide will equilibrate to form carbonic acid, which lowers the pH to approximately 5.6. This has been termed as the natural pH of precipitation. However, additional factors can influence the acidity of precipitation, for example: ionic species present and their concentration, type and atmospheric loading of solid particles, temperature, and the surrounding geology. (Likens et al., 1979; Effer, 1981)

Measurements over the past 200 years from the eastern United States and western Europe have indicated that overall pH of precipitation has decreased from near neutral to a slightly dilute concentration of sulphuric and nitric acid. Some regional examples have indicated extreme conditions, such in Scotland, where the precipitation during a storm reached a pH of 2.4. Ice pack measurements in Greenland indicated that pH has decreased over the past 180 years from 7.6 to 6.0. Other studies indicate the acidity of rain and snow is five to thirty times lower in industrial regions compared to virgin lands. (Likens et al., 1979)

The natural pH of precipitation has been defined as 5.6 (Likens et al., 1979; Effer, 1981). This value is derived from the pH expected when carbon dioxide is in equilibrium with water at standard conditions. However, the definition of acid rain can be misleading as it ignores global and localized acidizing and neutralizing abilities of the environment, and the specific weather and land-uses of the related areas (Effer, 1981). The acidity of precipitation depends upon many factors, none of which can be overlooked when assessing whether a region is experiencing abnormally low acid rain. Prior to the industrial revolution, the pH of precipitation already demonstrated substantial variations depending upon the surrounding geology and the natural events which may have occurred during the period. Such natural modifiers of pH include: volcanoes, tidal flats, marshes, oceans, regional land uses, surrounding geology, forest fires, and the weather. Because of the relatively low concentration spread over vast areas, an assessment of the global emissions from natural sources poses some difficulties. However, estimates of global contributions suggest 50 per cent of all sulphur precursors, and 90 per cent of all nitrogen precursors, are released from natural sources, although these estimates vary widely (Effer, 1981). Regardless, the evidence suggests that industrial activity has substantially increased sulphur emissions, globally doubling levels. The complex interactions of the environment demands that each region receive individual assessment to define the sources of all emissions, the potential environmental impacts, and the sensitive components which required higher levels of protection.

In the United States of America (USA), legislation in 1990 was developed to help reduce the problem of acid rain by imposing restrictions on sulphur dioxide emissions. The United States (US) Congress, through efforts of the Environment Protection Agency (EPA), have amended the Clean Air Act requiring utilities to reduce sulphur dioxide emissions from 17.9 to 8.9 million tonnes per year by the year 2000. (Leaf, 1990; Corocoran, 1991)

The US Congress has also proposed a plan which permits the granting of tradable allowances for polluting. The policy was intended to promote a cost efficient method of minimizing the release of sulphur precursors by transferring the design of control strategies to the independent operators (Corocoran, 1991). Utilities can buy or sell allowances to help meet the emissions requirements that the EPA will switch on in 1995. Those unable to balance their sulphur dioxide emissions and allowance ledgers will be charged hefty fines. Congress has provided another deterrent, top officers must assume personal liability and may be prosecuted for jail sentencing if their company's violate. Because utilities must also conform to state emission limits, no region is likely to wind up as a sulphur dioxide dumping ground. (Corocoran, 1991)

It is evident that methods for reducing sulphur dioxide emissions are desperately needed in all parts of the world. Efforts have been extended in response to investigate advanced coal cleaning technologies which will mediate acid rain problems. Flotation processes are considered as advanced coal cleaning technologies and some examples which relate to this study are: froth flotation, bulk or spherical agglomeration flotation, and emulsion flotation. (Mishra and Klimpel, 1987)

Froth flotation involves separating mineral matter from combustible material by promoting the surface hydrophobicity of combustible particles with chemical additions, and separating these activated particles with a chemically stabilized bubble system as the buoyant transport medium. Froth flotation generally uses low concentrations of reagents, (several kilograms per ton of raw feed coal or less) and for coal possessing natural hydrophobic surfaces, only a frother addition of several tenths of a kilogram is necessary. (Mishra and Klimpel, 1987)

Spherical agglomeration flotation combines large quantities of oil and intensive energy to cause the formation of macro-sized agglomerates after which flotation is used to separate the desired combustible agglomerates from the waste constituents. The concentration of oil varies with process conditions, ranging from 2 to 30 per cent based on the raw coal feed rate. (Mishra and Klimpel, 1987)

Emulsion flotation is essentially a cross between froth flotation and oil agglomeration and requires a combination of oil and chemical emulsifiers at a dosage level intermediate between froth flotation and agglomeration. Emulsion flotation involves emulsification of the oil phase prior to addition to the coal and water slurry. (Mishra and Klimpel, 1987)

Selective coal and oil agglomeration for desulphurization is a physio-chemical process which has been recognized as a process to remove pyrite and ash from bituminous coals (Hucko, et al., 1989). The process investigated in this study is similar to emulsion flotation as it combines both the agglomeration process and froth flotation together to facilitate the beneficiation of the feed stock coal. However, no chemical emulsifiers are employed, instead, high energy mixers are used to both disperse the oil into tiny droplets and provide for the collisions between the carbonaceous particles and oil droplets. The oil concentration levels investigated in this study are among the lowest reported in the literature. The process configuration is described in Figure 1.1 and consists of four steps:

- coal grinding or pyrite liberation,
- slurry conditioning or water wetting,
- selective coal and oil agglomeration, and
- pyrite and ash separation.

The pyrite and ash rich matter is liberated from the combustible matrix by grinding the coal. The degree of grinding required depends upon the size distribution of the pyrite and ash matter within the coal matrix, and will vary for different coals. Figure 1.2 below helps describe the operation.

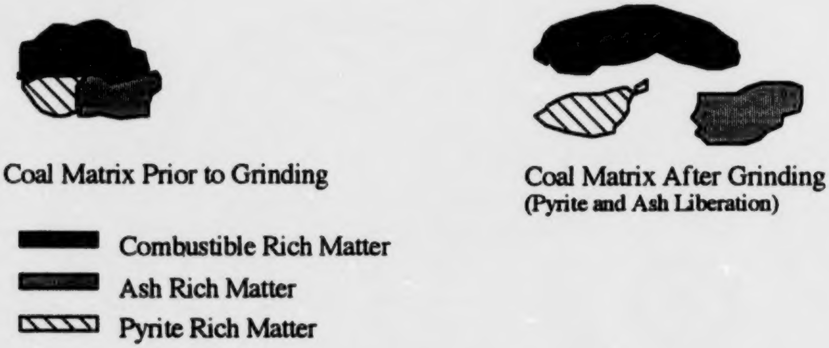
Coal Matrix Prior to Grinding

Coal Matrix After Grinding
(Pyrite and Ash Liberation)

Figure 1.2 Pyrite and Ash Rich Matter Liberation

Conditioning of the coal may involve water wetting the particle surfaces. In dry grinding operations water wetting is an important step, however, in wet grinding operations, most water wetting occurs during the grinding operation (Weiss, 1985). In more conventional flotation processing, conditioning provides for the dispersion of reagents, and contact time with the desired solids material. Conditioning tanks are also used as equalization vessels to dampen variations in the feed stock.

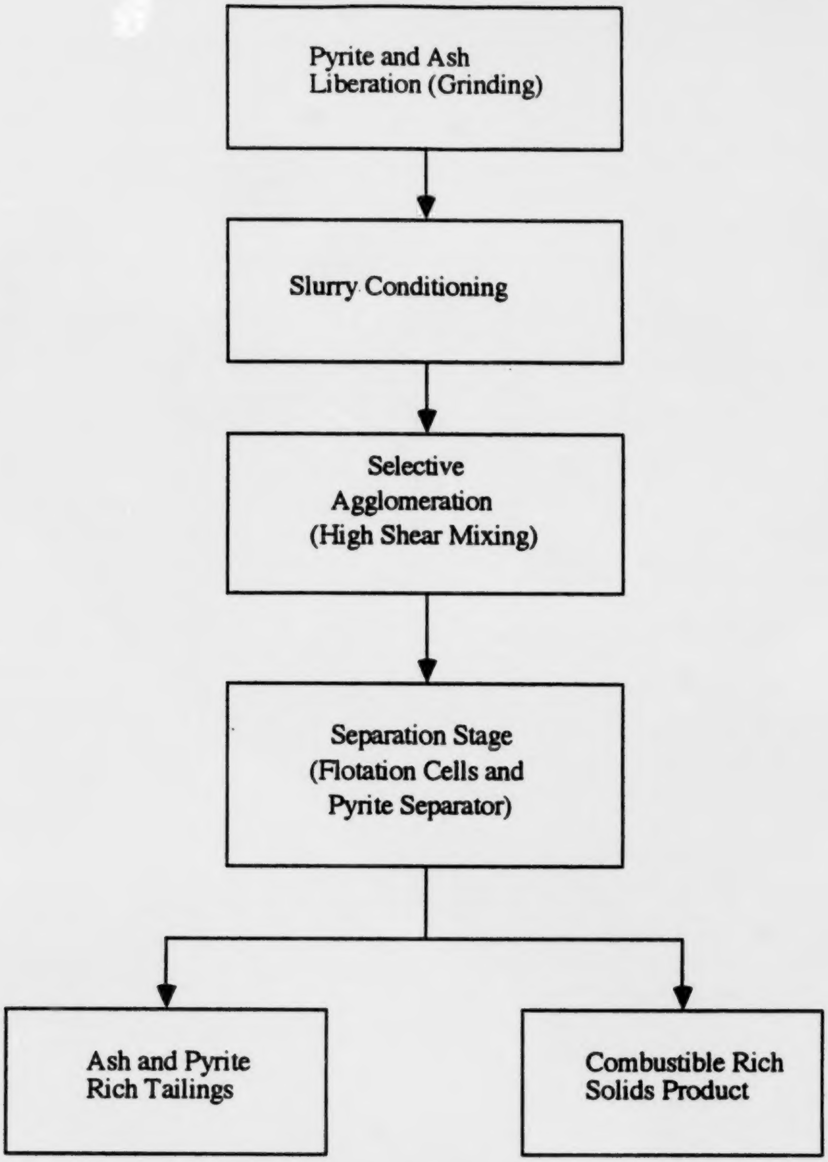
Pyrite and Ash Liberation (Grinding)
Slurry Conditioning
Selective Agglomeration (High Shear Mixing)
Separation Stage (Flotation Cells and Pyrite Separator)
Ash and Pyrite Rich Tailings
Combustible Rich Solids Product

Figure 1.1 Selective Coal and Oil Agglomeration Process

Figure 1.3 helps to describe the selective coal and oil agglomeration process. Oil concentration influences the product quality in terms of pyrite removal because of several mechanisms. The potential for pyrite entrapment with this process is most probable when operated at high oil concentrations, where secondary and tertiary agglomeration prevails (see Figure 1.3). In the primary agglomeration regime, where only a few discrete particles are combined, the process is operated at high energy levels and low oil concentration to promote the selective oil wetting of the combustible solids. The oil concentration is limited to discourage pyrite entrapment within the agglomerates, or oil wetting of their surfaces. High energy levels are used to promote maximum dispersion of the oil and contact with the carbonaceous surfaces (Liu, 1982). Capes et al. (1985) also discusses a similar concept for improving the oil agglomeration process by operating at lower oil levels to increase impurity rejection, yet high enough to maintain reasonable recovery. When low levels of oil are used (eg. 1 to 2 per cent or less) only the highest quality carbonaceous particles are expected to be captured by the process. The structures formed would be floc-like in nature, and would not respond to conventional agglomerations separation methods, such as screening. However, air flotation could be used to recovery these floc-like agglomerates, by adding a washing stage to ensure any entrained or trapped extraneous material is rejected before recovery.

The newly formed combustible flocs are hydrophobic in nature and larger in size and can be separated from the ash and pyrite rich matter by conventional flotation. Despite the selectivity of the primary agglomeration regime, pyrite and ash rich particles can report to the product phase during flotation by several mechanisms, thus lowering the product quality. Hence, the following study was undertaken to investigate the cleaning potential of the process.

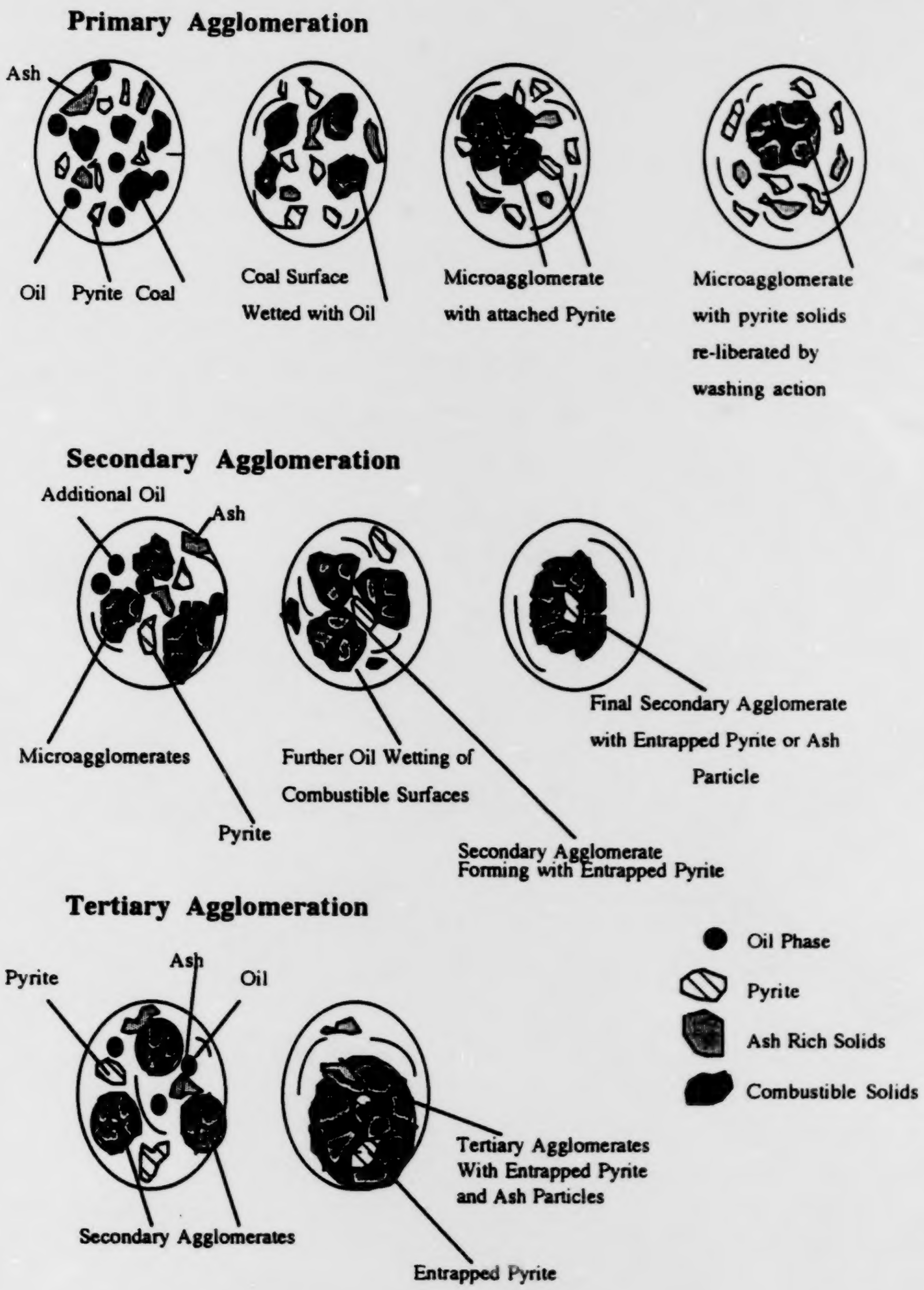
Primary Agglomeration
Ash
Oil
Pyrite
Coal
Coal Surface Wetted with Oil
Microagglomerate with attached Pyrite
Microagglomerate with pyrite solids re-liberated by washing action
Secondary Agglomeration
Additional Oil
Ash
Microagglomerates
Pyrite
Further Oil Wetting of Combustible Surfaces
Secondary Agglomerate Forming with Entrapped Pyrite
Final Secondary Agglomerate with Entrapped Pyrite or Ash Particle
Tertiary Agglomeration
Pyrite
Ash
Oil
Secondary Agglomerates
Tertiary Agglomerates With Entrapped Pyrite and Ash Particles
Entrapped Pyrite
Oil Phase
Pyrite
Ash Rich Solids
Combustible Solids

Figure 1.3 Primary, Secondary, and Tertiary Agglomeration

1.1 Purpose and Scope of Work

The study was undertaken in four phases to evaluate the process of selective coal and oil agglomeration as a method of reducing the sulphur and ash contents of a high volatile Bituminous A coal (Illinois No. 6) coal from the eastern United States.

Phase 1 involved the commissioning and construction of a bench scale continuous pilot plant (5 kg/hr) suitable for testing and evaluating the process.

Phase 2 involved the development of the experimental method with specific attention focused to apparatus design modifications to ensure test reliability and optimum process performance, and the economy of testing.

The Phase 3 objective was to perform a 2^5 factorial design to investigate how main and interactive effects impact recovery and cleaning efficiency. The following main factors were investigated:

- coal particle size,
- oil concentration,
- high shear energy input,
- temperature, and
- frother concentration.

Two additional factors which varied during the testing program are percent solids in the product phase and sample age.

Phase 4 involved developing linear regression equations to help describe how main factors and interactions impact CMR (%), TS (% daf) content of the product coal, and the ash (% db) of the product coal.

2.0 Sulphur Reduction

2.1 Strategies

In general, there are four key strategies to reduce sulphur dioxide emission levels during the combustion of coal.

- Switching to low sulphur coals as an alternative fuel source represents a longer term solution to reduce acid rain precursors. Although this strategy appear to be a straightforward solution, it has some economic and social limitations. Many low sulphur coals are lower in energy content, which would result in boiler derating. Furthermore, complete fuel switching in many cases would results in loss of local mining jobs. Blending of feed stocks of coal, oil and gas, may help to smooth the transition into the use of low sulphur coals. (Maronde and Deurbrouck, 1985)

In regions of the world such as China, where the domestic consumption of high sulphur coal is a major contributor of sulphur emission, fuel switching, or energy conversion using centralized systems where higher efficiencies and better control strategies can be implemented, would help reduce sulphur emission levels dramatically.

- Flue gas scrubbing systems are costly and difficult to economically justify when the life expectancy of the boiler is less than 10 years. The disposal of the sludge generated from the operation also presents some unsolved problems. (Maronde and Deurbrouck, 1985)

In developing countries, the transfer of advanced sulphur emission control technologies presents greater difficulties because of the complexity of operation, and the generally less favorable economic conditions. Livengood, et al., 1984, performed a comparative economic evaluation using computer simulation and data from over 20 operating plants in the USA and concluded that physical methods are more cost effective compared to flue gas scrubbing systems for 50 percent of the operations investigated, and had comparable costs for another 25 percent.

Despite any economic disadvantages, flue gas scrubbing can achieve very high sulphur reductions and can more easily accommodate changes in feed stock, and changing technology and environmental legislation is creating more favorable economics (Maronde and Deurbrouck, 1985). Hence, flue gas desulphurization will likely become a major environmental operation in the future operation of power plants.

- Increasing combustion efficiency and improving control and conservation strategies offers an opportunity for reducing sulphur emissions by lowering the overall amount of coal required for combustion. In less developed countries, where notably low combustion efficiencies are experienced, improvements of over 15 percent in combustion efficiency could be achieved by transferring to more efficient combustion technologies. This would reduce the coal required for combustion by almost one half, hence reducing the sulphur emission quantities respectively. However, in more technologically developed countries such as the USA, these high improvements margins cannot be expected, although more stringent power conservation measures might be implemented.

- Conventional and advanced coal cleaning processes are the simplest and most cost effective method to reduce the sulphur content of US coals, particularly those of the midwest and Appalachian regions. The general benefits of coal cleaning are described below. (Maronde and Deurbrouck, 1985)

-reduced transportation costs,
-reduced boiler maintenance,
-increased boiler capacity and efficiency,
-increased in plant availability,
-reduced in ash disposal costs, and
-initial segregation of sulphur rich particles.

Advanced physical cleaning processes offer the opportunity for initial segregation of sulphur rich matter. These processes often complement the transfer of the technology to existing mining and processing facilities and power plants, which generally utilize similar equipment.

Selective coal and oil agglomeration technology has been recognized throughout the literature as an advanced physical coal cleaning process with excellent potential for producing a superclean coal. The process relies on the differences in surface properties between the carbonaceous matter, and the ash and pyrite rich matter. The salient features and limitations of the process are listed below. (Hucko et al., 1989; Killmeyer, 1985; Capes et al., 1985; Pawlak et al., 1989; Knight, 1989; Nguyen et al., 1983; Armstrong et al., 1979; Mehrotra and Sastry, 1980; Baur, 1981; Chen and Nguyen, 1981; Brooks and Miles, 1987; Laurila, 1985)

Salient Features

- Selective in rejecting ash and pyrite rich matter, yet able to maintain high levels of combustible matter recovery.
- Reduced mass of tailings solids because of increased recovery of fines, thereby reducing waste treatment and handling costs.
- Modern, high-production mining techniques such as continuous miners and long wall miners produce a greater fraction of fines in the as-mined coal. Hence, coal and oil agglomeration provides for a potential reduction in the loss in heating value from tailings streams, thereby potentially improving the raw material economics.
- Advances in coal slurry technology may dramatically increase the demand for fine coal products.
- Relatively unaffected by the size and size distribution of the feed stock.
- Relatively unaffected by the degree of feed stock oxidation.
- Agglomeration produces a stable feed stock for the flotation process, reducing the impact of feed variations.

- Relatively easy technology transfer. Similar applications have been successfully tested at demonstration scale sizes as the process uses conventional unit processes and operations.
- Favorable economics when size enlargement processes are not considered.

Limitations

- Naturally hydrophobic surface of the pyrite surfaces causing inherently less process selectivity for pyrite rejection at high oil concentrations because of the increased probability of entrapment or oil coating of the pyrite particles.
- Historically, the process has been crippled by the costs associated with high oil contents and capital intensive processes required to produce a final handable product.
- Unable to separate organic sulphur components.
- Water intensive process.

To enhance the process selectivity in terms of pyrite rejection, a combined process of agglomeration and flotation was investigated in this study. The test coal was finely ground to liberate the pyrite and ash impurities. Oil and high mixing energy were added to cause the selective agglomeration of combustible rich particles with pendicular shaped bonds forming between the surfaces of the particles. These combustible rich structures were then separated using conventional flotation. Operating with the lowest oil concentrations possible, termed as primary agglomeration, allows for higher selectivity in terms of both ash and pyrite rejection.

Low shear mixing systems, and further oil addition, can be used to promote size enlargement and strength, however, because of the inherent economic disadvantages of the secondary and tertiary agglomeration regimes, and the large scope associated with the selective portion of the process, low shear mixing and higher oil additions were not considered in this process evaluation.

Work performed at Ontario Hydro has addressed the problem of high oil requirement for secondary and tertiary agglomeration by examining a process of pelletization rather than the traditional low shear mixing to enlarge the agglomerates from the cleaning circuit. The results were promising indicating a reduction of oil requirement of over 50 percent from the more traditional low shear mixer. However, the economics are not completely established as addition reagents such as emulsifiers and ashphalts were required, in addition to thermal drying and curing systems to ensure the adequate product handability criteria are satisfied. (Chen, 1981)

Hence, for the purposes of this study, one process configuration was selected whereby the mining operation, the oil agglomeration and flotation circuit, and the power plant were all in adjacent positions, thereby eliminating the requirement of any secondary or tertiary agglomeration. Only minimal oil additions are required, in the range of 0.5 to 1.5 percent dry basis (% db); where the process demonstrates the higher selectivity for pyrite rejection. Figure 2.1 depicts the overall process configuration, which also includes provision for flue gas scrubbing to remove the organic sulphur component. Locating the power plant operations adjacent to the mine site eliminates the expensive transportation costs, and dramatically reduces the overall oil addition levels by removing the stringent transportation criteria from the product handability characteristics. (Chen, 1981)

The optimum process configuration for sulphur removal will depend upon many factors. The site specific coal cleaning characteristics and the existing plant operations will influence the technologies selected. Regional economics, including the market conditions for sulphur rich byproducts, and the availability and cost of the raw resources required for the selected process, may also be major design factors. Regional technological capacities, and the socio-economical climate, are also factors which

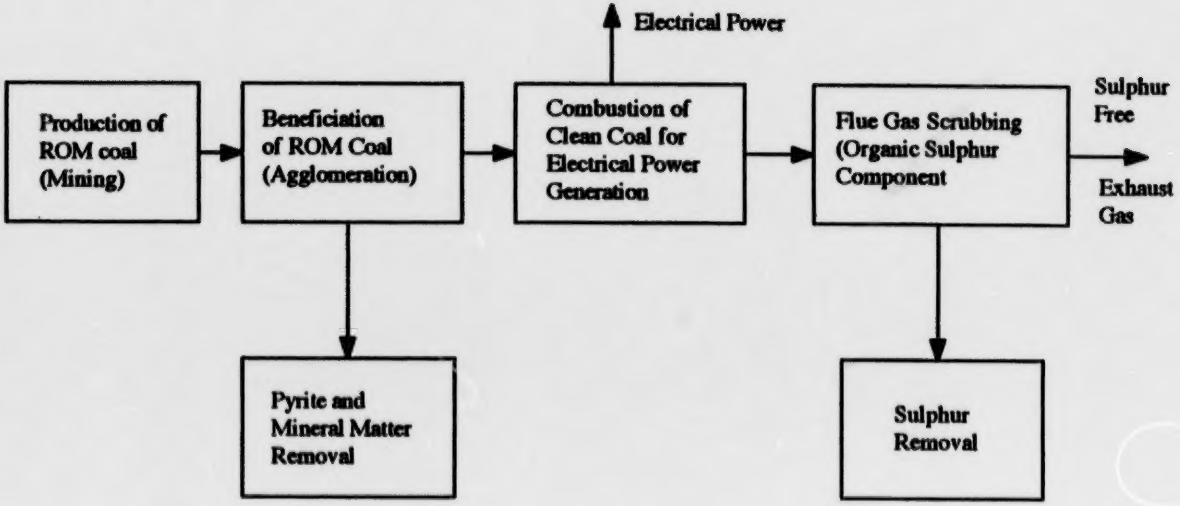
Production of ROM coal (Mining)
Beneficiation of ROM Coal (Agglomeration)
Pyrite and Mineral Matter Removal
Combustion of Clean Coal for Electrical Power Generation
Electrical Power
Flue Gas Scrubbing (Organic Sulphur Component
Sulphur Removal
Sulphur Free
Exhaust Gas

Figure 2.1 Process Configuration for Sulphur Free Power Generation

require careful consideration. For most coal fired power plants with high sulphur coal, the final process design requiring high removal levels for sulphur dioxide will involve a combination of both physical type processes to initially segregate ash and inorganic sulphur rich matter, followed by flue gas scrubbing or control systems to remove the remaining, sulphur dioxide.

2.2 Coal and Oil Agglomeration Process Description

The circuit configuration considered in this study is presented in the block diagram Figure 1.1, and consists of four steps:

- impurity liberation,
- water wetting,
- oil and coal agglomeration, and
- coal and oil phase separation.

In conventional operations, impurity liberation is achieved during the comminution operations. The impurities are typically disseminated within the coal matrix with a certain frequency and size distribution, or deposited in cleats within the coal. Crushing and grinding circuits are used to reduce the size of the feed stream such that the impurities, namely the pyrite and ash components, are liberated from the carbonaceous component. The level of grinding required depends upon how finely the ash and pyrite is disseminated in the coal matrix. Washability analyses are normally performed in parallel with grinding tests to determine the theoretical cleaning potential, and minimum grinding required.

In wet grinding operations, a water conditioning stage is not required as it occurs during the grinding operation. In this study, because a dry grinding system was used in this study, a water wetting stage was necessary. This mixing vessel also served as equalization for water and coal flowrate variations.

High shear mixing is responsible for the selective agglomeration of the combustible rich particles from the ash and pyrite rich particles. A pair of high shear reactors were used to supply the turbulence and time to disperse the oil phase, and provide mixing for sufficient collisions between the oil droplets and the combustible particles to ensure the combustible surfaces became oil wetted and agglomerated. Low levels of oil addition were used to improve the selectivity of the process, hence, the process was operated in the primary agglomeration regime, where only pendular shaped bonds are thought to exist and combustible solids are only loosely agglomerated or flocculated.

The flocculation of the combustible particles causes an increase in size, and the oil wetting enhances of the hydrophobic nature of the surface characteristics. Flotation systems rely on the same hydrophobic differences in surface characteristics to facilitate a separation. Hence, flotation was selected as a logical method for the recovery and separation of the combustible rich flocs from the ash and pyrite rich solids.

Further size enlargement promotes further deashing of the product, and ensures good dewatering capabilities. When the historically conventional method of low shear mixing for size enlargement is employed, addition oil, and mixing energy and time, must be provided to promote secondary and tertiary agglomeration.

2.3 Agglomeration

2.3.1 Fundamentals

The process of coal and oil agglomeration relies on the addition of an immiscible hydrocarbon which is preferentially attracted to carbonaceous rich particles causing the oil to wet the carbonaceous surfaces. Sufficient mixing energy is required to initially disperse the oil phase and promote collisions between the oil droplets and the combustible rich solids. The oil wetted combustible solids will continue to collide under mixing conditions, forming agglomerates, or floc type structures. Depending upon the specific attachment forces and the operating conditions, the newly formed agglomerate may be sufficient in size and strength to permit their separation and recovery. Coal and oil agglomeration is well recognized to preferentially wet carbonaceous matter resulting in the formation of agglomerates of various sizes depending upon processing parameters, while the mineral matter, which is typically hydrophilic in nature, remains in the water phase to be subsequently rejected. (Khoury, D., 1981; Mishra and Klimpel, 1987; Botsaris and Glazman, 1987; Liu, 1982)

Thermodynamics

Thermodynamic driving force for coal and oil agglomeration may best be described by the reduction in the total surface energy of the system. Thermodynamics of agglomeration are optimum when the following interface energies are predominant:

- solid-water interface energy is high;
- solid-oil interface energy is low; and,
- the oil-water interface energy is high (Mishra and Klimpel, 1987).

The system of internal forces responsible for the minimization of the surface energy can be related to either chemical and physical adsorption forces, chemical reactions between the oil and coal surface, or by the resolution of the surface energies where even weaker adsorption forces exist.

Kinetics

The kinetics of agglomeration are influenced by many factors, however, in most operative regimes, the following factors are of primary influence:

- the thermodynamic driving forces present,
- the concentration of oil added, and,
- the optimum selection of agitation and slurry concentration.

If extremely strong attachment forces exist between the type of oil selected and the carbonaceous particle surface characteristics, the process kinetics are intuitively increased because of the reduced probability of detachment, and increased rate of diffusion that the process will experience. Hence, for the coal and oil agglomeration process, if surface energy minimization forces are extremely high, the process kinetics will usually be rapid. However, it is theoretically possible, that even if strong forces of attachment between the oil and coal particles exist, forces of repulsion such as the electrostatic charges associated with both the oil and solid carbonaceous components may also exist. Studies have indicated that the forces of attachment for most agglomeration processes strongly counteract any electrostatic forces of repulsion which may be present (Labuschagne, 1986; Fan et al., 1982; Yang et al., 1988).

Mixing energy is a primary variable influencing the kinetics of the process, as sufficient energy is required to transport the oil droplets to close proximity of the carbonaceous rich particles so that the forces of agglomeration may become operative (Vanangamudi, 1984). The mixing energy, combined with the concentration of both the oil and solids, controls the rate at which agglomerates form and defines their final size. The shearing action of the mixer causes both agglomerate formation and rupture, allowing any captured hydrophilic ash particles to be released back to the tailings stream as the agglomerates are re-dispersed and reworked. However, the high shear mixing limits the agglomerates to relatively small sizes. (Mishra and Klimpel, 1987) The slurry density and oil concentration influences the kinetics of the process by ensuring a sufficiently high number of collisions within the system (Liu, 1982; Khoury, 1981; Mishra and Klimple, 1987).

Agglomerate Structure

Agglomerate structure is dependent upon the concentration and type of oil used. Figure 2.2 describes the expected response of increasing the oil concentration in terms of agglomerate structure. Various structures of agglomerates are predicted to exist over a range of oil addition levels, and in general, these structures demonstrate an increase in both size and strength as the oil concentration is increased. Lower levels of oil addition cause the formation of pendular bonds between the carbonaceous solids which can be best described as a loosely formed floc structure, somewhat two dimensional in shape. As the concentration of oil is increased, the flocs strengthen and consolidate, developing a funicular structure which could best be described as the transition into a distinctively three dimensional funnel like agglomerate. As the oil concentration is further increased, limited spherical agglomeration can be observed and a transition begins as the funicular flocs begin to form spherical agglomerates (Botsaris and Glazman, 1989; Mishra and Klimpel, 1987). As the mixing time and oil addition is further increased, the agglomerates will increase in size and reach a peak size and strength once the capillary region is approached, where 100 per cent of the pore volume is occupied by the oil phase. If the oil concentration is further increased, reverse agglomeration will prevail, and the agglomerates will exist as pasty lumps and the carbonaceous solids are held in suspension within the bridging liquid without any distinct individual agglomerate structures. (Liu, 1982)

2.3.1.1 Transport Mechanism

Agglomeration can be described in terms of transport and attachment mechanisms. Within each regime of the agglomeration process, different forces may dominate. Figures 2.3 a & b describe the possible forces responsible for the transport

Figure 2.2 is Restricted by Copyright

Figure 2.2 Structural Formation During Agglomeration (After Botsaris and Glazman)

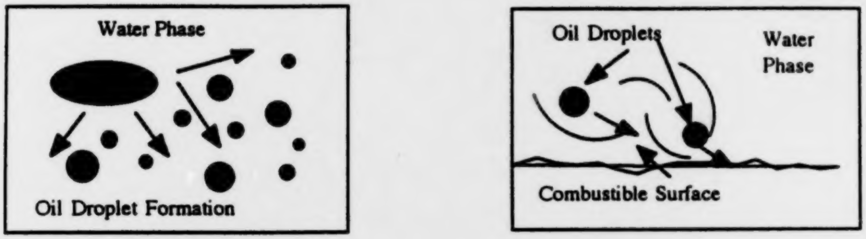

a. Oil Droplet Formation
-energy dispersion, and immiscible nature, results in droplet formation.

b. Transport of Oil Droplet
- Brownian motion,
- gravity,
- collision theory, and,
- diffusion.

Figure 2.3 Transport Mechanisms

of oil to the combustible surfaces (Weber, 1972; Alberty and Daniels, 1980; Botsaris and Glazman, 1989).

The transport mechanism begins with the dispersion of the oil binder into tiny droplets (see Figure 2.3 a.). The immiscible nature of the oil and its surface energy characteristics, combined with highly turbulent mixing regime, results in the formation of tiny oil droplets. The final droplet size is a function of the existing intermolecular adhesive forces holding the oil together, and the shear forces of the mixing system tending to tear the oil droplet apart. The final size of the droplets is dependent upon several physical and chemical factors. Physical factors may include: oil viscosity, temperature, mixing characteristics, and the slurry rheology. Chemical or physio-chemical factors may include: emulsion stabilizers present, pH, water chemistry, and the surface energy makeup of the slurry. The rate of dispersion is also influenced by similar factors, the most predominant factor being the mixing characteristics. Studies investigating the effect of pre-emulsification of the oil phase on agglomeration have indicated that the largest portion of the high shear energy input is consumed in dispersing the oil phase (Bensley, et al. 1977; Capes et al., 1985).

The remaining portion of the energy input is utilized primarily to transport the oil droplets to the carbonaceous surfaces. The transport of the oil droplets can be described by considering the fundamental forces responsible for liquid to solid transport (see Figure 2.3.b.). Listed below are the four main transport phenomena which are active in any similar mixing system:

- Brownian motion,
- gravity,
- inertia impact, and
- diffusion.

Brownian Motion

Brownian motion is observed when dispersed colloids demonstrate random movement by bombardment from molecules of the dispersing medium. When this random motion creates collisions and subsequent agglomeration, it is sometimes called perikinetic flocculation. For particles typically less than 1 micron is size, Brownian motion can be a predominant factor, however, above 1 micron in size, other factors are usually predominant (Weber, 1972). The impact of Brownian motion as a transport mechanism can be considered to be fairly limited because the particles are larger and mixing is turbulent.

Gravity

Gravity can be classified as a transport factor in systems where differential settling is a dominant potential. Larger, or denser particles may overtake and collide with one another in settling systems, or in fixed bed or counter current reactors, where gravity may cause particle and collector/reactor grain collisions. In the agglomeration process, gravity will be of minimal influence because of the turbulent mixing.

Inertia Impact

The transport factor related to agitation can be best termed as inertia impact. Agitation has been attributed with increasing the rate of collisions between particles in many systems. In mixing systems, velocity profiles are designed to promote variations in both spatial and temporal aspects. Particles and droplets will be effected by these hydraulic patterns, and the variations will cause and increase in intraparticle contacts. (Weber, 1972). The frequency of collisions of individual particles will depend upon the resolution of forces related to the particle momentum, imparted as a result of the mass and velocity due to the turbulence of the mixing regime, and the hydraulic drag forces created by the mixing of the slurry, and the particle shape.

Within the coal and oil agglomeration system strong attachment forces exist between the oil droplet and carbonaceous surfaces, permitting the use of high mixing velocities. Kinetic modeling of agglomeration has indicated that the process kinetics are strongly dependent upon mixing energies imparted on the slurry (Ahmed and Jameson, 1983). Furthermore, in highly turbulent mixing regimes such as these, inertia impact is known to be the predominant contributor to the transport of oil droplets and carbonaceous particles (Weber, 1972; Gilchrist, 1984).

Diffusion

It is possible that diffusion may be responsible for the transport of oil droplets to the coal surface. Within the mixing regime, there will exist instantaneous resolutions of forces where impact inertia alone will not be sufficient to cause the collision of oil droplets and solids surfaces. Furthermore, forces of repulsion may exist due to the electrochemical nature of the particles. In this case, the transport of the oil droplet may occur as a result of diffusion across a boundary layer. The gradient of the system is related to the minimization of surface energy of the system, or any other attractive forces present in the system. Likely, both the solid particles and oil droplets will demonstrate a similar electrochemical charge in a water solution, and hence, some forces of repulsion will exist phenomenally defining a boundary layer related to these forces. The attractive forces between the coal surfaces and oil droplets represents the theoretical gradient of attraction whereby the oil droplet is caused to diffuse across a boundary layer to hydrophobic surfaces of the combustibles solids.

Inertia impact is thought to be the predominant force contributing to the transport mechanism, however, in weakly agglomerating systems, diffusion across a boundary layer may be a contributing component.

2.3.1.2 Attachment Mechanisms

The attachment of the oil droplet to a combustible solid surface depends upon a number of possible forces. Figure 2.4 describes the possible forces acting in the system, and they are also listed below:

- minimum surface energy,

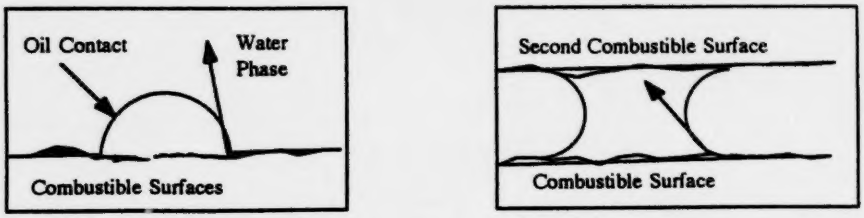

a. Oil wetting of surfaces:
- minimum surface energy,
- adsorption,
- repulsion, and
- shear forces.

b. Formation of coal & oil contacts
- surface energy,
- repulsive forces,
- adsorption,
- chemical bonding,
- shear forces and entrapment.

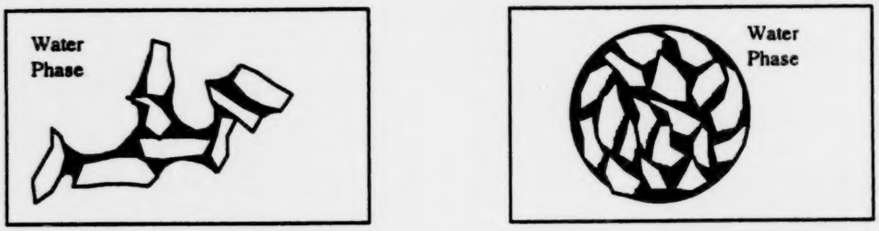

c. Pendular and Funicular Floc Formation

d. Agglomerate formation

Figure 2.4 Attachment Mechanisms

- adsorption,
- repulsive forces,
- chemical bonding,
- entrapment, and
- shear forces.

Surface Energy

Molecules at the surface of a liquid are attracted to the bulk of the liquid because of cohesive forces within the liquid are greater than the adhesive forces at the interface. The inward attraction gives rise to surface tension because the outside layer of molecules is tending to contract. Examples of the effect of surface tension are the formation of spherical droplets, the rise of fluids in capillary tubes, the migration of liquid through a porous solid, and the spreading of oil on the surface of a carbonaceous particle. (Alberty and Daniels, 1980)

By definition, the surface tension of a liquid is the interfacial force that opposes the expansion of surface area. For example, a drop of mercury resists spreading on a steel plate and tends to retain its spherical shape. The resistance to spreading is related to the surface energies at each of the interfaces of the drop. The mercury drop minimizes its total surface energy by maintaining its spherical shape. "Because molecules of mercury are attracted to one another by cohesion forces more strongly than they are by adhesion forces to molecules of the solid plate or molecules of air at the liquid-solid and liquid-gas interfaces, respectively, those molecules of mercury at the surface will be pulled mainly toward the interior of the drop" (Alberty and Daniels, 1980). The drop tends to decrease its exposed surface area because of the strong intramolecular attractions, and enlarging the surface area would require overcoming the attachment forces within the liquid phase. (Alberty and Daniels, 1980; Weber, 1972)

Depending upon the resolution of the relative molecular cohesion and adhesion forces in a system, different surface systems will be formed. Figure 2.5.a-e. depicts

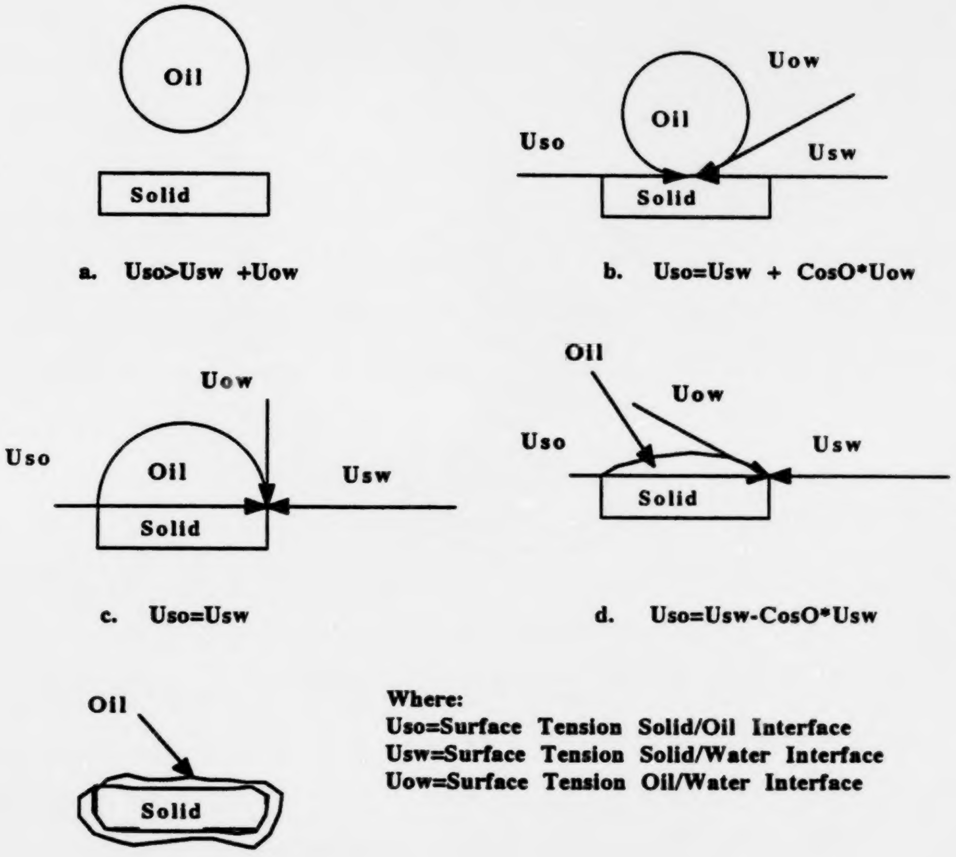

a. Uso>Usw +Uow

b. Uso=Usw + CosO*Uow

c. Uso=Usw

d. Uso=Usw-CosO*Usw

e. Uso< Usw + Uow

Where:
Uso=Surface Tension Solid/Oil Interface
Usw=Surface Tension Solid/Water Interface
Uow=Surface Tension Oil/Water Interface

Figure 2.5 Surface Tension Phenomena

five different minimum surface tension regimes possible in a liquid and solid system. Because the system is a resolution of interfacial forces, the forces of attraction and repulsion within the system cannot be distinguished. However, the consideration of these cases is useful in demonstrating the fundamentals of coal and oil agglomeration, and the later, the flotation process.

Figure 2.5.a represents a system where the intermolecular cohesion forces of the oil phase are prevalent. The repulsion forces between both the oil/water and the solid/oil could be also be large, resulting in high surface tensions between these components. Attractive forces between the solid/water may also be large, resulting in a low surface tension at this interface, effectively inhibiting the attachment of oil droplets to the solid particles. Some examples of this system may include clay solids, which are known to adsorb water, low rank coals such as lignite, which demonstrate significantly higher equilibrium moisture contents, or oxidized coal, whereby the surface functional groups demonstrate increased hydrophilic behavior. The equation helps define the force system by indicating that the surface tension of the solid/oil interface exceeds the combined surface tension of the both the solid/water and oil/water interfaces. Hence, the minimization of the surface energy of the system indicates that the immiscible oil phase will formulate small droplets within the water phase without attaching to the solid surfaces. The final size distribution of the oil droplets will depend upon the resolution of the intermolecular cohesive and the mixing shear forces.

Figure 2.5.b represents the case where the attraction at solid/oil interface may be large enough to cause the attachment of the oil droplet. The large contact angle indicates other forces may also be predominant. Hence, the small contact area at the solid/oil interface may be a result of predominant attractive forces at the solid/water or oil/water interfaces. The equality summarizes the possibilities by indicating that the solid/oil surface tension is equivalent to the resolution of the solid/water and the oil/water interfacial surface tensions. Attachment angles such as these are typical of conventional flotation systems, where the bonds are somewhat weaker than those experienced in the agglomeration process.

In Figure 2.5.c, the degree of oil wetting has increased. The equality provided indicates the surface tension between the solid/oil, and the solid/water interfaces, are equivalent. The surface tension between the oil/water interface is higher than both other interfaces, resulting in the attachment of the oil droplet onto the solid surface to satisfy the minimization of surface energies.

Stronger attachment forces at the oil/solid interface exist in Figure 2.5.d The equality indicates the largest surface tension exists at the solid/water interface. Hence, the predominant forces acting in this system are likely the repulsive forces at the solid/water interface, and perhaps, the oil/water interface, resulting in comparatively high surface tensions. A relatively lower surface tension at the solid/oil interface, or the existence of adsorption forces, would cause the droplet to effectively further flatten, or spread about the solid. The forces diagram suggests the particle may be highly hydrophobic as the surface tension of the solid/water interface is higher than the resolution of the solid/oil and oil/water interfaces.

In Figure 2.5.e, the surface tension at the solid/oil interface is lower than the combined surface tensions of both the solid/water and oil/water interfaces. In this force diagram, strong attractive forces between the solid and oil likely exist, and both these components are also likely to be hydrophobic, indicating extremely high surface tension would exist at the solid/water and oil/water interfaces. Hence, the oil droplet completely flattens and wets the entire solid surface.

The attachment forces typical of coal/oil agglomeration would be best represented by force diagrams 2.5.c,d, and e, where extremely strong attachment forces between the coal and oil can develop, and the oil phase wets the carbonaceous surface very well.

Adsorption

The action of adsorption results in the concentration of a substance ar the surface or interface of another. Adsorption can involve a variety of interfaces, including: liquid-liquid, gas-liquid, gas-solid, or liquid-solid interfaces. The absorbate is the substance being concentrated, and phase absorbing is the adsorbent. When molecules of one phase interpenetrate to form an almost uniform concentration within the second phase is defined as absorption. (Weber, 1972)

In coal and oil agglomeration, absorption of the oil phase onto the combustible solid surface is unlikely because of the viscous nature of the oil, and that the thermodynamic driving force is related to surface energies. Agglomeration processes which utilize light hydrocarbons may exhibit limited potential for intraparticle penetration via chemical bonding.

Adsorption forces exist between the carbonaceous surfaces and the oil droplets. However, these forces are highly interactive with surface energy interactions, as the combined attractive forces between the combustible surfaces and the oil droplets, and the repulsive forces between the water, solid, and oil phases will tend to cause the oil droplet to spread over the carbonaceous surface. For example, when the oil concentration exceeds a critical level, the carbonaceous solids become dispersed in the oil phase, not as spherical agglomerates, but as discrete particles. The free mineral matter subsequently agglomerates within the water phase (Liu, 1982).

There are several types of adsorption. The forces of adsorption may be related to the solvent-disliking (lyophobic) character of the solute relative to the solvent, or the strong attraction for the solid phase. Many systems will involve a combination of such molecular forces. (Weber, 1972)

The first factor influencing the level of adsorption is the solubility. For adsorbents which are extremely hydrophilic in nature, the forces of adsorption can be considered to be minimal. However, if the solute is extremely hydrophobic, the substance will likely demonstrate potential for adsorption interactions (Weber, 1972). Such is the case for coal and oil agglomeration. The oil and carbonaceous phases are both considered to be hydrophobic in nature, and the oil is immiscible in the water phase. Hence, with both the combustible solids and the oil phase demonstrating a hydrophobic nature, the potential for adsorption forces to exist are very high.

Adsorption may be solely dependent upon the direct attraction or affinity of the solute for the solid. Three principal types of adsorption mechanisms: electrical attractions, Van der Waals forces, or forces as a result of chemical attractions. Electrical attraction is sometimes termed as exchange adsorption, and has been used to describe ion exchange systems (Weber, 1972).

Physical adsorption has been classified as synonymous with Van der Waals forces, used to describe with the molecule is attached but is allowed to undergo some movement on the surface without detaching. Van der Waals forces are normally found at low temperatures, and is characteristically have low energies related to the bonding. (Weber, 1972; Capes et al., 1985; Nelson, 1989; Botsaris and Glazman, 1989)

When molecules are affixed to a specific site on the surface or interface they are considered to be chemically adsorbed, and undergo direct chemical interaction. These chemical reactions exhibit higher energies of adsorption, as the strong local bonds are formed. (Weber, 1972)

Characterizing the adsorption forces in coal and oil agglomeration as either physical and, or, chemical; or determining to what extent combined adsorption forces may exist, has not been clearly defined. Furthermore, because surface tension phenomena also interacts, determining the predominant components is further complicated. However, based upon the nature of the system, and the relative spontaneous agglomeration tendencies only under specific conditions, indicates the adsorption forces are predominantly physical in nature.

Repulsive Forces

The surface chemistry of coal may possess active sites which are either hydrophobic or hydrophilic in nature. Oxidized coal sites, ash swaps within a combustible rich surface, and the coal rank, all provide examples which demonstrate the hydrophilic characteristics causing forces of repulsion to exist between the oil and carbonaceous rich particles. Coal surfaces develop electrochemical charges in a water suspension. These electrochemical charges can be responsible for the development of forces of repulsion inhibiting the collision of coal particles and oil droplets. Investigations describing the point of zero charge have indicated that the electrochemical characteristics can influence both the kinetics and thermodynamics of agglomeration. These forces of repulsion may effect the kinetics of the process by inhibit the collision between the oil and coal and tend to increase the energy input requirements. Systems demonstrating high attractive forces of adsorption, the electrochemical characteristics may tend to inhibit the kinetics, while the final equilibrium oil wetting, or thermodynamics or agglomeration, will be reached provided sufficient energy and time are permitted (Sadwoski et al., 1988). However, the electrochemical forces of repulsion can effect the thermodynamics in weakly agglomerating systems, if these forces of repulsion exceed the attractive forces present between the oil and coal.

Chemical Bonding

Most of the literature in investigating agglomeration technology suggests that chemical bonding in coal and oil agglomeration is limited. However, it may be possible that some specific functional groups within the coal and oil phases interact chemically to form a bond, as it is sometimes difficult to distinguish between strong chemical adsorption forces and chemical bonding. Furthermore, if the coal and oil agglomeration process is chemically altered by pH, or ionic strength, chemical bonding may become a more significant force. Based on previous in agglomeration studies, chemical bonding usually is a minor force (Liu, 1982; Mishra and Klimpel, 1987).

Entrapment

Free particles of either ash or pyrite can be entrapped by the simultaneous collision and subsequent formation of combustible agglomerates. The potential for entrapment will depend on many factors, some being as follows: slurry concentration, oil concentration, shear forces, agglomerate size and shape, and the strength of attachment responsible for the entrapment of the free ash and or pyrite particles.

The potential for ash or pyrite entrapment is greatest during secondary and tertiary agglomeration where the oil concentration levels are high, and the least likely within the primary agglomeration stage where the oil concentration levels are the lowest. Figure 1.3 helps to describe these trends and how they relate to oil concentration.

Shear Forces

The shear forces are directly related to the turbulence and intensity of mixing imparted into the slurry. The mixing action is highly turbulent, possessing high velocities and rapid changes in direction over relatively short distances, resulting in maximum particle and oil droplet collisions and shear. The shape and density of the particles will also influence the shear forces which act upon a agglomerate because of drag and momentum forces. To maintain successful agglomeration, the mixing energy must be sufficiently high in turbulence and intensity to ensure rapid particle contact, however, the mixing energy must be sufficiently low to ensure the shear forces do not exceed the attachment forces and eventually disrupt the agglomerate formation (Capes et al., 1985; Botsaris and Glazman, 1989).

2.3.2 Process Variables

There are many important operative variables in the process of coal and oil agglomeration, of which the following are considered to be the most important:

- High energy input is first required to disperse the oil phase and supply the energy to facilitate the contact between the oil droplets and the coal surfaces (Mishra and Klimple, 1987).
- The addition of heavy oil, either alone or as a blended base to promote the agglomeration of the carbonaceous solids. Heavy oil is responsible for the formation of larger agglomerates because of the stronger intraparticle bonds which it forms (Mishra and Klimple, 1987).
- Lighter oils play an important role as they are often employed to improve the selectivity of the process for ash and pyrite rejection (Mishra and Klimple, 1987).

Other process variations and variables influencing agglomeration are categorizing as feed variations, chemical and physical parameters, and equipment components.

2.3.2.1 Feed Variations

Surface oxidation and coal rank

Coal demonstrates unique and varied properties when compared with other substances. Although coal possesses strong intermolecular forces, it is considered to be highly unstable and will weather in almost any condition which exposes the material to the natural environment. Coal's lack of stability creates problems associated with coal utilization, transport, and storage include self-heating and spontaneous combustion as well as progressive changes in handling, beneficiation, specific energy, liquefaction, and carbonizing properties (Nelson, 1989).

In its natural habitat, coal exist underground, in a water saturated and oxygen free environment. Changing anything related to its natural environment such as moisture content, temperature, or the oxygen partial pressure will surely influence the chemical and physical properties of the coal. The change in the coal characteristics is known as weathering, has been studied thoroughly and is known to adversely affect physical and chemical properties of coal. The weathering process alters the interpretation and test methods for coal samples, thereby having important implications with respect to fundamental research on coal. (Nelson, 1989)

Weathering refers to the air oxidation of the organic and mineral matter (chemical weathering), microbial oxidation or pyrite (biological weathering), and variation in moisture content which may alter the physical characteristics (physical weathering). Therefore, controlling the environment in which coal is exposed prior to utilization is very important in preventing any adverse alterations to the general properties of the coal. (Nelson, 1989)

Air oxidation influences the wetting characteristics of the combustible matter, by affecting the oxygen content of the organic matter. The newly oxidized components within the coal's organic matrix are more hydrophilic, reducing the dissimilar differences between the coal's organic and mineral matter components. The practical consequence of the reduced dissimilarity as it becomes more difficult to separate mineral matter based upon surface properties. Hence, the process of oxidation will have some level of influence on the performance of either the agglomeration or flotation process, although the later is expected to be more sensitive. Dewatering and drying of coal becomes more energy intensive and less efficient as oxidation increases. Furthermore, the surfaces become more polar and acidic and may influence slurry rheology, as well as increasing the potential for corrosion. (Nelson, 1989; Botsaris and Glazman, 1988 Venkatadri et al., 1988; Labuschagne, 1986)

The hydrophobicity of coal is dependent upon its rank, the characteristics of the mineral matter contained in the coal, and the carbon content. Bituminous coal are known to be more susceptible to oxidation compared to low grade sub-bituminous coal and lignite because of the -OH group content of the coal. The inherent moisture content of lignite can exceed 30 % and climb up to 40 % by mass, compared to relatively low values of between 1 to 5 % for bituminous coals. The coalification process gradually removes the -OH functional group which leads to the formation of semi-bituminous and eventually bituminous and anthracite coals. Structural changes also contribute to the hydrophobicity of coal. The carboxyl group is gradually replaced by more hydrophobic aromatic groups. The maximum angle of contact for an air bubble has been estimated to be within a range between a low volatile bituminous coal and semi-anthracite coal. The contact angle becomes lower with the higher rank anthracite coals. The mineral matter can also impact the hydrophobicity of the coal, and the specific composition and size consistency within the matrix will impact the hydrophobicity of the coal. The carbon to hydrogen ratio has been used as a general indicator of coal hydrophobicity, all this factor can only be used as a rule of thumb. Studies have shown that the process of oxidation, which increases the -OH and -CO functional groups, tends to reduce the hydrophobicity of the coal. The reduction in hydrophobicity has been attributed to the increase in oxygen functional groups within the coal structure. (Mishra and Klimpel, 1987) Further support is provided by distinguishing the lower-rank sub-bituminous and lignites by their greater oxygen content and the hydrophilic nature of their surfaces. "The light oils which are used successfully with bituminous coals are not able to wet the lower-rank coals and form only emulsions with no discrete agglomerates when agitated with them is a water slurry. If heavier oils, such as coke oven tars and pitches as well as petroleum crude oils and their higher boiling components, are used as conditioners, distinct agglomerates are formed with the lower-rank coals. Apparently the nitrogen, oxygen, and sulphur functional groups of these complex oils are able to adsorb sufficiently well on the relatively hydrophilic surfaces of the lower-rank coals to form agglomerates" (Botsaris and Glazman, 1988).

Impurity content, size distribution

The impurity content, type and size distribution directly effects the performance of oil wetting of the combustible surfaces, as high slimes content has been known to interfere with the performance of both coal and oil agglomeration, and froth flotation. Postulations have been made that some humic materials can be leached from the coal forming a weak humic acid in the aqueous phase which subsequently can adsorb onto clay material, rendering then somewhat hydrophobic (Botsaris and Glazman, 1988) If large amounts of these types of clays are present in the process, which might be the case in some recycle streams, the hydrophobic clays may compete in the process by promoting an oil-water clay-stabilized emulsion which interferes with agglomeration and blinds the separating screen. Removal of these clay components from the process stream will help eliminate the interference and restores the hydrophobic-hydrophilic distinction between the organic component and the mineral matter. (Botsaris and Glazman, 1988) Problems such as these are more typical in the treatment of tailings pond solids where the mineral matter has extended periods to interact with humic acids leached from the organic matter. However, excessive mineral matter content also physically interferes with the coal agglomeration process, resulting in higher energy levels to ensure a overall high process efficiency.

Oil agglomeration is considered to be a high recovery process because of the strength of the coal-oil bond. Carbonaceous particles with non-liberated impurities are therefore recovered so that impurity particles which are rejected are virtually barren of coal matter. Oil wettability appears to be unaffected by (or swamps) large areas of hydrophilic impurity islands in the surface of carbonaceous particles and the high strength of the coal and oil bonds allows the particles to be recovered with the agglomerates. (Botsaris and Glazman, 1988) This fundamental process characteristic influences the ability of the coal and oil agglomeration process to reject finely disseminated particles of pyrite found in the organic matter. Only if the pyrite is sufficiently liberated from the organic matrix will the process be able to reject the pyrite fraction. Similarly for ash particles, if they coexist with a large fraction of carbonaceous matter, recovery into the product phase is likely to occur.

Variations in quality

Variations in the feed properties can cause serious process disturbances. For example, variations in degree of weathering, or mineral matter content can easily cause serious disturbances in impurity rejection, and or combustible matter recovery. Feed variations must be minimized to enable the process to operate at an optimum set of process conditions without continuous upsets.

2.3.2.2 Chemical Factors

The oil type and concentration are the most important chemical factors in coal and oil agglomeration. The type of oil used can influence both the physical and chemical components of agglomeration. In the physical sense, heavier oils tend to demonstrate a more viscous nature and form stronger intraparticle bonds. Hence, when agglomerates are formed with heavier oils, the intraparticle bonds between the solid and oil have more internal strength than those formed with the lighter oils. The viscosity of the oil will also influence the energy requirements to ensure sufficient dispersion of the oil phase, and in this manner, will influence both the thermodynamics and kinetics of oil wetting. In general, for heavier oils, higher energy levels are required to ensure sufficient oil dispersion and oil droplet and particle collisions. Bensley et al. (1977) however, investigated the impact of oil emulsification and found substantial decreases in energy input can be realized. Despite the energy limitations, heavier oils offer the advantage of stronger intraparticle bonding. The stronger intraparticle bonds can influence both the process economics as well as the process selectivity (see Figure 1.3) by reducing the overall oil concentration required.

The chemistry of the oil also plays an important role on both the thermodynamics and kinetics of agglomeration. Despite the kinetic dependency of the process on sufficient energy to supply the transport of the oil to the surface of the desired particle, if strong chemical attractions between the oil droplets and the combustible particles exist, the process kinetics can be strongly influenced. Such is the case with lower rank coals, such as lignite and sub-bituminous coals, which do not readily agglomerate with the less viscous lighter oils typically used with bituminous coal, but agglomerate more readily when heavier oils, substantial higher in viscosity, are used. The heavier oils have complex functional groups, which are more strongly attracted to the lower rank coals. Heavier oils are also used with bituminous coal, with sufficient energy input, and tend to improve combustible matter recovery, however, at the expense of reduced process selectivity for impurity rejection, such as ash and pyrite. Studies have indicated, that in general, lighter oil is responsible for improving the process selectivity for ash and pyrite rejection of bituminous coals, while the heavier oils tend to be less selective but promote better combustible matter recoveries when sufficient energy levels are added to properly disperse the heavier oil. Investigation into the impact of pre-emulsification of the oil phase have supported this trend indicating that heavier oil are capable of high recoveries when sufficient dispersion and collision between the droplets and carbonaceous particles occur. However, these same studies found that heavier oil will demonstrate the same levels of ash rejection are possible provided sufficient energy and time are added to the mixing system. (Bensley et al., 1977; Mishra and Klimpel, 1987; Liu, 1982)

Lighter oils have been characterized as more selective when compared to the heavier oils. The lighter oils may include fuel oil, and kerosene, while the heavier oils may include bunker C, crude oil, or coal tar. The heavy oils are hypothesized to contain functional groups capable of altering the mineral oxide surfaces to sometimes produce hydrophobic surfaces, allowing these impurities to report to the product phase (Mishra and Klimpel, 1987). Other research has indicated differing solids settling rates of the tailings produced by agglomeration with different oils. Experimental evidence and observations indicate that the heavier oil tailings produce flocculation of the tailings solids, which produced the faster solids settling rates. The residual oil component in the tailings phase appeared to promote the flocculation of the mineral matter to increase its settling rate. Hence, the poorer process selectivity may not be necessarily dependent upon the oil density, as other studies have indicated that the use of pre-emulsification of heavy oil results in no loss of ash rejection potential as the density of the oil was varied. They postulated that the impurities present in the heavy oil, rather than the density, strongly influence the process selectivity for both the ash and pyrite rich particles. Their investigations demonstrate that the laboratory addition of impurities to the oil phase reduce selectivity and increase the ash content of the agglomerate product. Other works have also indicated similar trends. (Bensley et al., 1977; Mishra and Klimple, 1987)

Lighter oils tend to be more selective because of the efficient dispersion and higher level of purity than the heavier oils. However, heavier oils demonstrate higher carbonaceous recovery and dewatering capabilities when sufficient energy input is added to promote dispersion and transport. The heavier oils also appear to demonstrate stronger intraparticle bonding, which results in lower oil concentration levels required to facilitate recovery. The lower oil concentration levels affect the process in terms of both process economics, as oil costs are often the crippling component of the process, and process selectivity, as lower oil concentrations, reduce the probability of pyrite and ash entrapment (see Figure 1.3). (Mishra and Klimpel, 1987; Liu, 1982; Botsaris and Glazman, 1989)

Oil concentration is an important variable influencing the process in terms of product quality, and process economics, relating back to the high cost associated with oil. In terms of traditional coal and oil agglomeration, (see Figures 1.3 and 2.2) an increase in oil concentration will influence the structure of the forming agglomerant. Based upon the more traditional process separation steps selected, such as mechanical screening systems, the agglomerate structure will affect the combustible matter recovery, the process selectivity, and the product dewatering. The agglomerate structure in traditional coal and oil agglomeration process is influenced over a wide range of oil concentrations (e.g. 5 to 15 % db). (Mishra and Klimpel, 1987; Liu, 1982; Botsaris and Glazman, 1989)

In this study, primary agglomeration was followed directly by flotation to separate the combustible matter from the impurities. Hence, the operative range of oil concentration was reduced to a much lower range of 0.5 to 1.5 % db. When agglomeration and flotation are employed as a combined process, the concentration of oil used influences the combustible matter recovery levels dramatically until the local requirement to established to maintain high combustible recoveries (e.g. >98 % CMR). After the operative requirement is met, additional oil will no longer effect the recoveries, however, some structural changes in the froth can be expected and the solids concentration of the product will increase. The process selectivity continues to be affected as additional oil is used, particularly in terms of pyrite removal. At low levels of oil addition, only loosely consolidated floc structures will form resembling pendular and funicular structures. Separation at this time is favored to minimize the oil coating and entrapment of the pyrite and ash rich particles. High wash nozzles are used to increase the impurity removal from the combustible flocs prior to recovery. The impact of froth washing in terms of ash and pyrite removal is documented by the work of others. (Mishra and Klimpel, 1987; Liu, 1982; Botsaris and Glazman, 1989)

2.3.2.3 Physical Parameters

Solids Concentration

The solids concentration will influence the kinetics of agglomeration, as high percent solids increases the probability of oil droplet and particle collisions, while a lower percent solids results in a slower rate of collision. The slurry density must be low to avoid the entrapment and oil coating of impurities, yet sufficiently high to maintain rapid wetting kinetics. The optimum selection is related to the surface characteristics of the impurities and their relative hydrophobicity, the chemistry of oil, the energy input in the process, and the agglomeration kinetics. Strongly hydrophilic impurities allow for higher percent solids to be used, while impurities such as pyrite which are less hydrophilic, require lower percent solids to be used. Agglomeration processes used solely for ash rejection can experience solids concentrations as high as 30 to 50 percent, while for systems designed for pyrite rejection will use a range from 10 to 30 percent. (Mishra and Klimple, 1987; Liu, 1982)

Size Consistency

Feed stock grinding is employed to ensure an adequate impurity liberation. Size reduction must be sufficient to cause the liberation of impurities contained in the coal, otherwise, the impurities will report to the product because they are physically attached to the combustible rich particles. The desired size range depends upon the breakage characteristics of the feed stock, the relative size distribution of the impurities within the feed stock, and the cost of grinding. Some impurities are so finely disseminated within the coal that liberation reaches a point where increases in grinding produces minimal increases in impurity liberation. Furthermore, the cost of grinding becomes incrementally more expensive at the finer sizes due to the loss of natural breakage patterns in the coal, and the somewhat elastic behaviour of coal in these lower size ranges. These factors define a practical size distribution which can be employed for the process.

Experimental evidence indicates that the agglomeration process demonstrates continued improvements in ash rejection when the feed stock coal is reduced to a mean particle diameter of 3 microns because of the high process selectivity for ash rejection and the higher degree of ash liberation at the smaller sizes. (Liu, 1982; Mishra and Klimpel, 1987; Capes et al., 1981). Capes et al. (1981) performed investigations into the effect of size on ash rejection and surmised that the additional rejection in ash content at the smaller sizes may also be dependent upon how the oil concentration interacts with feed stock particle size. "The reason for this effect of particle size seems to be related to the forms of agglomerates produced as oil concentration increases and to the increase in strength of intraparticle bonding which occurs as particle size decreases. With the lowest oil levels a loosely consolidated floc (e.g., approximately 100 to 300 microns in diameter) structure is formed which is able to trap ash particles and cause them to report with the agglomerates. As oil concentration increases, this voluminous two-dimensional floc structure is replaced more and more by discrete more compact three-dimensional larger agglomerates (e.g., approximately 300 to 800 microns in diameter) which do not trap ash particles as easily in the inter-agglomerate space" (Capes et al., 1981). Similar supportive work describing these effects in terms of pyrite reduction from the product phase does not exist. Pyrite rich particle attachment and entrapment within agglomerates occurs in the opposite trend at these lower sizes than ash particles because of the natural hydrophobicity of the pyrite surfaces. Increasing the oil concentrations into similar ranges (e.g. 10 to 40 % db) would surely result in extremely low pyrite reductions (Pawlak et al., 1988).

Size consistency also influences the process because of the increase in surface area of the combustible particles. It is well noted that the robust nature of coal agglomeration, specifically related to the strength of the oil and coal bonding mechanisms, results in the process being relatively unaffected by the size and degree of oxidation of the feed stock coal. However, the increase in particle surface area can result in a higher oil requirement to maintain high combustible matter recovery. Hence, although increasing the impurity liberation by extensive grinding allows a high potential for impurity rejection, the additional oil and other reagents required to maintain a high combustible matter recovery can reduce the removal potential because of how these factors affect the process selectivity.

The size consistency and surface characteristics also influence the process in terms of pathways by which impurities may report with the product phase. Listed below are the major pathways by which impurities may report to the product phase:

- non-liberated pyrite and ash,
- natural pyrite and ash flotation,
- oil coated pyrite and ash particles,
- impurity attachment or entrapment within combustible agglomerates, and
- hydraulic entrainment.

Pyrite and ash components may still be attached to the combustible rich particles, and contribution of this pathway will depend upon the size distribution of the impurities within the coal matrix and the level of grinding used to promote the liberation of the impurities. The inherent ash of the coal is a term used to describe the ash component of the combustible matrix and is considered, practically speaking, as impossible to remove from the coal by physical processes. Depending upon the deposition of pyrite this impurity can also be so finely disseminated within the coal matrix that grinding the feed stock for physio-chemical process removal is limited.

Pyrite, unlike most ash minerals, demonstrates natural hydrophobicity. In coal flotation and agglomeration processes, this has been a problem as pyrite can naturally attach to air bubbles, or agglomerate with combustible rich particles. This surface characteristic of pyrite influences the impurity recovery pathways listed above. Pyrite can naturally attach to the air bubbles during flotation to be recovered in the product phase. The size consistency of the impurity within the feed stock coal can influence the natural flotation of pyrite because of the level of grinding required. The angle of bubble attachment is influenced by the size of the particle as very fine particles are not easily attached to large bubbles. The mass density of pyrite influences natural flotation as finer particles of pyrite have lower gravitational and drag forces effecting their rejection into the product stream.

Pyrite and ash particles can become oil coated, entrapped or attached during high shear mixing resulting in their recovery with the product phase. Much of this potential is determined by the chemistry and concentration of the oil and the surface characteristics of the pyrite and ash particles. Oxidized pyrite surfaces demonstrate a lower tendency for natural flotation, oil coating, entrapment or attachment to combustible agglomerates. Several studies have investigated the use of selective chemical depressants, or biological systems for pyrite surface oxidation. However, the process are often crippled by high costs, and complex chemical, biological and mechanical system requirements. Ash particles demonstrate a much lower hydrophobicity, however, some limited data suggests the activation of hydrophobic tendencies are possible. (Mishra and Klimple, 1987; Capes et al., 1981; Nelson, 1989)

The hydraulic entrainment of impurities is dependent upon the process of flotation rather than agglomeration. Ash impurities are most influenced by this pathway, because of their lower density and naturally fine size distribution when clay minerals are present. Furthermore, when feed stock coals demonstrate a significantly high ash content, the probability of hydraulic entrainment of ash impurities is higher. Pyrite particles are typically in lower concentration and significantly higher in density lowering the probability of hydraulic entrainment.

High Shear Turbulence and Intensity

A distinctive characteristic of the agglomeration process is the strength of the attachment forces, permitting the use of extremely high mixing energies to ensure the rapid collision of the particles and oil droplets. The mixing stage is essential to the coal oil agglomeration process as it serves to promote the thermodynamic driving forces, and influences the kinetics of the process (Vanangamudi and Rao, 1984). According to Bensley (1977) the addition of energy is consumed in the functions listed below, of which the initial dispersion of the oil into droplets is the most substantial component of the energy input requirement.

- Emulsification of the oil phase.
- Entrainment of oil by coal particles.
- Distribution of the oil droplets.
- Coalescence of emulsified droplets with coal particles.
- Pendular flocculation of oil coated coal particles.
- Growth of agglomerates from flocculated nuclei.

Others have provided a similar description as intense mixing initially disperses the oil phase and then provide additional energy to promote the contacts between the oil droplets and carbonaceous particles so the pendular bonds are able to form (Liu, 1982). Investigations into the impact of pre-emulsification of the oil phase prior to addition to the high shear mixing vessels have demonstrated a significant reduction in energy input required to complete the contact and agglomeration of carbonaceous material. Furthermore, these investigations indicate that lower oil requirements are experienced to maintain high carbonaceous matter recovery, however, the studies also indicate that oil emulsification has no significant effect on product ash. The increase in recovery of organic matter when using emulsified oil is attributed to better collection of the ultrafine coal particles. This is believed to result from more efficient distribution of the oil throughout the system and the elimination of agglomerates containing disportionately high amounts of oil phase above that required to maintain adequate strength. (Bensley et al., 1977)

High shear mixing promotes the modification of the as the coal slurry undergoes a change, as its appearance reveals a distinct mixture of black agglomerates in a light colored slurry of clay. This is referred to as slurry inversion and is accompanied by a distinct change in mixing torque. (Capes et al., 1981)

High shear mixing characteristics are extremely turbulent, with very high tip speeds in the range of 8 to 30 m/sec, and power consumption in the range of 10 to 40 kW/m^3. Increased energies are experienced when high percent solids and agitator speeds are used (Capes et al., 1981; Mishra and Klimple, 1987; Nelson, 1989). Higher energy levels are required when high density and viscous oils are used. This is substantiated by the work of Bensley et al., (1977) which indicated the rate controlling factors for energy input is the dispersion and distribution of the oil phase into droplets throughout the mixer. When heavier oil were emulsified, inversion times were reduced by a factor of ten. The time and mixing energy and characteristics interact, and in general as the intensity and turbulence of the energy input is increased, the time required decreases.

High Shear Mixing Time

Investigations have suggested an optimum mixing time for each operative mixing energy level, after which additional time does not improve the combustible matter recovery, and may reduce the recovery if excessive times are added. Furthermore, excessive mixing will cause the oil coating of pyrite particles, and even ash particles, intuitively reducing product quality and even recovery. Very little work has been performed on how the energy input levels (eg. kW/m^3) and mixing time interact to influence product quality and recovery. However, their exist some limited data to suggest in terms of ash rejection, that higher mixing intensities and shorter mixing times promote better product quality for the similar carbonaceous recoveries. Work performed describing the impact of these mixing energy variables has not been investigated extensively for pyrite reduction (Mishra and Klimple, 1987). However, studies have hypothesized that although pyrite is hydrophobic in nature, carbonanceous material demonstrates a greater hydrophobic tendency and higher energy level inputs with low oil concentration may cause improved process selectivity for pyrite rejection. Intuitively, added time with lower mixing energies, in weakly turbulent regimes may result in lower selectivity because of the lack of proper dispersion and distribution of the oil phase which would result in less than optimum use of the oil phase. (Drzymala, et al., 1986).

The high energy mixing allows for effective transport of oil droplets to the solids surfaces, and improves the selectivity of the process by maintaining rapid process kinetics and minimizing the exposure time of pyrite and ash surfaces to the oil droplets under high energy conditions. Furthermore, the high energy helps minimize the oil required to ensure adequate surface wetting through maximum dispersion, and transport of oil droplets to the combustible surfaces. Hence, when the mixing time and oil content required are at a process optimum; the process selectivity should improve.

Temperature

The impact of temperature on the process of agglomeration has not been extensively investigated, other than to preheat the oil prior to high shear mixing. The physical impact would be related to higher oil dispersion efficiencies, as a reduction of the viscosity of the oil phase. If complex chemical interactions exist in the process, temperature may alter both the thermodynamics or kinetics of the process. All these factors may influence the process in terms of oil concentration required to maintain high recoveries, which influences the process in terms of pyrite selectivity.

2.3.2.3 Mixing Designs and Configurations

Mixer Design

Various mixing configurations and designs have been utilized in the process of agglomeration, all which focus on the following fundamentals:

- maximum dispersion of the oil phase,
- maximum contact between the combustible solids and oil droplets,
- minimum contact between oil droplets and ash and pyrite rich solids, and
- cost effectiveness.

Impellers can be designed to produce either extremely high shear profiles, or no shear characteristics at all. No shear will develop in the stream leaving an axial-flow impeller. Flow from marine and hydrofoil are design examples, producing uniform velocities from centerline to tip with virtually minimal shear across the entire stream leaving the impeller. (Bowen, 1986)

The radial-flow turbine impellers are different as they produce large shear forces. The rotation of the impeller causes the fluid in front of the impeller in a radial direction, resulting in a discharge flow similar to a pump impeller. The fluid at the tip of the impeller blade has a tangential velocity equal to the peripheral velocity of the turbine. As a result of these tangential- and radial-velocity components a flow stream in the form of jets is produces. However, the development of shear forces within a mixing system depends not only on the high mixing velocities, but also on the existence of large differentials in velocity and direction within a small spatial distance (Bowen, 1986).

The two critical design components for shear sensitive mixing processes are the shear and circulation flow rates (Bowen, 1986). The high shear forces provide enough momentum and turbulence to ensure that adequate emulsification of the oil phase, and particle collisions occur. The shear rate is related to both the magnitude and distribution of velocities over the spatial region of the shear forces. The average shear rate is determined by calculating the difference between the centerline, or maximum velocity, and the point at which the velocity levels off, and dividing this difference by the distance between the two points (Bowen, 1986).

The radial flow produced by the high shear impellers is diverted by the tank walls and baffles to above and below the impeller in a circular manner. This circulating flow is not important in terms of shear, but is important because if a reasonable turn over rate within the mixer is not obtained the mixing time becomes unreasonable. Hence, there is no real advantage of producing extremely high shear rates within sufficient flow within the mixer to ensure the contents are circulated into the zone of high shear. (Bowen, 1986).

In terms of power consumption and generating high shear forces within the mixing region, the shear rate and circulation flow rate are opposing design parameters which must be optimized to achieve the best mixer design. The most critical design components of a high shear mixer to achieve the optimum balance between shear rate and circulating flow rate are as follows:

- rotational speed,
- impeller diameter,
- impeller width,
- tank diameter,
- baffle width, and
- oil injection point and impeller location.

The maximum tangential velocity achieved in mixing is directly related to the speed of rotation, hence, both the shear rate and circulation rate are directly related to the rotational speed. It terms of shear rate, the magnitude of the shear forces developed during mixing are not only related to the maximum velocity, but the shape of the velocity profile. Increasing speed causes a higher velocity, and sharper profile indicating more rapid changes in velocity over the shear force region. Increasing the speed of rotation has a direct effect on the discharge flow rate. Hence, the circulation rate has been found to vary linearly with increases in the speed of rotation. (Bowen, 1986)

The impeller diameter impacts the discharge flow rate, which impacts the circulating flow rate. Bowen (1986) through his investigative work revealed that the circulation rate is exponentially related to the impeller diameter to the third order for the experimental ranges considered. Because of the complex interactions between impeller diameter, tank diameter, and impeller width; the following mathematical expressions were developed to express shear rate and circulating flow.

- D/T ratio,

where D is the impeller diameter, T is the tank diameter, and the

- W/D ratio,

where W is the impeller width.

The impeller diameter causes the development of shear forces within the mixer because the discharge velocity is directly proportional to the impeller tip speed. Large diameter impellers have higher tip speeds which causes high tangential velocities, and very narrow velocity profiles to exist within the mixing regime. Large changes in velocity over small spatial distances is the fundamental source of shear within any mixer, hence, the impeller diameter can cause a significant change in the shear profile of a mixer. However, both the tank diameter, and impeller width, interact with the impeller diameter in terms of both increasing shear rates and causing an increase in circulating flow. Bowen (1986) developed shear rate equations based upon experimental works which indicated "that, for geometrically similar impellers at the same D/T ratio, the average shear rate varies only with speed, and is independent of diameter (but not the D/T ratio). Suggestions that the ratio of maximum/average shear rates increases with increasing impeller diameter per se do not appear to be warranted. If the impeller diameter is doubled (with speed and D/T held constant), not only do the velocities double, but also do the widths of the impeller and the velocity profile; therefore, all of the increases cancel out and the shear rates remain constant. On the other hand, if the tank diameter is held constant and D/T is increased, the shear rate increases as $D^{0.3}$".

The impeller width effects both the shear rate and circulating flow rate. "Velocity measurements made by Cooper and Wolf on six 100 mm disk turbines, with the blade width to diameter ratio (W/D) varying from 0.15 to 0.40, revealed that turbines with W/D ratios of 0.15 to 0.25 have parabolic radial-velocity profiles similar to those already examined, whereas those with ratios of 0.30 to 0.40 have profiles with a blunter shape and higher velocities. In the region of W/D of 0.20, discharge flows varied almost linearly with blade width; above this region, a limiting value of flow was approached. Unfortunately, no data were presented to substantiate these generalizations." (Bowen, 1986)

Bowen (1986) in the same work investigated circulating flow for three W/D ratios: 0.1, 0.2, and 0.4. The flow from the most narrow widths was exactly proportional to the W/D. However, when the W/D was increased up to 0.2 to 0.4, the circulating flow only increase at a rate of 1.74. Cooper and Wolf also observed that above a W/D of 0.25, the rate of increase in flow starts to drop off. If this phenomenon did not occur, a linear relationship could easily be developed describing the discharge flow data. Hence, the discharge flow was observed to be proportional to blade width below a W/D of 0.25. (Bowen, 1986)

The blade width also influences the shear stresses developed because the velocity profile varies. As the impeller width is decreased, the velocity profile becomes more narrow, and the shear rate is increased accordingly.

Bowen (1986) demonstrated that reducing the blade width in half will double the shear rate for the same tank diameter and rotational velocity. The reduction in blade width decreases the circulating flow, therefore, the impeller diameter must be increased to restore a reasonable recirculation, which increases the power. The selection of the appropriate impeller must consider both the required shear rates and recirculation flow rates, with the optimum design likely based upon power consumption. (Bowen, 1986)

In selecting a mixer design, both the shear rate and circulating flow rates must be considered. The important factors in the design are:

- impeller to tank diameter ratio (D/T),
- impeller width to diameter ratio (W/D), and
- baffle configuration.

It has been suggested that a D/T of less than 0.2 is not practical because of the extremely high power consumption required to ensure sufficient circulation. Increasing the D/T increases the shear rate, however, the tank effects limit any direct increase in shear with D/T ratio. Investigative work indicates the optimum ranges to be between 0.3 to 0.5.

The selection of the W/D ratio depends upon the desired shear rate, circulation flow rate, and power consumption. "It is evident that W/D ratios of less than the industry standard of 0.2 will increase shear rates and, at the same time, reduce the power required. Additionally, lower W/D ratios will produce a more economical balance between the rate of shearing and the rate of circulation in the vessel." (Bowen, 1986)

Configurations

Mehrotra et al., (1984) and Mishra and Klimple (1987) both have provided excellent reviews of the various agglomeration circuits investigated. Historically, the most notable variations in the process configurations and mechanical designs were as follows:

- The Trent process, whereby large quantities of oil (e.g. 30 percent by mass) were added to coal and water slurry and mixed for extended periods at low Rpm (e.g. 150 RPM). This process achieved commercial operation in the 1920's, however, it was abandoned because of the high cost of oil. Large agglomerates were formed and separated from the water by screening, and a subsequent process to briquette the product. The material was then sold as domestic fuel.

- In the 1950's, the Convertol process emerged at a commercial level in Germany, and subsequently was pilot studied in the USA. This process utilized phase inversion mills, which dramatically downside the mixer sizes, and oil requirement to the 3 to 15 % db ranges. High speed centrifuges were used to separate the combustible matter from the ash and water phases.

- In the 1960's, the National Research Council of Canada developed their process called spherical agglomeration. The coal was initially contacted with low concentrations of lighter oils in high shear mixing vessels to cause preferentially wetting was achieved, the slurry was delivered to lower shear mixings vessels, where additional oil and energy were added to promote additional growth, and agglomerate compaction. The compaction improved the strength and dewatering characteristics of the agglomerates. The agglomerates were then separated from the water and ash phase by screening.

- In the 1970's, the Shell Pelletizing Separator (SPS) process emerged. Shell developed a novel mixing system called the shell pelletizing separator. The SPS was designed specifically to remove small particles (eg. 5 microns) of soot from gasification wash water. The design involves a long narrow unit which results in very uniform flow through the mixer and excellent contact between the carbonaceous matter and oil phase. The fundamentals of the design are related to plug flow mixing characteristics and the resulting minimization of short circuiting through the mixer. The result was a significant reduction in the oil and energy input requirements. It is this multi-vessel effect in a single unit, and the mechanical contact of soot and oil which was unique. The SPS resulted in very uniform and hard pellet formation and very good ash rejections. Sieve bends were used to separate the final pellets from the water and liberated ash phase.

- The Central Fuel Research Institute (CFRI) process was developed in India and uses colloidal mills to facilitate the initial dispersion and contact of the oil and combustible surfaces. Secondary agglomeration occurs in flotation cells where additional oil and energy are added to promote further growth of the agglomerates, and air is added to facilitate the separation of the carbonaceous matter from the water and ash phases.

- The Broken Hill Proprietary Process utilized a pre-emulsification step prior to oil addition to the coal slurry. The emulsification stage eliminated the need for intensive high shear mixing to cause the contact between the carbonaceous and oil phases because the oil water emulsion dispersed very easily in the mixer.

2.4.0 Flotation

2.4.1 Fundamentals

Flotation is a process which combines of physical and chemical forces to concentrate finely sized minerals. The process relies on the differences on surface properties of the solids and water to cause a separation. Hydrophobic particles are floated to the surface by the attachment of finely dispersed air bubbles and are skimmed from the surface and collected as the product phase. Hydrophilic particles, which prefer the water phase, do not attach to the air bubbles and remain in the water phase to report to the tailings stream. (Liu, 1982)

Coal and oil agglomeration followed by flotation differs from conventional coal air flotation and ultrafine bubble air flotation by several distinct characteristics, the primary factors being related directly to the coal and oil agglomeration process itself.

Thermodynamics

The probability of successful attachment of an air bubble depends on both the thermodynamics and kinetics of the system. The thermodynamics of flotation are similar to those of agglomeration, where the primary driving force is related to the minimization of surface energy. The surface energy minimization causes the attachment of an air bubble to the solid particle surface, which subsequently results in its separation from the remaining slurry phase due to the combined buoyancy of the attached air bubble. Various chemical additions, termed as surface modifiers or collectors can alter or enhance these particle surface characteristics, and will improve the process recovery, or in other cases, the process selectivity. A number of forces may be responsible for the attachment, or the chemical interaction of the surface modifiers to the surface of the combustible surfaces. In this study, the coal and oil agglomeration process is used to increase the hydrophobicity and size of the combustible solids to enhance their response to air flotation. Hence, the predominant forces responsible for the successful flotation of the combustible matter is related to the coal and oil attachment forces, and the resulting hydrophobicity of the oil phase. The oil phase is highly hydrophobic in nature, and results in strong air bubble attachment forces. Surface energy forces are predominant in maximizing the flotation recovery of a desired component, when the following conditions exist: (Liu, 1982; Khoury, 1981; Botsaris and Glazman, 1989; Mishra and Klimple, 1987)

- the surface energy of the solid-water interface is high,
- the surface energy of the solid-air bubble interface is low, and
- the surface energy of the air bubble-water interface is high.

Kinetics

Process kinetics depend upon several factors, and the relative predominance of these factors can change depending upon the operative ranges. The most predominant factors of this process are listed below:

- the process thermodynamics,
- the slurry and air bubble concentration,
- the mixing energy and air input, and
- the particle and air bubble size distribution.

Flotation thermodynamics can impact on the process kinetics particularly if the attachment forces between the particle surface and the air bubbles are low. If the oil concentration is small, the kinetics of flotation can be effected, as the combustible surfaces may not be properly oil coated, or oxidized surfaces may remain exposed. However, for the purposes of this investigation, the process thermodynamics are large as the hydrophobicity of the agglomerated combustible solids high, and a frother is added to further promote the attachment process. In this process, if successful agglomeration has occurred, the thermodynamic driving forces for air bubble attachment would be high because of the hydrophobic nature of the agglomeration. Hence, the thermodynamics are not likely a predominant rate controlling kinetic step in the flotation of agglomerates.

The slurry density of the flotation process is a predominant component contributing to the kinetics of agglomerate flotation. As the percent solids of the slurry is increased, the rate of collisions between the air bubbles and combustible agglomerates also increases. The concentration of the air bubbles also influences the process kinetics, because as the concentration increases, the probability of collisions between the air bubbles and the coal and oil agglomerates increases. In the limiting case, however, the mass flow of the air bubbles may be increased to levels which may decrease the stability of the froth and create undesired turbulence resulting in excessive detachment of coal and oil, hence decreasing the overall rate of successful flotation of combustible.

The flotation kinetics are also strongly influenced by the degree of mixing in the vessel, as this energy provides for the necessary collisions to provide transport of the air bubble to the surface of the combustible agglomerate. Without this mixing energy, the transport, or contact, between the air bubble and combustible solid would rely on the forces of diffusion, and Brownian motion, which would result in slow process kinetics with conventionally designed systems. However, excessive agitation will result in high detachment forces, resulting in either negative, or no improvements in process kinetics.

The surface area and angle of attachment between the combustible surface, and the air bubble are influenced by the size distribution of both the air bubble and feed coal, which in turn influences the strength of attachment. The air bubble size distribution must match the size distribution of the feed coal distribution. Conventionally designed flotation machines have evolved to supply the air addition and shear forces responsible for producing appropriate concentration and size distribution of air bubbles. Chemical additions in the form of frothing agent also influence the bubble size distribution by altering the surface tension of the water phase. As the surface tension is decreased, the bubbles will grow fewer and larger in size. In ultrafine flotation systems, where particles in the 5 micron range are separated by column flotation, specially designed diffusers to control air bubble particle size distributions are used, as well as specially designed counter current plug flow cells to ensure adequate opportunity for contact occurs.

2.4.1.1 Transport Mechanisms

The same basic transport phenomena which exist in the agglomeration stage are operative in the flotation stage:

- Brownian motion,
- gravity,
- inertia impact, and
- diffusion.

Brownian Motion

The phenomena of Brownian motion is expected to be minimal as a result of the relatively turbulent mixing environment which is employed in the flotation stage. Small particles of combustible matter (e.g. 1 micron) may respond to such forces and report to the froth phase by attaching to larger combustible particles or agglomerates bound for the froth phase.

Gravity

Gravity as a transport force cannot be overlooked, although it is not considered to be a predominant transport phenomena. The air bubbles are in a constant migration to the surface or the froth phase, however, detachment of combustible agglomerates would result in the downward migration of the particle towards the tailings phase. Hence, gravity causes the counter current migration between the air bubbles and sinking particles. This will increase the probability of the re-transport of a detached combustible solids with an air bubble by virtue of the opposing directions and increased momentum.

Inertial Impact

Inertial impact is directly related to the mixing energy of the system, and is the predominant force acting in the transport of air bubbles to the agglomerate surfaces.

The turbulent mixing of the flotation machines causes the air bubbles and combustible agglomerates or particles to collide, providing the opportunity for attachment to occur.

Diffusion

Diffusion of the air bubble to an agglomerate surfaces can be rate controlling, depending upon the electrochemical nature of the system. Surface characteristics can influence the force of attraction and repulsion within the system. Forces of attraction between the combustible surfaces and the air bubbles provide the theoretical driving force for the flotation process, however, particles can demonstrate electrical charges in the water solution which can result in forces of repulsion. If these forces are large compared to the attractive forces, the thermodynamics and kinetics of the process will be affected. If the attractive forces are stronger, the kinetics of the process tend to be slower, and provided sufficient time and appropriate mixing is provided, equilibrium recoveries will be observed. Extensive research has been performed investigating the impact zeta potential, or a particles' point of zero charge. These investigations generally indicate that the electrochemical nature of the particles influence both the kinetics and thermodynamics of the process. In processes demonstrating strong attraction forces, the electrochemical nature of the system tends to impact the kinetics, and to a lesser degree the equilibrium recovery of the process. In systems demonstrating weak attractive forces, the attachment may depend upon the point of zero charge for the particle. If such forces of repulsion exist, the process of flotation may be diffusion controlled as the air bubble will be required to diffuse across a boundary layer before achieving successful attachment.

2.4.1.2 Attachment Mechanisms

The flotation process depends upon the same component forces as agglomeration. Figure 2.5 can also be used to help describe the attachment to an air bubble, and the theory of surface energy minimization as it applies to the flotation process. The following attachment forces are expected to be operative in the flotation process, although not all are predominant forces as surface energy minimization is the predominant component:

- minimum surface energy,
- adsorption,
- repulsive forces,
- chemical bonding,
- entrapment, and
- shear forces.

Surface Energy Minimization

Forces of attachment in the flotation process are typically weaker than those demonstrated in the coal and oil agglomeration process. Figure 2.5 b. and c. represent physical descriptions of the typical attachment that a flotation process may demonstrate, indicating weaker attachment forces exist because of the smaller contact angle. The weaker bonds require mixing to be less turbulent to provide for air bubble formation and dispersion, and collision between the air bubbles and agglomerates. The solid surfaces demonstrating a hydrophobic nature will preferentially attach to the air bubbles and leave the water phase and report to the surface as a froth phase. Strong hydrophobic forces may or may not exist, as some systems rely on the resolution of the intramolecular and intermolecular attractions, and the point of particle zero charge to promote attachment, sometimes resulting in fairly weak attachment forces. Such systems demonstrate slower flotation kinetics, require relatively quiet flotation machines where turbulence is minimized.

Solids possessing strong hydrophobic surfaces, do not require any surface modification, or enhancement of the hydrophobic nature. However, most flotation systems require chemical additions to enhance the hydrophobicity, which often rely on selective adsorption forces between chemical additions referred to as collectors and modifiers to alter the solid surfaces. These chemical additions may be specifically designed with polar and non-polar end molecules, or may simply act as a electrochemical neutralizer, thereby reducing the surface to a point of zero charge making the transport of an air bubble to the particles' surface more probable.

Adsorption and Repulsion Forces

Adsorption and repulsion forces may both exist within flotation systems. Surface collectors are used to alter or enhance the particles' hydrophobic nature. The collector tends to attach preferentially to the desired particles surface, either by adsorption forces or by surface energy minimization. The actual mechanisms will vary for each system, however, the presence of some form of adsorption forces are highly likely. The opposite end of the collector is very hydrophobic and results in the tail end of the collector attaching itself to the air bubble and causing the formation of the froth phase.

The electrochemical nature of the solids may cause forces of repulsion to exist within the system. If the charge of the particle is highly negative, the electrochemical charge inhibits air bubbles, or collectors from approaching close enough to the particle for the adsorption forces, or surface energy minimization to prevail. Hence, the chemistry of the system sometimes requires change involving the use of pH or ionic strength alteration to reduce the electrochemical charge of the particles to zero state. At the zero charge, collector molecules or air bubbles can approach relatively freely, allowing easier attachment.

Chemical Bonding

The possibility of chemical bonding occurring between the air bubble and the hydrophobic particle surface is very unlikely. The most likely potential for any chemical bonding to occur is between the collector, or in this process the agglomerant and solid surface. In conventional flotation processes, chemical bonding is extremely limited, and at best, chemical-adsorption forces may be present between the desired particles and the collector molecules.

Entrapment

The potential for particle entrapment during the flotation process is a recognized possibility. Studies investigating the use of froth washing and column flotation operate on the premise that if froth drainage is maintained at the maximum, without reducing recovery, an optimum tradeoff between quality and quantity of the product can be obtained. In the coal and oil agglomeration process, pendular bonds between the particles exist, generating a loose floc like structure. These type of structures increase the potential of entrapment of particles which are not typically oil wetted.

Shear Forces

Shear forces play a similar role in the process of flotation as in coal and oil agglomeration. The mixing energy of flotation supplies the energy necessary to perform the following functions:

- formation and dispersion of the air bubbles,
- maintain all particles in suspension, and
- provide the necessary energy required to facilitate collisions.

Excessive energy increases shear forces within a flotation cell and would result in the detachment of an air bubble from the desired particles. Conventional flotation machines have evolved to provide adequate dispersion and mixing without generating excessive shearing forces. However, work performed in the area of ultrafine bubble flotation for recovery of super clean coals have required alternative flotation machine designs which provide finely dispersed bubbles, and enhanced bubble and particle contact with minimal shearing zones.

2.4.2 Process Variations

Process variations influencing flotation can be defined as feed variations, chemical and physical parameters, and machine components.

2.4.2.1 Feed Variations

Coal Rank

The degree of hydrophobicity of coal is thought to vary with coal rank. Lignite and subbituminous coal tend to be less hydrophobic, and do not respond as well to the flotation process and usually require enhancement with surface modifiers. Bituminous coals respond best to the flotation process, as they demonstrate the strongest hydrophobic behaviour. Anthracite coals do not respond as well to the flotation process, being the highest in carbon content. Although no definite explanation for how coal rank influences these trends concerning hydrophobicity have been developed, some hypothesis have be proposed related to the carbon to hydrogen ratio of the coal, the complexity and variation of organic functional groups present (eg. usually oxygen), the concentration and type of mineral impurities present, and the more inert nature of the higher rank coals are some explanations which have been presented. Because the chemical and physical composition of coal varies so extensively, it is apparent many factors could influence the relative hydrophobicity of a specific coal.

Feed stock Variations

If the feed stock demonstrates large variations in surface characteristics, the optimization of the flotation process can be greatly effected. For this reason, most operating circuits are developing circuits with adequate equalization or blending of the feed stock, and advanced monitoring before processing to enable adjustments to be implemented to the circuit prior to the arrival of variations into the processing circuit. Any variation in surface characteristics, size, impurity type and concentration will influence the process and alter performance either in terms of recovery or selectivity.

The type and concentration of mineral impurities present in the coal can also influence the operation of the flotation process. High clay contents have be known to interfere with both the transport and attachment of air bubbles and may even compete for the collector additions. Some impurities may also alter the chemistry of the flotation water, which may impact the electrokinetic behavior of the flotation process. Pyrite for example has been identified to produce various complexes in some flotation process which results in the depression of the carbonaceous material.

The size distribution of the feed stock to the flotation circuit is defined for conventional systems to be best between about 100 to 500 μm. Particles larger in size tend to detach because of strong forces associated with drag and gravity. Transport and subsequent attachment of smaller particles are also difficult. Transport is thought be inhibited because the particles tend to follow the fluid hydraulic patterns, as they have insufficient momentum to maximize the potential of mixing eddies. Hence, the probability of collisions is somewhat reduce for smaller particles, unless the collision or mixing system is adjusted. Furthermore, the smaller surface area limits the strength of attachment because the air bubbles tend to be too large for strong attachment to be achieved. Hence, attachment to the smaller particles is believed to be followed by a higher probability of detachment because of the reduced surface area associated. Investigative work into ultrafine bubble flotation has indicated by decreasing the bubble size can result in enhanced recovery of fines fraction, provided high frequency of collisions can be promoted, and quiet mixing conditions can be maintained. Work in the area of column flotation has indicated some promising results.

The distribution of the impurity in the coal matrix also influences the process indirectly because finer grinding of the feed stock is required for impurities which are disseminated within the matrix. The disseminated impurity will limit the performance of conventional flotation systems because the bubble size distribution typically produced is too large to permit effective attachment of particles. However, utilizing coal and oil agglomeration prior to conventional flotation circuits help overcome this limitation as the smaller carbonaceous particles can be combined to cause the formation of larger particles.

Oxidation

Oxidation has impact on the chemical and physical characteristics of coal, altering the: calorific value, combustion properties, site storage facility design, coal cleaning properties, and the carbonization, gasification, and liquefaction properties.

Coal oxidation has been divided into three stages. The first stage involves the superficial oxidation of the coal surface by the development of coal-oxygen complexes with acid characteristics. The second stage involves the transformation of the organic components of coal into hydroxyl carboxylic or humic acids. In stage three, the humic acids become water soluble acids. (Taylor, et al., 1981)

Oxidation of the coal surfaces appear to reduce the flotation performance by effecting both the thermodynamic driving force of the process, and effecting the kinetics of the transport and attachment steps of the process. Once oxidized, the coal surface may contain function groups which do not demonstrate hydrophobic behavior, tending to be more hydrophilic in nature. This strongly influences the potential recovery of carbonaceous material as the thermodynamic driving force for the attachment of an air bubble relies on the hydrophobic behavior of the coal surface. The addition of collectors can be used to enhance the hydrophobicity of the oxidized surface, however, the negative electrokinetic behavior of the particles has increased as a results of the oxidation. Therefore, the zeta potential of the oxidized particles, which in this case tend to behave as forces of repulsion, will inhibit collisions more strongly once the coal surface has been oxidized. This can effect both the thermodynamics and kinetics of the process. Even if a net positive thermodynamic driving force exists, the probability of successful transport and attachment of an air bubble and carbonaceous particle is reduced because of the stronger forces of repulsion produced by the more negatively charged particles (Davidson, 1990). The process of coal and oil agglomeration demonstrates extremely strong interparticle attractions between the oil phase and coal particles, hence, it provides a process to enhance the hydrophobic nature of the oxidized coal relatively easily, and overcome any possible hydrophobic surface characteristics which may exist.

2.4.2.2 Chemical Parameters

- **Collectors**

To facilitate a successful flotation system, the particles requiring separation must be sufficiently hydrophobic in nature. Surfactants, known as collectors, are added to most flotation systems to improve the hydropobic nature of the desired particles. Collectors are organic molecules which adsorb to the surface of selected particles rendering it water repellent by attaching itself to the surface and displacing the hydrated water layer allowing for the attachment of air bubbles. The head of the collector molecule tends to attach to the surface of the solid, and the tail attaching to the air bubble. The action of the collector is to shear the surrounding water layer from the solid surface because of the stronger attachment forces of the collector. The collector tail demonstrates strong attraction for the air bubbles within the system resulting in the formation of a froth phase consisting of the desired particles. (Wills, 1984)

Collectors have been classified as either non-ionizing or ionizing. Non-ionizing collectors are virtually insoluble and render the desired particle hydrophobic by coating the surface with a very thin film. Non polar light and heavy oils are examples of non-ionizing collectors and are typical in coal flotation and agglomeration processes. (Wills, 1984)

Ionizing collectors are used extensively in the hard rock mineral processing industry to clean selected minerals from the host rock components. Ionizing collectors are heteropolar, consisting of both a non polar and polar end of the molecule. The non polar end of the molecule is water repellent or hydrophobic, while the polar end of the molecule tends to react with the water layer surrounding the desired particle, and may be selectively attracted by specific mineral surfaces. Figure 2.8 provides a description of a classification system. These collectors are first classified as anionic or cationic, depending upon nature of the polar end of the collector. The polar end of the collector is responsible for attaching to the desired particle surfaces, rendering the particle hydrophobic because the non polar end of the collector is hence oriented toward the water phase. The attachment mechanisms can be chemical, electrical, or physical in nature, depending upon the specifics of the system. The collector addition levels are low in general, relying on the development of a monolayer of collector on the surface of the desired particle surface. Increasing the collector dosage levels above this level is costly, can reduce selectivity, and in some cases reduce the overall recovery because of reactions or attractions between collector molecules thereby altering the surface of the mineral particle. (Wills, 1984)

- **Frother**

The addition of frother promotes the stability of a bubble system to provide the transport of the desired particles to the surface where they can be removed to the product phase. The frother molecule is similar to ionizing collectors, being primarily heteropolar, consisting of non polar and polar ends. The frother tends to alter the surface tension of the system, as the polar end interacts with the water phase, and the non polar end tends to be hydrophobic tending to interact with the air phase. In this manner, the addition of frother allows for the alteration of the surface tension of the system, and permits the control of the bubble system the size distribution, concentration, and stability. (Wills, 1984) Observations in both the laboratory and plant have indicated that the addition of frother increases the possibility of particle-bubble contact, and second, the efficiency of attachment. (Mishra and Klimpel, 1987)

Fundamentally, the frother acts in the liquid phase only, and does not have a direct impact on the mineral surface. However, in practical terms some form of interaction between the frother and other reagents does occur. (Wills, 1984). In general, however, there are several guidelines which are used to define the best frother. (Mishra and Klimple, 1987)

- The bubble must be sufficient in stability to allow for product recovery, yet provide for proper drainage to enhance the removal of entrapped impurities.
- The product phase must break down with relative ease, as very persistent froths will result in difficult handling problems.
- The frother must be fairly resilient to changes in feed stock solids, and the water chemistry and temperature.
- Frothers must be easy to disperse in the medium.
- The reagent must be relatively cheap, abundant, and safe to use.

2.4.2.3 Physical Components

- **Slurry Concentration**

Slurry concentration effects combustible matter recovery, process selectivity, and depending upon the system, can be interactive with other variables including chemical additions, and energy and air input. In general terms, a high slurry concentration increases the probability of collisions between the air bubbles and the combustible agglomerates thereby increasing the kinetics of flotation. However, improved flotation kinetics is usually accompanied by a loss in process selectivity as the probability of contact between an air bubble and a particle rich in impurities is also increased. Furthermore, the probability of impurity entrainment with the product phase via insufficient drainage time, or a higher density froth phase is also higher (Weiss, 1985; Singhal et al., 1983). Most commercial applications of flotation attempt to operate with the highest slurry concentration possible as this factor directly impacts the size of flotation equipment required, and the magnitude of wastewater streams required by the process.

High slurry concentrations can also reduce the efficiency of the process by causing poor dispersion of the flotation collectors and air bubbles. This can result in over feeding chemicals, or providing insufficient mixing energy or air input. Utilizing agglomeration followed by flotation, high solids concentration and flotation energy input may result in further agglomeration during the flotation stage. Larger agglomerates may serve to entrap or entrain particles rich in impurities which may otherwise have reported to the tailings phase. Singhal et al. (1983) indicated in their studies of slurry concentration, that the impact of solids concentration may vary with collector and frother dosages, suggesting interactions may exist.

- **Energy input**

Energy input during the flotation stage serves three purposes: to generate air bubbles sufficient in volume and size to recover the desired component, to provide for intimate contact between the air bubbles and particles, and to provide sufficient mixing energy to maintain the particles in suspension.

Mechanically induced air systems require some form of mixing energy to control the volume of air and size of air bubbles, although the air bubble size may also be controlled by the addition of frother, or the volume by an air blower. Convention flotation machines have specially designed venturi impellers for air generation and as the rotational speed of the impeller is increased, the volumetric input of air into the cell is also increased. The impeller design is such that it shears the incoming air into uniformly sized air bubbles, and at the same time the flotation slurry is drawn into the impeller via a similar venturi and released simultaneously into the rotating impeller blades. This action provides for excellent contact between the solids and air bubbles.

Hence, the level of mixing required is directly related to the slurry concentration. The mixing level must be high enough to ensure adequate volumes of air are generated, yet low enough to ensure that over mixing of the slurry does not occur. At lower slurry concentrations, high enough mixing must be used to ensure contact between the solids and air bubbles occur.

The impeller design and location are such to minimize the disturbance on the surface of the cell, yet maintain adequate mixing of the slurry to discourage segregation of solids within the cell. Most impellers are located deep within the cell where the maximum contact time between the solids and air bubbles can be obtained, and the minimum impact of hydraulic dead zones in the cell can be obtained. Most impeller designs contain a shroud over the impeller to ensure the surface of the cell is not excessively disturbed. The location of the impeller also serves to maintain a quite surface.

High energy input can reduce process selectivity by several possible mechanisms. High mixing energy will result in larger volumes of air input, thereby increasing the probability of recovering particles of impurities to the surface to be added into the product phase. The added energy may provide for further agglomeration of impurities, or may oil coat pyrite or ash surfaces by attrition of any extra oil which may exist on the combustible agglomerate surfaces. The newly coated or agglomerated impurities will report directly to the product phase. High energy input causes an increase in turbulence within the cell, which may result in the easier entrainment of the solids into the product phase.

The flotation energy input also provided mixing to ensure contact occurs between the desired combustible agglomerates and the air bubbles to allow of the attachment and the subsequent journey upward to the product phase. However, the mixing energy can also provide for collisions between the air bubbles and impurities. Hence, the solids concentration, mixing energy, and frother concentration may all be somewhat related in terms of recovery and process selectivity.

- **Particle size and distribution**

The optimum particle size depends upon the density and type of flotation machine used as this often determines the air bubble size generated. The flotation of coarse particles is limited because of turbulence effects of the mixing system tend tear apart the solid/bubble attachment points with less resistance (Weiss, 1985). Particles about 500 microns in size begin to demonstrate limitations in flotation. Particles of this size are often too large and are subject to the velocity gradients and easily detach, or do not stay properly suspended in the flotation cell and report to dead portions of the cell (Weiss, 1985; Olson, 1985).

Small sized particles also demonstrate reduced flotation performance, however, the reason are less obvious. Below about 50 microns, reduced rates of recovery are often observed. Predictions suggest that the smaller particles have less surface area available to provide for a strong attachment point between the air bubble and solid. Other predictions indicate collisions between air bubble and solid particles are limited because the particles lack sufficient inertia to cause a high frequency of collisions. The fine solid particles tend to follow the hydraulic pattern of the mixer, thereby reducing the potential for air bubble and particle collisions (Weiss, 1985; Olson, 1985).

The particle size distribution of the feed stock coal can also influence flotation performance. If the feed coal particle size distribution is too wide, demonstrating large fractions of both fine and coarse particles, the average bubble size cannot be properly selected to optimize the process performance. Hence, a narrow enough feed coal size distribution is desirable so as to match the distribution or air bubble sizes.

The use of coal and oil agglomeration reduces the problems associated with feed coal particle size and distribution as the process of agglomeration produces a very uniform and consistence feed stock in terms of agglomerate size and distribution. Hence, the flotation rate and equilibrium recovery is improved dramatically when the feed stock coal is agglomerated prior to flotation, especially when the original feed stock contains an excessive fraction of fine materials.

- **Temperature**

Comparatively little work has been performed on the effect temperature has on flotation performance. Physical impacts related to changes in temperature might be changes slurry rheology and viscosity, changes in the solubility levels and the evaporation rates for the frother and collector, and changes related to the surface tension of the solution.

Changes in viscosity may effect the efficiency of collisions, and may promote further exchange of chemical reagents, or agglomeration during the flotation process.

Changes in collector or frother solubility, or increases in the rate of evaporation across the open flotation cell, may have dramatic impact on flotation performance. If at higher temperatures for example, frother concentrations are effectively reduced by evaporation, recoveries could be reduced dramatically.

The chemistry of the flotation system may also change with temperature. An increase in temperature decreases the surface tension of the liquid. A decrease in the liquid surface tension improves the likelihood of successful flotation as this promotes the easier formation of air bubbles. However, lowering the surface tension excessively will result in the formation of extremely large bubbles which may reduce the opportunity for proper collisions and attachments to occur. Furthermore, if the surface tension of the solution is extremely low, surface energy minimization may promote single air bubbles remain in the water phase (Alberty and Daniels, 1983).

Temperature may also influence the adsorption forces of collectors or binders within the system. However, most adsorption forces which exist in either agglomeration or flotation systems are physical in nature, and if chemical adsorption forces exist, they are weak in nature. Hence, the overall impact of temperature has on the adsorption forces can be expected to be minimal for small changes in temperature. (Alberty and Daniels, 1983; Weber, 1972)

2.4.2.4 Equipment Components

The design of flotation machines has evolved over the past 50 years based upon plant experience and research and development. Radical changes in design, however, are rare based upon the risk associated in pilot testing new ideas at larger enough scales to prove the design as a commercial success. Hence, the designs tend to be more traditional, relying on older proven technologies. The most dramatic design change which has occurred in the past 20 years and operates with commercial success is cells which have been increased in size. The cost effectiveness of the economy of scale has resulted in cells becoming 15 to 30 times larger in size in the past 20 years. (Weiss, 1985; Mishra and Klimple, 1987).

Flotation machines can be categorized into four main groups:

- mechanical,
- pneumatic,
- froth separator, and
- column flotation cells.

Mechanical flotation machines are most common and they can be either self aerating or supercharged. Self aerating flotation machine operate on the principal that the rotation of the impeller also acts as a venturi drawing air into the cell. Supercharged cells are also mechanical cells which also contain an air blower to supplement the air flow of the mechanical system. The self aerating cells are most common. (Mishra and Klimple, 1987).

Pneumatic cells utilize an air blower system, or dissolved air flotation systems to provide both the air bubbles and sufficient agitation to ensure contact between the particles and air bubble. These cells are less common in commercial applications. (Mishra and Klimple, 1987)

The froth separator has had no application in North America, however, it has found some acceptance in the Soviet Union. It is also mechanical in nature, however, the feed is delivered at the top of the cell rather from the side or bottom as in most common cells. (Mishra and Klimple, 1987).

Column flotation is the most recent advance and is beginning to gain some commercial interest. The column cell is based upon the counter-current plug flow of air bubbles and feed and appears to offer promise of both high recoveries and product qualities. The counter-current directional patterns provide for deeper layers of froth formation where sprinkling and high drainage can be used to improve quality. The plug flow pattern provides a uniform time distribution for particles, allowing for better optimization of operating variables. The counter current design ensures for a high frequency for air bubble and particle collision for difficult to float particles.

A flotation machine must provide for several essential components to ensure proper flotation performance.

- Adequate mixing of feed slurry

The flotation machine must provide enough mixing to maintain the feed coal in suspension, particularly to avoid the segregation of particles based upon size or density. Otherwise, short circuiting or settling of coarse or heavier particles would occur in dead zones of the cell. (Mishra and Klimple, 1987)

- Minimal turbulence in froth zone

Despite the requirement of adequate mixing to ensure the slurry is well mixed, the froth zone of the cell must have minimal turbulence. Hence, near the surface of the froth, or the transition zone, where a rising air bubble enters the froth zone of the cell, quiescent or smooth conditions must exist to ensure air bubbles are detached from the particle. Excessive mixing will cause the froth zone to disrupt, resulting in bubble breakage and detachment. Therefore, mixing must be controlled to a proper balance to ensure good mixing in the slurry phase, yet quiet conditions at the surface of the froth zone. Very often , impeller baffles are employed to promote these type of mixing conditions. (Mishra and Klimple, 1987)

- Air bubble generation and even dispersion

The flotation machine must provide an adequate volume of air and disperse the air throughout the cell volume, and to some degree control the size distribution of the bubbles. Experience has indicated the dispersion of the air bubbles throughout the cell is extremely important, especially when cells are very large and insufficient dispersion will result in dead zones or an effective loss in flotation capacity. (Mishra and Klimple, 1987)

- Efficient froth removal

A froth removal device is an important component of any effective flotation machine. The froth removal system must ensure rapid removal of the froth zone from the cell, allowing for sufficient time for the froth to properly drain, yet ensure dead zones in the zone do not exist resulting in detachment back to the slurry zone. Often froth sprinkling or washing is employed to enhance the drainage of any attached impurities (Miller, 1969; Weiss, 1985). Modern approaches are to provide for a plug flow approach to the removal from the froth zone, whereby each particle of the froth phase has the same or similar time in the zone. This provides for better optimization of the flotation process because of the increased consistency in time within the froth zone. (Mishra and Klimple, 1987)

3.0 Design Specifications

The coal and oil agglomeration process involves four main stages (see Figure 1.1). The first stage involved grinding the feed coal, which served to liberate the pyrite and ash rich material from the combustible rich material of the coal matrix. A dry grinding hammer mill system was used in this investigation, and was performed off site of the pilot plant. In the second stage, dry coal was fed to the conditioning vessel where water and energy were added to promote wetting of the surfaces. After water wetting, the coal slurry was fed to the high shear stage, where oil and mixing energy were added to promote the agglomeration of the combustible solids. Separation was the final stage, and involved primary froth flotation cells and the pyrite separator. Figure 3.1 describes the bench scale primary flotation cell and its specially designed conical bottom to minimize solids accumulations during testing. Figure 3.2 describes the bench scale pyrite separator which was invented in this study; and tested as a unit process to enhance rejection of ash and pyrite rich solids.

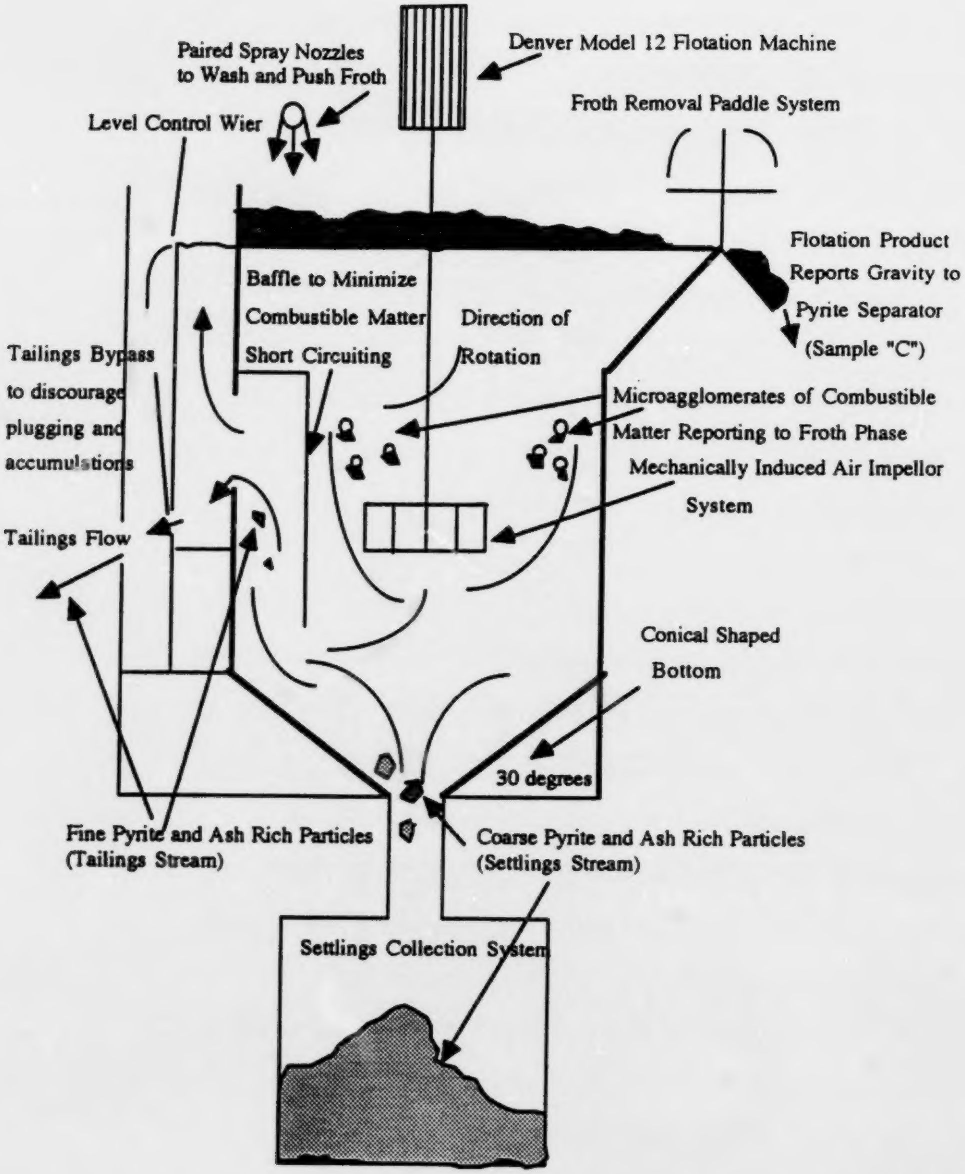
Paired Spray Nozzles to Wash and Push Froth
Denver Model 12 Flotation Machine
Level Control Wier
Froth Removal Paddle System
Flotation Product Reports Gravity to Pyrite Separator (Sample "C")
Baffle to Minimize Combustible Matter Short Circuiting
Direction of Rotation
Tailings Bypass to discourage plugging and accumulations
Microagglomerates of Combustible Matter Reporting to Froth Phase
Mechanically Induced Air Impellor System
Tailings Flow
Conical Shaped Bottom
30 degrees
Fine Pyrite and Ash Rich Particles (Tailings Stream)
Coarse Pyrite and Ash Rich Particles (Settlings Stream)
Settlings Collection System

Figure 3.1 Bench Scale Primary Flotation Cell No. 1

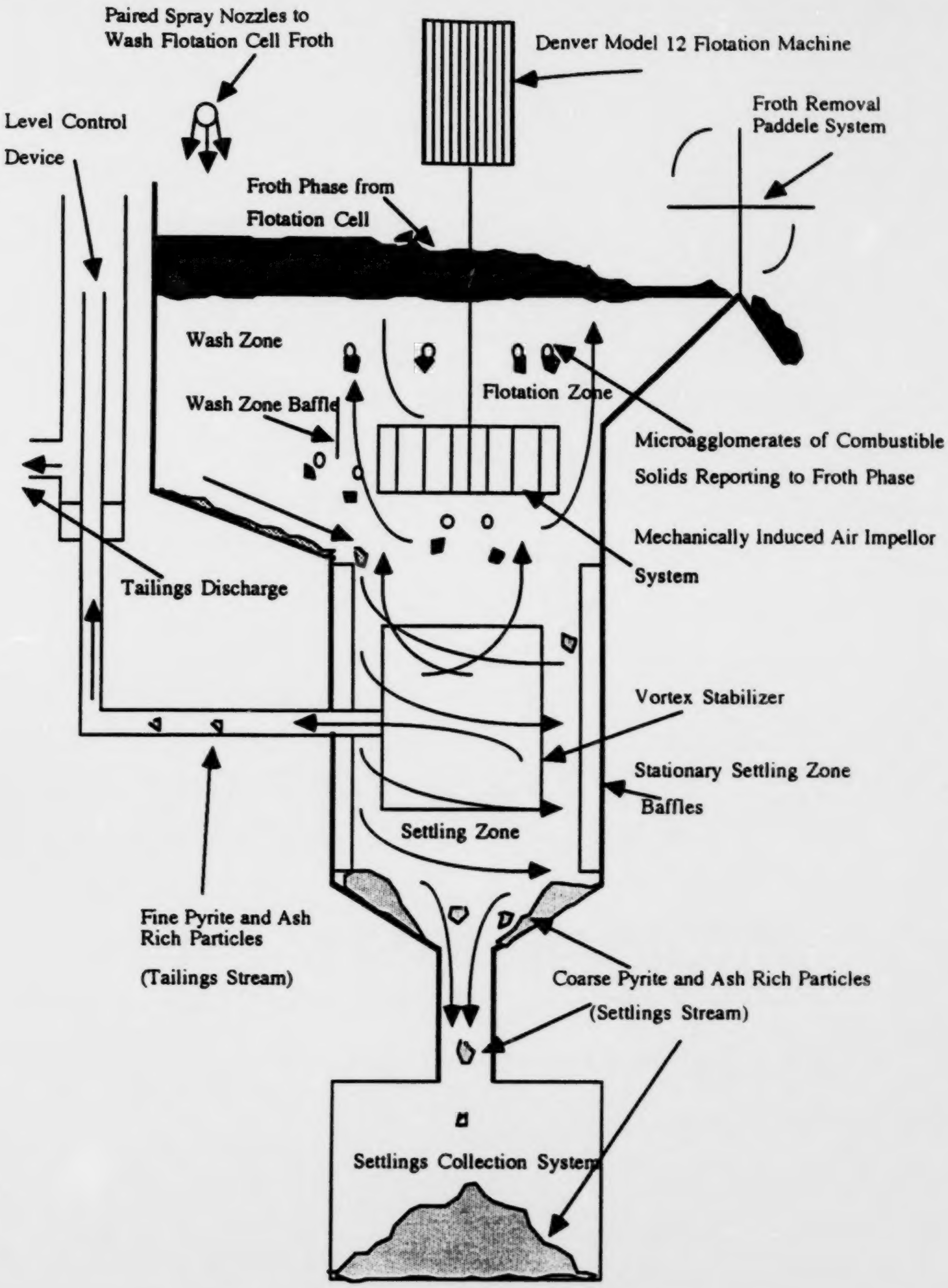
Paired Spray Nozzles to Wash Flotation Cell Froth
Denver Model 12 Flotation Machine
Level Control Device
Froth Removal Paddele System
Froth Phase from Flotation Cell
Wash Zone
Wash Zone Baffle
Flotation Zone
Microagglomerates of Combustible Solids Reporting to Froth Phase
Mechanically Induced Air Impellor System
Tailings Discharge
Vortex Stabilizer
Stationary Settling Zone Baffles
Settling Zone
Fine Pyrite and Ash Rich Particles
(Tailings Stream)
Coarse Pyrite and Ash Rich Particles
(Settlings Stream)
Settlings Collection System

Figure 3.2 **Bench Scale Pyrite Separator**

3.1 Flow Schemes

During the experimental program, two flow schemes were investigated. Phases 1 and 2 of the experimental program utilized flow scheme 1 (see Figure 3.3). The results from these tests were used to develop the experimental method and apparatus, from which flow scheme 2 (see Figure 3.4) emerged and the Phase 3 experimental program was performed. Flow schemes 1 and 2 vary in the added primary flotation capacity, the additional high shear mixing capacity, the specially designed primary flotation cell which possesses a conical shaped bottom for pyrite and ash rejection, and the settling vessels which served to remove the accumulating solids from the processing stream.

3.1.1 Flow scheme 1

Flow scheme 1 is described in Figure 3.3. The coal was fed dry with an auger system into a 1 L conditioning vessel where both water and energy are added to prepare the coal slurry. The coal slurry gravity fed into the high shear mixers where oil and energy was added to promote the agglomeration of the combustible solids. After agglomeration, the modified coal slurry reported to the separation phase, consisting of a single primary flotation cell and the pyrite separator. No settlings vessels existed on either the flotation cell or the pyrite separator, and the heavier particles were allowed to accumulate within these vessels during testing.

3.1.2 Flow scheme 2

Flow scheme 2 is described in Figure 3.4. The dry coal fed into a 2 L conditioning vessel, where water and energy are also added. The slurry reported by gravity into two high shear mixers, where oil and energy are added. The modified slurry reported by gravity into the separation stage, which consists of two flotation cells and the pyrite separator. The primary flotation cell and the pyrite separator were both equipped with conical bottoms and settling vessels, permitting the removal of the heavier particles from the processing stream.

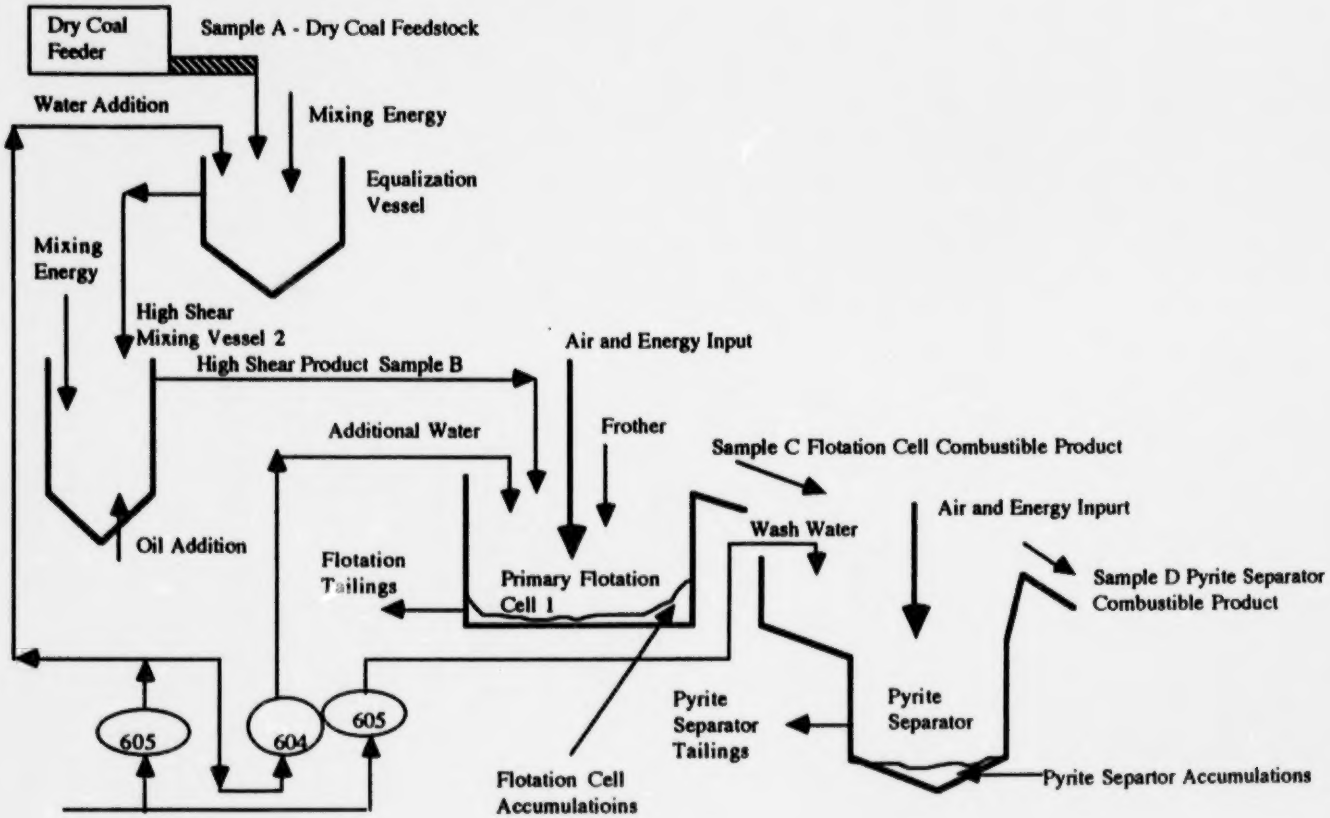
Dry Coal Feeder
Sample A - Dry Coal Feedstock
Water Addition
Mixing Energy
Equalization Vessel
Mixing Energy
High Shear Mixing Vessel 2
High Shear Product Sample B
Air and Energy Input
Additional Water
Frother
Sample C Flotation Cell Combustible Product
Air and Energy Inpurt
Wash Water
Oil Addition
Flotation Tailings
Primary Flotation Cell 1
Sample D Pyrite Separator Combustible Product
605
604
605
Pyrite Separator Tailings
Pyrite Separator
Flotation Cell Accumulatioins
Pyrite Separtor Accumulations

Figure 3.3 Bench Scale (5 kg/hr) Continuous Coal and Oil Agglomeration and Flotation Pilot Plant for Ash and Pyrite Removal - Flow Scheme 1

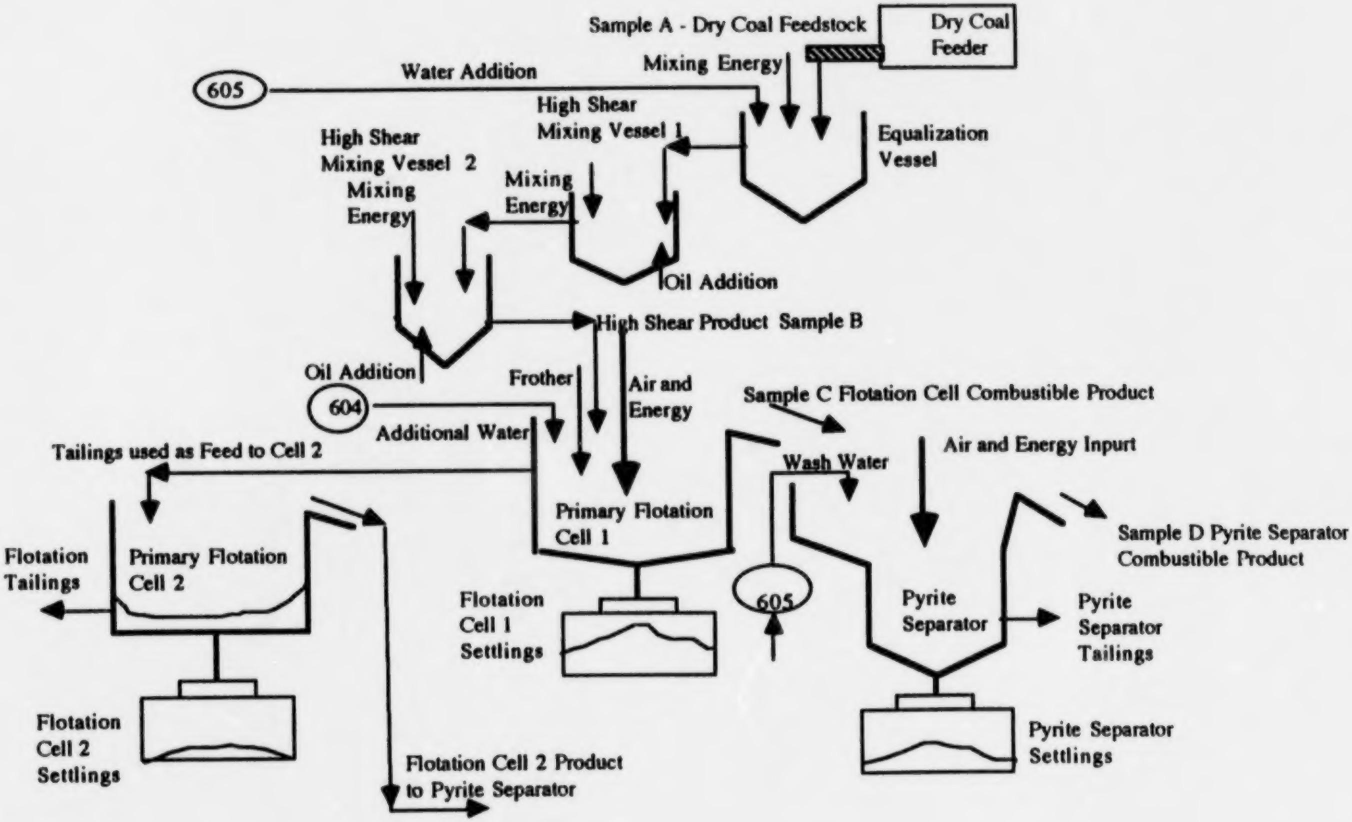
Sample A - Dry Coal Feedstock
Dry Coal Feeder
Mixing Energy
Water Addition
605
Equalization Vessel
High Shear Mixing Vessel 1
High Shear Mixing Vessel 2
Mixing Energy
Mixing Energy
Oil Addition
High Shear Product Sample B
Oil Addition
604
Frother
Air and Energy
Additional Water
Sample C Flotation Cell Combustible Product
Air and Energy Inpurt
Wash Water
Tailings used as Feed to Cell 2
Primary Flotation Cell 1
Sample D Pyrite Separator Combustible Product
Flotation Tailings
Primary Flotation Cell 2
Flotation Cell 1 Settlings
605
Pyrite Separator
Pyrite Separator Tailings
Flotation Cell 2 Settlings
Pyrite Separator Settlings
Flotation Cell 2 Product to Pyrite Separator

Figure 3.4 Bench Scale (5 kg/hr) Continuous Coal and Oil Agglomeration and Flotation Pilot Plant for Ash and Pyrite Removal - Flow Scheme 2

3.1.3 Operating Test Conditions

Table 3.1 Summary of Operating Test Conditions

Operation/Process	Range	Comments
Coal feed rate (kg/hr)	2.5 to 7.5	Held constant @ 4.63 kg/hr
Equalization		
-Time (min.)	8.0	Held constant
-RPM	1200 & 1500	Held constant
-% Solids	28	Held constant
High shear mixing		
-Time (min.)	3.7 to 9.4	Varied with test program
-RPM	1600 to 2000	Varied with test program
-% solids	28	Held constant
-Energy Input (J/L)	10.4 to 15.6	Varied with test program
Flotation cells		
-Time (min.)	8.0	Held constant
-RPM	1100	Held constant
-% solids	15.5	Held constant
-Air input (L/min.)	4.5	Held constant
-Volume (mL)	5560	Held constant
Pyrite separator		
-Time (min.)	4.4	Held constant
-RPM	1100	Held constant
-% Solids	5.7	Held constant
-Air input (L/min.)	5.4	Held constant
-Wash water (mL/min.)	600	Held constant
-Volume (mL)	4650	Held constant
Oil concentration (% daf)	.93 to 2.08	Varied with test program
Frother conc. (% daf)	.012 to .038	Varied with test program
Temperature (°C)	20 to 40	Varied with test program
Particle size (d_{50} in μm)	90 to 200	Varied with test program
Sample age (days)	1 to 45	Varied with test program
% Solids in froth phase (%)	7 to 25	Varied with test program

3.2 Coal Grinding and Feeding Systems

3.2.1 Coal Grinding

The grinding apparatus consisted of the Mikro-Pulverizer (Model #1 SH), which is manufactured by Pulverizing Machinery, a division of MikroPul Corporation. The cast iron and steel unit is designed specifically for the grinding of coal, and is a totally enclosed fan cooled system. The system employs a screw feeder, 44 mm in diameter. The grinding chamber is fabricated from hardened steel, and the hammers themselves are hardened by a proprietary hardening process. The rotational speed can be varied from 3450 to 9600 RPM (Pulverizing Machinery, 1989).

"The pulverizer consists essentially of a rotor assembly, fitted with hammers and operated generally at high rotor speeds. The grinding action is one of impact between the rapidly moving hammers and the particles. The inertial energy of the moving hammers transfers to the particle being ground, thus causing the particle size reduction. Basically, there are three methods which will control the fineness of ground product produced" (Pulverizing Machinery, 1989). The retaining screens inserted at the discharge of the grinding chamber is the primary source of size control. Rotor speed is the second method of controlling the particle size. The hammer selection can also impact the particle size and distribution. Two types of hammers are available, stirrup and bar type. Stirrup type hammers produce a finer size due to the slicing action of their shape, and the bar type hammers are used where coarse sizes, and narrower distributions are required. (Pulverizing Machinery, 1989)

3.2.2 Coal Feeding

The coal feed was purchased from Accurate Inc., (Model 302) and is equipped with a 19 mm stainless steel auger (SS 304), and a unique vinyl flexible hopper which is massaged with two external paddles, chain driven by the drive motor to provide for gentle vibration free agitation of the feed coal ensuring uniform mass flow. Figure 3.5 summarizes the operational performance in terms of mass flow and percent relative error

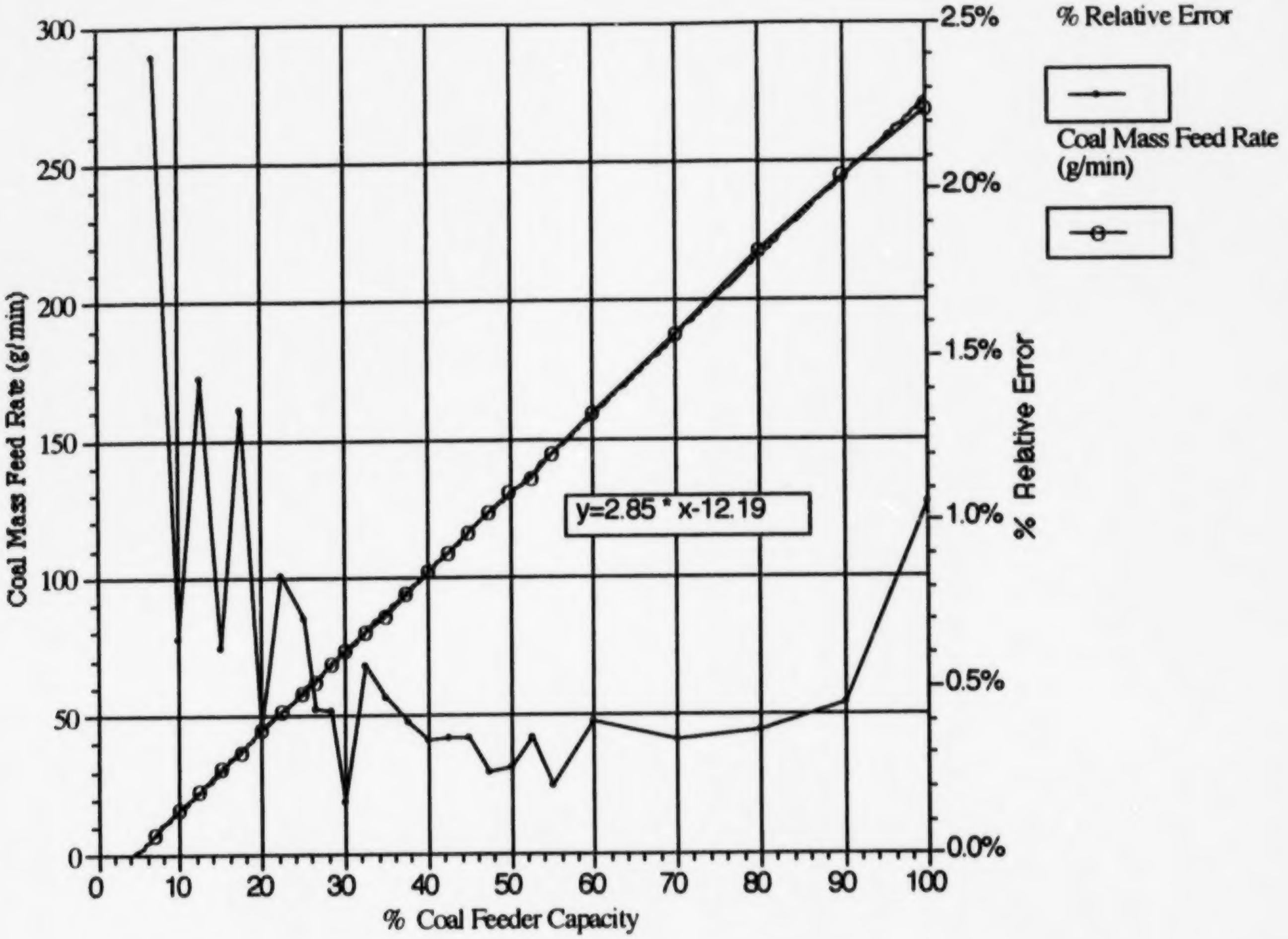

Figure 3.5 Coal Mass Feed Rate (g/min) and % Relative Error versus % Coal Feeder Capacity

against percent coal feeder capacity. The feed rate was highly reliable and accurate (less than 1 percent error), and was equipped with a digital readout for total helix revolutions, and a variable speed 93 W DC gear motor drive . The volumetric capacity of the hopper is about 37 liters.

3.3 Slurry Conditioning

The cylindrical shaped conditioning vessel for flow scheme 1 is fabricated from 6.35 mm cast acrylic pipe and plate. The vessel has a conical shaped bottom with an internal diameter of 139 mm, a centerline height of 210 mm, and a outside height of 195 mm. The conditioning vessel has a working volume of 1.5 L at the normal operating RPM of 1200.

The cylindrical shaped conditioning vessel for flow scheme 2 has a working volume of 2.0 L and a diameter of 150 mm. An operating RPM of 1500 was used during the experimental program.

The mixer used for both flow scheme 1 and 2 was a 93 W variable speed motor with a RPM readout, and a stainless steel four bladed turbine impeller, 12.5 mm in depth and 50.8 mm in width.

3.4 High Shear Mixing

The cylindrical high shear mixer vessels have conical shaped bottoms and are fabricated from 6.35 mm cast acrylic pipe and plate. High shear mixer 1 has a diameter of 139 mm, an outside height of 195 mm and a centerline height of 210 mm. High shear mixer 2 has an inside diameter of 126 mm, an inside height of 206 mm and a centerline depth of 230 mm. The operating volume for both mixers are provided as a function of rpm's in Figure 3.6 and Table 3.2, both being fairly similar. However, the baffle design is somewhat different for high shear mixer 1. Both vessels contain four baffles along the entire height of the vessels with a width of 12.5 mm (e.g. 9 % and 9.9 % of high shear mixers 1 and 2 tank diameter, respectively). Within high shear mixer 1, a small gap between all four baffles and the vessel wall exists

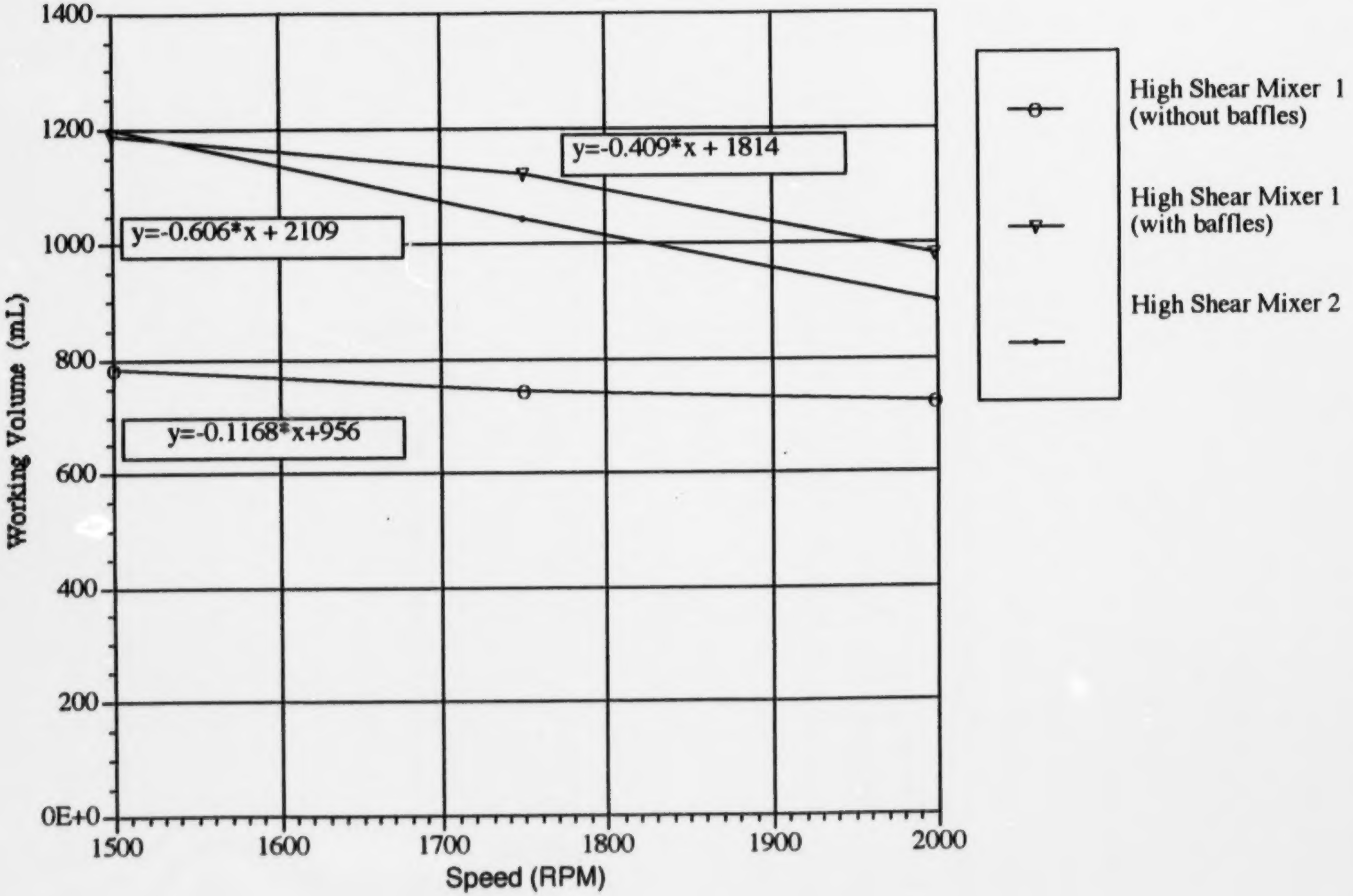

Figure 3.6 High Shear Mixers 1 and 2 Volume (mL) versus Speed (RPM)

continuously along the entire length of the baffles (e.g. 3 to 4 mm). Within high shear mixer 2 the baffles are fabricated flush to the wall over the entire length of the baffle. The power consumption reflects this design difference as high shear mixer 1 normally demonstrated a energy consumption of about 10 to 20 J/L, while high shear mixer 2 demonstrated an energy consumption of about 33 to 35 J/L. In flow scheme 1, only one stage of high shear mixing was used. High shear mixer 2 was utilized for that function, while in flow scheme 2, both high shear mixers were utilized.

Table 3.2 High Shear Mixing Volume versus RPM

Vessel	RPM	Average Volume (mL)
High shear mixer for flow scheme 1 (without Baffles)	1500 1750 2000	785 744 726
High shear mixer 1 for flow scheme 2 (with Baffles)	1500 1750 2000	1420 1184 982
High shear 2 for flow schemes 1 and 2 (with Baffles)	1500 1750 2000	1202 1046 899

The high shear mixers are equipped with 93 Watt motors, complete with a variable speed controller (0 to 2600 rpm) with both RPM and torque readout (in-oz). Both mixer impellers are stainless steel four bladed turbines, with a width and depth of 60 mm, and 16 mm, respectively, positioned 50 mm from the bottom of the vessels directly above the oil addition by about 2 to 3 mm. The impeller width to diameter ratio is 0.31, and the impeller diameter to tank diameter ratio are 0.37 and 0.40 for high shear mixers 1 and 2, respectively.

3.5 Separation Systems

3.5.1 Flotation Cells

Both primary flotation cells are 140 mm square, one fabricated from 6.35 mm cast clear acrylic, and the other from stainless steel. Both cells have a working volume of about 2.75 L at 1100 rpm and air input rate of 4.95 L/min. The flotation cells are equipped with overflow weirs for control of surface level in the cell, and a variable speed froth removal paddle device. Flotation cell 1 contains a conical bottom and settling vessel to facilitate enhanced removal of solids which accumulation in the bottom of the cell (see Figure 3.1). Flotation cell 2 does not contain this salient feature, however, in this tailings scavenging scenario, minimal solids accumulation was experienced.

Flow scheme 1 used cell 2 and single stage flotation as a mean of product separation, while flow scheme 2 consisted of two stage primary flotation with cell 1 serving as the first stage. The unique design of flotation cell 1 evolved from the operating experience gained with flotation cell 2 and flow scheme 1.

A standard Denver Flotation Machine, model D12, was used for the first stage of primary flotation, and was equipped with the following: a speed controller, a tachometer, and a mechanically induced aeration impeller. The air input rate of cell 1 was 5.4 L/min. at the normal operating speed of 1100 rpm. The variation of the air input verses RPM for this cell is provided in Figure 3.7 and Table 3.3. The second primary flotation cells was a Wemco Flotation Machine with the same peripheral equipment as the Denver Machine. The air input of cell 2 was 5.7 L/min. at the normal operating speed of 900 rpm.

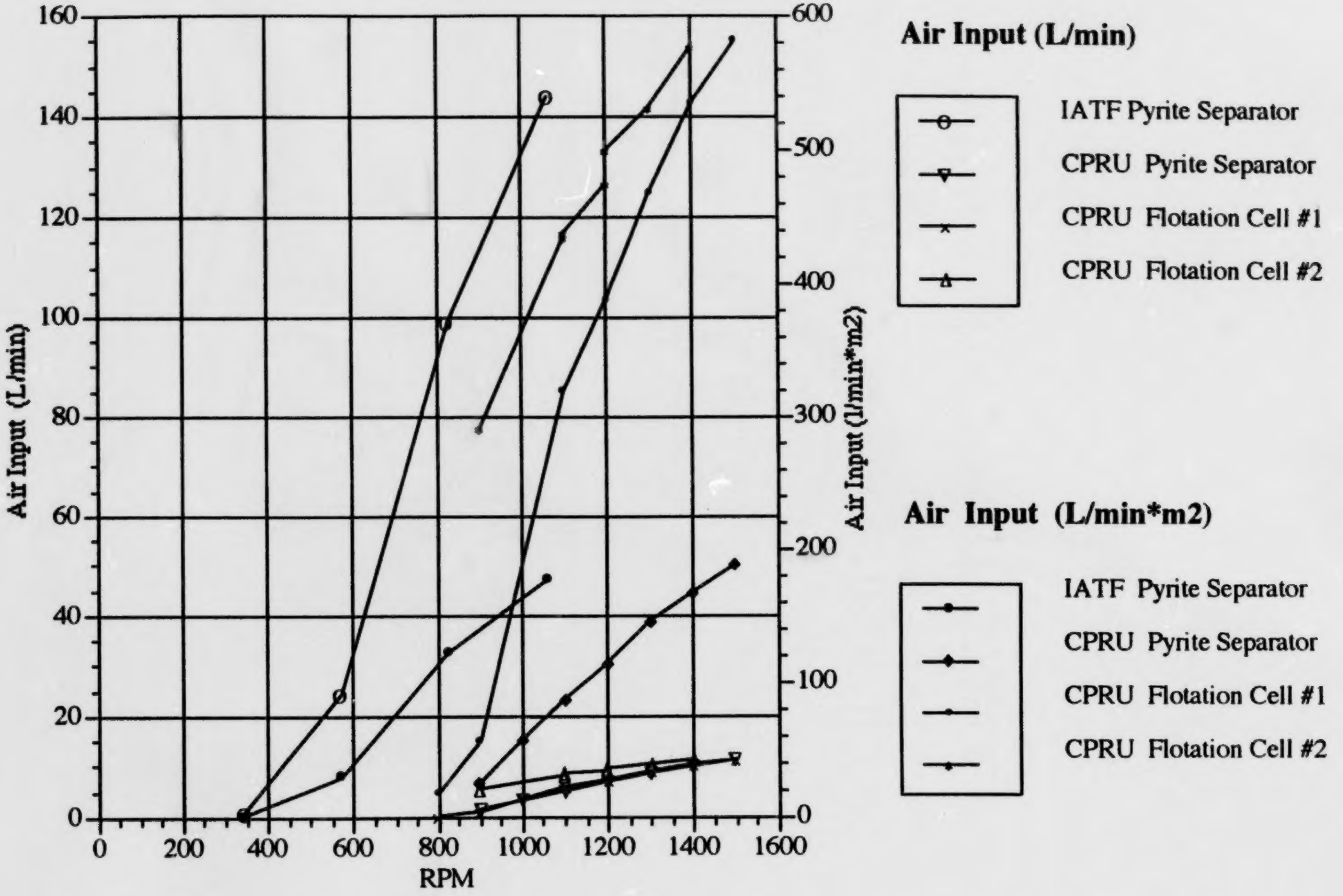

Figure 3.7 Air Input (L/min and L/min*m^2) versus RPM

Table 3.3 Air Input (L/min.) versus RPM

Vessel	RPM	Air Input (L/min.)	Air input (L/min*m^2)
Primary Flotation Cell 1 (Denver Cell)	900	.7	35.7
	1100	4.5	229.6
	1200	7.6	387.8
	1300	8.7	443.9
	1400	10.1	515.3
	1500	10.8	551.0
Primary Flotation Cell 2 (Wemco Cell)	900	5.7	290.8
	1100	8.7	437.3
	1200	9.6	487.8
	1300	10.4	531.6
	1400	11.3	576.5
Pyrite Separator (Denver Cell)	900	1.6	103.9
	1000	3.6	233.9
	1100	5.4	275.5
	1200	7.0	454.7
	1300	9.0	584.6
	1400	10.3	669.1
	1500	11.7	760.0

3.5.2 Pyrite Separator

The pyrite separator was used in both flow scheme 1 and 2 as the second stage separation of beneficiation, and has an overall working volume of 4.75 L at an operating RPM of 1100. The air input rate was about 5.4 L/min. at this operating RPM. The pyrite separator is cylindrical in shape and has three distinct zones:

- the washing zone,
- the settling zone, and,
- the flotation zone (see Figure 3.2).

The washing zone is rectangular in shape with a length of 104 mm, a width of 85 mm, and a depth of 103 mm. The volume of the wash zone is about 1.1 L, however, the zone is equipped with high penetration water wash nozzles, hence, the working volume is lower. The water wash nozzles can operate from the 6 to 30 kg/hr range, and penetrate the froth about 25 to 50 mm.

The settling zone is 140 mm in diameter and 149 mm in height, and is equipped with a flow stabilizer which is cylindrical in shape with a diameter of 60 mm and an height of 88 mm. The bottom of the settling zone is conical in shape at an angle of 30 degrees with the horizontal, and is equipped with four stationary baffles 90 mm in height and 12 mm wide, along the wall of the settling zone.

The flotation zone is also cylindrical with a diameter of 140 mm, and a height of 149 mm. A stationary baffle between the washing zone and the flotation zone was used to dampen the action of the flotation impeller within the washing zone.

A Denver Flotation Machine, Model D12, was used with the pyrite separator, and was equipped with the following: a speed control system, a tachometer, a mechanically induced aeration impeller, and a level control device. The air input versus rpm's is also provided in Figure 3.7 and Table 3.3.

3.6 Water Flowrate Controls

Water was added at the conditioning stage, at the flotation stage, and at the pyrite separator. The water addition was controlled by the rotameter configuration provided in flow scheme 1 and 2 (see Figure 3.3 and 3.4). The rotameters are manufactured by Matheson, series 604 and 605, and the flow rate plots are provided in Figure 3.8 and Table 3.4. The series 604 operated within the 50 to 180 mL/min. range and was used to feed the flotation cell. The 605 series operated within the 100 to 550 mL/min. range and was used to feed the conditioning vessel, the flotation cell, and the hydraulic separator wash water.

The rotameter arrangement for both flow scheme configurations are somewhat different as additional water was added to the weir region of primary flotation to eliminate solids accumulation within this vessel in flow scheme 2. Both rotameter arrangements are described in Figures 3.3 and 3.4, respectively.

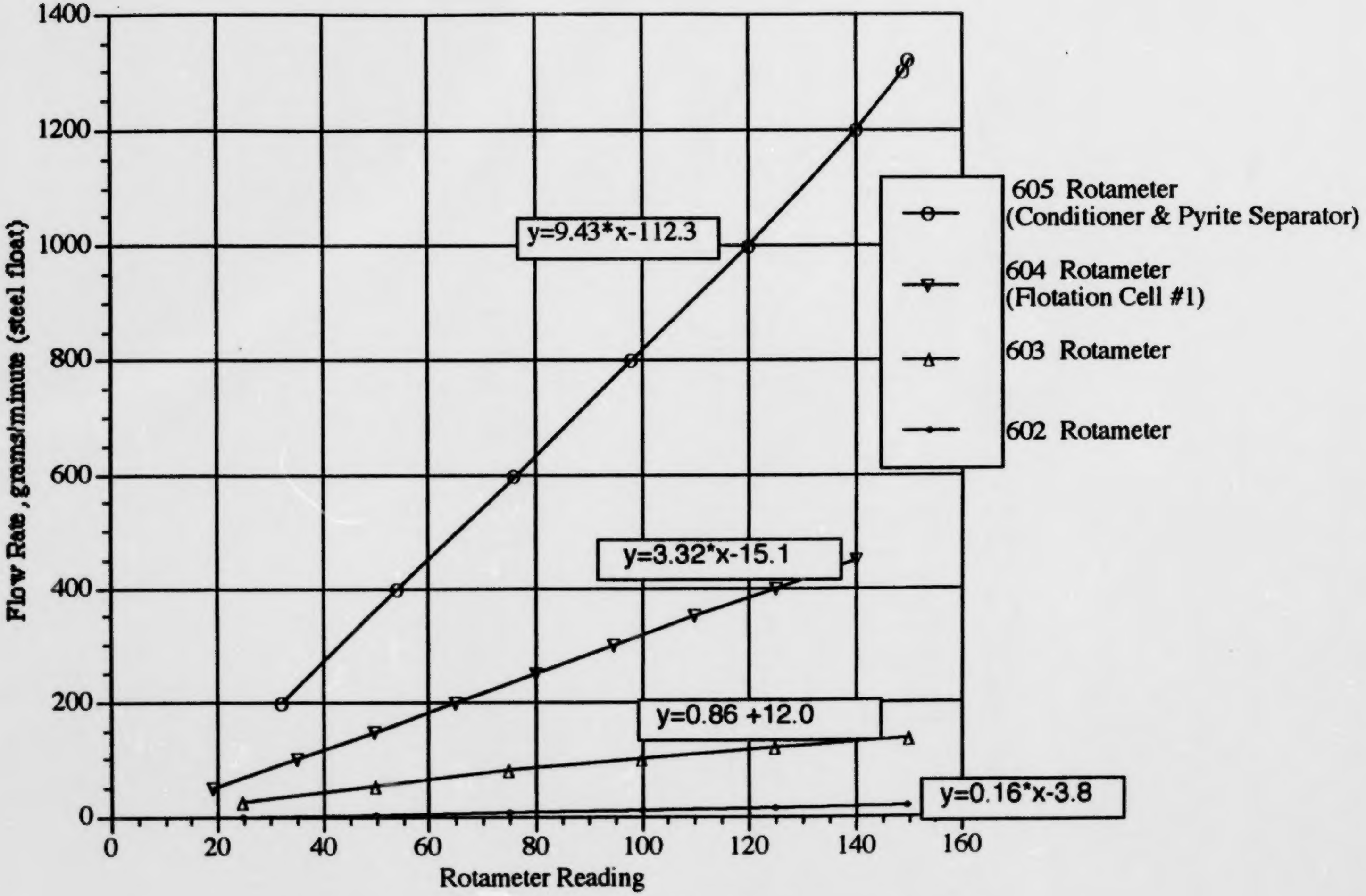

Figure 3.8 Conditioner, Flotation Cell 1, and the Pyrite Separator Water Mass Flow Rates versus Rotameter Setting

Table 3.4 Water Flow Rates (g/min.) versus Rotameter Setting

Location	Rotameter Model #	Rotameter Scale Reading	Water Flow Rate (mL/min.)
Flotation Cells	604	19	50
		35	100
		50	150
		65	200
		80	250
		95	300
		110	350
		124	400
		140	450
	603	25	28
		50	56
		75	81
		100	103
		125	122
		150	135
	602	25	1.5
		50	3.5
		75	6.7
		100	11.1
		125	15.8
		150	20.6
Pyrite Separator	605	32	200
		54	400
		76	600
		98	800
		120	1000
		140	1200
		149	1300
		150	1323

3.7 Frother Additions

Frother addition to the flotation circuit was achieved with a small centrifugal pump and a continuously stirred reservoir tank with a 1 percent Methyl Isobuty Carbinol (MIBC) stock solution. The pump demonstrated high levels of precision, however, it demonstrated limited accuracy between test days, and hence, required calibration prior to each day of testing. A calibration plot for the experimental program is provided in Figure 3.9 and Table 3.5.

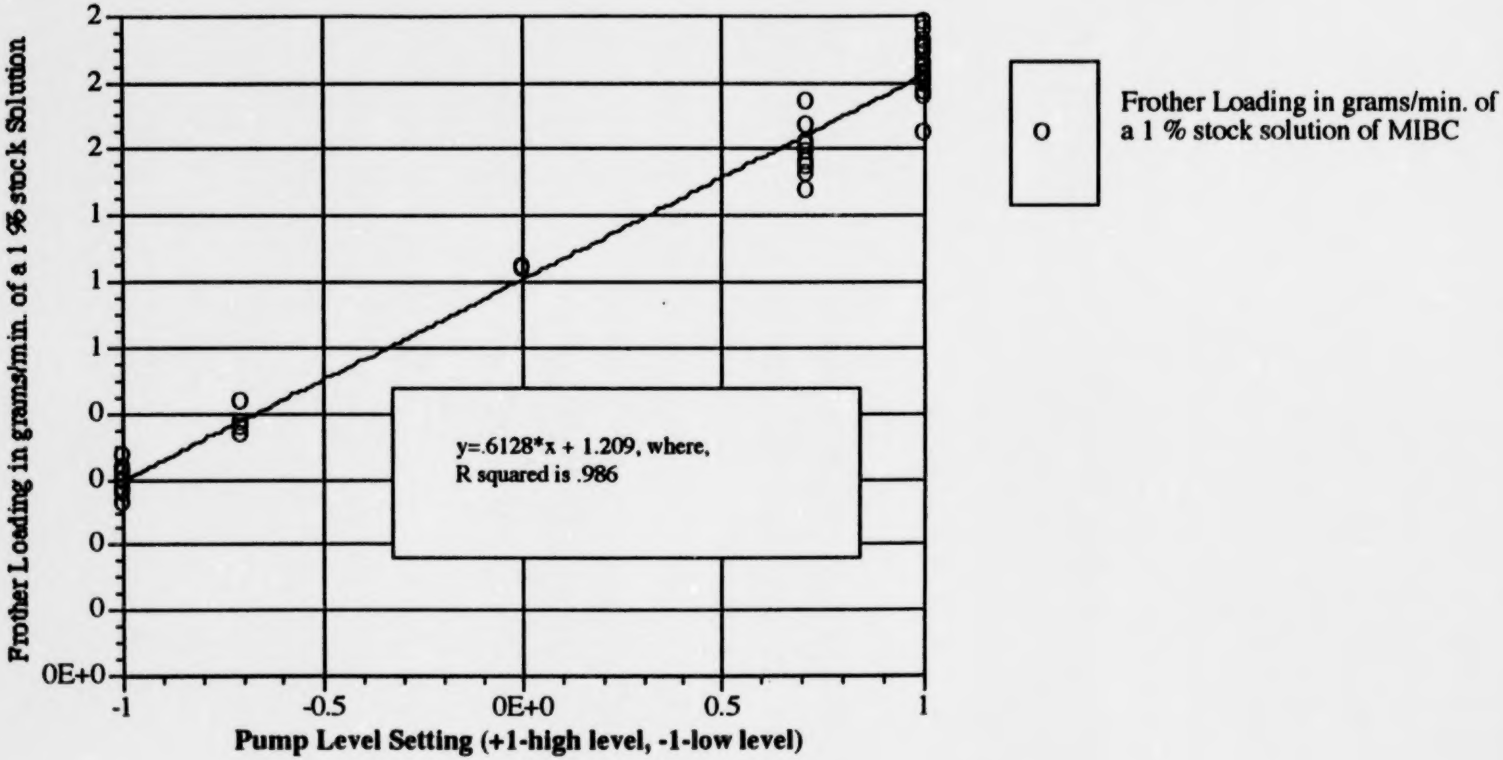

Figure 3.9 Frother Loading in grams/min of a 1 % Stock Solution of MIBC versus Pump Capacity level, (eg. -1 representing low level capacity, and +1 representing high level capacity)

Table 3.5 Frother Mass Flow (gram/min.) & % Relative Error vs. Experimental Level

Experimental Level	Readings (gram/min.)	Average (gram/min.)	% Relative Error
-1	0.62, 0.59, 0.62, 0.64, 0.56, 0.6, 0.62, 0.64, 0.57, 0.67, 0.57, 0.57, 0.57, 0.53, 0.64	0.60	6.5
-1/2	0.84, 0.77, 0.74, 0.77, 0.76, 0.74	0.77	4.8
0	1.25,1.24		
1/2	1.61, 1.62, 1.56, 1.67, 1.56, 1.61, 1.74, 1.62, 1.59, 1.62, 1.62, 1.55, 1.53, 1.53, 1.48	1.59	4.0
1	1.83, 1.91, 1.87, 1.83, 1.85, 1.90, 1.83, 1.86, 1.76, 1.85, 1.98, 1.86, 1.83, 1.84, 1.77, 1.84, 1.79, 1.81, 1.8, 1.86, 1.92, 1.84	1.85	2.7

3.8 Oil Additions

Oil was added to either high shear mixer with a gear pump. The pump output is controlled by a variable speed 400 W motor operating in the range of 4.6 to 72 RPM, (e.g. model G.M., Precision Metering Pump, manufactured by Nichols Zenith). A calibration plot is provided in Figure 3.10 and Table 3.6.

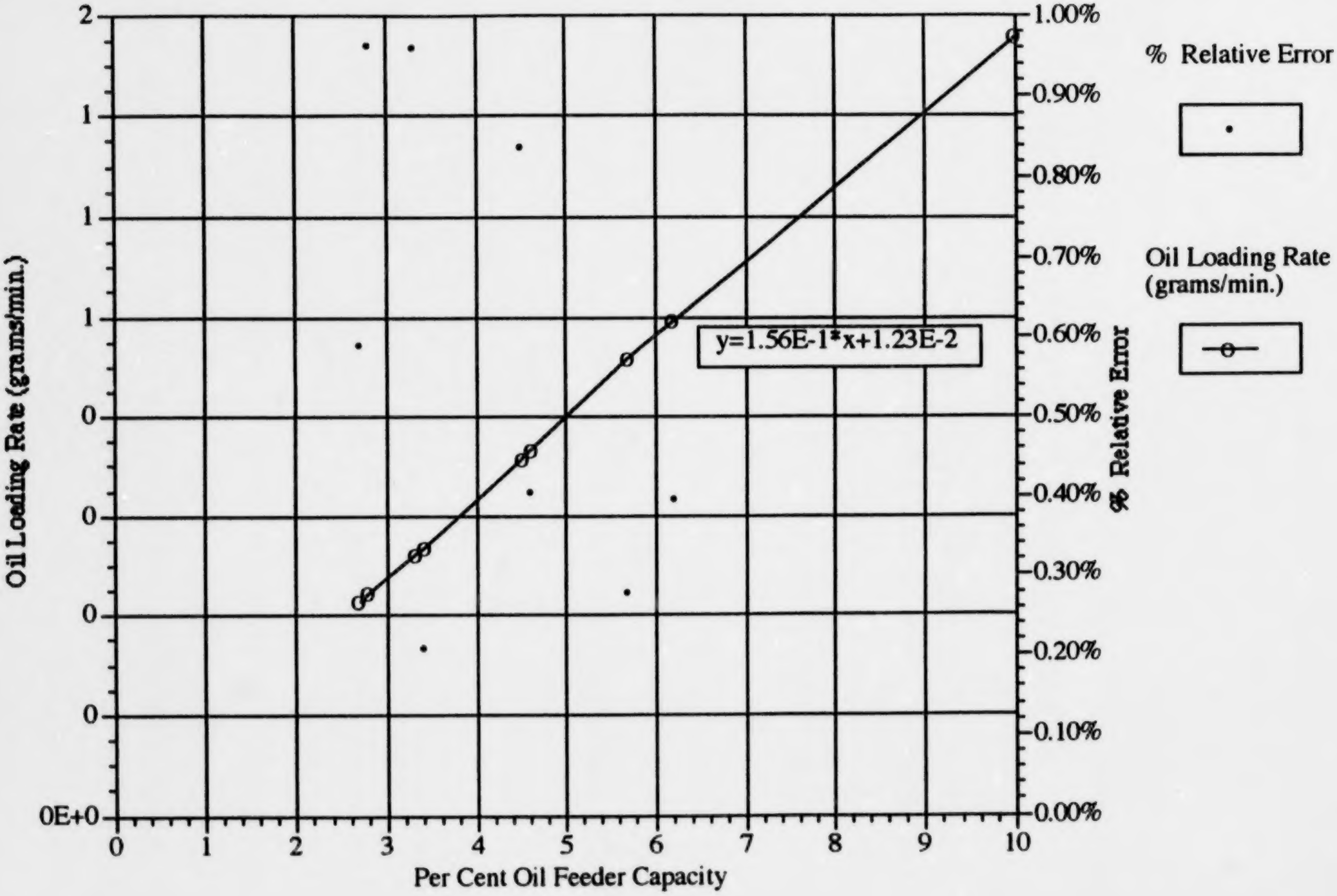

Figure 3.10 Oil Loading Rate (grams/min) and % Relative Error versus % Oil Feeder Capacity

Table 3.6 Oil Mass Flow (gram/min.) & % Relative Error vs. % Capacity

% Pump Capacity	Oil Rate (gram/min.)	% Relative Error
2.7	.427	.59
2.8	.445	.96
3.3	.523	.96
3.4	.538	.21
4.5	.716	.84
4.6	.734	.40
5.7	.915	.28
6.2	.995	.40
10.	1.56	

4.0 Experimental Method

The experimental program included three phases of work.

Phase 1	Commission Tests.
Phase 2	Development of Experimental Method.
Phase 3	Experimental Investigations.

The commission tests involved debugging the apparatus using observations and process measurements to evaluate the apparatus reliability and accuracy.

The development of experimental method involved detailed mass balance tests with extended run times to quantify apparatus repeatability and steady state conditions. These experiments defined the time for steady state conditions to prevail, and the minimum sampling and analysis program required for obtaining representative results.

The experimental investigations were based upon a 2^5 factorial design. Washability tests were performed on feed samples to help establish the theoretical cleaning potential for the test coal. The test results were used to assess the theoretical performance of the process.

4.1 Phase 1 Commission Testing

These tests involved debugging and determining the rates and relative errors for all process equipment. Section 3.0 describes specifications and summarizes the calibration plots and percent relative error for all major equipment. These results indicate the most important parameters such as coal feed rate, oil and frother feed rates, and high shear mixer speed, power and volume, can all be measured with a high level of precision and accuracy.

4.2 Phase 2 Development of Experimental Method

The development of the experimental method consisted of three test series:

- test series 1 - sample preparation and collection;
- test series 2 - steady state analysis and repeatability; and
- test series 3 - apparatus modifications.

The majority of these tests were performed with process flow scheme 1, from which the apparatus modifications developed and were used to generate flow scheme 2.

4.2.1 Series 1 Sample Preparation and Collection

4.2.1.1 Feed Coal Preparation

The feed coal required rigorous blending and grinding preparations. Initially, 500 liters of the test coal was collected and extensively blended prior to grinding. The blending procedure involved mixing the coal within a large conical pile. Large shovels were used and the conical pile was mixed by continuously displacing the bottom most material to the top of the pile for 3 hours. The sample was then divided repetitively until each sub-sample was approximately 15 to 20 kg in size. The sub-samples were then randomly placed back into the barrels in preparation for the dry grinding of the sample.

The dry grinding procedure involved calibration to generate the desired size distributions. A hammer mill was used with 250 μm (60 mesh) and 150 μm (100 mesh) classification screens. Each barrel of coal was used to generate a sample of the fine (d_{50}=47 μm and d_{80}=88 μm), coarse (d_{50}=80 μm and d_{80}=208 μm) and medium (d_{50}=73 μm and d_{80}=154 μm) size distributions. All these samples were generated in a three day period and followed the same blending procedure as provided for the initial sample. However, the 15 to 20 kg sub-samples of the fine and coarse size distributions were stored in air tight bags and the medium distribution was stored in a barrel open to ambient air conditions for 40 to 45 days. When the medium size distribution testing program was to begin, the sample was again thoroughly blended and divided into 15 to 20 kg sub samples and stored in air tight bags.

4.2.1.2 Feed Coal Sample Collection

Experimental evidence indicated variations in instantaneous samples can be quite large, which can cause a significant problem in the assessment of the process performance. Hence, a feed coal composite sampling program was selected to define both the mass flow rate and the assay components. These results were used to evaluate process performance.

Samples and feed rate measurements were taken approximately every 30 minutes for a 30 second interval, to generate a composite sample for each size distribution of the test coal. The sample was then riffled down to approximately a 500 g sample. The remaining feed sample was stored in an air tight jar for washability and size distribution analysis. The sub-sample was further pulverized, blended and subsequently further sub-sampled into a 5.0 mL air tight vial (see Section 4.2.1.3). Normally, approximately 2.5 mL was submitted for laboratory analysis.

4.2.1.3 Feed Sample Preparation for Assay Analysis

All feed samples collected during the testing program were prepared with the following procedure:

- the sample was first riffled sub sampled to approximately 500 g;
- the 500 g sub-sample was pulverized to 100 percent less than 50 μm.; and
- the 500 g sub-sample was then extensively blended on a clear plastic sheet.

The blending process involved crossing the axis of a conical pile via each corner of the plastic. Once a long windrow was formed by the blending action, the opposite corners of the plastic sheet were rolled until a windrow of sample formed in the opposite direction. This procedure effectively rolled the bottom material over the top, and caused the sample to cross axis with each blend. This procedure was repeated 10 times for each sample prior to sub-sampling the material.

- The sub-sample was extracted from at least 10 locations from the last windrow to collect approximately 2.5 mL for laboratory analysis.

4.2.1.4 Product and Tailings Stream Sample Preparation

The product and tailings streams were prepared in a similar method as the feed sample, with the addition of the following procedure.

- Once the product sample was collected, the total slurry mass was recorded, and the sample was then pressure filtered to remove the majority of the water phase. The sample was subsequently placed in the oven at approximately 55 °C to drive off the remaining water.
- Following a 12 to 16 hour drying time, the samples were removed from the oven and weighed. Approximately 24 hours later the sample was weighed again to ensure the moisture content had reached equilibrium. If no changes were observed in the sample mass, it was prepared for analysis. Tables in section 8 summarize the moisture contents of all the product samples prepared during the phase 3 testing program, and the results indicate very consistent moisture contents were observed over the testing program.

4.2.2 Series 2 Steady State Analysis and Repeatability

A step tracer test was performed to evaluate steady state conditions. A sodium chloride salt solution, a feed pump, two conductivity probes, and a charge recorder were used to perform the test. Two start-up procedures were evaluated, the first involved tracer being added with initially a very small volume of water within the conditioner and agglomeration vessels. The second method investigated start-up conditions when both the conditioner and high shear vessels were initially full of water. Conductivity was monitored in the high shear mixer, and the flotation cell tailings stream.

Figure 4.1 defines the concentration profile observed in the high shear mixer. Two conductivity probes were submerged within the mixer, and used to measure salt concentration with time. The results indicate the mixer achieves near steady concentration after about 15 minutes in tracer study 1 at a flowrate which is equivalent to about half the volumetric flowrate applied in the test program. The concentration profile

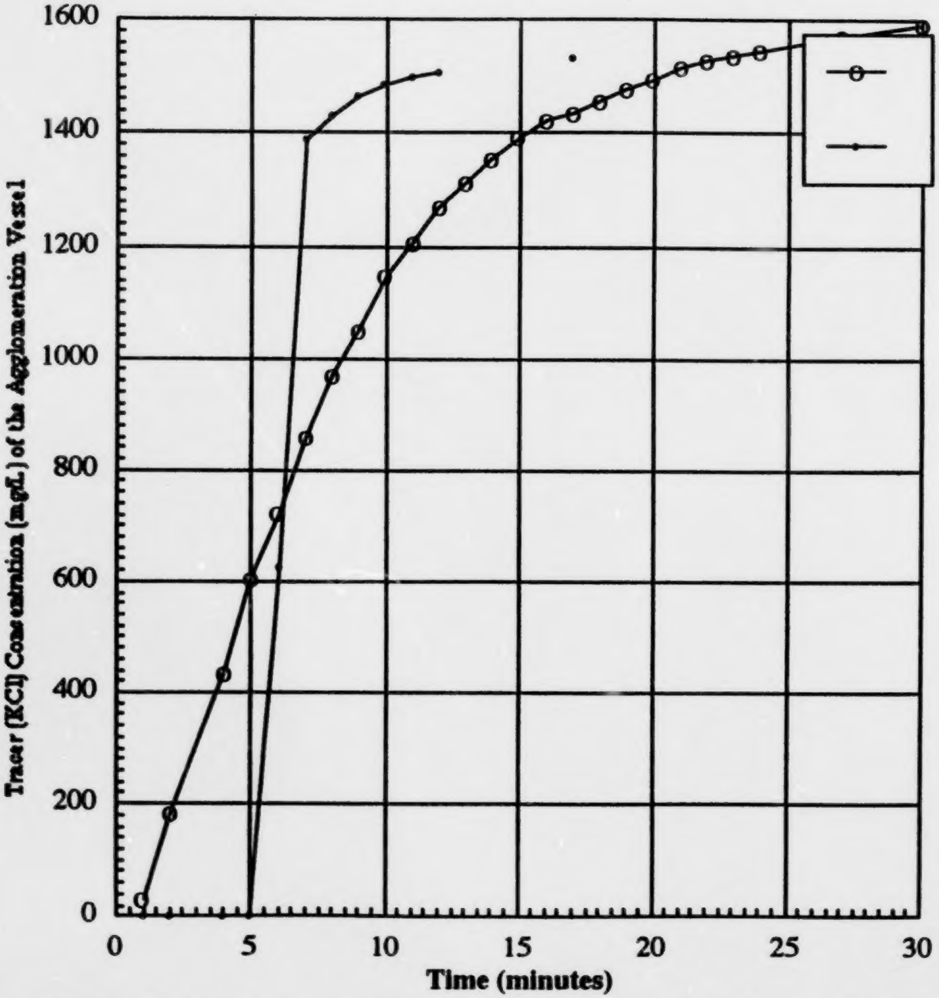

Chart Speed - 300 mm/hr
Tap Water Background subtracted from profile
 -ionic interactions neglected
 -assume water density = 1.0g/mL
Stock Salt Solution = 250 g/L (KCl)
Step Input Rate = 2.43 g/min
 -assume density of salt solution = 1.134 g/mL
 -Cmax=1678 mg/L

Tracer Study #1
-Conditioner -starting volume 750 mL
 -operating volume 784 mL
 -720 RPM's
 -water flowrate 317 g/minute
-Agglomeration -starting volume 1400 mL
 -1200 RPM's
 -operating volume 1400 mL
 -water flowrate 317 g/minute
-Flotation -starting volume 2744 mL
 -1100 RPM's w/o air
 -operating volume 2744 mL
 -water flowrate 649 g/minute

Tracer Study #2
-Conditioner - starting volume 0 mL
 -all other factors the same as Tracer study #1
-Agglomeration -starting volume 0 mL
 -all other factors the same as Tracer study #1
-Flotation -all factors the same as Tracer study #1

Figure 4.1 Step Input Salt Tracer (KCl) Concentration at the High Shear Vessel versus Time (minutes)

in tracer study 2 required approximately the same time, but the profile is not as sharp as tracer study 1.

Figure 4.2 is presented as a normalized profile. The normalization procedure involved dividing the concentration, C(t), at time (t), by the maximum concentration (Cmax), and plotting these values against the normalized time. Normalizing the time involved dividing the profile times, (t), by the theoretical hydraulic retention time of the vessel. Tracer Study 1 reached 84 percent of the calculated equilibrium concentration in about 1 hydraulic retention time at the high shear stage. Tracer Study 2 reached 51 percent of the calculated equilibrium concentration in about 1 hydraulic retention time. Based upon the sharper response of the high shear stage, the start-up procedure was developed based upon Tracer Study 1.

Once the salt solution reached the flotation cell, Tracer Study 1 demonstrated only a slightly sharper response. Figure 4.3 and 4.4 demonstrate this evaluation. Figure 4.3 summarizes the change in salt concentration with time after the initial step input. Figure 4.4 provides for the normalized profile. Equilibrium conditions were met after about 30 minutes in both Tracer Study 1 and 2, with only minimal difference in the profiles observed at the beginning of the profile. These profile are typical of continuous stirred tank reactor (CSTR) behavior, and may be used to predict the behavior of the from the tailings solids of the flotation cell. The froth or product phase, however, will follow an entirely different residence time distribution pattern.

Two batch flotation kinetic tests were performed and combined to characterize the behaviour of the froth phase. The results of the test indicate that the froth phase does not behave as a CSTR, but rather demonstrates a different residence time distribution. Figure 4.5 provides the plot of the percent interval solids recovery versus mean interval time in minutes and indicates a nominal mean residence time of approximately 1.0 minute. The nominal mean residence time is defined by the centroid of the profile. Figure 4.6 is a normalized plot of the resident time distribution and is

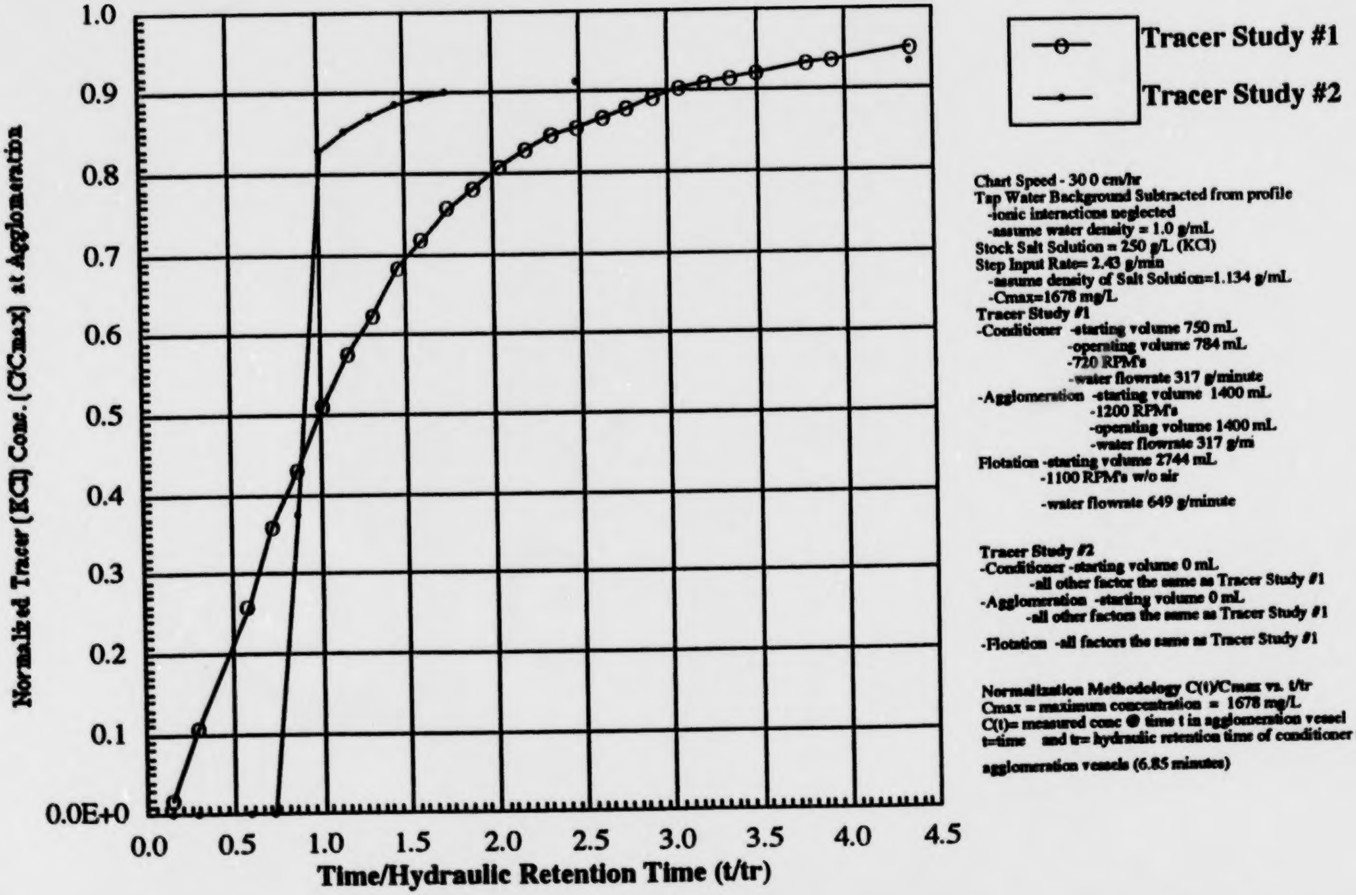

Chart Speed - 30 0 cm/hr
Tap Water Background Subtracted from profile
-ionic interactions neglected
-assume water density = 1.0 g/mL
Stock Salt Solution = 250 g/L (KCl)
Step Input Rate= 2.43 g/min
-assume density of Salt Solution=1.134 g/mL
-Cmax=1678 mg/L
Tracer Study #1
-Conditioner -starting volume 750 mL
-operating volume 784 mL
-720 RPM's
-water flowrate 317 g/minute
-Agglomeration -starting volume 1400 mL
-1200 RPM's
-operating volume 1400 mL
-water flowrate 317 g/mi
Flotation -starting volume 2744 mL
-1100 RPM's w/o air

-water flowrate 649 g/minute

Tracer Study #2
-Conditioner -starting volume 0 mL
-all other factor the same as Tracer Study #1
-Agglomeration -starting volume 0 mL
-all other factors the same as Tracer Study #1

-Flotation -all factors the same as Tracer Study #1

Normalization Methodology C(t)/Cmax vs. t/tr
Cmax = maximum concentration = 1678 mg/L
C(t)= measured conc @ time t in agglomeration vessel
t=time and tr= hydraulic retention time of conditioner and

agglomeration vessels (6.85 minutes)

Figure 4.2 Normalized (C/Cmax) Step Input Salt Tracer (KCl) Concentration at the High Shear Vessel versus Normalized Time (t/tr)

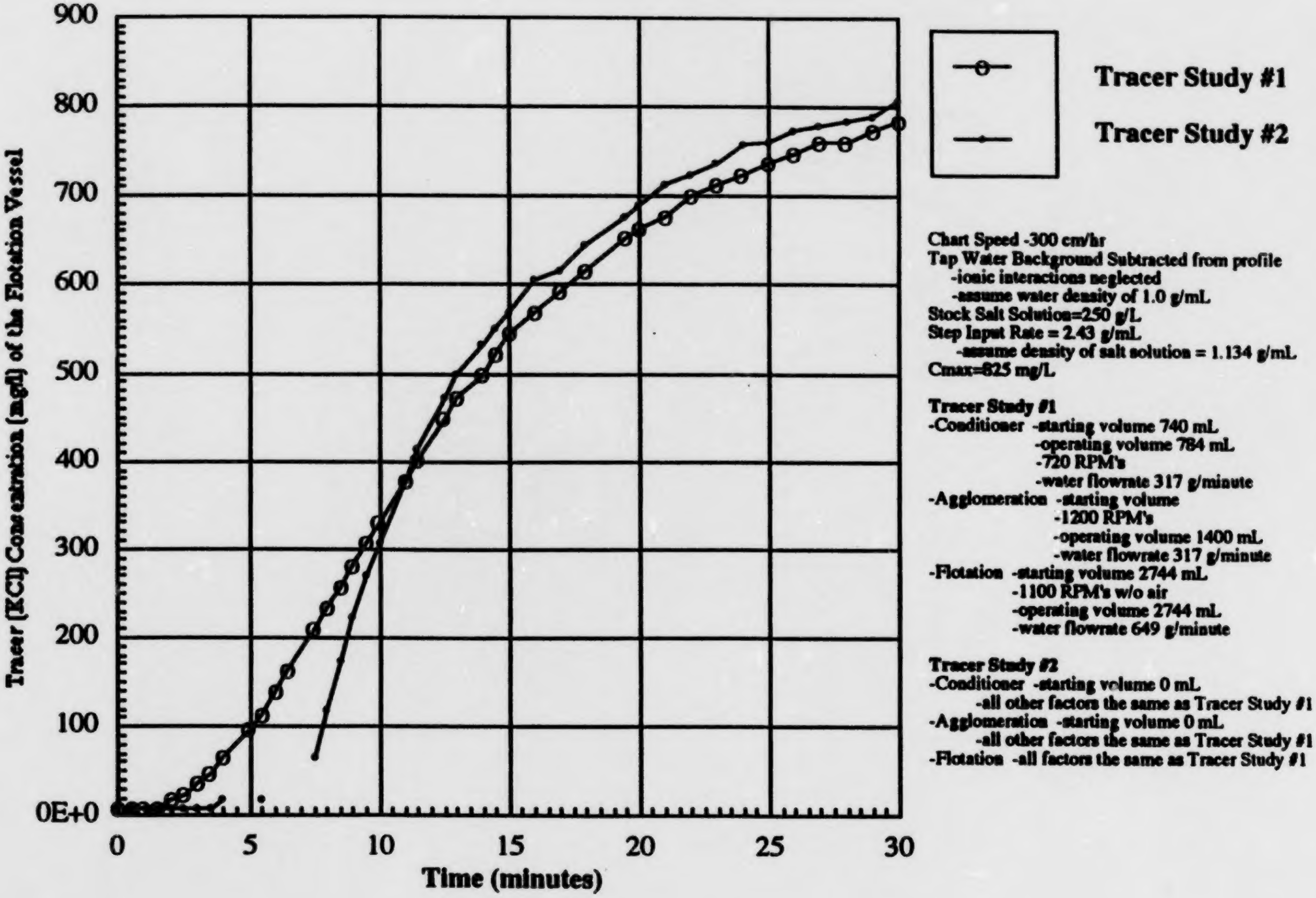

Chart Speed -300 cm/hr
Tap Water Background Subtracted from profile
  -ionic interactions neglected
  -assume water density of 1.0 g/mL
Stock Salt Solution=250 g/L
Step Input Rate = 2.43 g/mL
  -assume density of salt solution = 1.134 g/mL
Cmax=825 mg/L

Tracer Study #1
-Conditioner -starting volume 740 mL
  -operating volume 784 mL
  -720 RPM's
  -water flowrate 317 g/minute
-Agglomeration -starting volume
  -1200 RPM's
  -operating volume 1400 mL
  -water flowrate 317 g/minute
-Flotation -starting volume 2744 mL
  -1100 RPM's w/o air
  -operating volume 2744 mL
  -water flowrate 649 g/minute

Tracer Study #2
-Conditioner -starting volume 0 mL
  -all other factors the same as Tracer Study #1
-Agglomeration -starting volume 0 mL
  -all other factors the same as Tracer Study #1
-Flotation -all factors the same as Tracer Study #1

Figure 4.3 Step Input Salt Tracer (KCl) Concentration at the Flotation Vessel versus Time (minutes)

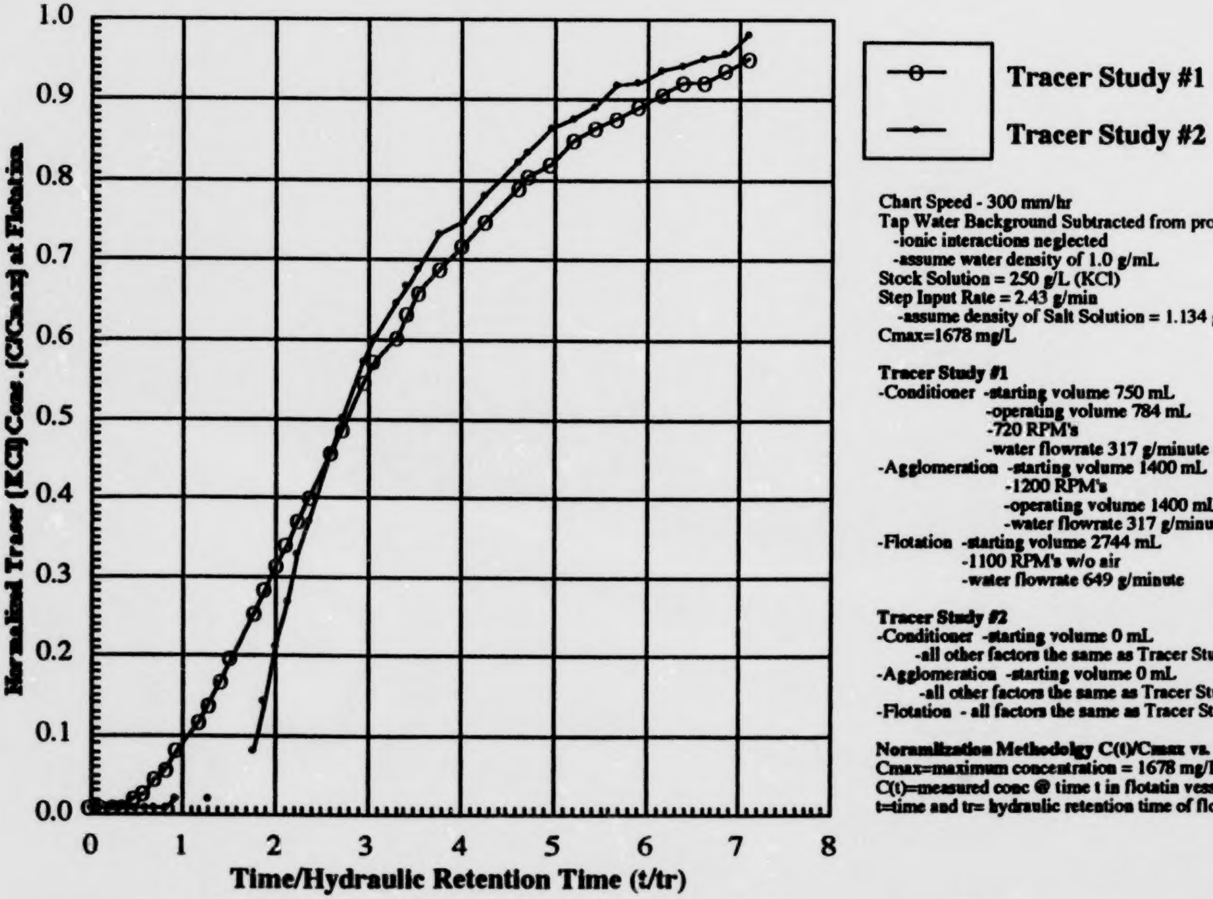

Chart Speed - 300 mm/hr
Tap Water Background Subtracted from profile
-ionic interactions neglected
-assume water density of 1.0 g/mL
Stock Solution = 250 g/L (KCl)
Step Input Rate = 2.43 g/min
-assume density of Salt Solution = 1.134 g/mL
Cmax=1678 mg/L

Tracer Study #1
-Conditioner -starting volume 750 mL
-operating volume 784 mL
-720 RPM's
-water flowrate 317 g/minute
-Agglomeration -starting volume 1400 mL
-1200 RPM's
-operating volume 1400 mL
-water flowrate 317 g/minute
-Flotation -starting volume 2744 mL
-1100 RPM's w/o air
-water flowrate 649 g/minute

Tracer Study #2
-Conditioner -starting volume 0 mL
-all other factors the same as Tracer Study #1
-Agglomeration -starting volume 0 mL
-all other factors the same as Tracer Study #1
-Flotation - all factors the same as Tracer Study #1

Noramlization Methodolgy C(t)/Cmax vs. t/tr
Cmax=maximum concentration = 1678 mg/L
C(t)=measured conc @ time t in flotatin vessel
t=time and tr= hydraulic retention time of flotaiton cell (4.2 L) minutes

Figure 4.4 Normalized (C/Cmax) Step Input Salt Tracer (KCl) Concentration at the Flotation Vessel versus Normalized Time (t/tr)

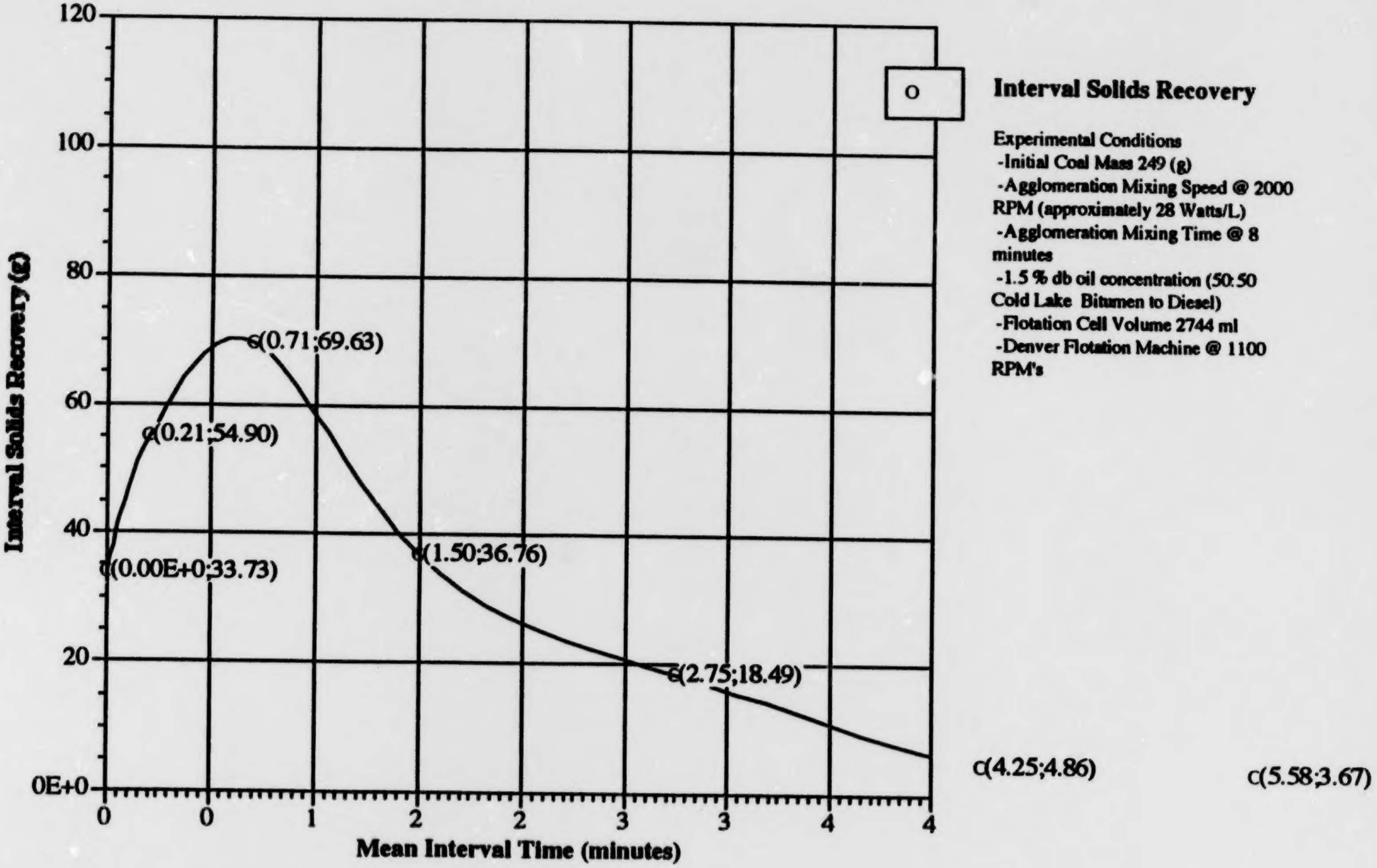

Figure 4.5 Interval Solids Recovery (g) versus Mean Interval Time (minutes)

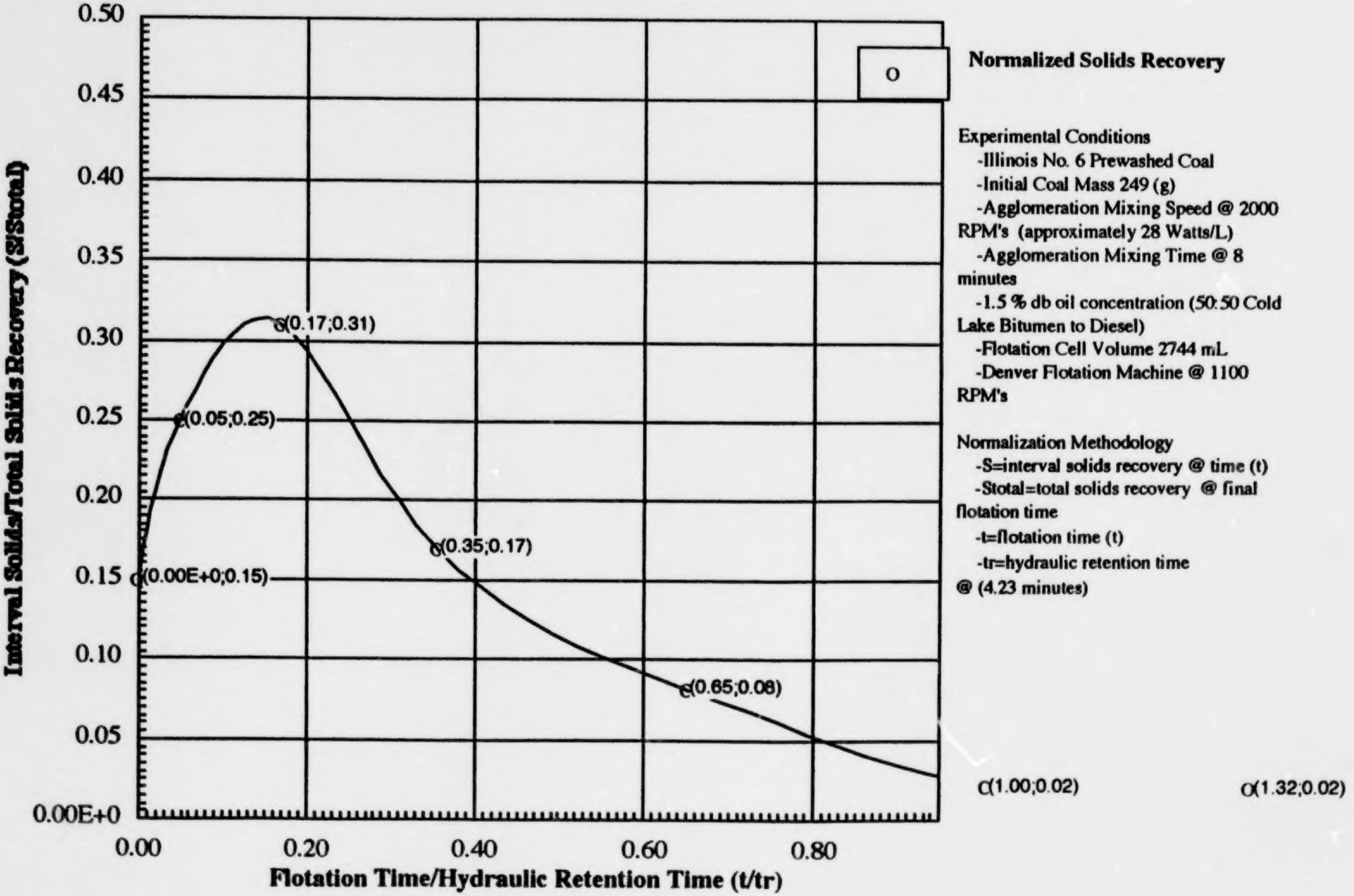

Figure 4.6 Normalized Solids Recovery (S/Stotal) versus Normalized Time (t/tr)

obtained by dividing the interval solids recovery by the total recovery plotted against the flotation time divided by the hydraulic retention time. This plot indicates a corresponding nominal mean residence time of about 0.2 of a hydraulic retention time. Figure 4.7 summarizes the combustible matter recovery (%) versus flotation time (minutes), the results indicate 100 percent recoverable solids are captured after about 6 minutes of flotation.

Detailed mass balance tests (d5, d6, d7) were performed with flow scheme 1 to develop the experimental method. These tests involved sampling programs to evaluate the steady state response and close the solids mass balance. The first sampling protocol involved instantaneous sampling, which required 1 minute samples to be extracted from various locations in the process. The second sampling protocol involved an extended sample collection program whereby all main streams were collected for every 30 minute interval. Both tailings streams and the product phase were monitored for solid mass flowrate, percent solids, and the ash and the total sulphur contents.

Figures 4.8, 4.9 and 4.10 and Tables 4.1, 4.2 and 4.3 are all provided for the evaluation of the instantaneous sampling campaign, as the total sulphur and ash contents at key locations in the process are plotted against run time to evaluate steady state conditions. The results from the instantaneous sampling program suggest the product stream reaches steady state within 30 minutes. However, the results also indicate the apparatus is demonstrating high sulphur accumulation and creep within the tailings streams, and a slight creep within the product phase. The results also indicate that large variations in mass flowrate and assays can be expected with a 1 minute sampling interval, indicating that a longer sampling intervals would be required to obtain reliable process response measurements.

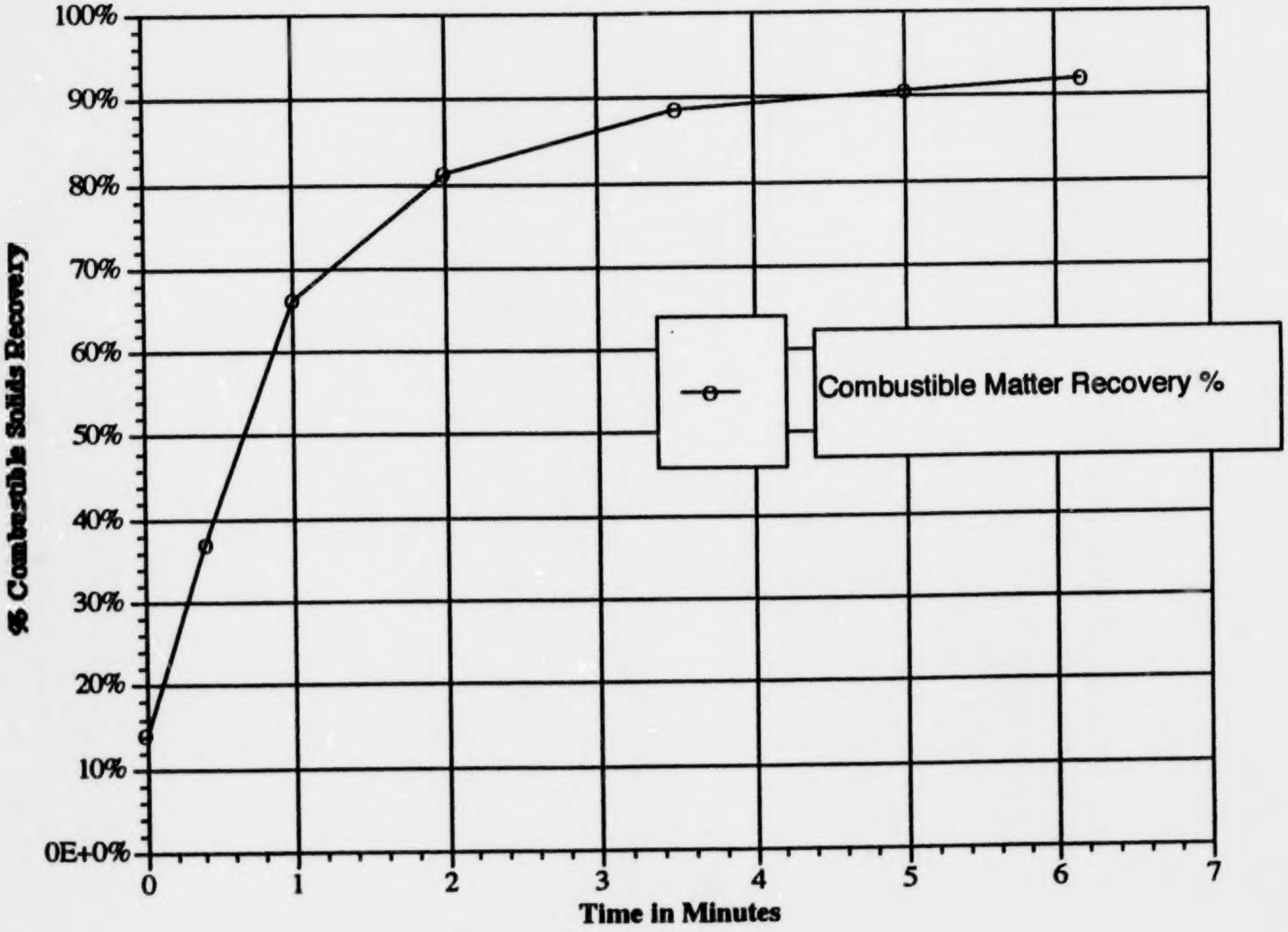

Figure 4.7 Batch Flotation Kinetic Study of Prewashed Illoinois 6 Coal

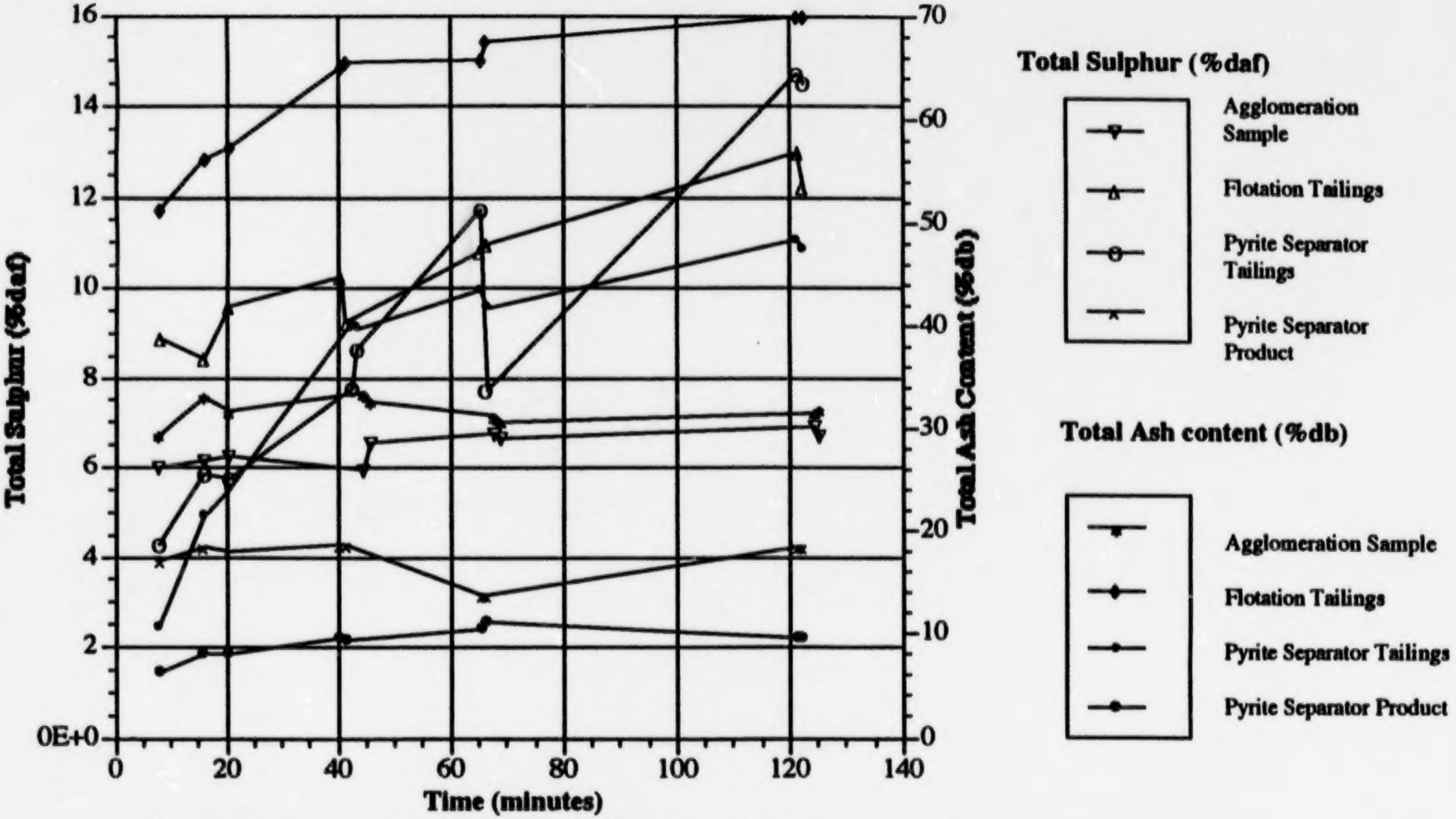

Figure 4.8 Repeat Test Intervals for Total Sulphur (%daf), and Ash Content (%db) versus Run Time (minutes) for the One Minute Sampling Intervals during Test D5

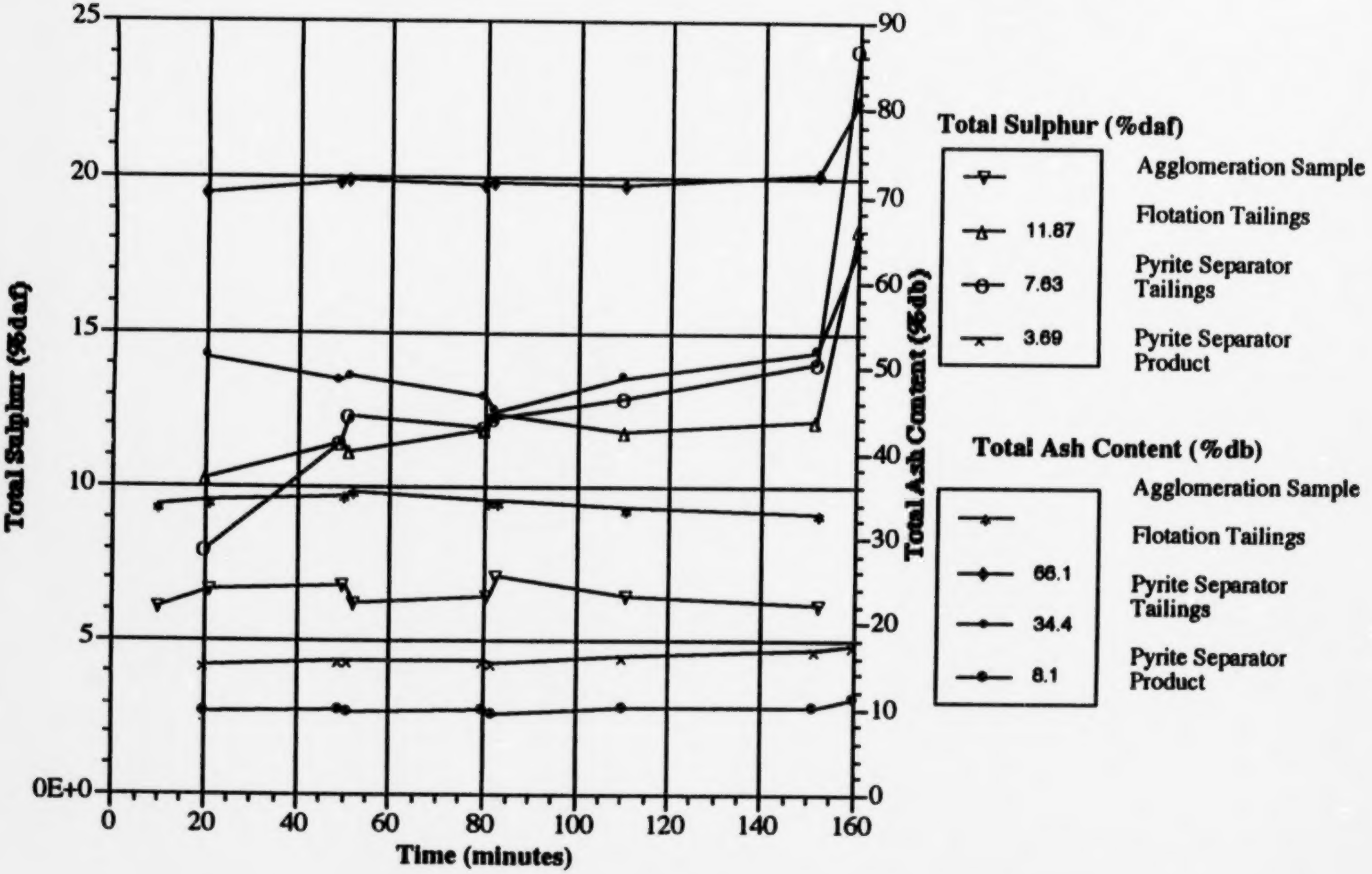

Figure 4.9 Repeat Test Intervals for Total Sulphur (%daf), and Ash Content (%db) versus Run Time (minutes) for the One Minute Sampling Experiment for Test D6

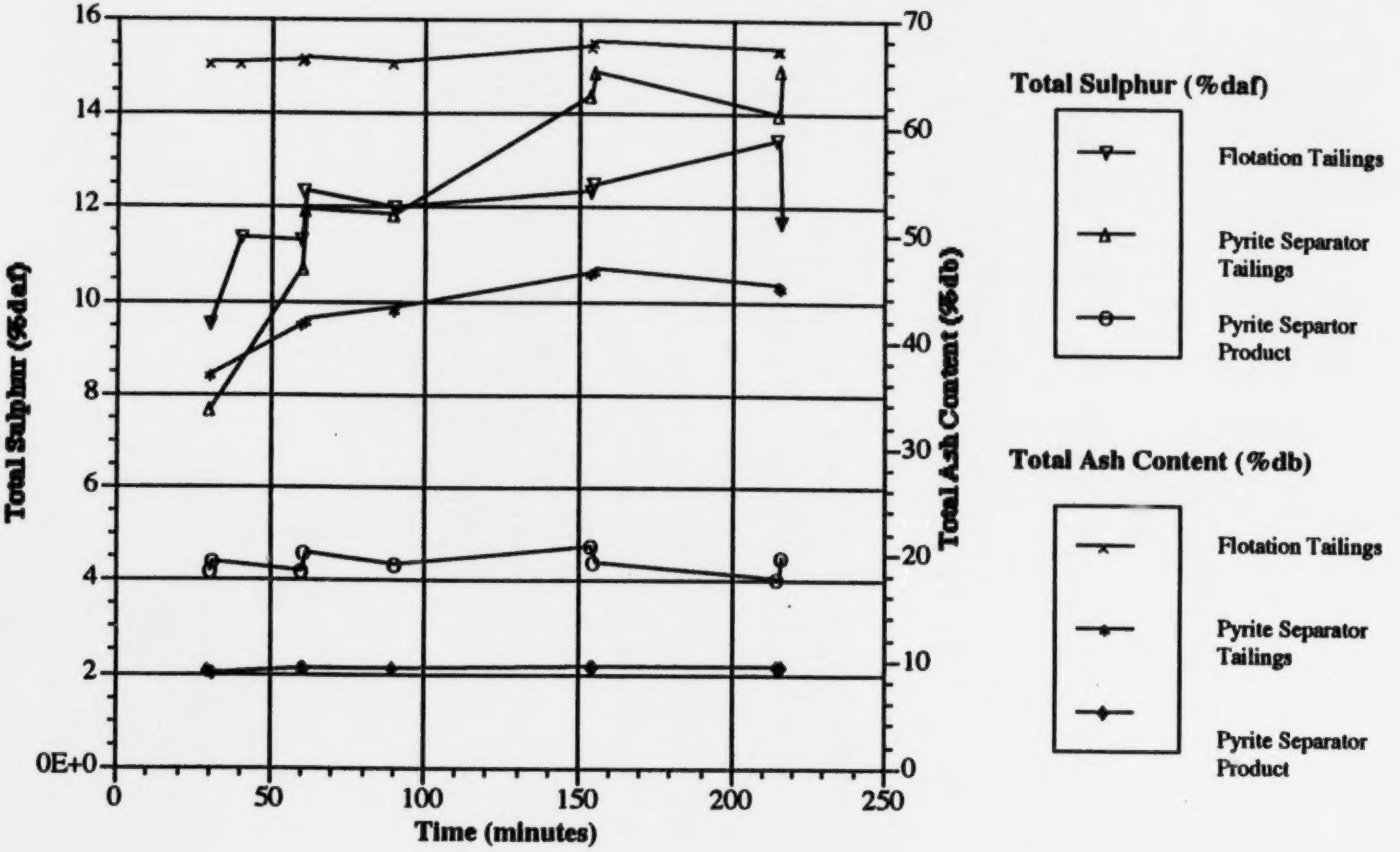

Figure 4.10 Repeat Test Interval for Total Sulphur (%daf), and Ash Content (%db) versus Run Time (minutes) for the One Minute Sampling Experiment for Test D7

Table 4.1 Steady State Results For Test D5 (1 minute Sample Interval)

	Time Range	High Shear Product		Flotation Tailings		Pyrite Separator Tailings		Product		
#	Time (min.)	Ash % db	TS % daf	Ash % db	TS % daf	Ash % db	TS % daf	Rate g/min.	Ash % db	TS % daf
1	8	29.4	5.99	51.4	8.91	10.7	4.26	13.5	3.95	6.4
2	16	33.2	6.17	56.1	8.41	21.4	5.83	30.5	8.00	4.22
3	20.5	31.7	6.28	57.3	9.59	24.1	5.77	23.4	8.10	4.12
4	41			65.1	10.25	40.4	7.78	34.8	9.6	4.26
5	43	33.5	5.93	65.4	9.24	39.8	8.62		9.4	4.28
6	64	32.7	6.54							
7	65.5	31.3	6.76	65.7	10.80	43.5	11.74	35.5	10.6	3.15
8	66.5	30.7	6.68	67.5	10.97	41.8	7.70	38.2	11.3	3.19
9	121.5	31.9	6.90	69.8	12.97	48.4	14.72	45.8	9.7	4.23
10	122.5	32.0	6.71	70.0	12.22	47.5	14.54	51.1	9.7	4.21

Table 4.2 Steady State Results for Test D6 (1 minute Sampling Interval)

	Time Range	High Shear Product		Flotation Tailings		Pyrite Separator Tailings		Product		
#	Time (min.)	Ash % db	TS % daf	Ash % db	TS % daf	Ash % db	TS % daf	Rate g/min.	Ash % db	TS % daf
1	9	33.9	6.11	66.1	11.87	34.4	7.63	36.4	8.10	3.69
2	20	34.4	6.64	70.2	10.28	51.8	7.97	51.2	9.8	4.35
3	49	35.0	6.81	71.4	11.46	48.5	11.48	38.9	10.0	4.35
4	51			71.6	11.13	49.0	12.28	17.9	9.8	4.33
5	80	35.6	6.26	71.3	11.88	46.6	11.94	39.8	9.9	4.35
6	82	34.4	6.42	71.4	12.38	44.9	12.27	22.3	9.3	4.27
7	83	34.4	7.11							
8	110	33.6	6.43	71.2	11.82	48.8	12.87	41.2	10.1	4.47
9	151.5	32.9	6.18	72.4	12.16	51.9	14.04	37.01	10.1	4.69
10	160			80.7	18.41	64.0	24.09	12.8	11.3	4.85

Table 4.3 Steady State Results for Test D7 (1 minute Sample Interval)

Test	Time Range	High Shear Product		Flotation Tailings		Pyrite Separator Tailings		Product		
#	Time (min.)	Ash % db	TS % daf	Ash % db	TS % daf	Ash % db	TS % daf	Rate g/min.	Ash % db	TS % daf
1				66.1	9.53	37.0	7.68	35.9	9.0	4.22
2				66.0	11.35			41.1	8.9	4.43
3				66.3	11.31	41.8	10.72	39.9	9.4	4.21
4				66.6	12.37	42.1	11.98	36.5	9.4	4.61
5				66.1	12.01	43.2	11.87	39.7	9.4	4.35
6				67.6	12.36	46.6	14.43	42.22	9.6	4.76
7				68.1	12.52	46.9	14.89	43.4	9.6	4.39
8				67.3	13.47	45.5	14.01	43.4	9.5	4.08
9				67.3	11.74	45.3	14.97	40.1	9.5	4.50

Figures 4.11 and 4.12, and Table 4.4 provide the results for the extended sample collection program (30 minute sampling interval) which was performed in conjunction with the instantaneous sampling program to evaluate the steady state profiles and test repeatability. The results also indicated the product phase reaches steady state within approximately 20 to 30 minutes, but the accumulation of sulphur, ash and coarse coal within the flotation cell and the pyrite separator, causes a steady creep in sulphur throughout the process. Hence, some apparatus modifications were required to eliminate these accumulations and improve experimental repeatability. Nevertheless, flow scheme 1 still demonstrated a high level of experimental repeatability and reproducibility by evidence of Figures 4.13 and 4.14 summarizing results with respect to combustible matter recovery, and the product quality.

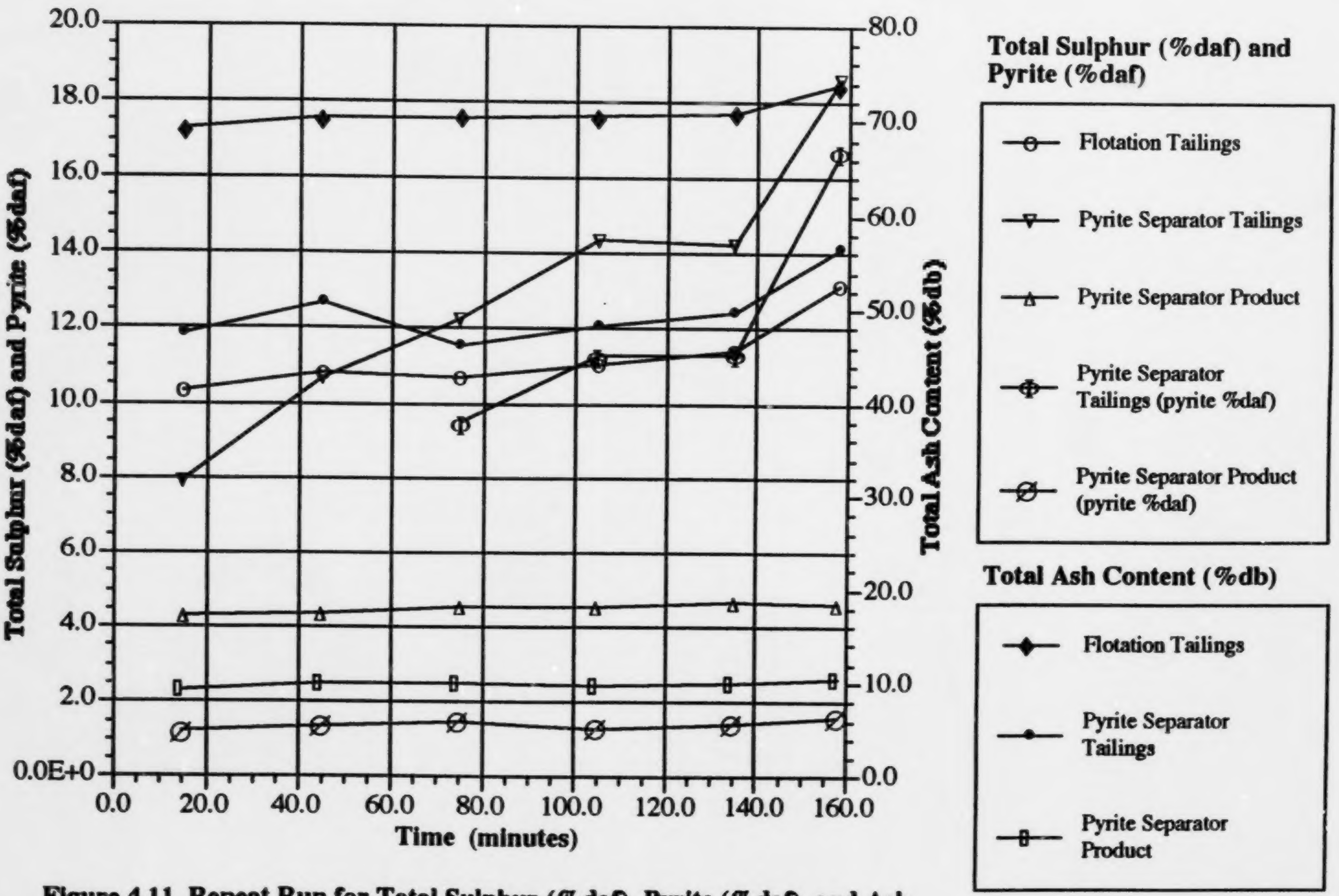

Figure 4.11 Repeat Run for Total Sulphur (%daf), Pyrite (%daf), and Ash Content (%daf) versus Run Time (minutes) for the Thirty Minute Composite Sampling Experiment for Test D6

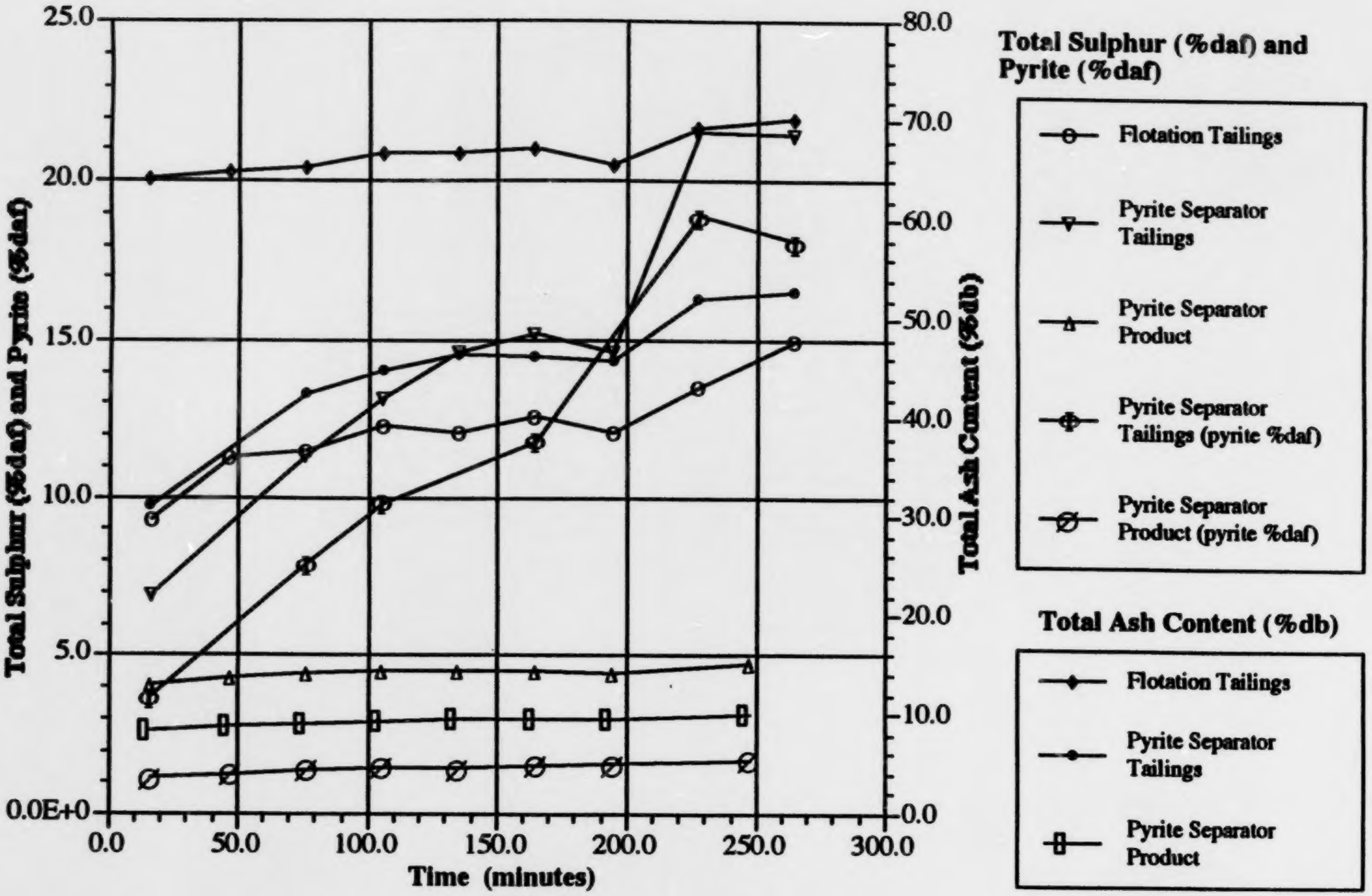

Figure 4.12 Repeat Run for Total Sulphur (%daf), Pyrite (%daf), and Ash Content (%daf) versus Run Time (minutes) for the Thirty Minute Composite Sampling Experiment for Test D7

Table 4.4 Steady State and Repeatability Analysis -Test D6 (30 min. Intervals)

	Time Interval	Flotation Tailings		Pyrite Separator Tailings		Product Phase					Process Responses			
#	min.	Ash % db	TS % daf	Ash % db	TS % daf	PS % daf	Rate g/m	Ash % db	TS % daf	PS % daf	CM R	TS Red.	Red.	Ash Red.
1	0-30	69.0	10.37	47.4	7.93		23.4	9.3	4.31	1.21	74.4	60.0	44.0	84.3
2	30-60	70.2	10.81	50.8	10.68		38.6	9.9	4.37	1.36	78.9	46.5	43.2	82.5
3	60-90	70.4	10.63	46.3	12.29	9.49	32.9	10.0	4.57	1.49	74.5	51.7	40.6	85.0
4	90-120	70.5	11.08	48.4	14.40	11.29	37.3	9.8	4.55	1.32	78.1	48.2	40.9	83.4
5	120-150	70.8	11.42	49.8	14.25	11.33	38.6	10.1	4.68	1.43	77.5	49.0	39.2	83.6
6	150-166	73.9	13.16	56.5	18.63	16.69	16.7	10.6	4.61	1.62	73.0	61.6	40.1	87.6

Table 4.4 Steady State and Repeatability Analysis -Test D7 (30 min. Intervals)

	Time Interval	Flotation Tailings		Pyrite Separator Tailings		Product Phase					Process Responses			
#	min.	Ash % db	TS % daf	Ash % db	TS % daf	PS % daf	Rate g/m	Ash % db	TS % daf	PS % daf	CM R	TS Red.	PS Red.	Ash Red.
1	0-32	64.2	9.32	31.2	6.95	3.69	23.9	8.3	4.11	1.16	72.4	50.1	41.3	84.8
2	32-62	65.0	11.3				38.8	8.9	4.29	1.27	75.5	51.9	38.7	83.6
3	62-91	65.5	11.52	42.5	11.36	7.93	38.3	9.1	4.43	1.40	74.9	50.7	36.7	83.7
4	91-120	66.8	12.28	44.9	13.20	9.85	40.8	9.4	4.50	1.47	75.5	51.3	35.7	83.6
5	120-150	66.7	12.05	46.7	14.64		42.9	9.5	4.50	1.44	76.3	53.2	35.7	82.8
6	150-180	67.2	12.56	46.3	15.17	11.79	39.7	9.6	4.53	1.55	76.1	54.5	35.2	83.0
7	180-210	65.7	12.09	45.9	14.65		38.6	9.6	4.47	1.58	74.9	55.4	36.1	83.4
8	210-285						33.1	10.1	4.73	1.68	80.5	50.5	32.4	81.6
9	210-245	69.3	13.54	52.2	21.55	18.88								
	245-285	70.4	14.97	53.0	21.46	18.09								

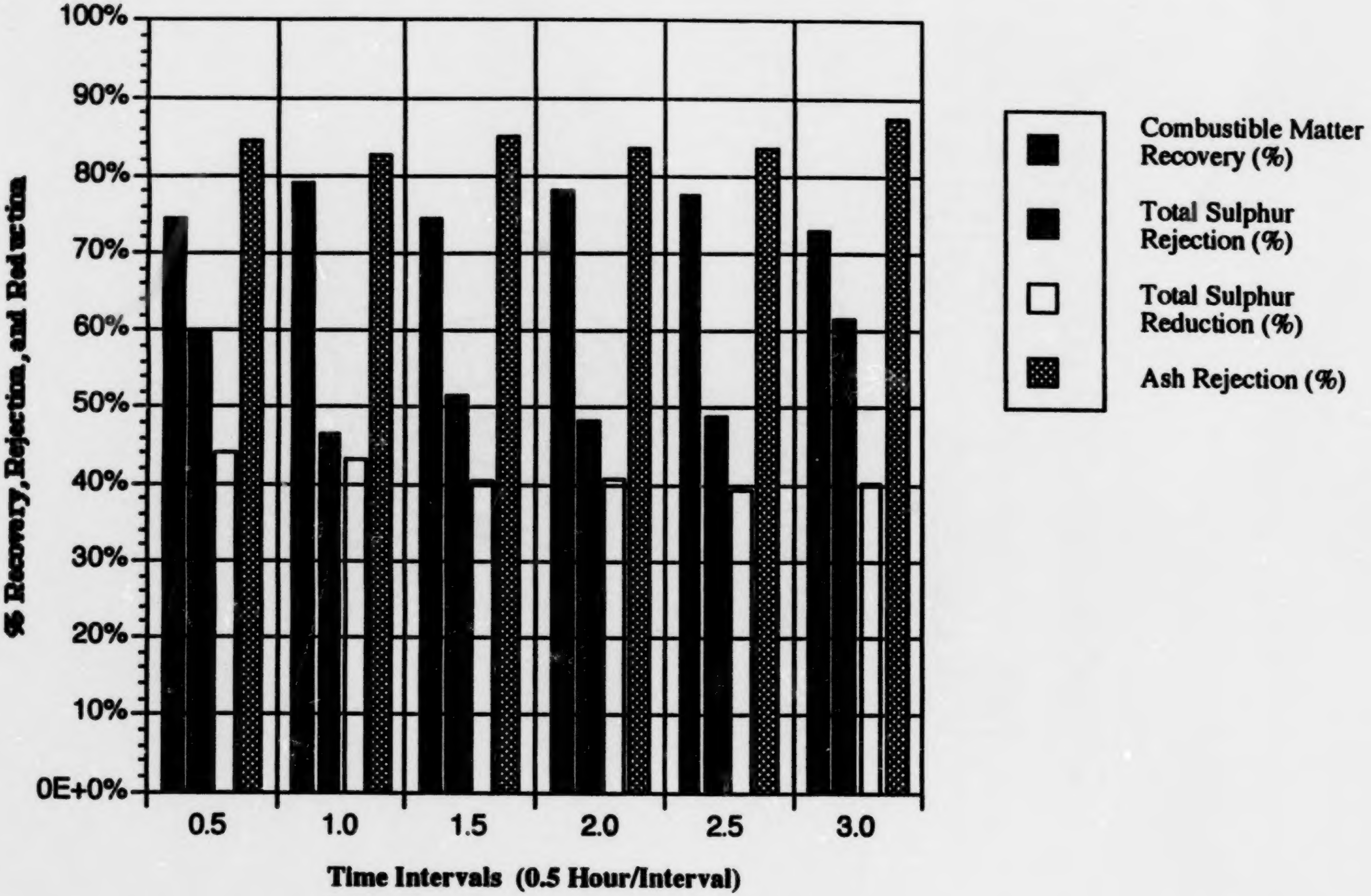

Figure 4.13 Combustible Matter Recovery (%), Total Sulphur Rejection (%), Total Sulphur Reduction (%), and Ash Rejection (%) versus Run Time (hours) for Test D6

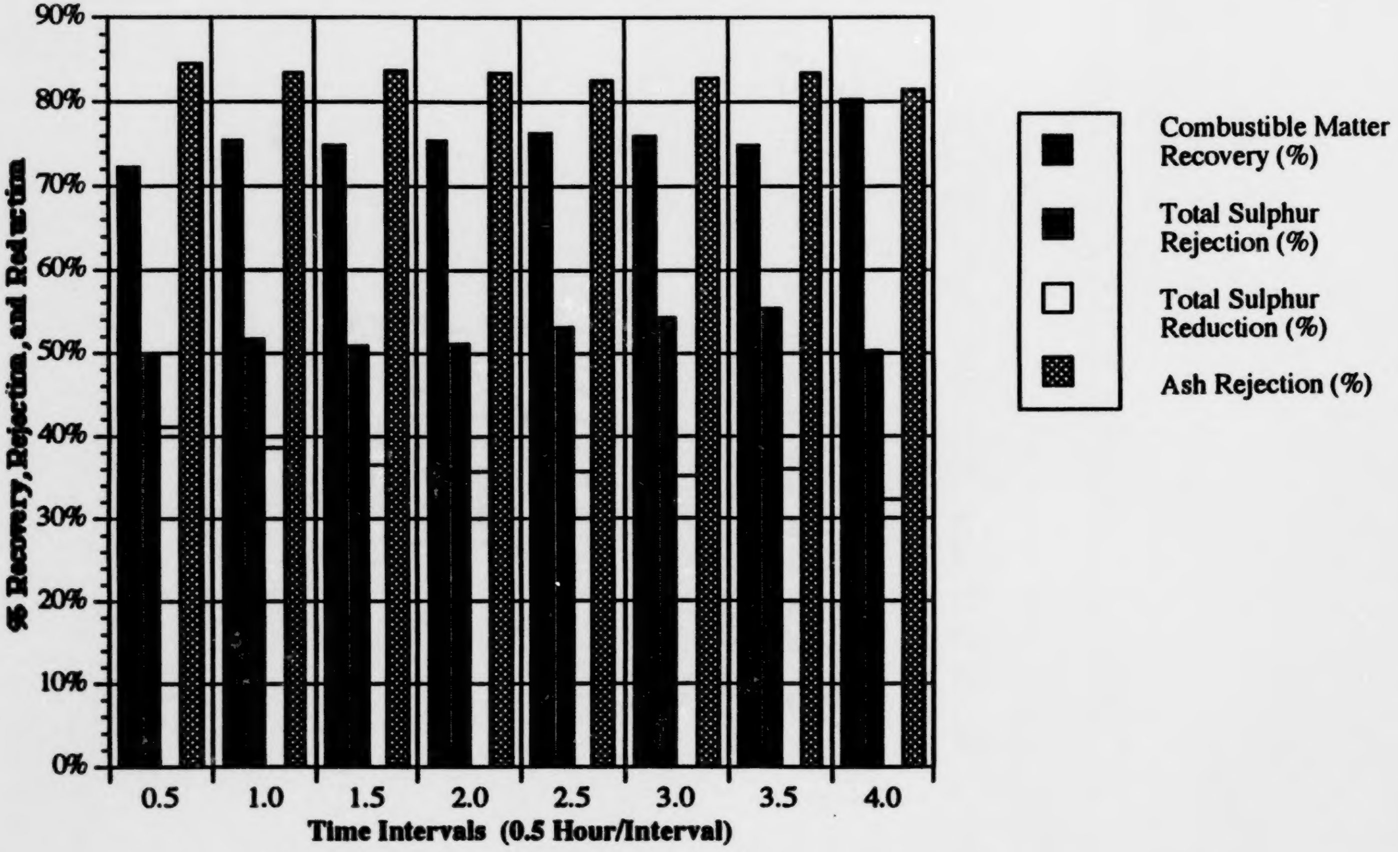

Figure 4.14 Combustible Matter Recovery (%), Total Sulphur Rejection (%), Total Sulphur Reduction (%), and Ash Rejection (%) versus Run Time (hours) for Test D7

The detailed mass balances are summarized for flow scheme 1 and 2 in Tables 4.5 and 4.6, respectively. The results indicated over 95 percent of the total solids, combustible solids, ash solids, and sulphur solids were accounted for in the mass balance preparation for either flow scheme 1 or 2.

Based upon these investigations, it was concluded that a 50 minute unsteady state period was used to permit the system to achieve steady state after process changes were implemented within the apparatus. However, the apparatus would first require further modification to eliminate any sulphur and ash accumulation within the apparatus.

Table 4.5 Detailed Mass Balance For Tests D6 (Flow Scheme 1)

Stream Designation	Combustible Solids (grams)	Ash Solids (grams)	Total Sulphur Solids (grams)	Pyrite Solids (grams)	Total Solids (grams)
Feed Conditions	7043.2	3832.6	502.2	254.3	10875.8
Conditioner Accumulation	32.52	41.7	10.1	9.2	74.2
High Shear Accumulation	16.5	8.1	1.3	.6	24.6
Flotation Cell Accumulation	114.3	309.6	63.9	61.2	423.9
Pyrite Separator Accumulation	14.8	17.2	5.2	4.9	32.0
Samples Extracted	852.5	442.4	54.4		1294.9
Flotation Cell Tailings	802.3	1934.2	89.4		2736.5
Pyrite Separator Tailings	460.5	447.0	58.3		907.5
Pyrite Separator Product	4430.9	469.6	199.9	60.2	4900.5
Total Solids Recovered	6724.2	3669.8	482.4		10,394.0
% Recovery of Solids	95.5	96.0	96.1		95.6

Table 4.5 Continued. Detailed Mass Balance For Test D7 (Flow Scheme 1)

Stream Designation	Combustible Solids (grams)	Ash Solids (grams)	Total Sulphur Solids (grams)	Pyrite Solids (grams)	Total Solids (grams)
Feed Conditions	13,264.9	6236.7	928.5	512.0	19512.6
Conditioner Accumulation	37.4	38.4	11.6	11.2	75.8
High Shear Accumulation	20.1	7.4	1.3	.7	27.5
Flotation Cell Accumulation	103.0	299.4	58.6		402.4
Pyrite Separator Accumulation	52.3	49.6	24.0	21.4	101.8
Samples Extracted	556.3	243.7	35.2		800.0
Flotation Cell Tailings	1797.6	3610.6	219.9		5408.3
Pyrite Separator Tailings	907.8	727.0	124.1		1634.8
Pyrite Separator Product	9225.6	11,003.8	414.5	136.9	10,229.4
Total Solids Recovered	12,700.2	5979.3	889.1		18,679.9
% Recovery of Solids	95.7	95.6	95.8		96.0

Table 4.6 Detailed Mass Balance for Tests E 12-18 (Flow Scheme 2)

Stream Designation	Combustible Solids (g/min.)	Ash Solids (g/min.)	Total Sulphur Solids (g/min.)	Pyrite Solids (g/min.)	Total Solids (g/min.)
Feed Conditions	53.1	24.3	3.2	1.7	77.9
Flotation Cell #1 Settlings	.65	1.91	.41	.37	2.56
Pyrite Separator Settlings	.52	.41	.09	.08	.93
Flotation Cells Tailings	2.71	10.28	.37		12.99
Pyrite Separator Tailings	6.82	4.94	.50		11.76
Pyrite Separator Product	40.75	5.58	1.70	.58	46.33
Total Solids Recovered	57.45	23.12	3.07		74.57
% Recovery of Solids	96.9	95.3	94.9		95.7

Table 4.6 Detailed Mass Balance for Tests e13-3 (Flow Scheme 2)

Stream Designation	Combustible Solids (g/min.)	Ash Solids (g/min.)	Total Sulphur Solids (g/min.)	Pyrite Solids (g/min.)	Total Solids (g/min.)
Feed Conditions	49.85	22.94	3.17		72.79
Flotation Cell #1 Settlings	.27	.72	.18		.99
Pyrite Separator Settlings	1.75	1.31	.29		3.06
Flotation Cells Tailings	.63	3.07	.07		3.70
Pyrite Separator Tailings	11.48	13.30	1.09		24.78
Pyrite Separator Product	35.37	4.51	1.51		39.88
Total Solids Recovered	49.50	22.91	3.14		72.40
% Recovery of Solids	99.3	100	99.1		99.5

4.2.3 Series 3 Apparatus Modifications

Based upon the investigations performed with flow scheme 1, several apparatus modifications were made to eliminate the accumulation of sulphur and ash rich particles in the process. Flotation cell 2 was designed and fabricated with conical shaped bottoms, and settling vessels to remove any sulphur or ash rich particles that would normally accumulate in the bottom of the flotation cell. Furthermore, settling vessels were also installed in the pyrite separator to remove any bottom accumulations. Solid rubber stoppers were installed in the conditioning, and high shear mixers to eliminate accumulations in the small cylindrical space associated with the bottom drain valve.

In addition to these modifications, a second flotation cell and a second high shear mixer was installed to expand the capabilities of the apparatus for investigation of operating parameters. Commissioning tests were performed to demonstrate repeatability and these results are presented in Table 4.7 and Figure 4.15.

Table 4.7 Steady State Analysis and Test Repeatability for Flow Scheme 2

Test Interval	Run Time	Product Phase		
#	min.	Ash % db	TS % daf	Comb. Rec. %
E9-1 to 2	65	10.40	4.64	75.2
	85	10.80	4.64	77.1
E9/3 to 6	95	8.0	3.99	67.1
	125	8.3	4.01	68.1
	155	8.2	3.98	64.0
	185	8.1	3.97	62.2
E 10/9 -10	75	14.6	4.31	46.4
	86	15.0	4.28	46.7
E 10/11-12	145	14.2	4.06	80.0
	156	14.3	4.07	77.9
E 11/14-16	215	13.8	4.86	86.4
	227	14.0	4.92	86.6
E 12 1 to 3	55	12.3	3.56	70.0
	115	12.0	3.61	72.8
	175	12.0	3.54	70.3

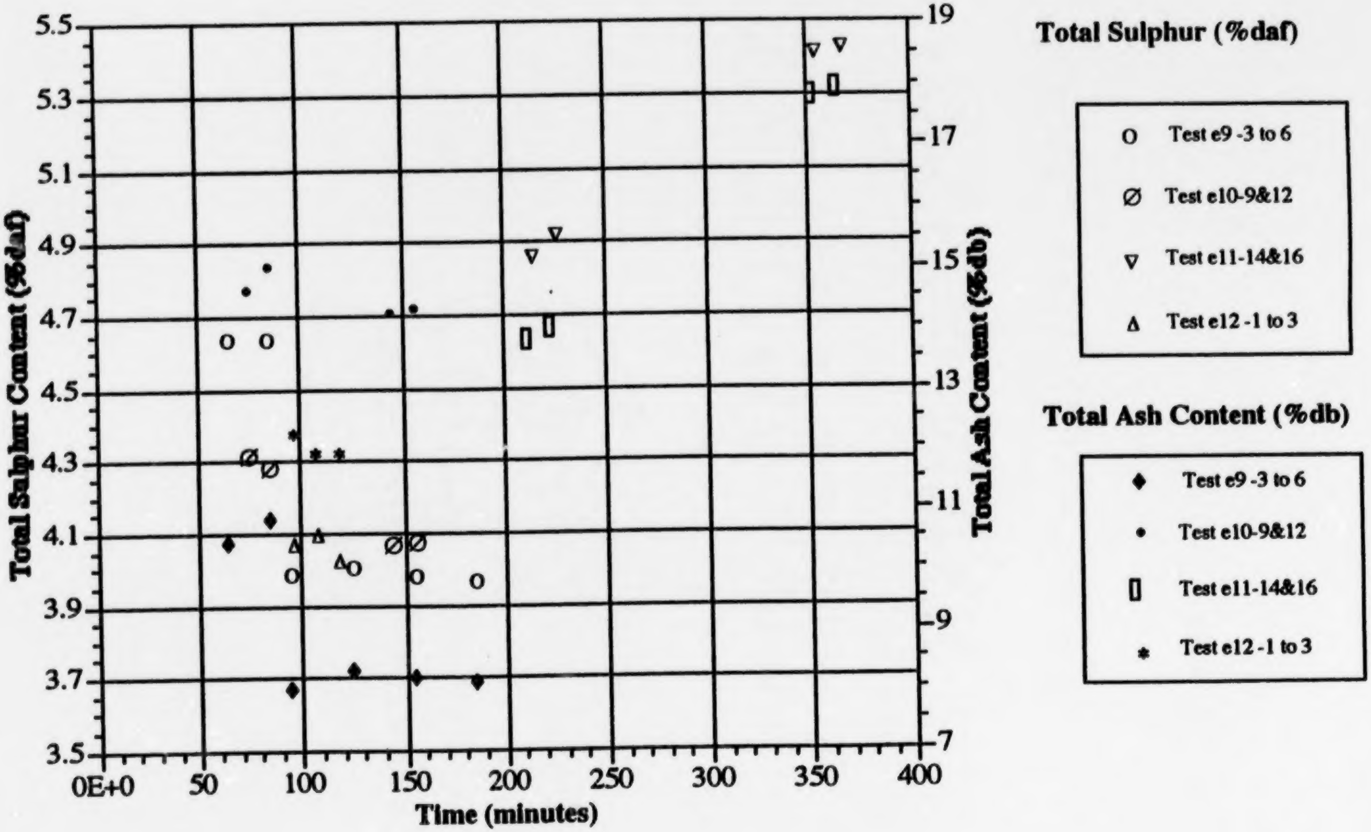

Figure 4.15 Repeat Runs for Total Sulphur (%daf), and Ash Content (%db), versus Run Time (minutes) for a Ten Minute Sampling Interval for Experiments E9,E10,E11,E12, and E13.

4.3 Phase 3 Experimentation Investigations

Two test methods were developed and used in the experimental program. A system performance method was used to improve the economy of experimentation and was based upon feed and product measurements and samples only. The detailed mass balance involved the measurement of all streams, and was used primarily to evaluate the individual process performance of the flotation and the pyrite separator stages, and to provide detailed information related to experimental method.

4.3.1 System Performance

The system performance method was used to generate the data base from which the process could be evaluated. The product phase was sampled 50 minutes after a process change was implemented. A 10 minute sample was extracted from which the mass flow rate and assay analysis of the product was determined. The composite feed sample and mass flow rate measurements completed the basis from which a performance calculation was derived.

4.3.2 Detailed Mass Balance Experimental Procedure

The detailed mass balance experiments involved a comprehensive sampling program. The entire process was sampled in detail during a 10 minute interval. The sampling program is described in below and in Figure 4.16:

- the pyrite separator product,
- the pyrite separator tailings,
- the pyrite separator settlings,
- both flotation cells products (only for assays),
- the flotation tailings, and
- the flotation settlings.

4.3.3 Washability Tests

The composite sample collected during tests E10 and E11 were sub-divided utilizing a bench scale riffle sampling device. A sample of approximately 200 g was

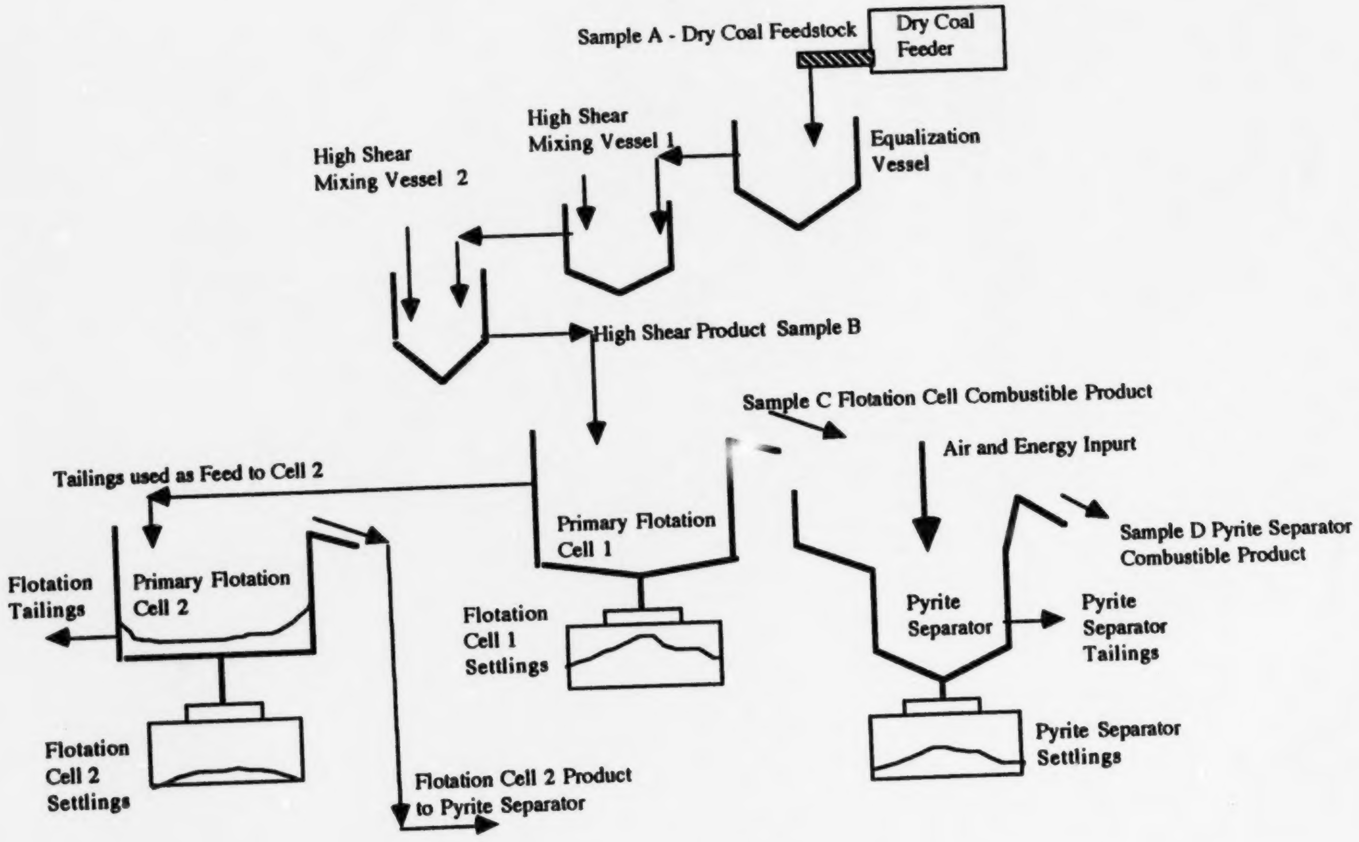
Sample A - Dry Coal Feedstock
Dry Coal Feeder
Equalization Vessel
High Shear Mixing Vessel 1
High Shear Mixing Vessel 2
High Shear Product Sample B
Sample C Flotation Cell Combustible Product
Air and Energy Inpurt
Sample D Pyrite Separator Combustible Product
Primary Flotation Cell 1
Flotation Cell 1 Settlings
Pyrite Separator
Pyrite Separator Tailings
Pyrite Separator Settlings
Tailings used as Feed to Cell 2
Flotation Tailings
Primary Flotation Cell 2
Flotation Cell 2 Settlings
Flotation Cell 2 Product to Pyrite Separator

Figure 4.16 Sample Location for Flowsheet 2

submitted for washability analysis at the University of Alberta, Department of Mining, Metallurgy, and Petroleum Engineering. The sample was subsequently further subdivided into two samples, one for wet screen analysis and the second for washability analysis. Because of the extremely high mineral matter content of the sample, static washability analysis would not produce reliable results, as the extremely fine mineral matter would hang-up because of the fluid viscosity and resulting drag forces, inhibiting the differential settling. Hence, the procedure used relied on increasing the gravitational forces to promote a distinct rate of differential particle settling. The procedure followed the steps below:

- Heavy media liquids were prepared for specific gravity's of 1.4, 1.5, 1.6, 1.8 and 2.0 g/cm^3. The heavy liquids were selected as to not influence the total sulphur content, or mineral matter content of the sample.
- Ten samples approximately 8 g in mass were sub-sampled from the composite sample using standard protocol from ASTM sampling procedures. These samples were subsequently prepared into 50 mL centrifugal vials. The sample was mixed thoroughly within the vial and spun at various speeds in a laboratory centrifuge until distinct float and sink fractions could be observed.
- The float and sink fractions were then separated and the same procedure was performed again to ensure particle entrapment did not cause either a portion of the floats to report to the sinks fraction, or vise versa. The resulting floats and sinks were combined and dried for mass determinations, and subsequently prepared for moisture, ash and total sulphur analysis.

4.4 Experimental Design

Five main factors and their interactive effects on Combustible Matter Recovery (% CMR), and Total Sulphur (% daf) and Total Ash (% db) content in the product phase, were investigated. In addition, two main factors varied with the experimental program, percent solids in the product phase and sample age. Table 4.8 summarizes all main factors of the experimental program.

Table 4.8 Main factors of the Experimental Design

Main Factor Numbers	Main Factor Descriptions
X1	% Solids in Pyrite Separator Product
X2	Oil Concentration % daf
X3	Frother Concentration % daf
X4	Energy Input J/L
X5	Average System Temperature (Celsius)
X6	Feed Coal Particle Size (d80)
X7	Sample Age (Days)

The experimental program used factorial experimental design to investigate five main factors, and the program is divided into two blocks of testing. The first block of tests investigated high (1) and low (-1) variable levels of the five main factors. The second block of tests were performed at the center point levels (0), and mid range levels (+.707 and -.707) to further investigation the process response surface. The sample used in the second block of tests was aged for 45 days after grinding to the center point size level. Table 4.9 summarizes the measured set points, ranges of investigations, and the percent relative error associated with the measured set points.

Table 4.9 Experimental Set Points

Main Factor Number	Description	Code Main Factor	Measured Set Point	Range
X1	% Solids in Product			7 to 25 %
X2	Oil Content (% daf)	+1	2.08	0.93 to 2.08 %
		-1	0.93	
		0	1.48	
		+.707	1.87	
		-.707	1.07	
X3	Frother Content (% daf)	+1	.038	0.012 to 0.038 %
		-1	.012	
		0	.026	
		+.707	.033	
		-.707	.017	
X4	Energy Input (kJ/l)	+1	15.6	10
		-1	10.4	
		0	13.2	
		+.707	14.9	
		-.707	11.0	
X5	Average System Temperature (Celsius)	+1	45	
		-1	20	
		0	29	
		+.707		
		-.707		
X6	Feed Coal Particle Size (d_{80})	+1	200	90 to 200 μm
		-1	90	
		0	150	
X7	Sample Age (Days)	+1	41-45	1 to 45 days
		-1	1-10	

5.0 Analytical Procedures

Six assays were determined by laboratory analysis and the methods and equipment used are summarized below in Table 5.1.

Table 5.1 Summary of Analytical Instruments and Methods

Assay Type	Method or Analyzer Used
Moisture (%)	Leco TGA 500 Proximate Analyzer, Based upon ASTM Instrument Proximate Analysis.
Ash (% db)	Leco TGA 500 Proximate Analyzer, Based upon ASTM Instrument Proximate Analysis.
Total Sulphur (% db)	Leco SC432 Sulphur Determinator, ASTM - D2492-90
Pyrite Sulphur (% db)	ASTM - D2492-90
Sulphatic Sulphur (% db)	ASTM - D2492-90
Organic Sulphur (% db)	By difference

The moisture determinations were based upon weight loss at 110 °C in a inert atmosphere of nitrogen gas. For each batch of samples prepared for analysis, laboratory prepared standards are also submitted for analyses. The analyzer was calibrated every morning and afternoon with an approved National Bureau of Standards Reference Material (NBS RM) usually provided by the instrument manufacturer.

Ash determinations are performed in two stages. The first stage of combustion is performed at 450 to 500° C for approximately 1 hour to drive off the SO_2 from the sample. The second stage involves combustion at 750° C in an air oxidizing atmosphere, from which the ash content was determined. Laboratory standards are also submitted with each batch of samples as a quality control and assurance program, and calibrations were performed daily with NBS RM standards to confirm analyzer accuracy. All moisture and ash contents were performed in duplicate.

The total sulphur determinator contains a furnace which combusts the sample at 1400° C in a pure oxygen atmosphere. The combustion products are then passed through scrubbing and filtering systems to clean the gases of particulate and water. The clean gas stream was then fed through an infared detector to determine the sulphur content. The infared detector is calibrated for the SO_2 wave length, and the calibration provides for the sulphur determination. The SO_3 and SO_2 equilibrium can influence the calibration, hence, the estimated sulphur content of the sample was required prior to determination to ensure the instrument was calibrated is the appropriate range. Laboratory standards are performed every five samples to ensure ongoing quality control and assurance. Calibrations with NBS RM were performed every morning and afternoon in the sulphur ranges corresponding to the estimated content of the samples being analyzed. Every total sulphur analysis was performed in duplicate.

The pyrite determinations involve a hydrochloric extraction to remove all iron except that associated with pyrite. All the sulphatic sulphur component is extracted in this step. The sulphatic sulphur extract was analyzed for sulphur content by Inductively Coupled Argon Plasma Atomic Emission Spectrometry (ICAP AES). The iron pyrite remaining in the residual was extracted with nitric acid and this sample was also analyzed for pyrite iron by ICAP AES. Laboratory standards were prepared for both extraction procedures.

6.0 Calculations

Experimental calculations are categorized as main factor dimensional analysis, process performance calculations, and regression analysis calculations.

6.1 Main Factor Dimensional Analysis

To facilitate the analysis of the results, the dimensional form of all main factors within the experimental program were analyzed. When possible, a dimensionless form for the main factor was utilized. Wherever not possible, the industrially accepted dimensional form of the main factor was utilized. Table 6.1 contains the algorithms used to express all factors in the appropriate form. Included are the following:

- Percent solids content in the product phase is represented as the total dry mass of solids material divided by the total mass of water and solids which is recovered in the product phase.

- Oil content used in the high shear mixer is expressed on a % daf basis as the total oil mass flow rate divided by the total carbonaceous solid mass feed rate. The total carbonaceous solids mass flow rate is based upon the ash determinations for the feed coal.

- Frother content used in the process is also expressed on a % daf basis as the total frother mass flow rate divided by the carbonaceous solid mass feed rate.

- Energy input to the high shear mixers is given as the total power per unit volume, and is expressed in J/L. This calculation was provided by the measurement of impeller torque and revolutions per minute, and the hydraulic detention time and volume of the mixing system.

- System temperature is expressed in °C and is determined as the average temperature within the high shear mixers, primary flotation cells and the pyrite separator.

- Feed coal particle size is expressed as the d_{50}, which is the size where 50 percent of the feed coal will pass in a wet screen analysis. The d_{50} size is determined based upon a logarithmic model describing each feed coal particle size distribution. The calibrated model form is based upon the Gaudin-Schumann model for particle size distribution (Weiss, 1985).

- Sample age is expressed in days lapsed from the grinding of the feed coal into their respective size distributions, until when the actual tests were performed.

Table 6.1 Algorithms Describing the Main Factors Dimensional Analysis

Main Factor	Algorithm
Solids content (%)	(dry product solids mass(g/min.)/total product mass(g/min.))
Oil content (% daf)	(oil mass rate(g/min.)/carbonaceous solids rate(g/min.))
Frother content (% daf)	(frother mass rate(g/min.)/carbonaceous solids rate(g/min.))
Energy input (J/L)	(power input(W)*detention time(min.)/Slurry Flowrate(L/min.)), where power in Watts is described as, torque(N-m)*w(revolutions/s), which is expressed as, J/s or Watts, and detention time over slurry flowrate is described as, Rt/Q, which is expressed as, s/L/s, combining the two expression yields energy input expressed as, J/L
Temperature (^{o}C)	(high mixer temperature+primary flotation cell temperature+pyrite separator temperature)/3
Particle size d_{50}(microns)	-Model Calibration of Particle Size Distribution Based on a Gaudin-Schumann model form of $y =(x/k)^m$, where, x =particle size in microns, and, y =% of feed coal passing the size x. -Determination of d_{80} is based upon the calibrated model expressed in microns.
Sample age (days)	(date of test run-date of grinding)

6.2 Process Performance Calculations

To evaluate the results from the experimental program, the following process performance responses were calculated. Table 6.2 provided for the algorithms used in these calculations.

- Combustible Matter Recovery (CMR (%)) is calculated based upon the carbonaceous matter flow rate of the product phase divided by the carbonaceous matter flow rate of the feed coal.

- Total Sulphur Content (TS (% daf)) in the product phase is expressed on a % daf basis and is based upon the sulphur, ash, and moisture determinations. The value is calculated as the dry mass of total sulphur divided by the dry mass of total carbonaceous matter within the sample. Percent daf is an independent expression of sulphur content; and is preferred over % db because changes in ash content would artificially alter the total sulphur assay.

- Total Ash Content (Ash (% db)) in the product phase is expressed on a % db. This value is based on the ash and moisture determinations of the sample, and is calculated as the dry mass of ash divided by the dry mass of total solids.

- The theoretical cleaning potential of both ash and total sulphur (TCPA & TCPS) were estimated based upon washability analysis of float and sink tests at various density fractions. The TCPS and TCPA are plotted against the recovery of combustible matter based upon the separate density fractions analyzed.

- The total sulphur emission rate per unit of energy (kg/kJ) is determined by relating the total sulphur content of the product (% daf) to the estimated energy content of the product expressed in kJ/kg. The energy content of the product is adjusted in accordance to the product quality in terms of ash content.

Table 6.2 Algorithms Describing the Process Performance Calculations

Process Response	Algorithm
CMR (%)	(combustibles in product(g/min.)/combustibles in feed(g/min.)), which can be further defined as, (product rate (g/min.)*(100-moisture(%))*(100-ash(% db)))/(coal feed rate(g/min.)*(100-moisture(%))*(100-ash(% db)))
TS (% daf)	(total sulphur in sample(g)/combustibles in sample(g), which is defined as, sulphur in sample(g)/(sample mass(g)*(100-moist.(%))*(100-ash(% db)))
ash (% db)	(total ash in sample(g)/combustible is sample(g), which is defined as, ash in sample(g)/(sample mass(g)*(100-moist.(%)))
TCPA &TCPS	graphic evaluation (see Figures 8.1 and 8.2)
Sulphur Emission (kg/kJ)	(Mass of Coal (kg/hr)*(TS % db))/(Mass of Coal (kg/hr)*Q), where, Q_C is the heat content of the product at its specified ash content, (see Table 7.4 and Figure 7.1)

Other performance calculations used extensively in the industry, and included in the Section 8 summary of results, are described in Table 6.3. These include total ash rejection (%), total sulphur and pyrite rejections, inorganic sulphur rejection, total sulphur and pyrite reduction, and inorganic sulphur reduction. The fundamental distinction between rejection and reduction calculations is rejection is based upon solids mass balance flows, and reduction is based only on changes in chemical assay analysis. Reduction calculations are preferred for reporting sulphur removals because of the dependency of the sulphur rejection calculation on the ash component.

Table 6.3 Rejection and Reduction Algorithms

Component	**Algorithm**	**Calculation**
Total Sulphur (TS.)	Rejection	({[TS. Feed Coal (kg/hr)]-[TS. Product (kg/hr)]} /[TS. Feed Coal (kg/hr)])
Pyrite Sulphur (PS.)	Rejection	({[PS. Feed Coal (kg/hr)]-[PS. Product (kg/hr)]} /[PS. Feed Coal (kg/hr)])
Ash	Rejection	({[ASH Feed Coal (kg/hr)]-[ASH Product (kg/hr)]} /[ASH Feed Coal (kg/hr)])
Total Sulphur (TS)	Reduction	({[TS Feed Coal (% daf)]-[TS Product (% daf)]} /[TS Feed Coal (% daf)])
Pyrite Sulphur (PS)	Reduction	({[PS Feed Coal (% daf)]-[PS Product (% daf)]} /[PS Feed Coal (% daf)])

7.0 Feed Coal Characterization

Table 7.1 summarizes the proximate analyses of the test coal. The results indicate the average as received moisture content is 8.6 percent, the range is from 6.58 to 9.85 percent. The volatile matter is 30.56 % db, and the fixed carbon content is 31.36 % db. These average values can also be expressed on a % dmmf basis by means of the Parr formula to assist in characterizing the test coal. Hence, Table 7.1 also indicates the volatile matter is 48.2 expressed on a % dmmf basis, and the fixed carbon is 49.5 % dmmf. The average ash content of the test coal is 33.0 % db, and the mineral matter is 36.6[a] % db.

Table 7.1 Proximate Analysis of Test Coal

Component	%	Range	% db	% daf	% dmmf
As Received Moisture	8.07[a]	6.58 to 9.85[a]			
Volatile Matter			30.56	45.6	48.2
Fixed Carbon			31.36	46.8	49.5
Ash Content			33.0[b]		

[a] This mineral matter content was estimated with the use of the Parr equation (see section 2.4.3)

[b] This data represents the analysis of the coal samples extracted for the experimental program. All other information in this table was based upon analysis of the coal samples received by the Alberta Research Council which were very similar in characteristics, and which, in effect represent the bulk source of the test coal for this experimental program.

Table 7.2 contains the ultimate analysis for the test coal providing information describing the carbon, hydrogen, nitrogen, oxygen, and chlorine contents, expressed on a % db, % daf and % dmmf bases. The results indicate the test coal contains 45.97 % db carbon, 3.46 % db hydrogen, 0.8 % db nitrogen, and 7.43 % db oxygen.

Table 7.2 Ultimate Analysis[a] of Test Coal

Component	% db	% daf	% dmmf
Carbon	45.97	68.6	72.5
Hydrogen	3.46	5.16	8.14
Nitrogen	0.80	1.19	1.26
Oxygen (by difference)	8.39	12.5	13.2

[a] These ultimate analysis results are based upon the bulk coal samples received by the Alberta Research Council, which were similar in chemical contents, and were used to characterize the test coal prior to experimental investigations.

Table 7.3 summarizes the ash and sulphur contents of the three samples extracted from the test coal bank, and used in the experimental program. These include ash and sulphur assays for the fine, coarse and medium size distributions. The average ash content of the coal samples used in the experimental program was 33.0 % db, and did not appear to vary significantly in the program. The average total sulphur content was 6.63 % daf, and did appear to demonstrate a variation between the three barrel samples used in the test program. The pyrite sulphur content was 4.36 % daf and constitutes approximately 66 % of the total sulphur in the coal. The sulphatic and organic levels were 0.63 % daf and 2.31 % daf, respectively.

Table 7.3 Ash and Sulphur Contents of the Test Coal

Coal Sample Description	Total Ash Content % db	Total Sulphur Content % daf	Pyrite Sulphur Content % daf	Sulphatic Sulphur Content % daf	Organic Sulphur Content % daf
Fine Coal d_{80}=90 μm	32.7	6.62	4.36	.55	2.26
Coarse Coal d_{80}=200 μm	34.1	6.90	4.60	.69	2.30
Medium Coal d80=150 μm	32.2	6.37	4.01	0.66	2.36
Averages	33.0	6.63	4.36	.63	2.31
Standard Deviation	0.98	0.27	0.30	0.07	0.05
% Relative Error	3.0	4.0	6.8	11.6	2.2

Table 7.4 and Figure 7.1 describe how the heat content of the test coal varies with ash content. The heat content is provided both in kJ/kg and BTU/LB, and is plotted against the final ash content of the coal, expressed in % db. The calorific value determinations were developed using an adiabatic calorific reactor following ASTM standards.

Table 7.4 Calorific Value versus Sample Ash Content

Ash (% db)	Heat Content (Btu/LB)[a] % db basis	Calorific Value[a] (kJ/kg) % db basis	Calorific Value[a] (kJ/kg) % daf basis	Calorific Value[b] (kJ/kg) % dmmf basis
39.0	8350	19,409	32,896	Not Applicable
10.6	12,760	29,660	33,177	33,696
6.8	13,380	31,101	33,370	33,732

[a] Linear regression of the above data is provided in Figure 7.1.

[b] Calculation of heat content based upon a % dmmf basis was performed by means of the Parr formula, (see Berkowitz, 1979)

Based upon these results and ASTM Standards, the test coal was classified as a High Volatile A Bituminous Coal Sample.

Table 7.5 and Figures 7.2, 7.3 and 7.4 describe the particle size distributions of each of the test coals prepared. These figures contain the cumulative percent passing and retained masses plotted against the screen size. The results indicate that Test E10 has a d_{50} of 80 μm and d_{80} of 208 μm. The finest size is Test E11, which had a d_{50} of 47 μm and a d_{80} of 88 μm. The medium size distribution was Test E12, which had a d_{50} of 73 μm and a d_{80} of 154 μm.

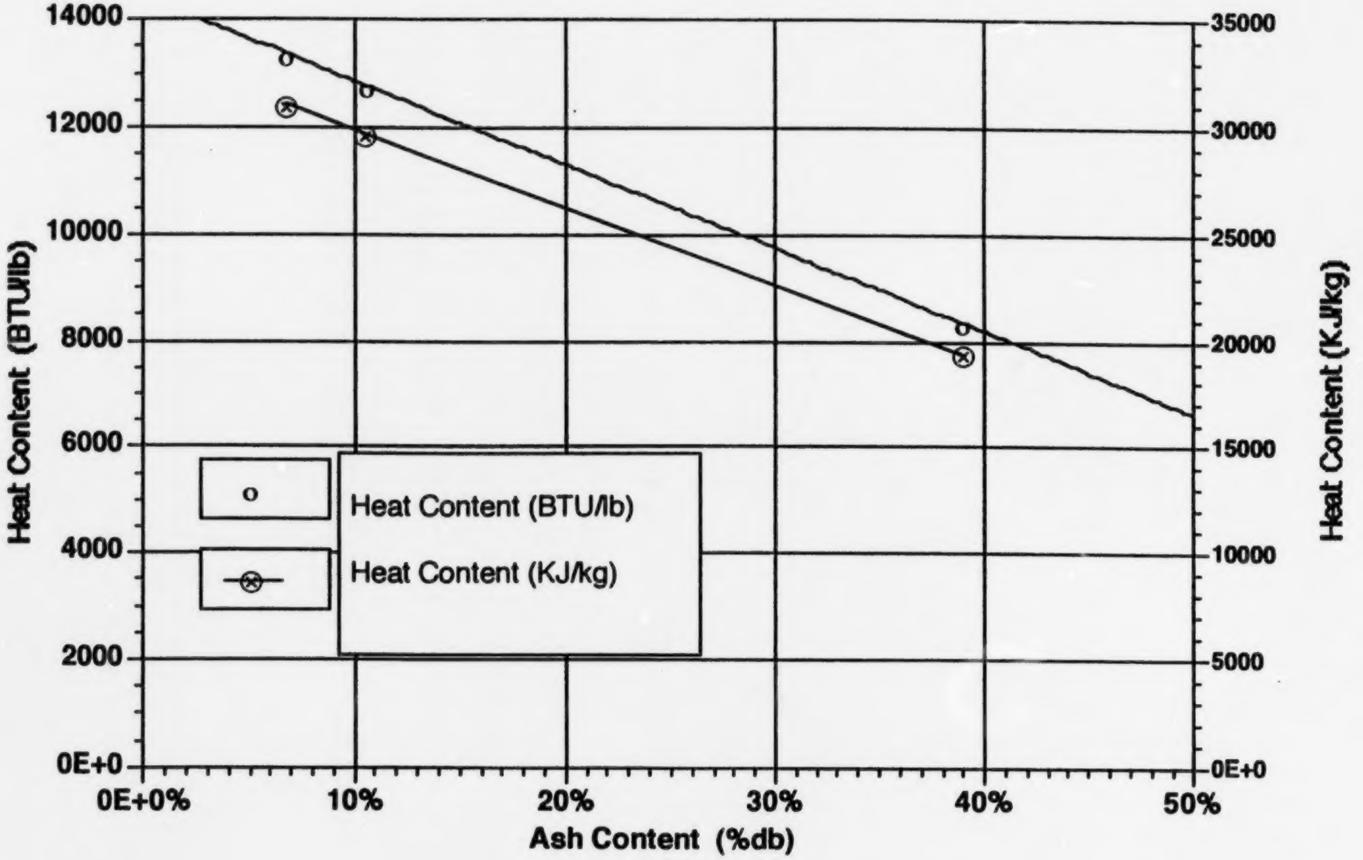

Figure 7.1 Heat Content of Illinois No. 6 ROM Coal (BTU/LB and kJ/kg) versus Ash Content (% db)

Table 7.5 Size Analysis Data for Test Coals E10, E 11, and E 12

Coarse E10
d50=80 um
sg

screen	wt g	wt %	cum wt % pass	pass size um	cum wt % retain	ret. size um
>300	8.11	2.98%	100.00%	-	2.98%	300
>212 to 300	46.33	17.01%	97.02%	300	19.99%	212
>150 to 212	30.85	11.33%	80.01%	212	31.32%	150
>150 to 75	57.87	21.25%	68.68%	150	52.57%	75
>75 to 53	18.21	6.69%	47.43%	75	59.26%	53
>53 to 45	8.95	3.29%	40.74%	53	62.54%	45
>45 to 38	6.15	2.26%	37.46%	45	64.80%	38
-38	95.85	35.20%	35.20%	38	100.00%	
total	272.32	100%				

Medium E12
d50=73 um
sg

screen	wt g	wt %	cum wt % pass	pass size um	cum wt % retain	ret. size um
>300	0.40	0.4%	100.0%	-	0.39%	300
>150 to 300	21.18	20.5%	99.6%	300	20.92%	150
>75 to 150	28.95	28.1%	79.1%	150	48.98%	75
>53 to 75	8.83	8.6%	51.0%	75	57.54%	53
>45 to 53	4.05	3.9%	42.5%	53	61.47%	45
>38 to 45	1.92	1.9%	38.5%	45	63.33%	38
-38	37.83	36.7%	36.7%	38	100.00%	
total	103.16	100.0%				

Fine E11
d50=47 um
sg

screen	wt g	wt %	cum wt % pass	pass size um	cum wt % retain	ret. size um
>150	16.80	7.06%	100.00%	-	7.06%	150
>106 to 150	14.70	6.17%	92.94%	150	13.23%	106
>75 to 106	23.80	9.99%	86.77%	106	23.22%	75
>53 to 75	30.80	12.93%	76.78%	75	36.16%	53
>45 to 53	10.70	4.49%	63.84%	53	40.65%	45
>38 to 45	14.97	6.29%	59.35%	45	46.94%	38
-38	126.35	53.06%	53.06%	38	100.00%	-
total	238.12	100%				

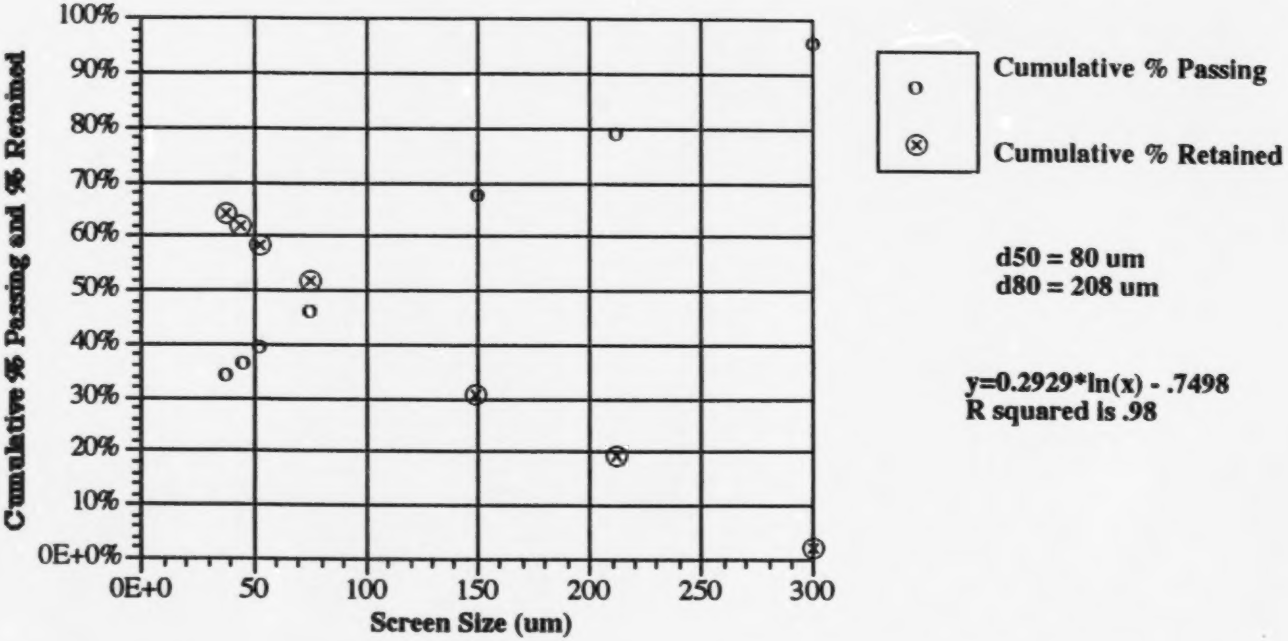

Figure 7.2 Cumulative % Passing and % Retained vs. Screen Size for Tests E 10 and E 13

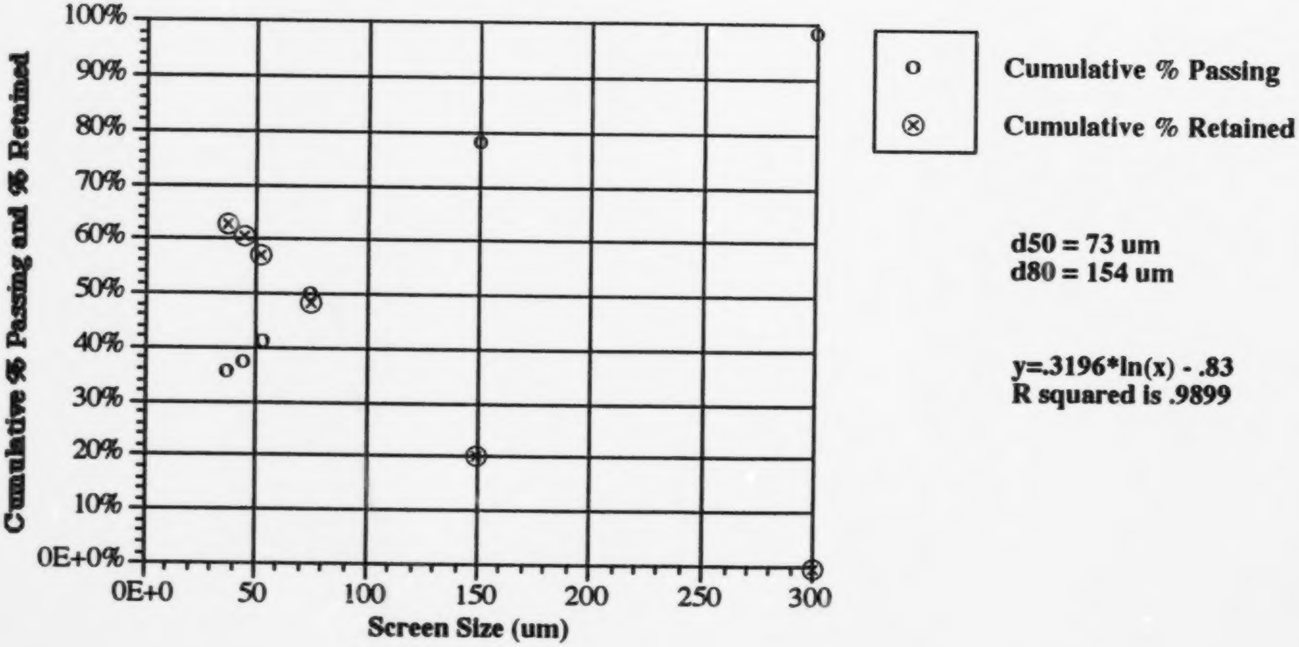

d50 = 73 um
d80 = 154 um

y=.3196*ln(x) - .83
R squared is .9899

Figure 7.3 Cumulative % Passing and % Retained vs. Screen Size for Test E 12

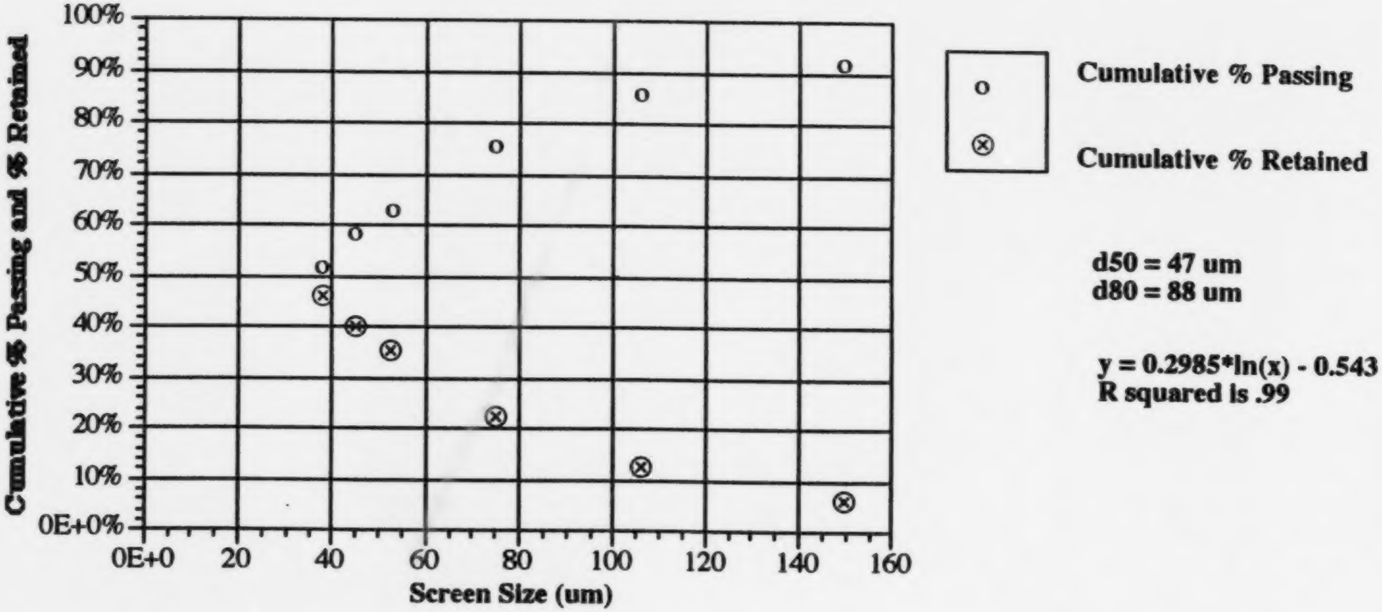

d50 = 47 um
d80 = 88 um

y = 0.2985*ln(x) - 0.543
R squared is .99

Figure 7.4 Cumulative % Passing and % Retained vs. Screen Size for Test E 11

8.0 Results

8.1 Process Performance

Figure 8.1 was prepared to compare the sulphur removal efficiency of the process to the theoretical potential based upon the washability tests performed. It contains the sulphur washability data collected for the tests E 10 and E 11, and all product TS (% daf) assays determined during the test program. Figure 8.2 contains a similar graphical analysis prepared for the ash content from the washability analysis, and product samples generated from the experimental program. The raw data and washability analysis is provided in Tables 8.1 and 8.2.

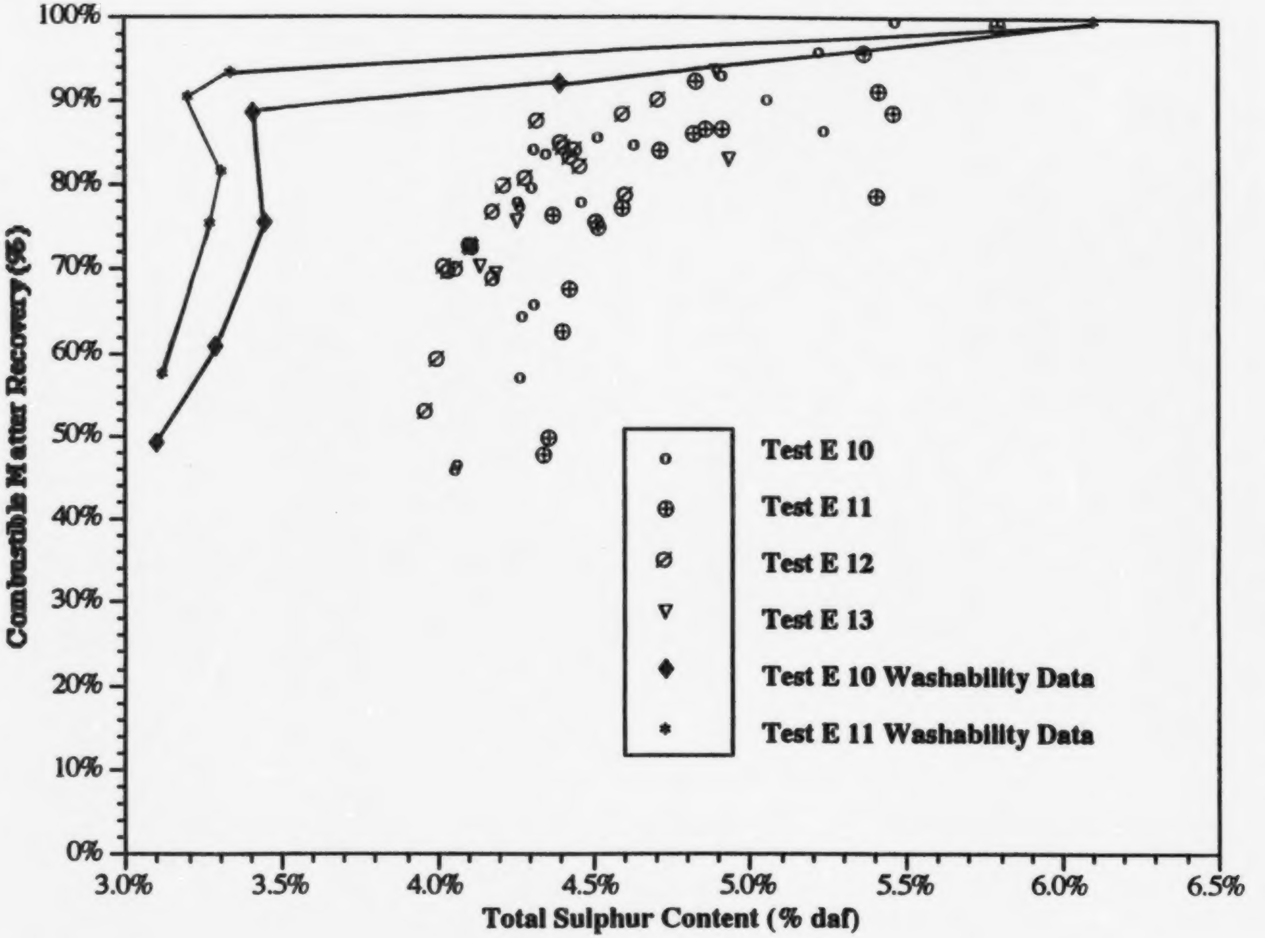

Figure 8.1 % Combustible Matter Recovery vs. Total Sulphur Content (% daf) for Tests E 10, E 11, E 12 and E 13

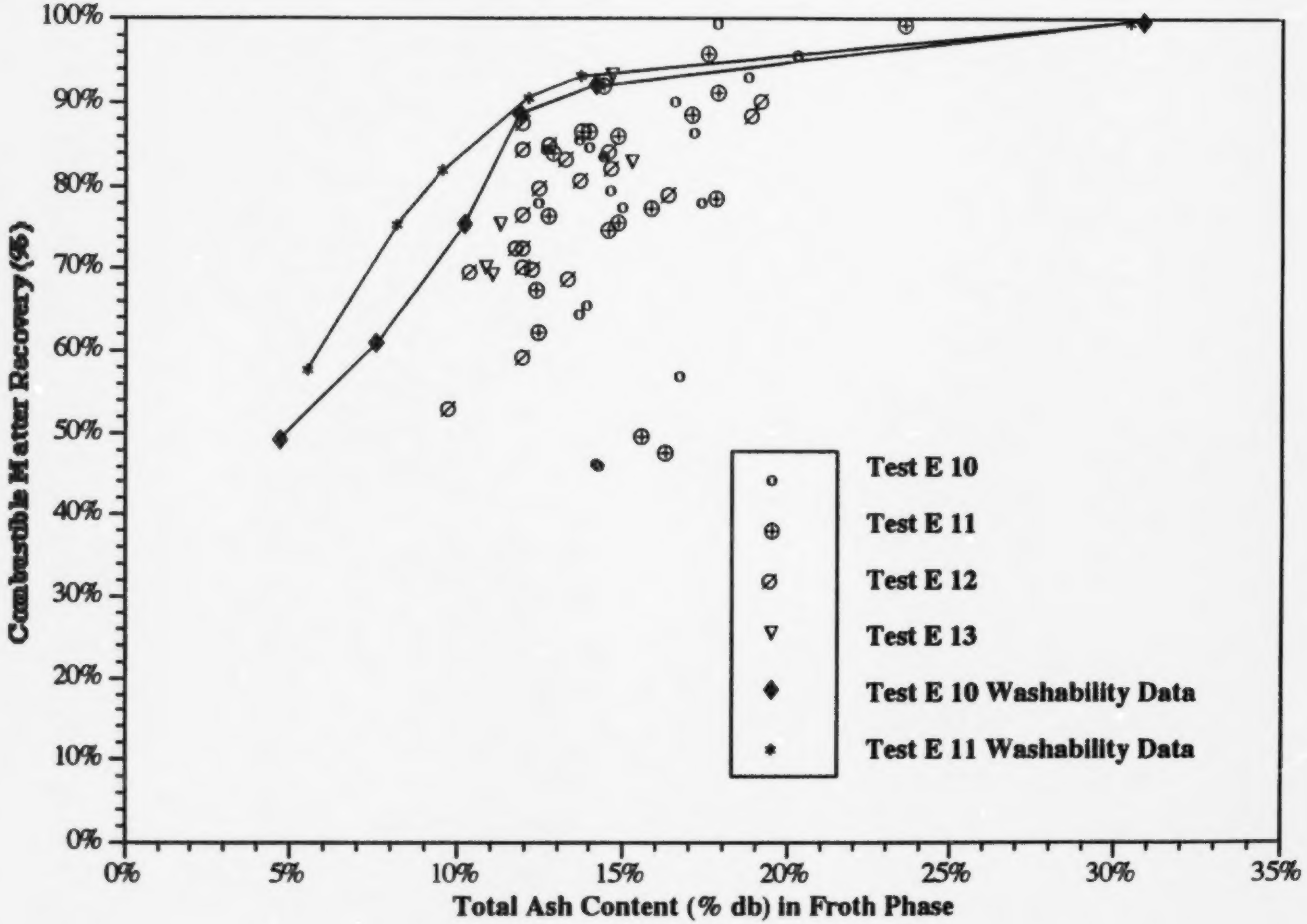

Figure 8.2 % Combustible Matter Recovery vs. Total Ash Content (% db) for Tests E 10, E 11, E 12 and E 13

Table 8.1 Raw Results from Washability Analysis for Tests E10 and E11

Coarse E10
d50=80 um

sg	Mass g	Wt % Feed	Ash %db Float/sink	Wt % Tot. Ash	Feed Ash % db	TS Wt % db Float/Sink	% Wt of TS in Feed	Feed TS % db
<1.4	3.05	35.88%	4.73%	1.70%		2.95%	1.06%	
>1.4	5.45	64.12%	47.21%	30.27%	31.97%	4.82%	3.09%	4.15%
<1.5	3.88	45.75%	7.63%	3.49%		3.04%	1.39%	
>1.5	4.60	54.25%	51.94%	28.18%	31.67%	5.20%	2.82%	4.21%
<1.6	4.97	58.33%	10.24%	5.97%		3.10%	1.81%	
>1.6	3.55	41.67%	61.40%	25.58%	31.56%	5.78%	2.41%	4.22%
<1.6(R)	5.20	61.54%	11.23%	6.91%		3.09%	1.90%	
>1.6(R)	3.25	38.46%	64.83%	24.93%	31.85%	5.53%	2.13%	4.03%
<1.8	6.20	69.66%	11.90%	8.29%		3.00%	2.09%	
>1.8	2.70	30.34%	75.15%	22.80%	31.09%	7.42%	2.25%	4.34%
<2.0	6.70	74.44%	14.20%	10.57%		3.09%	2.30%	
>2.0	2.30	25.56%	79.68%	20.36%	30.93%	7.63%	1.95%	4.25%
				avg	31.51%		avg	4.20%
				std	0.41%		std	0.10%
				% re	1.31%		% re	2.49%

Fine E11
d50=47 um

sg	Mass g	Wt % Feed	Ash %db Float/sink	Wt % Tot. Ash	Feed Ash % db	TS Wt % db Float/Sink	% Wt of TS in Feed	Feed TS % db
<1.4	3.48	42.75%	5.55%	2.37%		2.95%	1.26%	
>1.4	4.66	57.25%	49.21%	28.17%	30.54%	5.33%	3.05%	4.31%
<1.5	4.45	57.05%	8.25%	4.71%		3.00%	1.71%	
>1.5	3.35	42.95%	60.19%	25.85%	30.56%	5.91%	2.54%	4.25%
<1.6	4.88	62.89%	9.57%	6.02%		2.99%	1.88%	
>1.6	2.88	37.11%	66.60%	24.72%	30.74%	6.62%	2.46%	4.34%
<1.6(R)	5.30	65.03%	9.76%	6.35%		2.89%	1.88%	
>1.6(R)	2.85	34.97%	66.72%	23.33%	29.68%	6.75%	2.36%	4.24%
<1.8	6.15	71.51%	12.14%	8.68%		2.81%	2.01%	
>1.8	2.45	28.49%	75.78%	21.59%	30.27%	7.71%	2.20%	4.21%
<2.0	6.75	75.00%	13.72%	10.29%		2.88%	2.16%	
>2.0	2.25	25.00%	80.69%	20.17%	30.46%	8.36%	2.09%	4.25%
				avg	30.37%		avg	4.27%
				std	0.37%		std	0.05%
				% re	1.23%		% re	1.15%

Table 8.2 Washability Analysis for Test Coals E10 and E11

Coarse E10
d80=200 um

sg	Wt % in Fl Frac	Acc Wt %	Ash %db in Fract	Fract. Wt % Tot Ash	Acc Wt % Tot Ash	Ash % db	% Comb in Fract	% Comb of Tot	% Rec comb	% db TS in Fract	Fract. of TS in Sample	Acc. Wt % TS %db	Ts %db	TS %daf
<1.4	35.9%	35.9%	4.7%	1.70%	1.70%	4.73%	95.3%	34.2%	49.5%	2.95%	1.06%	1.06%	2.95%	3.10%
<1.5 +1.4	9.9%	45.8%	18.2%	1.79%	3.49%	7.63%	81.8%	8.1%	61.2%	3.37%	0.33%	1.39%	3.04%	3.29%
<1.6 +1.5	12.6%	58.3%	19.7%	2.48%	5.97%	10.24%	80.3%	10.1%	75.8%	3.32%	0.42%	1.81%	3.10%	3.45%
<1.8 +1.6	11.3%	69.7%	20.4%	2.32%	8.29%	11.90%	79.6%	9.0%	88.9%	2.49%	0.28%	2.09%	3.00%	3.41%
<2.0 +1.8	4.8%	74.4%	47.7%	2.28%	10.57%	14.20%	52.3%	2.5%	92.5%	4.40%	0.21%	2.30%	3.09%	3.60%
>2.0	25.6%	100.0%	79.7%	20.36%	30.93%	30.93%	20.3%	5.2%	100.0%	7.63%	1.95%	4.25%	4.25%	6.15%
	100.0%			30.93%				69.1%			4.25%			

Fine E11
d80=90 um

sg	Wt % in Fl Frac	Acc Wt %	Ash %db in Fract	Fract. Wt % Tot Ash	Acc Wt % Tot Ash	Ash % db	% Comb in Fract	% Comb of Tot	% Rec comb	% db TS in Fract	Fract. of TS in Sample	Acc. Wt % TS %db	Ts %db	TS %daf
<1.4	42.8%	42.8%	5.6%	2.37%	2.37%	5.55%	94.5%	40.4%	58.1%	2.95%	1.26%	1.26%	2.95%	3.12%
<1.5 +1.4	14.3%	57.1%	16.3%	2.33%	4.71%	8.25%	83.7%	12.0%	75.8%	3.15%	0.45%	1.71%	3.00%	3.27%
<1.6 +1.5	5.8%	62.9%	22.5%	1.31%	6.02%	9.57%	77.5%	4.5%	82.3%	2.89%	0.17%	1.88%	2.99%	3.31%
<1.8 +1.6	8.6%	71.5%	30.9%	2.66%	8.68%	12.14%	69.1%	6.0%	91.0%	1.50%	0.13%	2.01%	2.81%	3.20%
<2.0 +1.8	3.5%	75.0%	46.1%	1.61%	10.29%	13.72%	53.9%	1.9%	93.7%	4.32%	0.15%	2.16%	2.88%	3.34%
>2.0	25.0%	100.0%	80.7%	20.17%	30.46%	30.46%	19.3%	4.8%	100.7%	8.36%	2.09%	4.25%	4.25%	6.11%
	100.0%			30.46%				69.5%			4.25%			

8.2 Regression Analysis

Table 8.3 contains the summary of all the regression work performed in the testing program. The table contains the regression title, the statistically significant terms at a probability of 0.01, the adjusted R^2 ,and the corresponding Table reference from Appendices 2 to 6.

Tables A2.1 through A6.6 contains the details of the regression work performed on CMR (%), TS (% daf) in the product phase, and ash (% db) in the product phase for the testing program, and Table 8.4 is provided as an example and contains the following:

- the main or interaction title,
- the term designated for the factor or interaction,
- the numerical value of coefficient,
- both the standard error and coefficient,
- the tolerance,
- the calculated "t" statistic for each coefficient,
- the probability level,
- the Multiple R value, R^2, and the adjusted R^2,
- the standard error of estimate, and,
- the analysis of variance summary.

Tables A2.1 to A2.10 contain the regression results for Test E 10. Tables A3.1 to A3.11 contains the regression results for Test E 11. Size was not considered in either of these regression analyses, as it was not varied within the experiments. The regression work was performed to individually evaluate tests E10 and E11. Subsequently, the results were combined to evaluate particle size and sample age and were summarized in Tables A4.1 through A4.3. Tables A5.1 to A6.6 summarize the regression work performed for CMR (%), TS (% daf) and ash (% db) for the combined tests E 10, E 11, E 12 and E 13.

Table 8.3 Summary of Regression Work

Regression Title	Appendix Reference	Statistically Significant Terms at a Probability of 0.01	Terms Tested	Adjusted R^2
Test E10	Appendix 2			
CMR (%) Coded Matrix	Table A2.1	Constant, Oil, Frother, Energy and Temperature	5	0.78
CMR (%) Coded Matrix	Table A2.2	Constant, Oil, Frother, Energy, Temperature, and Oil*Frother Interaction	12	0.96
CMR (%) Coded Matrix	Table A2.3	Constant, Oil, Frother, Energy, Temperature, and Oil*Frother Ineraction	7	0.96
CMR (%) Coded Matrix	Table A2.4	Constant, Oil, Frother, Energy, Temperature, and Oil*Frother Interaction	6	0.96
CMR (%) Raw Data Matrix	Table A2.5	Constant, Oil, Frother, Energy, Temperature, and Oil*Frother Interaction	6	0.96
TS (% daf) Coded Matrix	Table A2.6	Constant, Oil, Frother, Energy and Temperature	5	0.87
TS (% daf) Coded Matrix	Table A2.7	Constant, Oil, Frother, Energy, Temperature, Oil*Frother, Oil*Energy, Frother*Temperature, Oil*Energy*Temperature, Oil*Frother*Temperature	10	0.98
TS (% daf) Raw Data Matrix	Table A2.8	Constant, Oil, Frother, Frother*Temperature,	10	0.96
TS (% daf) Raw Data Matrix	Table A2.9	Constant, Oil, Frother, Energy, Frother*Temperature,	5	0.97
ash (% db) Raw Data Matrix	Table A2.10	Constant, Oil, Frother, Energy, Temperature, % Solids	6	0.94

Regression Title	Appendix Reference	Statistically Significant Terms at a Probability of 0.01	Terms Tested	Adjusted R^2
Test E11				
CMR (%) Coded Matrix	Table A3.1	Constant, Oil, Frother, Energy, Temperature	5	0.80
CMR (%) Coded Matrix	Table A3.2	Constant, Oil, Frother, Temperature, Oil*Frother	9	0.90
CMR (%) Coded Matrix	Table A3.3	Constant, Oil, Frother, Temperature, Oil*Frother	5	0.92
CMR (%) Raw Data Matrix	Table A3.4	Constant, Oil, Frother, Temperature, Oil*Frother	5	0.92
TS (% daf) Coded Matrix	Table A3.5	Constant, Oil, Frother,	5	0.81
TS (% daf) Coded Matrix	Table A3.6	Constant, Oil, Frother, Temperature, Frother*Temperature	6	0.95
TS (% daf) Coded Matrix	Table A3.7	Constant, Oil, Frother, Temperature, Frother*Temperature	5	0.94
TS (% daf) Raw Data Matrix	Table A3.8	Constant, Oil, Frother, Frother*Temperature	5	0.94
TS (% daf) Raw Data Matrix	Table A3.9	Constant, Oil, Frother, Frother*Temperature	4	0.94
ash (% db) Raw Data Matrix	Table A3.10	Constant, % Solids, Oil, Frother, Temperature	6	0.95
ash (% db) Raw Data Matrix	Table A3.11	Constant, % Solids, Oil, Frother, Temperature	5	0.94

Table 3 Continued

Regression Title	Appendix Reference	Statistically Significant Terms at a Probability of 0.01	Terms Tested	Adjusted R^2
Tests E10 and E11				
CMR (%) Raw Data Matrix	Table A4.1	Constant, Oil, Frother, Energy, Temperature, Oil*Frother	6	0.92
TS (% daf) Raw Data Matrix	Table A4.2	Constant, Oil, Frother, Frother*Temperature, Size, Age	6	0.95
ash (% db) Raw Data Matrix	Table A4.3	Constant, Oil, Frother, Energy Temperature, Size, % Solids	7	0.94
Tests E10, E11 & E12				
CMR (%) Raw Data Matrix	Table A5.1	Constant, Oil, Frother, Temperature, Oil*Frother, Age	6	0.86
CMR (%) Raw Data Matrix	Table A5.2	Constant, Oil, Frother, Temperature, Oil*Frother, Oil*Age	6	0.88
TS (% daf) Raw Data Matrix	Table A5.3	Constant, Oil, Frother, Frother*Temperature, Size, Age	6	0.93
TS (% daf) Raw Data Matrix	Table A5.4	Constant, Oil, Frother, Frother*Temperature, Size*Oil, Size*Frother, Age*Oil, Age*Frother	8	0.95
ash (% db) Raw Data Matrix	Table A5.5	Constant, Oil, Frother, Energy Temperature, Size, % Solids, Age	8	0.81
ash (% db) Raw Data Matrix	Table A5.6	Constant, Oil, Frother, Energy Temperature, Size, % Solids, Age, Frother*Age, Size*% Solids	10	0.85

Table 3 Continued

Regression Title	Appendix Reference	Statistically Significant Terms at a Probability of 0.01	Terms Tested	Adjusted R^2
Tests E10, E11, E12 & E13				
CMR (%) Raw Data Matrix	Table A6.1	Constant, Oil, Frother, Temperature, Oil*Frother, Age	6	0.80
CMR (%) Raw Data Matrix	Table A6.2	Constant, Oil, Frother, Temperature, Oil*Frother, Oil*Age	6	0.81
TS (% daf) Raw Data Matrix	Table A6.3	Constant, Oil, Frother, Frother*Temperature, Size, Age	6	0.92
TS (% daf) Raw Data Matrix	Table A6.4	Constant, Oil, Frother, Frother*Temperature, Size*Oil, Size*Frother, Age*Oil, Age*Frother	8	0.93
ash (% db) Raw Data Matrix	Table A6.5	Constant, Oil, Frother, Energy Temperature, Size, % Solids, Age	8	0.82
ash (% db) Raw Data Matrix	Table A6.6	Constant, Oil, Frother, Energy Temperature, Size, % Solids, Age, Frother*Age, Size*% Solids	10	0.85

Table 3 Continued

Table 8.4 Regression Analysis of CMR (%) for Main Factors for Test E10

Variable	Term	Coefficient	Std. Error	Std. Coef.	Tolerance	T	Probability
Constant	C	80.1	1.8	0.0		43.7	0.000
Oil	x1	7.4	1.8	0.48	0.94	4.0	0.002
Frother	x2	8.1	1.8	0.53	0.98	4.5	0.001
Energy	x3	-3.2	1.8	-0.21	0.97	-1.8	0.102
Temp.	x4	-6.3	1.8	-0.40	0.97	-3.4	0.005

Multiple R: 0.92 R2: 0.84 Adjusted R2: 0.79
Standard Error of Estimate: 7.3

Analysis of Variance

Source	Sum-of-Squares	DF	Mean-Square	F-Ratio	P
Regression	3365	4	841	15.8	0.000
Residual	640	12	53.3		

The results above can be used to generate the following linear equation describing CMR (%):

$$\text{CMR}\ (\%) = 80.1 + 7.5*\text{oil} + 8.1*\text{frother} - 3.2*\text{energy} - 6.3*\text{temperature}$$

8.3 Graphical Evaluation

Figures 8.1 and 8.2 from Appendix 8 were prepared to evaluate the impact of the main factors and are presented below for example. The x-axis in each case represents the coded set points for each of the main factors, while the y-axis contains the three main responses considered in this investigation: CMR (%), TS (% daf) content in the product phase, or Ash (% db) content in the product phase. The remaining Figures describing the impact of the main factors on the process responses are summarized in Appendix 8.

Figures A8.1 to A8.3 were prepared for test E10 to demonstrate the effect of oil concentration on CMR (%), TS (% daf) content in the product, and Ash (% db) content in the product phase. Similarly, Figures A8.13 to A8.15 were prepared for test E11, and Figures A8.28 and A8.30 for test E12.

Figures A8.4 to A8.6 demonstrate the effect of frother on CMR (%) and product quality in terms of TS (% daf) and Ash (% db) for test E10. Figures A8.16 to A8.18 provide the same evaluation for test E11, and Figures A8.31 to A8.33 for test E12. Figures A8.7 to A8.9, A8.19 to A8.21, and A8.34 to A8.36 were constructed to investigate the effect of energy input for tests E10, E11, and E12, respectively. Figures A8.10 to A8.12, and A8.22 to A8.24 were developed to investigate the impact of temperature on process performance to tests E10 and E11. Figures A8.25 to A8.27 combine the results from tests E10 and E11 to demonstrate the impact of particle size on process performance. Figures A8.37 to A8.39 were constructed to demonstrate the impact that percent solids in the product phase has on TS (% daf) content of the product phase, Ash (% db) content of the product phase, and CMR (%).

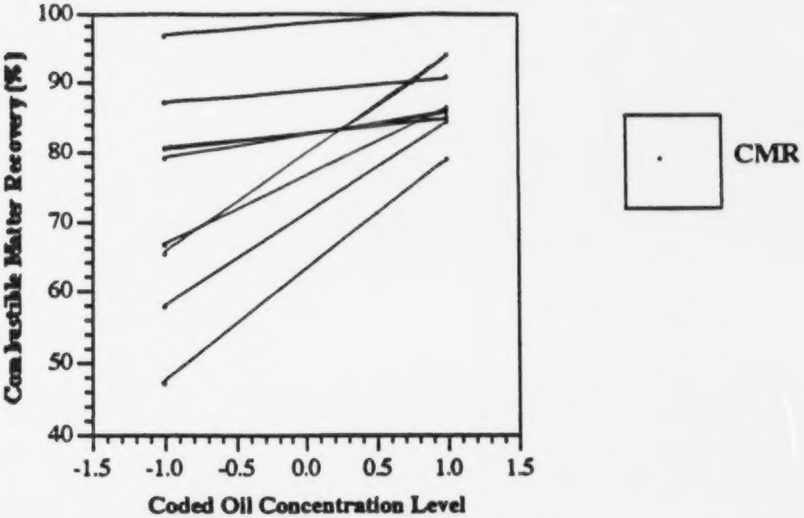

Figure A8.1 % Combustible Matter Recovery versus Coded Oil Concentration for Test E 10

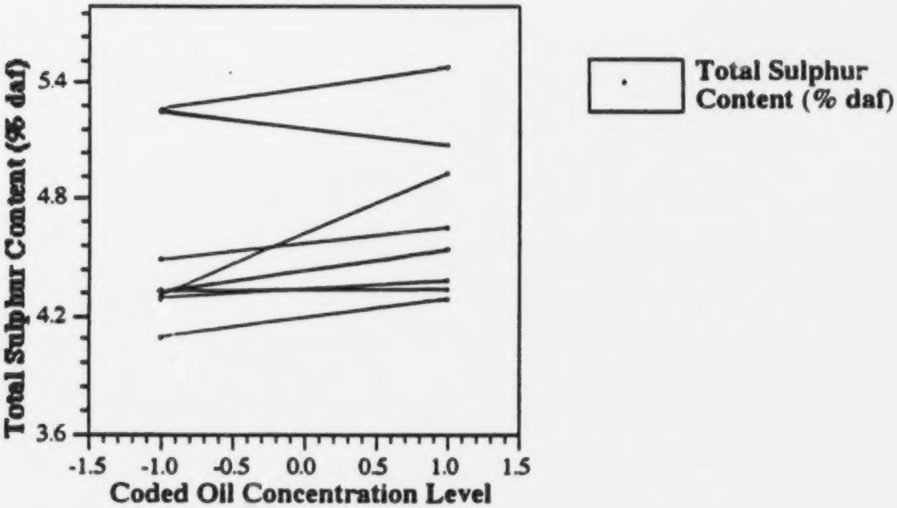

Figure A8.2 Total Sulphur Content (% daf) versus Coded Oil Concentration for Test E 10

Figure 8.3 **Example Figures A8.1 and A8.2**

8.4 Raw Data

All main factor variations and process responses are summarized in Tables 8.5 to 8.10. The table defines all operational set points for each main factor in the test matrix.

- Coal Feed Rate (in grams/min.)
- Oil Concentration (in grams/min., % db, % daf)
- Frother Concentration (in grams/min., % db, % daf)
- Energy Input (in terms of Speed, Time, and Torque)
- Temperature (in Celsius)
- Size (in d_{50} and d_{80})

A summary of the process performance calculations include the following.

- Product recovery rate (in grams/min.)
- % Solids in the product froth
- Product assays (moisture, ash, total sulphur)
- Combustible Matter Recovery (%)
- Total Sulphur Reduction (%)
- Total Ash Rejection (%)
- Sulphur Release (g/kJ)

Table 8.5 Summary of Main Factors for Test E10

Run	Int.	Coal Feed Rate g/min	Oil Conc. x2———>			Frother x3———>			Energy x4 ———>					Temperature x5—>				Size x6—>	
			Rate g/min	%db	%daf	Rate g/min	%db	%daf	Speed rpm	Time min hs 1	Time min hs 2	Torque in-oz hs 1	hs 2	C hs2	C fc1	C ps	avg C	d50 um	d80 um
e10	1	80.6	0.44	0.61%	0.93%	0.57	0.008%	0.012%	2000	3.7	***4.1***	18	28	26	21	19	22	80	208
e10	2	79.7	1.00	1.37%	2.08%	1.83	0.025%	0.038%	2000	3.7	***4.1***	18	28	25	19	18	21	80	208
e10	3	79.8	1.00	1.37%	2.08%	0.64	0.009%	0.013%	2000	3.7	***4.1***	18	28	24	19	17	20	80	208
e10	4	81.9	0.44	0.61%	0.93%	1.82	0.025%	0.038%	2000	3.7	***4.1***	18	28	24	19	18	20	80	208
e10	5	80.0	1.00	1.37%	2.08%	0.57	0.008%	0.012%	2000	3.7	***4.1***	18	28	46	46	44	45	80	208
e10	6	79.2	0.44	0.61%	0.93%	1.83	0.025%	0.038%	2000	3.7	***4.1***	16	27	47	46	45	46	80	208
e10	7	80.0	0.44	0.61%	0.93%	0.53	0.007%	0.011%	2000	3.7	***4.1***	17	28	47	46	44	46	80	208
e10	8	77.9	1.00	1.37%	2.08%	1.89	0.026%	0.040%	2000	3.7	***4.1***	17	28	44	43	45	44	80	208
e10	9b	79.8	0.44	0.61%	0.93%	0.54	0.007%	0.011%	2000	***3.7***	***4.1***	12	28	45	42	46	44	80	208
e10	10	77.7	1.00	1.37%	2.08%	1.85	0.025%	0.039%	2000	***3.7***	***4.1***	13	28	45	44	46	45	80	208
e10	11	77.9	1.00	1.37%	2.08%	0.61	0.008%	0.013%	2000	***3.7***	***4.1***	13	28	44	43	46	44	80	208
e10	12a	79.6	0.44	0.61%	0.93%	1.79	0.025%	0.037%	2000	***3.7***	***4.1***	13	27	46	45	44	45	80	208
e10	13	78.1	1.00	1.37%	2.08%	0.64	0.009%	0.013%	2000	***3.7***	***4.1***	14	28	26	20	19	22	80	208
e10	14	78.6	0.44	0.61%	0.93%	1.98	0.027%	0.041%	2000	***3.7***	***4.1***	13	28	24	19	19	21	80	208
e10	15	79.0	0.44	0.61%	0.93%	0.62	0.009%	0.013%	2000	***3.7***	***4.1***	13	28	31	21	22	25	80	208
e10	16	77.5	1.00	1.37%	2.08%	1.83	0.025%	0.038%	2000	***3.7***	***4.1***	13	29	25	21	20	22	80	208
e10	9b	78.1	0.44	0.61%	0.93%	0.53	0.007%	0.011%	2000	***3.7***	***4.1***	12	28	45	42	46	44	80	208
e10	12b		0.44	0.61%	0.93%	1.79	0.025%	0.037%	2000	***3.7***	***4.1***	13	27	46	45	44	45	80	208
avg		79.1																	

note: Italized and bold high shear mixing time indicates mixer is in use as an agglomeration vessel, otherwise, mixer is bypassed in process and serves only as an extended frontend slurry holding vessel.

Table 8.6 Summary of Main Factors for Test E11

Run	Int.	Coal Feed Rate g/min	Oil Conc. x2———> Rate g/min	%db	%daf	Frother x3———> Rate g/min	%db	%daf	Energy Speed rpm	x4 ———> Time min hs 1	Time min hs 2	Torque in-oz hs 1	hs 2	Temperature x5—> C hs2	C fc1	C ps	avg C	Size x6—> d50 um	d80 um
e11	1	76.6	1.00	1.38%	2.05%	0.62	0.009%	0.013%	2000	3.7	***4.1***	10	29	25	20	18	21	47	88
e11	2	80.1	0.44	0.61%	0.91%	0.57	0.008%	0.012%	2000	***3.7***	***4.1***	10	30	23	28	17	23	47	88
e11	3	74.4	0.44	0.61%	0.91%	1.83	0.025%	0.038%	2000	3.7	***4.1***	9	29	24	19	18	20	47	88
e11	4	80.2	1.00	1.38%	2.05%	1.83	0.025%	0.038%	2000	***3.7***	***4.1***	10	30	23	18	17	20	47	88
e11	5	78.4	0.44	0.61%	0.91%	0.57	0.008%	0.012%	2000	3.7	***4.1***	10	28	45	44	43	44	47	88
e11	6	79.8	1.00	1.38%	2.05%	0.57	0.008%	0.012%	2000	***3.7***	***4.1***	10	28	45	45	44	45	47	88
e11	7	75.1	1.00	1.38%	2.05%	1.83	0.025%	0.038%	2000	3.7	***4.1***	10	28	46	46	45	46	47	88
e11	8	78.2	0.44	0.61%	0.91%	1.84	0.025%	0.038%	2000	***3.7***	***4.1***	10	28	47	46	44	46	47	88
e11	9	76.0	1.00	1.38%	2.05%	0.58	0.008%	0.012%	2000	3.7	***4.1***	10	28	47	47	45	46	47	88
e11	10	77.3	0.44	0.61%	0.91%	0.57	0.008%	0.012%	2000	***3.7***	***4.1***	9	28	47	46	47	47	47	88
e11	11	77.1	0.44	0.61%	0.91%	1.76	0.024%	0.036%	2000	3.7	***4.1***	10	28	47	47	45	46	47	88
e11	12		1.00	1.38%	2.05%	1.84	0.025%	0.038%	2000	***3.7***	***4.1***	10	28	47	45	44	45	47	88
e11	13		0.44	0.61%	0.91%	0.58	0.008%	0.012%	2000	3.7	***4.1***	9	29	24	19	18	21	47	88
e11	14a	79.9	1.00	1.38%	2.05%	0.67	0.009%	0.014%	2000	***3.7***	***4.1***	10	30	28	19	18	22	47	88
e11	14b		1.00	1.38%	2.05%	0.67	0.009%	0.014%	2000	3.7	***4.1***	10	30	28	19	18	22	47	88
e11	15		1.00	1.38%	2.05%	1.76	0.024%	0.036%	2000	***3.7***	***4.1***	9	29	24	19	19	21	47	88
e11	16a	77.9	0.44	0.61%	0.91%	1.84	0.025%	0.038%	2000	3.7	***4.1***	10	30	24	19	19	21	47	88
e11	16b	73.0	0.44	0.61%	0.91%	1.84	0.025%	0.038%	2000	***3.7***	***4.1***	10	30	24	19	19	21	47	88
avg		77.4																	

note: Italized and bold high shear mixing time indicates mixer is in use as an agglomeration vessel, otherwise, mixer is bypassed in process and serves only as an extended frontend slurry holding vessel.

Table 8.7 Summary of Main Factors for Test E12 and E13

Run	Int.	Coal Feed Rate g/min	Oil Conc. x2———> Rate g/min	%db	%daf	Frother x3————> Rate g/min	%db	%daf	Energy Speed rpm	x4 ————> Time min hs 1	Time min hs 2	Torque in-oz hs 1	hs 2	Temperature x5—> C hs2	C fc1	C ps	avg C	Size x6—> d50 um	d80 um
e12	1	81.9	0.72	1.00%	1.48%	1.25	0.017%	0.026%	1600	***4.7***	***4.7***	8	20	32	31	31	31	73	154
e12	2		0.71	0.98%	1.46%	1.25	0.017%	0.026%	1600	***4.7***	***4.7***	9	21	32	31	31	31	73	154
e12	3		0.72	1.00%	1.48%	1.25	0.017%	0.026%	1600	***4.7***	***4.7***	8	20	32	31	31	31	73	154
e12	4	82.4	0.52	0.72%	1.07%	0.85	0.012%	0.017%	1800	***4.2***	***4.4***	12	26	27	24	23	25	73	154
e12	5		0.84	1.16%	1.73%	0.77	0.011%	0.016%	1800	***4.2***	***4.4***	11	24	27	24	24	25	73	154
e12	6	82.9	0.52	0.72%	1.07%	1.61	0.022%	0.033%	1800	***4.2***	***4.4***	11	26	27	24	23	24	73	154
e12	7	79.9	0.91	1.26%	1.87%	1.62	0.022%	0.033%	1800	***4.2***	***4.4***	12	25	27	24	23	24	73	154
e12	8	82.6	0.52	0.72%	1.07%	0.74	0.010%	0.015%	2000	***3.7***	***4.1***	11	30	26	21	20	23	73	154
e12	9	82.4	0.91	1.26%	1.87%	0.86	0.012%	0.018%	2000	***3.7***	***4.1***	11	30	24	19	18	20	73	154
e12	10	84.8	0.52	0.72%	1.07%	1.56	0.022%	0.032%	2000	***3.7***	***4.1***	11	30	23	19	18	20	73	154
e12	11	85.4	0.91	1.26%	1.87%	1.59	0.022%	0.033%	2000	***3.7***	***4.1***	11	31	24	20	19	21	73	154
e12	12	84.6	0.71	0.98%	1.46%	1.62	0.022%	0.033%	2000	***3.7***	***4.1***	11	30	24	20	19	21	73	154
e12	13	81.8	0.72	1.00%	1.48%	1.86	0.026%	0.038%	2000	***3.7***	***4.1***	11	31	25	20	19	21	73	154
e12	14	81.0	0.91	1.26%	1.87%	1.24	0.017%	0.025%	2000	***3.7***	***4.1***	12	30	25	20	19	21	73	154
e12	15	82.1	0.44	0.61%	0.91%	1.79	0.025%	0.037%	2000	3.7	***4.1***	11	30	22	18	17	19	73	154
e12	16		0.44	0.61%	0.91%	1.55	0.021%	0.032%	2000	3.7	***4.1***	11	31	23	19	17	20	73	154
e12	17	83.2	0.51	0.71%	1.05%	0.76	0.011%	0.016%	2000	3.7	***4.1***	11	31	23	19	17	19	73	154
e12	18		0.91	1.26%	1.87%	0.74	0.010%	0.015%	2000	3.7	***4.1***	11	31	23	19	17	20	73	154
e12	19	80.0	0.52	0.72%	1.07%	1.53	0.021%	0.031%	2000	3.7	***4.1***	11	32	23	19	17	20	73	154
e12	20	84.5	0.91	1.26%	1.87%	1.48	0.020%	0.030%	2000	3.7	***4.1***	11	31	23	19	18	20	73	154
avg		82.6																	
e13	1	72.6	0.44	0.61%	0.91%	1.64	0.023%	0.034%	2000	3.7	***4.2***	12	31	22	18	16	19	73	154
e13	2	76.5	1.00	1.38%	2.05%	0.64	0.009%	0.013%	2000	3.7	***4.2***	11	30	23	18	16	19	73	154
e13	3	77.8	0.72	1.00%	1.48%	1.12	0.015%	0.023%	2000	3.7	***4.2***	10	31	23	18	16	19	73	154
e13	4	75.9	0.92	1.27%	1.89%	1.6	0.022%	0.033%	2000	3.7	***4.2***	11	31	23	17	16	19	73	154
e13	5		0.44	0.61%	0.91%	1.87	0.026%	0.038%	2000	3.7	***4.2***	11	31	23	18	17	19	73	154
avg		75.7																	

note: Italized and bold high shear mixing time indicates mixer is in use as an agglomeration vessel, otherwise, mixer is bypassed in process and serves only as an extended frontend slurry holding vessel.

Table 8.8 Summary of Main Responses for Test E10

Run	Window	PRODUCT			Product Coal——>							
		FEED RATE g/min	%SOLIDS (FROTH)	Sample Age (Days)	% M	Ash %db	TS %db	TS %daf	CMR %	TSR %	AR %	SO2 Release g of SO2/J
e10	1	37.55	12.2%	0	3.4%	13.7%	3.69%	4.28%	64.8%	38.7%	60.1%	2.58E-03
e10	2	61.39	12.6%	0	3.2%	17.9%	4.49%	5.47%	99.9%	21.5%	47.8%	3.32E-03
e10	3	58.05	9.3%	0	3.2%	18.8%	3.99%	4.91%	93.4%	29.5%	45.2%	2.99E-03
e10	4	60.17	8.5%	0	3.2%	20.3%	4.17%	5.23%	96.1%	24.9%	40.8%	3.19E-03
e10	5	49.60	11.9%	0	3.3%	14.4%	3.73%	4.36%	84.1%	37.5%	58.0%	2.63E-03
e10	6	47.37	8.1%	0	3.2%	17.4%	3.69%	4.47%	78.4%	35.9%	49.3%	2.71E-03
e10	7	34.35	7.5%	0	3.3%	16.7%	3.56%	4.27%	57.3%	38.7%	51.3%	2.59E-03
e10	8	50.05	15.3%	0	3.3%	14.0%	3.99%	4.64%	85.2%	33.4%	59.2%	2.80E-03
e10	9a	27.21	9.1%	2	3.4%	14.2%	3.49%	4.07%	46.7%	41.6%	58.6%	2.46E-03
e10	10	48.95	15.6%	3	3.2%	12.7%	3.77%	4.32%	84.7%	38.0%	63.0%	2.61E-03
e10	11	45.24	14.4%	2	3.2%	12.5%	3.73%	4.26%	78.5%	38.8%	63.6%	2.57E-03
e10	12a	46.74	10.8%	2	3.2%	14.7%	3.68%	4.31%	80.0%	38.1%	57.3%	2.61E-03
e10	13	50.29	15.5%	3	3.2%	13.7%	3.90%	4.52%	86.0%	35.2%	60.1%	2.73E-03
e10	14	52.42	11.7%	3	3.4%	17.2%	4.34%	5.24%	86.8%	24.8%	49.9%	3.18E-03
e10	15	38.40	11.0%	2	3.5%	13.9%	3.72%	4.32%	66.1%	38.0%	59.5%	2.61E-03
e10	16	54.78	12.5%	2	3.3%	16.6%	4.22%	5.06%	90.5%	27.4%	51.6%	3.07E-03
e10	9b	27.06	8.9%	2	3.5%	14.3%	3.48%	4.06%	46.4%	41.7%	58.3%	2.45E-03
e10	12b	45.80	10.4%	2	3.4%	15.0%	3.63%	4.27%	77.9%	38.7%	56.3%	2.58E-03

Table 8.9 Summary of Main Responses for Test E11

Run	Window	PRODUCT			Product Coal————>							
		FEED RATE g/min	%SOLIDS (FROTH)	Sample Age (Days)	% M	Ash %db	TS %db	TS %daf	CMR %	TSR %	AR %	SO2 Release g of SO2/J
e11	1	49.60	20.6%	10	3.1%	12.9%	4.11%	4.72%	84.3%	28.7%	60.6%	2.85E-03
e11	2	36.42	15.8%	9	3.3%	12.5%	3.86%	4.41%	62.8%	33.4%	61.8%	2.66E-03
e11	3	59.12	12.2%	10	3.2%	17.6%	4.43%	5.37%	96.0%	18.9%	46.2%	3.26E-03
e11	4	66.79	6.7%	9	3.2%	23.6%	4.43%	5.80%	99.5%	12.4%	27.8%	3.55E-03
e11	5	30.07	9.8%	9	3.3%	15.6%	3.68%	4.36%	50.0%	34.1%	52.3%	2.64E-03
e11	6	45.62	11.3%	9	3.1%	14.9%	3.84%	4.51%	75.8%	31.8%	54.4%	2.73E-03
e11	7	55.37	16.2%	10	3.2%	14.4%	4.14%	4.84%	92.4%	26.9%	56.0%	2.92E-03
e11	8	46.80	10.0%	9	3.3%	15.9%	3.87%	4.60%	77.5%	30.5%	51.4%	2.79E-03
e11	9	45.16	16.7%	10	3.2%	12.8%	3.82%	4.38%	76.8%	33.8%	60.9%	2.64E-03
e11	10	29.17	8.8%	9	3.4%	16.3%	3.64%	4.35%	48.0%	34.3%	50.2%	2.63E-03
e11	11	44.68	12.9%	10	3.3%	14.6%	3.86%	4.52%	75.1%	31.7%	55.4%	2.73E-03
e11	12	51.96	13.4%	9	3.2%	14.9%	4.11%	4.83%	86.2%	27.0%	54.4%	2.92E-03
e11	13	39.20	17.2%	10	3.2%	12.4%	3.88%	4.43%	67.7%	33.1%	62.1%	2.67E-03
e11	14a	51.60	17.5%	9	3.1%	13.8%	4.19%	4.86%	86.8%	26.6%	57.8%	2.94E-03
e11	14b	51.79	17.6%	9	3.1%	14.0%	4.23%	4.92%	86.9%	25.7%	57.2%	2.97E-03
e11	15	55.04	14.2%	10	3.2%	17.1%	4.53%	5.46%	88.9%	17.5%	47.7%	3.31E-03
e11	16a	48.62	10.6%	9	3.2%	17.8%	4.45%	5.41%	78.8%	18.2%	45.6%	3.29E-03
e11	16b	56.49	12.1%	9	3.2%	17.9%	4.45%	5.42%	91.4%	18.1%	45.3%	3.29E-03

Table 8.10 Summary of Main Responses for Test E12 and E13

Run	Window	PRODUCT			Product Coal——————>							
		FEED RATE g/min	%SOLIDS (FROTH)	Sample Age (Days)	% M	Ash %db	TS %db	TS %daf	CMR %	TSR %	AR %	SO2 Release g of SO2/J
e12	1	43.64	17.3%	40	3.2%	12.3%	3.56%	4.06%	70.0%	38.7%	62.4%	
e12	2	45.26	17.8%	40	3.3%	12.0%	3.61%	4.10%	72.8%	38.0%	63.3%	2.47E-03
e12	3	43.67	17.9%	40	3.2%	12.0%	3.54%	4.02%	70.3%	39.2%	63.3%	2.43E-03
e12	4	32.13	23.8%	40	3.3%	9.8%	3.57%	3.96%	53.2%	40.2%	70.0%	2.38E-03
e12	5	42.65	28.6%	40	3.2%	10.4%	3.62%	4.04%	69.8%	39.0%	68.2%	2.43E-03
e12	6	51.02	15.1%	40	3.2%	13.7%	3.70%	4.29%	80.9%	35.2%	58.1%	2.59E-03
e12	7	54.18	15.0%	40	3.2%	14.6%	3.80%	4.45%	84.4%	32.8%	55.4%	2.69E-03
e12	8	36.77	15.3%	41	3.2%	12.0%	3.52%	4.00%	59.4%	39.6%	63.3%	2.41E-03
e12	9	45.2	19.8%	41	3.1%	11.8%	3.63%	4.12%	72.8%	37.8%	63.9%	2.48E-03
e12	10	52.61	18.4%	41	3.5%	13.3%	3.84%	4.43%	83.5%	33.1%	59.3%	2.67E-03
e12	11	53.67	25.5%	41	3.5%	12.8%	3.84%	4.40%	85.1%	33.5%	60.9%	2.66E-03
e12	12	52.88	14.4%	41	3.5%	14.7%	3.81%	4.47%	82.3%	32.5%	55.0%	2.70E-03
e12	13	51.72	12.4%	41	3.4%	16.4%	3.85%	4.61%	79.0%	30.4%	49.8%	2.79E-03
e12	14	50.19	20.7%	41	3.3%	12.5%	3.69%	4.22%	80.0%	36.3%	61.8%	2.54E-03
e12	15	61.03	7.9%	42	3.6%	19.2%	3.81%	4.72%	90.3%	28.8%	41.3%	2.87E-03
e12	16	59.76	7.3%	42	3.9%	18.9%	3.73%	4.60%	88.5%	30.5%	42.2%	2.79E-03
e12	17	43.44	8.3%	43	3.6%	13.4%	3.62%	4.18%	68.8%	36.9%	59.0%	2.52E-03
e12	18	48.38	13.6%	43	4.2%	12.0%	3.68%	4.18%	76.8%	36.8%	63.3%	2.52E-03
e12	19	54.39	21.9%	43	3.3%	12.0%	3.81%	4.33%	87.8%	34.6%	63.3%	2.61E-03
e12	20	53.02	24.4%	43	3.7%	12.0%	3.88%	4.41%	84.6%	33.4%	63.3%	2.66E-03
e13	1	37.85	20.5%	44	3.0%	10.9%	3.69%	4.14%	70.4%	37.4%	66.7%	2.49E-03
e13	2	38.01	21.8%	44	3.1%	11.1%	3.73%	4.20%	69.6%	36.6%	66.1%	2.53E-03
e13	3	41.24	24.6%	44	3.3%	11.3%	3.78%	4.26%	75.7%	35.6%	65.4%	2.57E-03
e13	4	53.22	19.0%	44	3.2%	14.7%	4.18%	4.90%	93.6%	26.0%	55.0%	2.96E-03
e13	5	47.14	20.5%	44	3.2%	15.3%	4.18%	4.94%	83.2%	25.5%	53.2%	2.99E-03

9.0. Discussion

Experimental Program

Three blocks of tests were performed in the experimental design. The original feed stock was extensively blended, and subdivided into equal quantities from which three different sized test coals were prepared: E10, E11, and E12. After these test coals were generated, each sample was extensively re-blended and stored as 10 kg samples in plastics bags.

Test E10 used a 2^4 factorial design in which the testing was executed immediately following sample preparation. In this manner, the feed coal was exposed to little opportunity for air oxidation.

Test E11 was the second 2^4 factorial design in which a finer grind of test coal was investigated. The potential for air oxidation was higher as E11 was not executed for 10 to 11 days after sample preparation. Hence, air exposure time also varied which increased the complexity of the data evaluation.

Test E12 was the third block of tests in which a mid particle size was investigated. The experimental program also included set points to investigate non-linearity within the response surface (eg. -.707 and +.707). Test E12 received higher opportunity for air oxidation because the sample was stored for 40 to 45 days before the test program could begin and be completed. During this period, the samples were stored in plastic bags at ambient temperatures which ranged between 18 and 28 °C, with an average value of about 24 °C.

Main Factors

Main factors of the investigation include the following:

- x1 oil concentration,
- x2 frother concentration,
- x3 energy input,
- x4 temperature,

- x5 particle size distribution,

These factors represented controlled variations within the factorial design. Two process variations, sample age, and product percent solids concentration, represent uncontrollable variations inherent in the testing program.

- x6 sample age, and
- x7 product percent solids concentration.

Main Responses

Three main responses were considered within this experimental program. Combustible Matter Recovery, (CMR %), was considered to be the valuable constituent and was termed as the first process response. Total sulphur content (TS % daf) of the product phase was the second response of the this investigation and was considered to be the most relevant environmental indicator of process performance. The primary purpose of the process is reduce the sulphur content prior to combustion in an effort to reduce acids and acid precursor in stack gases. The third response is the final ash content (ash (% db)) of the product stream, which also has environmental concerns, but for this study was considered to be of lesser importance when compared to the sulphur content of the product material.

Data Analysis

The process performance was evaluated in terms of total sulphur and ash removal. The washability data, which defines the process in terms of theoretical cleaning potential, and the experimental results were plotted and to measure process performance (see Section 9.1).

Linear regression was employed to analyze the main and interaction effects, and the work was supplemented by a graphic analysis of the main factor effects (see Sections 9.2 and 9.3 respectively).

9.1 Process Performance

Figures 8.1 and 8.2 contain the washability data describing the theoretical cleaning potential of test coals E10 and E11 with respect to CMR(%) versus the product quality in terms of TS (% daf) and ash (% db) contents. The results from tests E10, E11, and E12 are imposed over the washability results to provide for an evaluation of process performance.

The results in Figure 8.1 indicate the process lacks selectivity in the optimum areas identified by the washability analysis. The washability analysis indicates that the cleaning potential for sulphur demonstrates a steep slope up to about 90 CMR (%), after which the TS (% daf) content of the product phase begin to increase sharply, causing the curve to flatten. This region of rapid change is considered to be the optimum range, because it defines where the maximum CMR (%) and minimum TS (% daf) can be obtained.

The test coal contains 6.00 TS (% daf) based upon the washability results, and can be cleaned by the two stage agglomeration and flotation process to about 4.00 TS (% daf), while maintaining a CMR (%) range of 75 to 90 %. The washability results indicate a theoretical cleaning potential of between 3.2 and 3.8 TS (% daf) while maintaining a CMR (%) close to 90 %. These results indicate the process falls short of operating within these optimum regions of the washability curve, and performance has been classified as poor to fair with respect to TS (% daf) removal.

Figure 8.2 indicates the process is performing very well with respect to ash removal, as the optimum regions of the ash washability curve are achieved by the process. A broad range of test conditions can be used to generate these results, hence, the process is very robust with respect to ash rejection.

The test coals contains about 33 % ash (% db), and can be cleaned by the two stage agglomeration and flotation process to less than 15 %, yet still maintain a high CMR (%) in the 90 % range. Dewatering of the product would further reduce the ash content to the 13 to 14 % ash (% db) range. The washability results indicate a theoretical cleaning potential of between 10.5 and 11.5 ash (% db) at a CMR (%) of 90 %. These results indicate the process is capable of maintaining both very high ash (% db) removals and CMR (%), as the experimental results closely follow the theoretical cleaning potential of the coal with respect of ash (% db). Hence, the process performance has been classified as very good with respect to ash (% db) removal.

9.2 Regression Analysis

Tables A2.1 to A6.6 located in Appendices 2 to 6 summarize all the linear regression analyses performed in this study. Each table provides a summary of the regression equation, and relevant statistical information.

The results were divided into five groups to assist in the evaluation. Group 1 represents test E10, (see Appendix 2), group 2 represents test E11 (see Appendix 3), and group 3 represents the combined data from tests E10 and E11 (see Appendix 4). Groups 4 and 5 represent the combined data sets for tests E10, E11, and E12; and subsequently tests E10, E11, E12 and E13 (see Appendices 5 and 6).

The regression analysis employed a practical evaluation, by which engineering judgment was used to supplement the statistical evaluation of the regression equation. For each data set, the regression began by first testing the main factors for statistical significance. Subsequently, only logical interaction terms were added to the regression equation, until significant interactions were identified. All initial regression equations developed for tests E10 and E11 were performed first using a coded factor data for CMR (%) and TS (% daf), whereby all main factors were represented by their respective coded values. Once a final regression equation was established, the raw data matrix was substituted and the regression equation was tested again.

In the regression work performed for ash (% db), and for data groups 4 and 5, only the raw data matrix could be used because of other process variables (eg. % solids and sample age) which were not part of the original factorial design varied simultaneously during experimentation. The % solids in the product phase had minimal impact on CMR (%) and TS (% daf), and sample age differences between tests E10 and E11 were minimal, hence, the coded factor matrix data worked well for data groups 1 and 2 in terms of CMR (%) and TS (% daf).

9.2.1 Group 1 - Test E10

CMR (%) - Test E10

Table A2.1 provides the results for the first regression analysis performed on CMR (%) for test E10. The results indicate that all four main factors are statistically significant at a 0.005 level, except energy input which was rejected at a probability level of 0.1. The equation fit is fair, although a higher R^2 would improve the confidence in the regression. The signs and magnitude of the coefficients are supported by the graphic analysis (see Figures A8.1, A8.4, A8.7 and A8.10).

Oil and frother concentrations both have a large impact on CMR (%), and increase CMR (%) in similar proportions based upon the standardized coefficient. Hence, these factors are predominant in terms of CMR (%).

Temperature and energy both have a negative impacts on CMR (%), temperature being predominant compared to energy input based upon the standardized coefficient. In fact, the standardized temperature coefficient has nearly the same numerical value as oil and frother, indicating its importance to process performance.

Table A2.2 was used to investigate various interactions. The regression indicates that the interaction between oil and frother is strongly significant at a probability level of 0.003. The interaction between oil and temperature demonstrated marginal statistical significance at a probability level of 0.15, hence, it warranted further investigation.

Table A2.3 was used to investigate interactions between oil and frother, and oil and temperature. The interaction between oil and temperature was not statistical significant at a probability level of 0.01. However, the interaction between oil and frother continued to demonstrated statistical significance at a probability level of 0.001.

Table A2.4 summarizes the final regression equation for the coded factor matrix.

CMR(%)=79.7 + 7.87*Oil + 7.91*Froth - 2.79*Energy - 5.84*Temp - 5.63*Oil*Froth

- The impact of oil concentration in the regression is consistent with both the graphical evaluation and the literature review. The coefficient demonstrates a high level of statistical significance at a probability level of 0.001. Additional oil provides for increased contact between the carbonaceous surfaces and oil droplets, resulting in an improvement in oil wetting, and in the growth of agglomerates. The newly formed agglomerates are very hydrophobic and report to the product phase during the flotation stage.

- The impact of frother in the equation is also consistent with both the graphical evaluation and the literature review. The coefficient demonstrates a high level of statistical significance at a probability level of 0.001. Frother addition is important to the kinetics of flotation, whereby the surface tension of the water is lowered causing the formation of smaller air bubbles, higher in concentration, and a more resilient to rupture. Together, these factors contribute to increase the CMR (%) of the process.

- The regression work indicates an increase in temperature decreases CMR (%), and the graphical evaluation supports the trend. The increase in temperature is thought to alter the bubble system within flotation stage by a number of possible methods:

  -by the evaporation of the frother from the bubble phase,
  -by excessive bubble collapse, or
  -by allowing formation of bubbles too large for attachment.

  The results do not provide a conclusion of why increasing temperature reduces CMR (%), but the probable explanation is the evaporation of the frother, reducing the stability of the bubble system, allowing for excessive bubble rupture to occur.

- The interaction between the oil and frother indicates that the latter may play an additional role aside from increasing the kinetics of the process. The negative interaction between oil and frother indicates the addition of frother may weaken the attachment between the air bubbles and agglomerates. The flotation process is based primarily on surface energy minimization and the addition of frother reduces the surface tension of the water phase. Attachment forces may weaken because the air bubbles are more favored within the water phase. Furthermore, the correct match between bubble size, and particle size is an essential requirement of the flotation process. The reduction of bubble size may reduce the CMR (%) if bubbles become too small, as the surface area available for attachment, and the net buoyancy are both reduced.

- Test E10 results indicate that an increase in energy input decreases CMR (%), and the graphical evaluation supports this trend. The literature generally supports the opposite trend, as an increase in energy should improve dispersion and provide for better contact between the oil and carbonaceous particles by causing improved particle and droplet collisions. Limitations in the apparatus have likely caused the anomaly as the first mixer consumed less power during operation because of poor baffle construction in high shear mixer 1. Hence, when both mixers were operated to simulate higher energy levels, the initial conditions from high shear mixer 1 delivered lower shear levels causing less efficient initial oil dispersion and particle and droplet collisions. This fact has been attributed to be the cause of the lower CMR (%) at higher energy input.

Table A2.5 provides the results of the final regression analysis for CMR (%) performed with the raw data matrix. This analysis was performed against the raw data matrix. These results indicate an excellent adjusted R^2 value of 0.96, and a reduced equation using the raw data matrix is presented below, indicating the same trends as already identified in Table A2.4.

CMR(%) = 49.6 + 47.7*Oil + 2518*Froth - 0.40*Energy-.46*Temp - 1645*Oil*Froth

TS (% daf) - Test E10

Table A2.6 to A2.9 summarizes the regression work performed for TS (% daf) for test E10. Table A2.6 contains the initial regression of the main factors, which indicates the main factors are statistically significant at a probability level of 0.001, with the exception of oil addition and energy input, which demonstrate probability levels or 0.24 and 0.007. The impact of oil addition is supported by the graphical evaluation, as Figure A8.2 indicates that the TS (% daf) of the product phase increases with the addition of oil. Hence, the equation does not accurately describe the process, and a different equation involving interactions was considered.

These results were summarized in Tables A2.7 and A2.8. Table A2.7 includes the results from the coded factor matrix design, while Table A2.8 includes the results from the raw data matrix regression. These two regression equations demonstrate an interesting anomaly.

The results from Table A2.7 indicates that the equation which included four main factors, six interactions, and a constant, provide for an excellent fit for the data with an adjusted R^2 value of 0.98. This equation is extremely complex, and several of the interactions cannot be described by the process fundamentals Furthermore, third order interactions which are most commonly insignificant, tested as significant. It is probable that this equation is an expression which provides an excellent fit of the data without any regard to process fundamentals.

To further investigate the equation in Table A2.7, the raw data matrix was utilized in the regression analysis rather than the coded factor matrix, and the results stored in Table A2.8. If the equation accurately described the process, a similar level of statistical validity could be expected from each term in the regression when the raw data matrix was used to replace the coded factor matrix. However, only two main factors, one interaction, and the constant term tested as statistically significant. Hence, a final reduced equation was developed from the raw data matrix and is described in Table

A2.9 and appears to describe the process with an outstanding adjusted R^2 value of 0.97. The reduced equation is presented below.

TS (% daf) = 4.65 + 0.17*oil + 72.7*froth - 0.02*energy - 1.4*froth*temp

- The regression results indicate that as oil concentration is increased, the TS (% daf) content of the product phase also increases, although the results do not indicate that oil is a predominant main factor in the regression equation. The graphical evaluation of these results also support these trends as the slopes of the graphs are not as steep as other main factors. The most probable recovery pathways for pyrite as it related to oil additions are physical entrapment, oil wetting, or the attachment of pyrite to the agglomerates.

At higher oil dosage levels, (eg. above 2.5 % db), pyrite entrapment and oil wetting of pyrite surfaces reduce sulphur removal. A low oil concentrations, it is predicted that there is less opportunity for oil and pyrite particle collisions. By controlling other processes variables in an effort to reduce the oil concentration required, it was hoped the pyrite content in the product could be minimized. The results of the regression analysis and the graphic analysis are somewhat supportive, as the addition of oil was not a predominant variable in terms of TS (% daf). However, the variables which were manipulated in an effort to reduce the overall oil concentration required, did not provide for an overall improvement in sulphur removal because of other pathways by which the pyrite rich particles can report to the product phase.

- Pyrite responds naturally to the process of flotation under ideal conditions, and frother addition appears to provide for the enhanced recovery of pyrite particles. The increased recovery has been attributed to improved flotation kinetics because of a higher rate of collisions between the air bubbles and pyrite particles, smaller bubble sizes which are better able to attach to the smaller pyrite particles, and a more resilient froth.

- The impact of energy input on sulphur reduction was statistically valid only for test E10, where an increase in energy input resulted in a decrease in sulphur content.

The energy input results imply that a portion of the liberated pyrite reports to the product phase with the agglomerates, because this similar drop in TS (% daf) was observed in the CMR (%) results.

- The regression work revealed an interaction between frother and temperature. The negative sign on the term indicates that as temperature is increased, the sulphur content of the product is reduced. Increasing temperature lowers the impact of the frother either by promoting the evaporation of the frother, reducing the stability of the bubble system promoting excessive bubble rupture, or by weakening the force of attachment between the bubble and solid. It is probable that all these factors are responsible for the reduction in sulphur content.

The interaction between frother and temperature indicates that the flotation of pyrite particles occurs by different pathways than the carbonaceous agglomerates. The most probable pathways for pyrite rich particles to report to the product include entrapment and attachment to the agglomerates, or by natural flotation. The experimental program suggests that pyrite particles report by both pathways. The positive coefficient associated with the oil addition implies that pyrite is recovered with the agglomerate phase. However, the interaction between temperature and frother suggests that natural flotation of pyrite is occurring, as there exists no reference to the oil addition in the interactions. If all pyrite particles required oil addition for their successful recovery, some other form of interaction between the oil and frother, or oil and temperature might be expected, rather than a frother and temperature term. The CMR (%) regression equation supports this conclusion as strong interactions between oil and frother exist for a system primarily dependent upon oil wetting of the carbonaceous matter. Hence, the results imply the pyrite rich particles report by a combination of oil induced flotation with the agglomerate phase, and by natural flotation.

- The % solids of the product phase did not appear to impact TS (% daf). The results from the regression analysis and the graphs both support this observation. Hence, an insignificant mass of sulphur rich material reports to the product phase via hydraulic entrainment.

Ash (% db) - Test E10

Table A2.10 summarizes the regression work describing how the ash (% db) in the product phase varies with the main factors of the design. All the main factors and process variables, including the % solids in the product phase, tested statistically significant in terms of final ash (% db) at a probability level of 0.01, with the exception of oil addition which tested at 0.08. No interactions were identified in the regression and the adjusted R^2 was very high at 0.94, although the equation lacked consistency with expected trends.

Ash (%db) = 26.6 + 1.5*oil + 99.4*froth - 0.08*energy - 0.093*temp - 0.66*%solids

- The regression work indicates the ash (% db) increases when the oil is increased. The graphical evaluation indicates this is clearly inconsistent because an increase in oil tended to decrease the ash (% db). The literature review also indicates that the product ash content should decrease with an increase in oil additions. The reason is attributed to uncontrollable variations in the % solids in the product phase.
- The graphic evaluation of frother indicates minimal impact on the final ash (% db), however, the regression study indicated frother to be a predominant factor. The explanation is related to the uncontrolled variations in % solids and the substantial impact on the final ash (% db).
- The impact of energy input indicates the high shear mixers are reworking and reforming the agglomerates, and in doing so, causing the efficient removal of ash material from the agglomerates. The regression equation is supported by the graphic evaluation.

- The results indicate an increase in temperature reduces the final ash (% db) in the product phase. The probable explanation for this trend is related to the lower CMR (%) experienced at higher temperatures, being attributed to frother evaporation or bubble rupture.
- The % solids term in the equation appears to be the predominant factor in the expression related to ash (% db) in the product phase. An increase in % solids causes a corresponding decrease in the ash (% db) of the product phase. Figure A8.38 provides convincing support of this trend in which the ash (% db) is plotted against the % solids of the product phase.

9.2.2 Group 2 - Test E11

CMR (%) - Test E11

Tables A3.1 to A3.11 summarize the regression work performed on Test E11 with respect to CMR (%). Table A3.1 provides the regression analysis of all four main factors. These results indicate that oil, frother, and temperature remain as statistically significant main factors at a probability level of 0.005, however, energy input was insignificant at a probability of 0.9. Table A3.2 represents the regression work investigating the potential of interactions. These results indicate that the same interaction (eg. oil* frother) identified in test E10 is significant at a probability of 0.006. Table A3.3 represents the final regression equation for the coded factor matrix. The results from the regression has an adjusted R^2 value of 0.92, and the equation is presented below.

$$\text{CMR}(\%) = 73.9 + 8.7*\text{oil} + 9.51*\text{froth} - 6.1*\text{temp} - 4.4*\text{oil}*\text{froth}$$

Table A3.4 provides the results for the raw data matrix regression equation. The equation is presented below and does not indicate any difference in the form of the regression equation between the coded factor matrix results, and the raw data matrix results.

$$\text{CMR}(\%) = 34.3 + 42.1*\text{oil} + 2514*\text{froth} - 0.496*\text{temp} - 1345*\text{oil}*\text{frother}$$

- The same interaction of oil and frother is a significant contributor to CMR (%) for both tests E10 and E11. Hence, despite the absence of a significant energy term in the equation for test E11, almost the identical equation was generated independently for both tests E10 and E11.
- The standardized coefficients for the coded factor matrix equation suggests that frother addition has a larger impact on CMR (%) than oil addition over the experimental ranges investigated for test E11.

TS (% daf)- Test E11

Tables A3.5 to A3.10 summarize the regression work performed in analyzing TS (% daf) for test E11. The results suggest that three of the main factors, oil, frother, and temperature are statistically significant at probability levels of 0.03. However, energy input, not unlike what the equation for CMR (%) indicated, does not appear to be significant for this group of data. To further explore the possible similarity in trends, the interaction between frother and temperature was added to the equation. The adjusted R^2 value jumped from 0.81 to .95 when this interaction was added to the equation. Hence, Table A3.7 was developed as the final equation describing the coded factor matrix and is presented below. The goodness of fit was excellent with an adjusted R^2 value of 0.94.

TS (% daf) = 4.82 + 0.13*oil + 0.29*froth - 0.27*temp - 0.14*froth*temp

- The regression equation is distinctively different from what was obtained for the CMR (%) investigations for either tests E10 and E11, indicating different recovery pathways must exist. Furthermore, the equation appears to be similar as the form observed for test E10 TS (% daf) investigations.
- Energy input did not test as statistically significant for test E11 at a probability level of 0.05, while for test E10, it is statistically significant at a probability level of 0.001. This observation was also observed for the CMR (%) regression analysis when test E10 and E11 were compared.

- Frother and temperature are prominent factors in the regression analysis, and the interaction between frother and temperature tests statistically significant at a probability of 0.005.

- Oil addition was an influencing factor, although it appears to be a less predominant variable when compared to frother and temperature for the experimental ranges investigated.

Tables A3.8 and A3.9 were developed based upon the raw data matrix, and used to generate the final equation for TS (% daf) for test E11. Table A3.8 summarizes the final equation generated by the coded factor matrix regression work, and provided an excellent fit with an adjusted R^2 value of 0.94. However, the main factor of temperature tested as statistically insignificant at a probability level of 0.5, hence, Table A3.9 was developed to represent the final equation for the raw data matrix. Temperature was discarded from the equation further reducing the form to a single constant, two main factors, (eg. oil and frother), and one interaction, frother and temperature. The results of this final regression analysis indicate an excellent adjusted R^2 value of 0.94. The equation is listed below.

TS (% daf) = 3.88 + 0.34*oil + 83.4*froth - 1.34*froth*temp

- The final regression for the raw data matrix is similar to the equation developed for test E10, with the exception of the absence of energy input, the equation form is very similar. Furthermore, the rejection of energy input from this group of data appears to be consistent with the trends observed in the CMR (%) evaluation.

- The regression results from the coded factor matrix and the raw data matrix indicated that the significance of the main factor temperature was rejected at a probability of 0.05. However, the results of the regression work indicate the interaction of frother and temperature became a more predominant term in the equation, and the effect of temperature is contained in this expression.

- The regression equation has been simplified dramatically, yet maintained an excellent fit with the experimental data. Hence, the same equation will be considered initially when evaluating the combined data sets for tests E10 and E11.

Ash (% db) - Test E11

Tables A3.10 and A3.11 summarize the regression work performed on the ash (% db) in the product phase for test E10. Table A3.10 was used to investigate the final regression equation used in test E10. The results indicated the same equation provided a very good fit, with an adjusted R^2 value of 0.95, however, the energy input term tested as insignificant for test E11 at a probability level of 0.10. This trend was supported by the graphical evaluation of the results, as Figure A8.21 indicated that energy did not impact the final ash (% db) content of the product phase. Hence, energy input was removed from the equation and Table A3.11 was used to investigate the reduced equation. The resulting equation is listed below and demonstrated an adjusted R^2 value of 0.94.

Ash (% db) = 25.3 + 2.1*oil + 87.2*froth - 0.11*temp - 0.74*%solids

- The regression equation closely resembles the results obtained for test E10, however, energy input does not test as statistically significant at a probability level of 0.05. This trend in the data appears to be consistent with respect to all the regression work performed for test E11.

9.2.3 Group 3 - Test E10 and E11

CMR (%) - Test E10 and E11

Table A4.1 provides the regression work performed on the combined data set for tests E10 and E11. The regression equation fits the data very well with an adjusted R^2 value of 0.92. The reduced equation is described as follows.

CMR (%) = 45.6 + 43.1*oil + 2310*froth - 0.29*energy - 0.43*temp - 1307*oil*froth

- The same regression equation appears to fit very well for not only E10 and E11 independently, but also when the data sets are combined.

- Oil and frother are the predominant factors influencing CMR (%), and appear to have about the same impact over the experimental ranges investigated. Similarly, the interaction of oil and frother tested as statistically significant for the combined data set at a probability of 0.001.

- The impact of size on CMR (%) tested as insignificant at a probability of 0.10, and the results from the graphic analysis support this trend. The literature also supports this trend, as the process of agglomeration is not normally effected by even large variations in size. However, the flotation process is sensitive to particle size. The insignificance of particle size on CMR (%), indicates that the addition of oil and energy has resulted in the formation of small agglomerates eliminating any impact on the process of flotation. This data set represents the most dramatic change in size within the experimental program, hence, it is reasonable to conclude that particle size does not appear to impact the CMR (%) within the experimental ranges investigated.

- Sample age does not appear to impact CMR (%) for tests E10 and E11. The sample age investigated within this data set does not represent the largest variations within the design, hence, the only observation which can be stated is that a sample age of 9 to 10 days after preparation is not long enough to significantly impact CMR (%).

TS (% daf) - Test E10 and E11

Table A4.2 summarizes the regression work performed on the combined data set of tests E10 and E11. The regression equation used from both tests E10 and E11 raw data matrix was used in the analysis, except that size and sample age were added to the expression. The results of the regression analysis are excellent, with an adjusted R^2 value of 0.94. The equation is presented below for discussion.

$$\text{TS (\% daf)} = 6.08 + 0.28*\text{oil} + 78.3*\text{froth} - 1.39*\text{froth}*\text{temp} - 0.03*\text{size} - 0.08*\text{age}$$

- The results from the regression analysis indicate that the same equation used for tests E10 and E11 independently, worked very well for the combined data set, except size and sample age were added to the equation.

- Frother and temperature remain predominant factors impacting the TS (% daf) of the product phase. Oil addition increases the final TS (% daf) of the product phase, but is considered of lesser importance when compared to frother and temperature. Energy input did not test statistically for the combined data set for tests E10 and E11 at a probability of 0.01.

- The regression results indicate that a decrease in size causes an increase in sulphur content. The explanation might be related to the kinetics of flotation of the smaller pyrite particles, which are now lower in mass and can report to the product phase faster. The graphical results from Figure 8.26 support the trend indicating a decrease in size tended to increase the TS (% daf) content in the product phase.

- The regression results indicated that an increase in sample age, lowers the sulphur content of the product. The increased exposure to air oxidation provided additional time for the pyrite surfaces to oxidize. Oxidized pyrite is less hydrophobic, and therefore, would be less attracted to the oil phase, and would demonstrate less tendency for natural flotation.

Ash (% db) - Test E10 and E11

Table A4.3 contains the regression work performed on the combined data set for tests E10 and E11. The regression contains all the main factors, and the impact of size was added to the expression. The results of the regression appear very good with an adjusted R^2 value of 0.94, and followed the same basic equation as tests E10 and E11 did independently.

Ash(%db)=29+ 2.2*oil + 89.1*froth - 0.1*energy -0.1*temp - 0.03*size - 0.72*% solid

- The impact of size tested statistically significant at a probability level of 0.001, indicating that a reduction in size caused a corresponding reduction in the ash (% db) in the product phase. The graphical observation supports this trend as Figure A8.11 indicates a decrease in size caused a drop in final ash (% db) content.

- The impact of sample age test as insignificant at a probability of 0.05.

9.2.4 Group 4 - Test E10, E11 and E12

CMR (%) - Test E10, E11 and E12

Table A5.1 and A5.2 represent the regressions of CMR(%) for the combined data sets for tests E10, E11 and E12. This work was performed using the raw data matrix, because of test E12 does not represent a complete set of factorial set points. Table A5.1 represents the similar equation used to describe tests E10 and E11, however, the effect of energy input as a main factor has been removed because it tested insignificant at a probability level of 0.05. The equation is listed below and the data fits well with an adjusted R^2 value of 0.86.

CMR (%) = 34. + 44.3*oil + 2579*froth - 0.48*temp - 1520*oil*frother - 0.21*age

- The regression equation used to describe the combined data sets of tests E10, E11 and E12 is very similar to the equation used to describe tests E10 and E11, however, the impact of energy input was rejected when test E12 was added to the data set. The results of the regression analysis also suggest the possibility of non-linearity in the response surface because of the reduced fit of the regression when additional data was added.
- The impact of sample age on CMR (%) is statistically significant at a probability of 0.001, indicating as the sample is given prolonged exposure to air, natural oxidation reduces the recovery of combustible matter.

Table A5.2 was used to investigate a different regression analysis, whereby the equation was slightly modified. The equation is provided below and demonstrates a slightly better fit with an adjusted R^2 value of 0.88.

CMR (%) =32. + 46.7*oil + 2555*froth - 0.48*temp - 1500*oil*frother - 0.23*age*oil

The results of this regression work indicate very similar trends as described in Table A5.2, however, the impact of sample age has been coupled with oil concentration in this analysis. The results indicate the term is statistically significant at a probability of 0.001, and the regression performance is slightly improved.

TS (% daf) - Test E10, E11 and E12

Tables A5.3 and A5.4 represent the regression work performed for the combined data sets for tests E10, E11, and E12 for TS (% daf). This work was performed using the raw data matrix, because test E12 does not represent a complete set of factorial set points. The results contained in Table A5.4 are promising with an adjusted R^2 value of 0.93. The equation used in the regression is exactly the same as the equation developed for the combined data set for tests E10 and E11, with the addition of size and sample age. To further investigate the possibility of improvements, additional interactions consistent with process fundamentals were added to the expression. These results are contained in Table A5.4, and demonstrated an excellent regression with an adjusted R^2 value of 0.95.

$$TS(\%daf) = 3.9 + 0.66*oil + 107*froth - 1.4*froth*temp - 0.003*oil*size - 0.01*oil*age$$
$$- 0.37*froth*size - 46*froth*age$$

- The regression equation developed from the combined data sets from tests E10 and E11 have provided very good results for the combined data set of tests E10, E11, and E12 when sample size and age were added to the expression.
- Size and sample age appear to impact the TS (% daf) content of the product phase in a complex manner, as several interactions have tested as statistically significant at probability levels of 0.01 and lower. These new interactions appear to influenced by the two most important chemical factors of the process, oil and frother.

Ash (% db) - Test E10, E11 and E12

Tables A5.5 and A5.6 summarizes the results developed for the combined data sets of tests E10, E11 and E12. The equation evaluated in Table A5.5 follows the same form used for the combined data set for tests E10 and E11 alone, except sample age was added to the expression. The results of this regression analysis are fair providing an adjusted R^2 value of 0.81, however, it is obvious the impact of sample age and size has complicated the regression. Several interactions were investigated to identify any possible improvements. These results are contained in Table A5.6, and indicate that two additional interactions test as statistically significant at a probability level of 0.005. The equation is listed below, and the addition of the interactions increased the adjusted R^2 to 0.85.

Ash (% db) =33.9 + 1*oil + 63.5*frother - 0.06*energy - 0.1*temperature - 0.14*size - 1*%solids - 0.11*age + 4*froth*age + 0.009*size*%solids

- Both sample age and % solid in the product phase have a direct impact on the final ash (% db) content, causing a reduction as either variable increases.
- Two additional interactions tested as statistically significant and improved the overall regression: frother and sample age, and size and % solids.

9.2.5 Group 5 - Test E10, E11, E12 and E13

CMR (%) - Test E10, E11, E12 and E13

Table A6.2 and A6.3 were used to investigate the entire combined data set for tests E10, E11, E12 and E13. The same equations investigated in Tables A5.2 and A5.3 were used in the evaluation, and similar trends were observed. The results from Table A6.2 are listed below, and indicate the regression results to be fair with an adjusted R^2 value of 0.74. However, it is apparent that the goodness of fit has been reduced considerable and must be attributed to the complex impact of sample age, surface oxidation, or non-linearity in the response surface.

CMR (%) = 41.5 + 38.4*oil + 2132*froth - 0.47*temp - 1154*oil*froth - 0.27*age

In Table A6.2 the impact of sample age was replaced with the interaction of sample age and oil. The goodness of fit improved with this equation with an adjusted R^2 value of 0.81, however, the equation is only described as fair, as the impact of sample age has impacted CMR (%) in some complex manner. The equation is described below.

CMR (%)=38.1+ 40.9*oil + 2039*froth - 0.46*temp - 1074*oil*frother - 0.26*age*oil

The conclusion from this regression work is that the original regression equation provides for a valid description of the process. However, the impact of sample age on CMR (%) is complex, and to more thoroughly investigate and improve the evaluation, additional data would be required.

TS (% daf) - Test E10, E11, E12 and E13

Tables A6.4 and A6.5 provide the final regression for the combined data set of tests E10, E11, E12 and E13. The raw data matrix was used in these final regression works, and the results are very good as the adjusted R^2 values were .91 and .93 for tests for Tables A6.4 and A6.5, respectively. The final equation from Table A6.5 is provided below.

TS (%daf)=3.8+0.66*oil + 109*froth - 1.4*froth*temp - 0.004*oil*size - 0.01*oil*age

- 0.4*froth*size - 48*froth*age

The results from this regression analysis indicates the same equation developed for tests E10, E11 and E13 provides for very good fit when test E13 is also included in the data set.

Ash (% db) - Test E10, E11, E12 and E13

Tables A6.5 and A6.6 provide the final regression analysis results for the ash (% db) in the product phase. The same equation was investigated for the combined data set of tests E10, E11, E12 and E13. The goodness of fit for the regression analysis is fair, revealing an adjusted R^2 value of 0.82. When the interaction of frother and sample age, and size and % solids, where added to the expression in Table A6.6, the adjusted R^2 value increased to 0.85. However, the equation has some inherent limitations as it is not fully supported by the graphical analysis, hence, the overall validity can be classsified as marginal.

9.3 Graphic Evaluation

Figures A8.1 to A8.36 provide the graphic representation of all main factors, whereby the dependent axis contains the process responses, CMR (%), TS (% daf) , and ash (% db), and the independent axis contains the coded high and low set point values for each main factor. The representation was used to help assess the impact of main factor variations.

9.3.1 Oil Concentration

Figures A8.1 to A8.3 provides the evaluation of oil concentration with respect to CMR (%), TS (% daf), and ash (% db), for test E10, while Figures A8.13 to A8.15, and A8.28 to A8.30 provide the same evaluation for tests E11 and E12, respectively.

Figures A8.1, A8.13, and A8.28 indicate that CMR (%) increases when oil concentration is increased. Observations indicate that the most dramatic changes in CMR (%) occurred in Figures A8.1 and A8.13, while the changes experienced in Figure A8.28 were not as pronounced. The trend is related to the larger changes in set point values implemented for tests E10 and E11 (e.g. from +1 to -1), while test E12 experienced smaller set point changes (e.g. +0.71 to -0.71).

Figures A8.2, A8.14 and A8.29 indicate the TS (% daf) content of the product phase is also directly related to the oil concentration. These results indicate that the sulphur content of the product phase increases as the oil concentration is increased. The most pronounced changes are again observed in Figures A8.2 and A8.14, while A8.29 demonstrates smaller changes likely due to the narrow increment associated with the set point changes in oil concentration for test E12.

Figures A8.3, A8.15, and A8.30 provide for the evaluation of how changes in oil concentration impact the product ash content. Figures A8.3 and A8.15 provide convincing trends which indicate that the ash (% db) of the product decreases as the oil concentration increases, however, results in Figure A8.30 are not as conclusive as the data appear to have more scatter. It is likely that changes in set point values have reached their experimental limitation with respect to ash content as it relates to oil concentration, and systematic variations and disturbances within the apparatus account for the scatter in the data.

9.3.2 Frother Concentration

Figures A8.4 to A8.6 provide for the evaluation of how frother concentration impacts CMR (%), TS (% daf), and ash (% db) for test E10, while Figures A8.16 to A8.18 and A8.31 to A8.33 provide for the evaluation for tests E11 and E12, respectively.

Figures A8.4, A8.16, and A8.31 all indicate that the CMR (%) is strongly influenced by the concentration of frother. As the concentration of frother is increased, the CMR (%) is also increased. This trend is strongly supported in tests E10, E11, and E12, suggesting that frother concentration has similar levels of impact on the CMR (%) than the oil concentration within the experimental ranges investigated.

Figures A8.5, A8.17, and A8.32 all indicate that the TS (% daf) content of the product phase increases with the increase in frother concentration. A strong trend is observed in all three tests, indicating frother to be a major parameter influencing the total sulphur of the product phase.

Figures A8.6, A8.18, and A8.33 do not provide a strong argument that the frother concentration impacts the final ash content of the product phase. The results from Figure A8.6, A8.18 and A8.33 demonstrate a high level of scatter, and would be difficult to substantiate an impact of frother concentration except the data is simultaneously influenced by percent solids in the product phase.

9.3.3 Energy Input

Figures A8.7 to A8.9 provide for the evaluation of how energy input impacts CMR (%), TS (% daf), and ash (% db) for test E10, while Figures A8.19 to A8.21 and A8.34 to A8.36 provide for the evaluation for tests E11 and E12, respectively.

Figure A8.7 indicates that the added energy input decreased the observed CMR (%) for test E10. The results do not indicate a dramatic change, but they are consistent in nature. The results contained in Figure A8.19 did not appear to demonstrate the same trend for test E11, as a consistent decrease in CMR (%) with an increase in energy was not clearly observed. The results from test E12 are summarized in Figure A8.34 and are similar to test E10, indicating a decrease in CMR (%) with an increase in energy input. However, there is limited data demonstrating the impact of energy input variations for test E12.

Figure A8.8 indicated the TS (% daf) of the product phase decreased with an increase in energy input for test E10, although the results from tests E11 and E12, presented in Figures A8.20 and A8.35, were not conclusive as only a slight decrease in the TS (% daf) was demonstrated in test E12.

Figure A8.9, used to define test E10, indicated the ash (% db) of the product phase decreased consistently when the energy input to the apparatus was increased. However, Figures A8.21 or A8.36, which were used to describe the impact on energy input for tests E11 and E12, indicated the lack of any consistent variations in ash content as related to the increase in energy input.

9.3.4 Temperature Input

Figures A8.10 to A8.12 provide for the evaluation of how temperature increases impacts CMR (%), TS (% daf), and ash (% db) for test E10, while Figures A8.22 to A8.24 provide for the evaluation for test E11.

Figures A8.10 and A8.22 from tests E10 and E11 both indicate that an increase in temperature caused a decrease in CMR(%). Similarly, Figures A8.11 and A8.23 both indicate that an increase in temperature caused a decrease in the TS (% daf) of the product phase. Figures A8.12 describes the ash (% db) content of the product phase as temperature is varied for test E10, and indicates increasing temperature decreases the product ash content. However, Figure A8.24, which describes the impact of temperature on ash (% db) content for test E11 does not provide conclusive evidence indicating that the ash (% db) content of the product phase decreases with an increase in temperature as there exists too much data scatter.

9.3.5 Particle Size

Figures A8.25 to A8.27 provides for the evaluation of how particle size impacts CMR (%), TS (% daf), and ash (% db) for tests E10 and E11. Figure A8.25 indicates that the CMR (%) appears to be independent of size, as there is limited change in CMR (%) magnitudes observed between tests E10 and E11. Furthermore, the results contained in Figure A8.25 suggest the data is random, not demonstrating any trend with variation in size.

Figure A8.26 indicates that the decrease in size for test E11 consistently increased the TS (% daf) of the product phase. Figure A8.27 indicates the opposite trend for ash, as a decrease in size reduced the ash (% db) content of the product phase.

9.3.6 Percent Solids of Product Phase

Figure A8.37, A8.38, and A8.39 provide for the evaluation of how percent solids of the product phase impacts the TS (% daf), the ash (% db) contents, and the CMR (%). The results in Figure A8.37 suggests no trend exists between percent solids and TS (% daf) in the product phase. However, the results do indicate that the variations in TS (% daf) appear to be the largest in the lower percent solids region, hence, some hydraulic entrainment of pyrite is possible.

Figure A8.38 indicates a strong trend exists between the product percent solids and ash (% db) content. Furthermore, there does appear to be substantially more scatter in the data at the lower percent solids regions, and the process appears more consistent at the higher percent solids concentration. These results clearly indicate that the hydraulic entrainment of ash material is occurring.

Figure A8.39 indicates the percent solids of the product does not influence the CMR (%), indicating the hydraulic entrainment of carbonaceous material is unlikely.

9.3.7 Sample Age

There is insufficient data to prepare a proper graphic evaluation of air exposure time, however, regression techniques will be used to test if any trend exists.

9.4 Apparatus

The bench scale apparatus operated very well and most of the modifications implemented had positive impacts on both the results and operation of the plant.

1. Variations in coal feed rate would cause critical process disturbances which would invalidate much of the experimentation, hence, a reliable coal feed system was required. The coal feed system employed in this study operated with a high level of accuracy and reliability (eg. > 1 % relative error).

2. The gear driven oil feed pump also performed with the same high level of accuracy (eg. >1% relative error), providing a feed rate to the system with extremely low levels of estimated error. The oil addition was important because of the relatively large impact on the process expected from these additions, and because at very low oil addition levels small variations would cause large variations in the % relative error. The injection location of the oil was selected in the region of the mixer with the maximum velocity gradient and highest overall shear rate. This is considered to be the best location in terms of providing optimum dispersion and particle contact.

3. A centrifugal pump was used to feed the frother solution to the flotation cells. The pump performed with reasonable accuracy, indicating a % relative error of about 4.5 %. Hence, the pump required more attention during the testing program, therefore, visual confirmation of the pumping action was established to provide for the opportunity of semi-continuous monitoring of frother addition. A small back pressure device in the form of a line restriction was required to assist in stabilizing the performance of the pump.

4. The rotameters provided the test unit with a continuous supply of water within 5 % relative error. Variations in flow during the process were anticipated to be an

insignificant problem, as the process was equipped with a large equalization tank at the beginning of the process.

5. The high shear mixing system performed very well. The motors provided very consistent mixing, and were able to endure long periods of continuous testing without any mechanical or electrical problems. The mixer design for high shear vessel 1 had a poor baffle design, and resulted in inadequate shear and velocity gradient patterns when compared to high shear mixer 2, and caused some unexpected results.

6. The flotation cells performed very well. The following modifications were implemented to the cell to improve the performance.

- A weir control device was built to control level in the cell .
- A rotating paddle device was installed to skim the froth from the surface of the flotation cell down into the pyrite separator at a constant and uniform rate.
- Spray nozzles were added to wash and push the froth towards the pyrite separator at a constant and uniform rate, eliminating any dead zones on the cell surface, and help release impurities from the agglomerates.
- The agglomerated feed stock was fed directly into the flotation impeller for maximum dispersion within the cell and contact with air bubbles. The frother reagent was fed into the feed stock line to provide for fast and equal dispersion of the frother.
- An additional conical shaped bottom was added to the flotation cell to allow for heavier and larger particles to settle out of the slurry phase. The conical bottoms worked extremely well in reducing the accumulation of sulphur rich material which normally collects in the bottoms of cells without such design provisions. The conical bottoms and settling vessels eliminated the problem of sulphur creep in the product which would have caused problems related to process measurements in terms of TS (% daf), reducing the reliability of the data. The conical shaped bottoms in both the

flotation cell and pyrite separator dramatically improved the experimental method with respect to TS (% daf) measurements in the product phase.

7. The Pyrite Separator is a novel design developed to investigate the enhanced removal of pyrite from the product phase by exaggerating the three fundamental components of the flotation cell: froth washing, flotation of valuable constituents, and gravity settling of pyrite and ash rich particles. The performance of the pyrite separator was not extensively tested in this experimental program, hence, no firm conclusions were developed based upon its performance, However, no dramatic deficiencies in performance were observed either, and the unit appeared to operate in a manner in which its design had intended.

9.5 Experimental Method

1. The experimental results indicate that the apparatus and method provided for very good test repeatability. The development tests indicate excellent recovery of total solids, with the small losses being accounted for by sample handling. The development tests indicated the existence of sulphur creep in the product phase; being attributed to accumulations of sulphur rich solids within the flotation cells and pyrite separator. The installation of conical bottoms and settling vessels eliminated sulphur creep by immediately removing any solid accumulations from the vessels.

2. The development tests also indicated an interval sampling program provided reliable results. A 50 minute period of stabilization, followed by a 10 minute sampling interval was found to be sufficient to ensure a representative sample was extracted.

3. The sample handling and preparation methods provided for reliable results, and the quality assurance and quality control program within the analytical laboratory was excellent.

9.6 Data Analysis

1. Multiple linear regression analysis provided a good analysis of the data. However, multiple non-linear regression analysis would have been the preferred

approach to the evaluation because of the expected non-linearity of the response surface. Tests E10 and E11 represented the most reliable and complete set of data because of minimal sample oxidation and the orthogonal design of these tests.

2. Test E12 was designed to investigate non-linearity within the response surface primarily for oil and frother addition, however, the air exposure of the test coal complicated the data analysis and inhibited the non-linear regression analysis of the data, and in general, reduced the performance of the regression analysis. The possibility of non-linear effects of oil and frother is highly probable, and contributes to the lack of regression performance when the complete combined data set was evaluated using linear regression analysis, rather than non-linear.

10.0 Conclusions

10.1 Process Performance

10.1.1 TS (% daf)

Figure 8.1 describes the process in terms of CMR (%) versus TS (% daf) for the experimental conditions tested. The feed stock coal contains 6.00 % TS (% daf) based upon the washability results, and can be cleaned by the process to about 4.60 % TS (% daf), while maintaining a range of CMR (%) from 75 to 90 %. The washability results indicate a theoretical cleaning potential of between 3.2 to 3.8 % TS (% daf) can be achieved at a CMR (%) of 90 %. These results indicate that the process performed from poor to fair with respect to the removal of sulphur.

10.1.2 Ash (% db)

Figure 8.2 describes the process in terms of CMR (%) versus ash (% db). The feed stock coal contains 33 % ash (% db), and can be cleaned by the process to less than 15 % db, yet still maintain a CMR (%) of 90 %. Dewatering of the product would reduce the ash content to about 14 % db. The washability results indicate a theoretical cleaning potential of about 11.0 % ash (% db) at a CMR (%) of 90 %. These results indicate the process performs very well in terms ash removal.

10.2 Process Fundamentals

CMR (%)

CMR (%) appears solely dependent upon the successful oil wetting of the combustible surfaces. Other recovery pathways such as those related to natural surface hydrophobicity, or hydraulic entrainment, do not appear to impact CMR (%). The predominance of oil, frother, and their interaction supports the reliance of the process on oil addition. If other predominant interactions not related to oil addition existed, other pathways for recovery may seem possible. The regression work revealed minimal sensitivity for size or sample oxidation in terms of CMR (%), providing more supportive evidence that only a single pathway exists. Process fundamentals support this trend as the agglomeration process provides the oil and high shear mixing with which a consistent feed stock in terms of both size and surface hydrophobicity are produced, thereby minimizing any potential variations within the flotation performance.

TS (% daf)

In terms of TS (% daf), the process behaves distinctly different than that of the carbonaceous agglomerates. The sulphur rich particles report to the product via three pathways: as non-liberated pyrite, attachment within the agglomerate phase, or via natural flotation of the pyrite particles. The washability analysis indicates some pyrite is finely disseminated within the coal matrix and is non-liberated after grinding of the feed stock. This non-liberated pyrite will report to the product phase with the CMR (%).

The addition of oil increased the TS (% daf) of the product phase indicating that pyrite rich particles are captured within the agglomerates and report to the product phase during flotation.

The impact of frother and the interaction between frother and temperature are the most predominant factors in the regression equation, indicating that natural flotation of pyrite to the product occurs. It is difficult to quantify the contribution of each pathway, but the results suggest that the natural flotation of pyrite may be predominant because of the relative magnitude of the regression coefficients.

Ash (% db)

In term of ash (% db), the process behaves distinctly different than either the carbonaceous agglomerates, or the pyrite rich particles. The ash rich particles report to the product phase by three pathways: as non-liberated ash, entrapped or attached to a newly formed agglomerates, or via hydraulic entrainment with the water phase.

The washability analysis indicates some component of ash is finely disseminated within the coal matrix and is not liberated by conventional grinding methods, and thus, will report to the product phase with the CMR (%).The significance of oil, frother, and temperature main factors impacting the ash (% daf) of the product phase indicates that some ash rich particles are associated with the agglomerates. The strong influence of % solids in the product phase indicates that the hydraulic entrainment of ash particles into the product phase is a major pathway.

10.3 Main Factors and Interactions

10.3.1 CMR (%)

1. The regression and graphic evaluations indicate that oil concentration is a predominant factor influencing CMR (%), providing for substantial increases within the oil addition levels investigated. The improved CMR (%) has been attributed to more efficient oil wetting of the carbonaceous particles as oil concentrations increase.
2. The regression and graphic evaluations indicate that frother concentration is a predominant factor influencing CMR (%), increasing recovery over the ranges investigated. The increase in CMR (%) has been attributed to the more resilient froth system, higher in bubble concentration generated by the addition of frother.
3. The interaction between the oil and frother indicates that the latter may play an additional role aside from stabilizing the froth, as the interaction tended to decrease CMR (%). The negative interaction has been attributed to the reduction in bubble size because the reduced surface area available for attachment will likely inhibit recovery of larger sized agglomerates; and the bubble may be insufficient in buoyancy to recover the larger and heavier agglomerates.
4. High shear mixing is essential to the process of agglomeration, however, within this study, high energy levels were used resulting in minimal impact when energy variations were implemented.
5. The regression and graphic evaluation indicates a decrease in CMR (%) with an increase in temperature. The decrease in CMR (%) has been attributed to the evaporation of frother, allowing for a less stable bubble system.

6. Size tested insignificant at a probability of 0.05. Process fundamentals support this trend because agglomeration was employed with the intention that it would produce a flotation feed stock constant in size and hydrophobicity.

7. The impact of sample age is consistent with process expectations. Agglomeration is robust in terms of oil wetting highly oxidized carbonaceous surfaces and the regression analysis supports the trend as additional oil could be used to maintain high recoveries for the sample with the highest degree of surface oxidation.

8. The % solids of the product phase did not impact CMR (%). The results from the regression and graphic evaluation both support this observation.

10.3.2 TS (% daf)

1. The regression results indicate the addition of oil causes a moderate increase the TS (% daf) of the product phase within the experimental ranges investigated.

2. The regression indicates that frother is the predominant factor increasing the TS (% daf). Additional frother provides for increased recovery of pyrite particles, primarily by improved bubble sizes, and a more stable froth system.

3. Variations in high shear mixing had minimal impact on TS (% daf) content.

4. The interaction between frother and temperature indicates as the later is increased the TS (% daf) of the product is reduced. The negative interaction is most probably caused by promoting the evaporation of the frother.

5. The regression and graphical evaluation indicates that a decrease in size causes an increase in TS (% daf). The increase has been attributed to faster flotation kinetics because the pyrite particles are smaller in size, and lower in mass.

6. The regression results indicate that an increase in sample age lowers the sulphur content of the product. The increased exposure to air oxidation provided additional time for the pyrite surfaces to oxidize. The oxidized surfaces of pyrite are less attracted to the agglomerate phase, and would demonstrate less tendency for natural flotation, thereby reducing the sulphur content of the product phase.

7. The % solids of the product phase did not appear to impact TS (% daf). The results from the regression analysis and the graphs both support this observation.

10.3.3 Ash (% db)

1. The regression work indicates the ash (% db) in the product increases when the oil concentration is increased. The graphical evaluation has some level of scatter, but indicates the ash content decreases with an increase in oil. It is difficult to explain the discrepancy between the graphic analysis and regression analysis, and the comparison reduces the validity of the equation.

2. The significance of frother addition was not realized until the % solids was added to the regression. The graphical evaluation indicates as no conclusive comments can be made based upon the raw data. These results tend to further invalidate the regression equation.

3. The impact of energy input indicates the high shear mixers are reworking, and reforming the agglomerates, and in doing so, causing the efficient removal of ash material from the agglomerates. The regression is support by the test E10 graphic results.

4. The regression indicates an increase in temperature reduces the final ash (% db) in the product phase, and the trend is support by the graphic evaluation. A probable explanation is related to the increased potential for evaporation of the frother phase thereby reducing CMR (%). Less ash (% db) will report to the product phase if CMR (%) are lower.

5. The regression indicates as size is increased, the ash (% db) of the product phase also increases. The graphical evaluation contained in Figure 8.27 supports this trend, although the plot does contain considerable scatter in the data. Finer sized feed coals have higher levels of ash particle liberation, hence, high removal levels are possible.

6. The % solids term in the regression is the predominant factor in the regression equation related to ash (% db) based upon the standardized coefficient. An increase in

% solids causes a corresponding decrease in the ash (% db) in the product, because of reduced hydraulic entrainment of ash constituents. Figure 8.38 provides a convincing graphical support of this trend.

7. The regression indicated that an increase in sample age reduced the ash (% db) of the product phase. Increased levels of air exposure may have caused additional oxidation of the ash rich particles, rendering the ash rich particles even more hydrophilic than their natural state.This may also be accounted for by the reduced levels of CMR (%) experienced when the feed stock sample is exposed to oxidation.

11.0 Recommendations

1. Further fundamental investigations should be conducted to identify the major pathways by which the pyrite rich particles report to the product phase. The work should involve two phases.

    i. Phase 1 should involve fundamental mathematical model development to help quantify which flotation pathways are the most predominant mechanisms responsible for pyrite reporting to the product phase.

    ii. Phase 2 should include additional investigative work, whereby the experimental design is specific to identifying the major flotation pathways by which pyrite reports to the product phase.

2. Preliminary investigative work into pyrite depressants should be performed in an effort to improve the process performance in terms of sulphur removal. Combining agglomeration and flotation with the process of biologically oxidizing of pyrite surface appears to be an area warranting investigation.

3. Investigative work should be performed to evaluate the tailings management and treatment requirements associated with the process. The process is unique as it employs higher oil concentrations than other comparable flotation processes, and generates finely sized pyrite particles in the tailings stream. The higher oil concentration used in the process increases the potential for hydrocarbon contamination of the tailings stream. The finely sized pyrite increases the available surface area which will likely contribute to the severity of the acid mine drainage problems.

Cited References

Ahmed, N. and Jameson, G.J., (1983), "Kinetics of Agglomeration of Oil Droplets and Carbon Particles in a Stirred Vessel", The Eleventh Australian Conference on Chemical Engineering, Brisbane, September 4-7, 245-252.

Alberty, R.A. and Daniels, F., (1980), Physical Chemistry, Fifth Edition, John Wiley & Sons, Inc., New York, New York, USA.

Armstrong, L.W., et al., (1979), "A pilot-scale treatment of coal preparation plant effluent by the selective agglomeration process", CIM Bulletin, November, 89-92.

Baur, P.S., (1981), "Coal Cleaning: improve boiler performance and reduce SO2 emissions", Power, September, 125, 9, S-1.

Bensley, C.N., et al., (1977), "The Effect of Emulsification on the Selective Agglomeration of Fine Coal", International Journal of Mineral Processing, 4,173-184.

Berkowitz, N., (1979), An Introduction to Coal Technology, Academic Press, New York, NY, USA.

Botsaris, G.D. and Glazman, Y.M., (ed.), (1989), Interfacial Phenomena in Coal Technology, Marcel Dekker, Inc., New York, NY, USA.

Bowen, R.L. Jr., (1986), "Unraveling the Mysteries of Shear-Sensitive Mixing Systems", Chemical Engineering, June, 55-63.

Brookes, G.F. and Miles, N.J., (1987), "Coal Preparation - Some Thoughts for the Future", Mining Magazine, July, 52-57.

Capes, C.E., et al., (1976), "Application of Spherical Agglomeration to Coal Preparation", Proceedings from 7th International Coal Preparation Conference, June 3-5, Sydney, Australia, H, 2.

Capes, C.E., et al., (1981), "Selective Oil Agglomeration: An Answer to Fine Coal Treatment Problems", Coal: Phoenix of the '80's - Proceedings of the 64th CIC Coal Symposium, May 31 to June 3, Halifax, Nova Scotia, Cananda, 209.

Capes, C.E., et al., (1985), "Oil Agglomeration for Fine Coal Processing", 4th International Symposium on Agglomeration, June 3-5, Toronto, Ontario, Canda, 857.

Chen, C.H. and Nguyen, Y.V., (1981), "Pilot Plant Study of the Spherical Agglomeration Process", Coal: Phoenix of the '80's - Proceedings of the 64th CIC Coal Symposium, May 31 to June 3, Halifax, Nova Scotia, Canada, 217.

Corocoran, E., (1991), "Cleaning Up Coal", Scientific American, May, 108.

Davidson, R.M., (1990), "Natural Oxidation of Coal", IEA Coal Research, London, United Kingdom.

Drzymala, J., et al., (1986), "Selective Oil Agglomeration of Graphite in the Presence of Pyrite", Coal Preparation, 3, 89-98.

Effer, W.R., (1981), "Acid Rain: A Re-evaluation of some Issues", Coal: Phoenix of the '80's - Proceedings of the 64th CIC Coal Symposium, May 31 to June 3, Halifax, Nova Scotia, Canada, 594.

Fan, C.W., et al., (1982), "Coal and Pyrite Separation by Oil Agglomeration in Salt Solutions," US DOE Contract No. W-7408-Eng-82.

Freedman, B., (1981), "Trace Elements and Organics Associated with Coal Combustion in Power Plants: Emissions and Environmental Impacts.", Coal: Phoenix of the '80's - Proceedings of the 64th CIC Coal Symposium, May 31 to June 3, Halifax, Nova Scotia, Canada, 616.

Gilchrist, J. D., (1984), Extractive Metallurgy, 2nd Edition, Pergammon Press, New York, New York, USA.

Gorham, E., (1981), "An Air that Kills--Man's Alteration of the Chemical Climate", Coal: Phoenix of the '80's - Proceedings of the 64th CIC Coal Symposium, May 31 to June 3, Halifax, Nova Scotia, Canada, 610.

Hucko, R., et al., (1989), "Selective Agglomeration: An Interlaboratory Test Program", Annual Meeting Society of Mining Engineers, Feb. 27 to Mar 4, Las Vegas, Nevada, USA.

Khoury, D.L., (ed.), (1981), "Coal Cleaning Technology", Noyes Data Corporation, Park Ridge, NJ, USA.

Killmeyer, R.P., (1985), "Selective Agglomeration: Let's compare the emerging processes", Coal Mining, September, 45.

Klimpel, R.R., (1984), "Use of chemical reagents in flotation", Chemical Engineering, September 3, 75.

Knight, J.C, (1989), "Florence Mining's OK's Oil Agglomeration", Coal, May, 57.

Labuschagne B.C.J., (1986), "Relationships Between Oil Agglomeration and Surface Properties of Coal: Effect of pH and Oil Composition", Coal Preparation, 3, 1-13.

Laurila, M.J., (1985), "Five advanced cleaning processes bring desulfurization within reach", Coal Mining, Sept., 36.

Leaf, D.A., (1990), "Acid Rain and the Clean Air Act", Chemical Engineering Progress, May, 25.

Likens, G.E., et al., (1979), "Acid Rain", Scientific American, October, 241, 4, 43-51.

Liu, Y.A., (Editor), (1982), Physical Cleaning of Coal, Marcel Dekker Inc., New York, New York, USA.

Livengood, C.D., et al, (1984), "Coal Cleaning as a Sulfur-Reduction Strategy in the Midwest", First Annual Coal Conference, Sept. 17/21, Pittsburgh, Pennsylvania, 52.

Males, R.H., (1981), "Environmental Impacts of Coal Utilization", Coal: Phoenix of the '80s - Proceedings of the 64th CIC Coal Symposium, May 31 to June 3, Halifax, Nova Scotia, Canada, 632.

Maronde, C.P. and Deurbrouck, A.W., (1985), "Sulfur Reduction Potential of the Coals of the Northern Appalachian Region", Conference Proceedings, Coal Preparation, Apr 30 to May 2, Lexington, USA, 16.

Mehrotra, V.P. and Sastry, K.V.S., (1980), "Oil Agglomeration Offers Technical and Economical Advantages", Mining Engineering, August, 1230.

Mehrotra, V.P., et al., (1983), "Review of Oil Agglomeration Techniques for Processing of Fine Coals", International Journal of Mineral Processing, 11, 175-201.

Miller, F.G., (1969), "The Effect of Froth Sprinkling on Coal Flotation Efficiency", Society of Mining Engineers, AIME, June, 158.

Mishra, S.K., and Klimpel, R.R., (ed.), (1987), Fine Coal Processing, Noyes Publications, Park Ridge, NJ, U.S.A..

Moses, H. and Dahlman, R.C., (1981), "An Update of the CO_2 Issue - 1981", Coal: Phoenix of the '80's - Proceedings of the 64th CIC Coal Symposium, May 31 to June 3, Halifax, Nova Scotia, Canada, 602.

Nelson, C.R., (ed.), (1989), Chemistry of Coal Weathering, Elsevier Science Publishing Company Inc., New York, New York, USA.

Nguyen, Y., et al., (1983), "Coal Cleaning by Oil Agglomeration with Oil Recovery", Proceedings of Second Australian Coal Preparation Conference, Rockhampton, 10th-14th October.

Olson, T.J., (1985), "Froth Flotation for Fine-Coal Cleaning", EPRI, CS-4383, RP 1852-4.

Pawlak, W., et al., (1988), "Coal Upgrading by Selective Agglomeration", Proceedings: Twelfth Annual EPRI Contractor's Conference on Fuel Science and Conversion, February, Palo Alto, California, 5, 1.

Pawlak, W., et al., (1989), "Novel Applications of Oil Agglomeration Technology", Proceedings: Thirteenth Annual EPRI Conference on Fuel Science and Conversion, January, Palo Alto, California, 6, 1.

Sadowski, Z., et al., (1988), "Behavior of Oxidized Coal During Oil Agglomeration", Coal Preparation, 6, 17-34.

Singhal, I.K., et al., (1983), "Studies on the Effect of Variables on the Flotation of Coal Fines", Adv. Sci. Technol. Miner Benefic., India, Proc. Simp., 229.

Taylor, S.R., et al., (1981), "Surface Chemical Problems in Coal Flotation", AIP Conf. Proc., Vol. 70, (Chem. Phys., Coal Utiliz.), 344.

Vanangamudi M. and Rao, T. C., (1984), "Kinetic study of agglomerate growth in coal-oil agglomeration process, Fuel, 63, June, 738.

Venkatadri, R., et al., (1988), "Oil Agglomeration of Weakly Hydrophobic Coals and Coal/Pyrite Mixtures", Energy & Fuels, 2, 2, 145.

Weber, J., (1972), Physiochemical Processes for Water Quality Control, Division of John Wiley and Sons, Inc., New York, New York, USA.

Weiss, N.L., (Editor), (1985), SME Mineral Processing Handbook, SME, New York, New York, USA.

Wen, W.W. and Sun, S.C., (1977), "An Electrokinetic Study on the Amine Flotation of Oxidized Coal", Society of Mining Engineering, AIME, 272, June, 174.

Wills, W.W., (1984), Mineral Process Technology, Pergammon Press, New York, New York, USA.

Yang, G.C.C., et al., (1988), "Oil Agglomeration of Coal in Inorganic Salt Solutions", Coal Preparation, 5, 133-146.

Bibliography

Abbott, J. and Jenkinson, D.E., (1986), "An assessment of the Potential for the Reduction of Sulphur Contents of the UK Power Station Fuels", CIM, 10th International Coal Preparation Congress, September 1-5, Edmonton, 151.

Albaugh, E.W. et al., (1981), "Difference in the Behavior of 200 x 0 Kentucky No. 9 and Illinois No. 6 Coals in Surface Controlled Beneficiation", Coal: Phoenix of the '80's - Proceedings of the 64th CIC Coal Symposium, May 31 to June 3, Halifax, Nova Scotia, Canada, 254.

Andersen, N.E. and Hamza, H.A., (1981), "The Characterization of Oxidized Coal - A Review", Coal: Phoenix of the '80's - Proceedings of the 64th CIC Coal Symposium, May 31 to June 3, Halifax, Nova Scotia, Canada, 117.

Arbiter, N., and Weiss, N.L., (1970), "Design of Flotation Cells and Circuits", Trans. SME-AIME, 247, 340-347.

Arnold, B.J. and Aplan F.F., (1990), "Effect of Water Carryover in a Bank of Industrial Coal Froth Flotation Cells with a Comparison to Laboratory Test Results", Mining Engineering, SME, December, 1347.

Bajor, O. and Trass, O., (1988), "Modified Oil Agglomeration Process for Coal Beneficiation, I. Mineral Matter Liberation by Fine Grinding with the Szego Mill", The Canadian Journal of Chemical Engineering, 66, 2, 282.

Bensley, C.N., et al., (1977), "The effect of Emulsification on the Selective Agglomeration of Fine Coal", International Journal of Mineral Processing, 4, 173-184.

Botha, P.H., (1980), "An investigation of the flotation of three South African coals", Journal of the South African Institute of Mining and Metallurgy, November, 395.

Burger, J.R., (1980), "Froth Flotation is on the Rise", Coal Age, March, 99.

Bustamante, H. and Warren, L.J., (1984), "The Joint Effect of Rank and Grain Size on the Flotation of Australian Bituminous Coals', International Journal of Mineral Processing, 13, 13-28.

Campbell, J.A.L. and Sun S.C., (1970), " Bituminous Coal Electrokinetics", Society of Mining Engineer, AIME, June, 249, 112.

Chen, J.W, et al., (1981), "Coal Fines Recovery and Utilization", Coal: Phoenix of the '80's - Proceedings of the 64th CIC Coal Symposium, May 31 to June 3, Halifax, Nova Scotia, Canada, 244.

Darcovich, K., et al., (1988), "Surface Properties of Coal-Oil Agglomerates in the Floc Regime", American Chemical Society, 33, 4, 765.

Domini, J.C., (1981), "Determination of Surface and Bulk Oxidation of Coals by Fourier Transform Infrared Spectroscopy Using a Photoacoustice Detector", Coal: Phoenix of the '80's - Proceedings of the 64th CIC Coal Symposium, May 31 to June 3, Halifax, Nova Scotia, Canada, 132.

Drzymala, J, et al., (1986), "Influence of Air on Oil Agglomeration of Carbonaceous Solids in Aqueous Suspension", International Journal of Mineral Processing, 18, 277-286.

Ember, L.R., et. al., (1986), "Tending the Global Commons", C&EN, Nov., 14.

Feeley, T.J. III and Hervol, J.D., (1987), "Testing of Advanced Physical Coal Cleaning Processes -- Current Status", Fourth Annual Pittsburgh Coal Conference, September 28 to October 2, Pittsburgh, USA, 65.

Firth, B.A. and Nicol, S.K., (1981), "The Influence of Pyritic Sulphur on the Recovery of Fine Coal by Froth Flotation", First Australian Coal Preparation Conference, April 6/10, Newcastle, Australia, 157.

Fuerstenau, D.W. and Hanson, J.S., (1990), "Surface Modification of Coal in Advanced Flotation", U.S.DOE, Contract No DE-AC22-88PC88878.

Fuerstenau, D.W., et al., (1988), "Effect of Surface Functional Groups on the Flotation of Coal", Colloids and Surfaces, 8, 153-173.

Glass, R.W., et al., (1981), "Coal Cleaning for Control of Emissions", Coal: Phoenix of the '80's - Proceedings of the 64th CIC Coal Symposium, May 31 to June 3, Halifax, Nova Scotia, Canada, 658.

Grady, W.C., (1977), "Microscopic Varieties of Pyrite in West Virginia Coals", Trans. Society of Mining Engineers, Sept., 262, 268.

Gregory, F.W., (1982), "Oil Agglomeration of Coal Fines", International Energy Agency, June.

Harris, C.C. and Lepetic, V., (1966), "Flotation Cell Design," Mining Engineering, Sept., 18, 67-72.

Harris, C.C. and Raja, A., (1970), "Flotation Machine Impeller Speed and Air Rates as Scale-Up Criteria," Transactions, Institution of Mining and Metallurgy, 79, c295-297.

Harris, C.C., (1974), "Impeller Speed, Air, and Power Requirements in Flotation Machine Scale-up", International Journal of Mineral Processing, 1, 51-64.

Harvey, R.D. and DeMaris, P.J., (1987), "Size and Maceral association of Pyrite in Illinois Coals and their Float-Sink Fractions", Org. Geochem., 11, 5, 343.

Havs, M., et al., (1984), "Red herrings in acid rain research", Environ Sci Technol, 18, 6, 176a.

Hazra, S.K., et al., (1986), "Effects of Process Variables on Size Distribution of Oil-Agglomeration of Fine Coal", Coal Preparation, 3, 77-87.

Hazra, S.K., et al., (1988), "Significance of the Efficiency Index in Evaluating the Economics of Beneficiation of Coal Fines by the Oil Agglomeration Technique", International Journal of Mineral Processing, 24, 81-90.

Hileman, B., (1984), "Acid rain perspectives: A tale of two countries", Environ Sci Technol, 18, 11, 341a.

Hirose, T., (1984), "Coal Beneficiation by Oil Agglomeration", Ministry of Education, Science and Culture, Japan.

Jessap, R.R. and Stretton, J.L., (1970), "Electrokinetic Measurements on Coal and a Criterion for its Hydrophobicity", Fuel, 48, 317-320.

Josephs, L.L. and Ferris, D.D., (1990), "Engineering Development of Advanced Froth Flotation Pyrite Liberation Study and Round-Robin Flotation Report", DOE Contract No DE-AC22-88PC-88881.

Laskowski, J., et al., (1985), "Desulfurizing Flotation of Eastern Canadian High-Sulphur Coal", Processing and Utilization of High Sulfur Coals, 247.

Leonard, W.G., et al., (1981), "Coal Desulfurization and Deashing by Oil Agglomeration", Separation Science and Technology, 16, 10, 1589-1609.

Loo C.E. and Slechta, J., (1987), "The Effect of Pendular Flocculation on the Filtration of Fine Coal", Coal Prepartion, 5, 109-120.

Mazumdar, M, et al., (1988), "Statistical Relationship between Pyrite Grain Size Distribution and Pyritic Sulfur Reduction in Ohio Coal", International Journal of Coal Geology, 9, 371-383.

McCartney, J.T., et al., (1969), "Pyrite Size Distribution and Coal-Pyrite Particle Association in Steam Coals", United States Department of the Interior, Bureau of Mines, Report of Investigations 7231, February.

Miller, F.G. and Turbeville, R.M., (1986), "Coal Flotation - Past, Present, and Future", SME Annual Meeting, New Orleans, Louisiana, March 2-6, 1.

Miller, J.D., et al., (1988), "Improved Pyrite Rejection by Chemically-Modified Fine Coal Flotation", Coal Preparation, 6, 151-166.

Miller, K.J, (1973), "Flotation of Pyrite form Coal: Pilot Plant Study", US Dept. of Interior, Report of Investigation 7822.

Miller, K.J., (1988), "Importance of Classifying Circuitry on the Successful Application of Reverse Coal-Pyrite Flotation", DOE/PETC/TR-88/1, February.

Nguyen, Y.V. and Cheh, C.H., (1981), "Froth Flotation Studies on as Eastern US Coal", Coal: Phoenix of the '80's - Proceedings of the 64th CIC Coal Symposium, May 31 to June 3, Halifax, Nova Scotia, Canada, 174.

Nguyen, Y.V., and Row, R., (1985), "Oil Agglomeration of Coal with Oil Recovery", 4th International Symposium on Agglomeration, June 2-5, Toronto, Canada, 875.

Nicol, S.K., (1979), "Oil Agglomeration for Fine Coal Refuse Treatment", World Coal, August, 20.

Nicol, S.K., et al., (1977), "Effect on Agitation on Quality of Selectively Agglomerated Fine Coal", Trans. Int. Min. Metall., C86-C92.

Nimerick, K.H., (1980), "New Method of Oxidized Coal Flotation", Mining Congress Journal, September, 21.

Palmer, A.D., et al., (1990), "Relation between particle size and properties of some bituminous coals", Fuel, 69, February, 183.

Rao, A.C., et al., (1982), "Characteristic Curve for the Coal-Oil Agglomeration Process", International Journal of Mineral Processing, 9, 235-243.

Sablik, J. and Pawlik, J., (1983), "The Influence of the Finest Coal Particles on the Floatability of Some Three-Phase Systems", Powder Technology, 36, 1, 21.

Spitzer, D.P., (1984), "Why oxidized Coal Does Not Float", First Annual Coal Conference, Sept. 17-21, Pittsburgh, Pennsylvania, USA, 858.

Taweel, A. et al, (1981), "Adsorption: A Tool for Characterizing Coal Oxidation", Coal: Phoenix of the '80's - Proceedings of the 64th CIC Coal Symposium, May 31 to June 3, Halifax, Nova Scotia, Canada, 125.

Theodore, F.W., (1985), "Oil Agglomeration for Fine Coal Recovery as Commercialized at Conoco/Consol", 4th International Symposium on Agglomeration, June 3-5, Toronto, Ontario, 857.

Trass, O. and McCracken, T.W., (1985), "Grinding and Oil Agglomeration of Coal in the Szego Mill", 4th International Symposium on Agglomeration, June 2-5, Toronto, Ontario, Canada, 891.

Trass, O., et al., (1981), "Grinding of Coal Slurries with the Szego Mill", Coal: Phoenix of the '80's - Proceedings of the 64th CIC Coal Symposium, May 31 to June 3, Halifax, Nova Scotia, Canada, 235.

Vickers, F. and Ivatt, S., (1983), "The Preparation of Low Ash, Low Sulphur Coal", I.CHEME Symposium Series No. 83, 55.

Wen, W.W. and Sun S.C., (1977), "An Electrokinetic Study on the Amine Flotation of Oxidized Coal", Society of Mining Engineers, AIME, June, 174.

West, T.W. and Apodaca, L.W., (1986), "Redesigning fine coal circuits for better froth flotation", Coal Mining, September, 67.

Wojcik, W., et al., (1990), "Influence of Polar and Apolar Liquids on the Stability of the Pyrite-Air Bubble Aggregate", Canadian Metallurgical Quarterly, 29, 2, 93-96.

Appendices 1 to 6

Appendix 1

Mathematical Probability Models Describing CMR (%) TS (% daf) and Ash (% db)

A1 Probability Models

Three scientific descriptions and probabilistic models were developed to describe how the processes of agglomeration and flotation are linked together to facilitate the cleaning of bituminous coals. Models describing combustible recovery, pyritic sulphur reduction, and ash rejection were developed and presented in the following sections.

Figure A1 provides a schematic representation of the combustible matter recovery (CMR) model. The diagram divides the process into the agglomeration and flotation processes. Within the agglomeration process, particles can either report to the agglomerate phase, or remain in the water phase. If the particle is successfully oil wetted in the high shear mixing stage, it will report to the agglomerate phase. The particle will report to the water phase if oil wetting does not occur. Both the agglomerate phase and the water phase report to the flotation process of the model representation.

The flotation process is subdivided into three zones, the slurry, transition and froth zones (see Figure A2). The slurry zone represents the region where all the inputs to the system are initially mix together, and all phases (agglomerate, water, and air) coexist in this region. The transition zone represents the dynamic region of the process where attachment and detachment of particles occurs continuously. It is within this region that entrainment of solids to the product occurs. The froth zone represents the distinct phase of solids and air which rides on the surface of the transition zone. Agglomerates will report back and froth across the boundary of the froth and transition zones by various mechanisms.

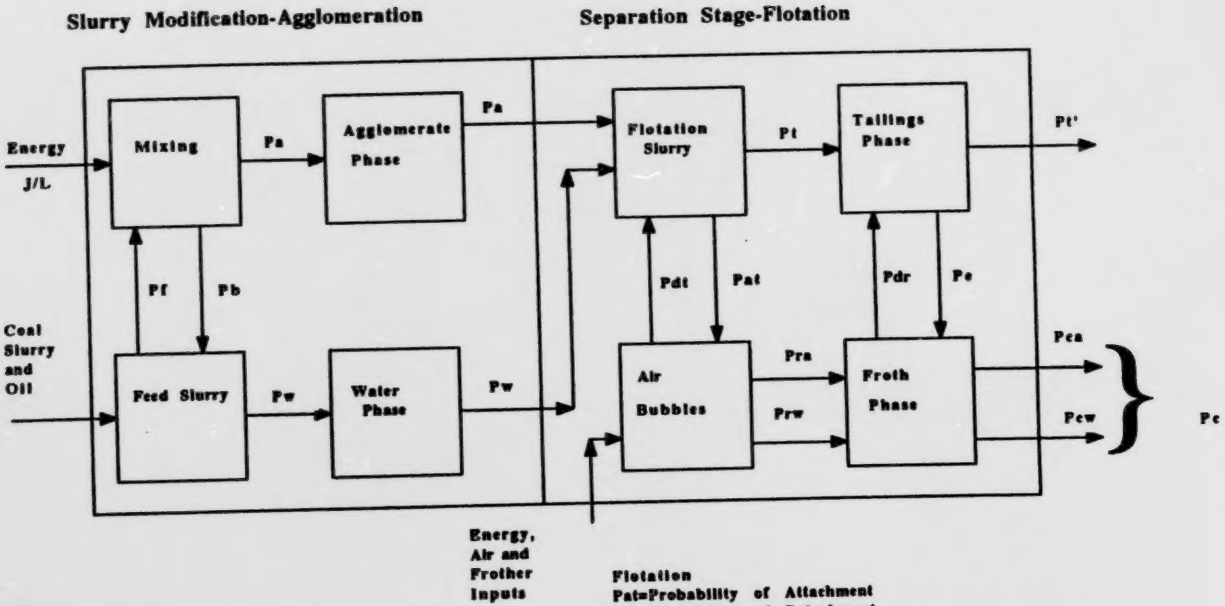

Agglomeration
Pa=Probability of Successful Agglomeration
Pf=Probability of Agglomeration Formation
Pb=Probability of Agglomerate Disruption
Pw=Probability of Particle Reporting to Water Phase

Flotation
Pat=Probability of Attachment
Pdt=Probability of Detachment
Prw=Probability of Particle from Water Phase Reporting to the Froth Phase by Flotation
Pra=Probability of Agglomerate Reporting to Froth
Pe=Probability of Entrainment
Pdr=Probability of Drainage
Pca=Probability of Agglomerates Reporting for Product
Pcw=Probability of Solid From Water Phase Reporting to the Product Phase
Pc=Probability of Combustible Recovery

Figure A1 Combustible Matter Recovery Model

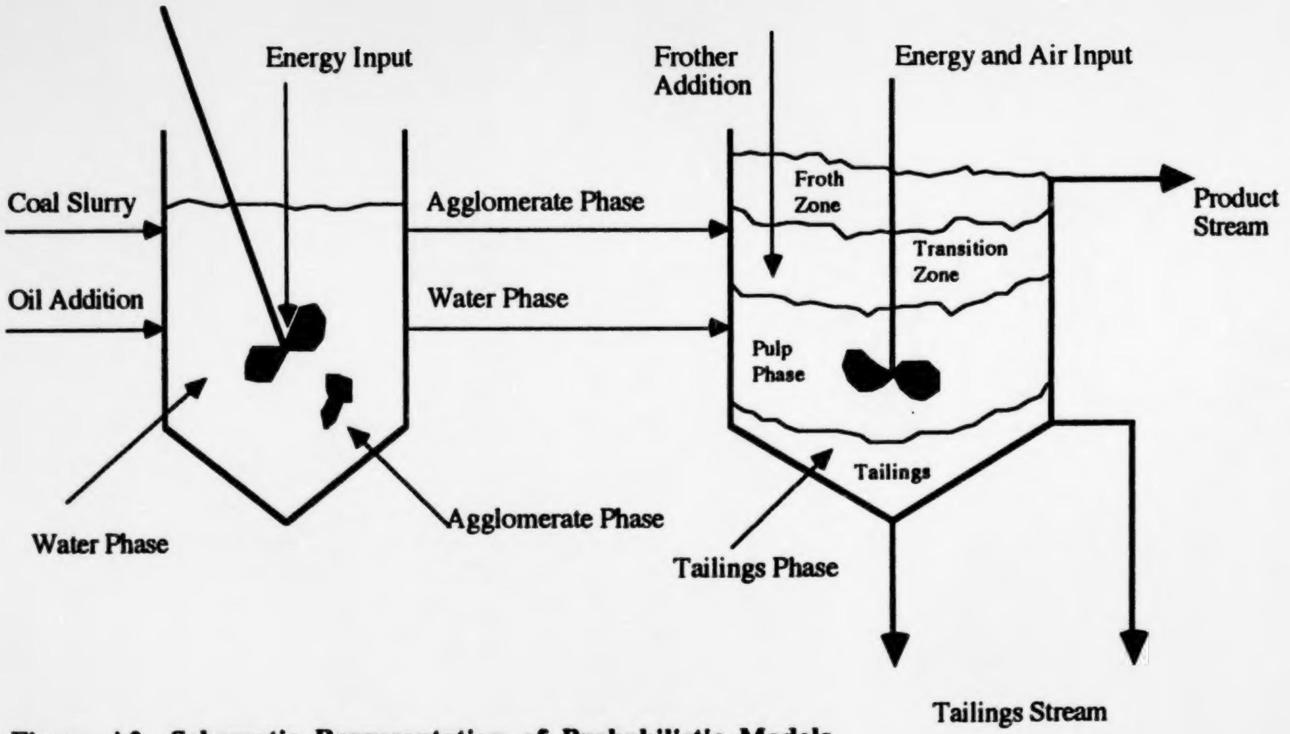

Figure A2 Schematic Representation of Probabilistic Models

A1.1 Combustible Matter Recovery Model

A1.1.1 Agglomeration

Agglomerate Phase

Figure A1 summarizes the block diagram of the proposed probabilistic model describing how the combustible solids report to the product phase. The model begins with the addition of mixing energy, coal slurry and oil. The probability of successful agglomeration, P_a, is given by the equation 1 which relates the outcome to the product of the probability of formation, P_f, by $(1 - P_b)$, where P_b is the probability of agglomerate breakage.

$P_a = P_f * (1 - P_b)$ eq. 1

Agglomerate Formation

P_f, the probability of formation can be defined in terms of transport and attachment mechanisms, where,

$P_f = P_{tr}{}^a * P_{attch}{}^a$ eq. 2

where,

$P_{tr}{}^a$ is the probability of successful agglomerate transport,

where,

$P_{tr}{}^a = (P_i{}^a + P_d{}^a)$ eq. 3

and,

$P_i{}^a$ is the probability of successful agglomerate transport by impact inertia,

$P_d{}^a$ is the probability of successful agglomerate transport by diffusion,

and, $P_{attach}{}^a$ is the probability of successful agglomerate attachment,

where,

$P_{attach}{}^a = (P_{sur}{}^a + P_{ad}{}^a + P_{ch}{}^a + P_{ent}{}^a)$,

and,

$P_{sur}{}^a$ is the probability of attachment via surface energy minimization,

$P_{ad}{}^a$ is the probability of attachment via adsorption forces,

P_{ch}^{a} is the probability of attachment via chemical bonding/interaction, and,

P_{ent}^{a} is the probability of attachment via particle entrapment.

therefore, the probability of successful agglomerate formation can be defined in terms of transport and attachment mechanisms as described below.

$$P_f^{a} = (P_i^{a} + P_d^{a}) * (P_{sur}^{a} + P_{ad}^{a} + P_{ch}^{a} + P_{ent}^{a}) \qquad \text{eq. 4}$$

Agglomerate Breakage

The probability of agglomerate breakage after formation is defined by the inequality related to the attachment and shear forces present in the mixer.

$$P_b = P_{sh}^{a} - P_{attach}^{a'} > 0, \qquad \text{eq. 5}$$

where,

P_{sh}^{a} is the probability that mixer shear forces exceed the attachment forces, and,

$P_{attach}^{a'}$ is the probability that the attachment forces are weaker than the shear forces within the mixer, (e.g. $(P_{sur}^{a'} + P_{ad}^{a'} + P_{ch}^{a'} + P_{ent}^{a'})$), therefore, the probability of successful agglomeration is described by the equations below.

$$P_a = (P_i^{a} + P_d^{a})*(P_{sur}^{a} + P_{ad}^{a} + P_{ch}^{a} + P_{ent}^{a}) *$$

$$(1 - (P_{sh}^{a} - (P_{sur}^{a'} + P_{ad}^{a'} + P_{ch}^{a'} + P_{ent}^{a'}))) \qquad \text{eq. 6}$$

where,

$(P_{sh}^{a} - (P_{sur}^{a'} + P_{ad}^{a'} + P_{ch}^{a'}))$ is > 0,

and,

$$P_a = (P_i^{a} + P_d^{a})*(P_{sur}^{a} + P_{ad}^{a} + P_{ch}^{a} + P_{ent}^{a}), \qquad \text{eq. 7}$$

where,

$(P_{sh}^{a} - (P_{sur}^{a'} + P_{ad}^{a'} + P_{ch}^{a'}))$ is < 0.

Water Phase

The probability of a combustible rich solid remaining distinctively part of the water phase solids, P_w, is given by the equation 8. The equation relates the P_w to the product of the probability of agglomerate breakage, P_b, and $(1 - P_f)$, where P_f is the probability of successful agglomeration.

$$P_w = (1 - P_f) + P_f * P_b \qquad \text{eq. 8}$$

Assuming similar transport and attachment mechanisms can be used to describe this probability, then equations 9 and 10 below can be used to further define the probability of a combustible rich particle remaining in the water phase.

$$P_w = (1 - (P_i^a + P_d^a) * (P_{sur}^a + P_{ad}^a + P_{ch}^a)) + (P_i^a + P_d^a) * (P_{sur}^a + P_{ad}^a + P_{ch}^a) * (P_{sh}^a - (P_{sur}^{a'} + P_{ad}^{a'} + P_{ch}^{a'})), \qquad \text{eq. 9}$$

where,

$(P_{sh}^a - (P_{sur}^{a'} + P_{ad}^{a'} + P_{ch}^{a'}))$ is > 0,

and,

$$P_w = (1 - (P_i^a + P_d^a) * (P_{sur}^a + P_{ad}^a + P_{ch}^a)) \qquad \text{eq.10}$$

where,

$(P_{sh}^a - (P_{sur}^{a'} + P_{ad}^{a'} + P_{ch}^{a'}))$ is < 0.

Assuming 100 coal particles consisting of combustible, ash and pyrite rich masses represent the sample set, then equation 11 below must also be true.

$$P_a + P_w = 1 \qquad \text{eq.11}$$

A1.1.2 Flotation

During flotation energy, water, air bubbles and frother are new inputs to the system. Combustible matter recovery by flotation can occur through four pathways:

- flotation of agglomerates formed during high shear mixing,
- flotation of agglomerates formed during flotation agitation,
- flotation of single combustible rich particles, sufficient in size and hydrophobicity to cause their reporting to the froth phase, and,
- combustible matter recovery by water entrainment, which for this model is neglected.

The model does not discriminate between agglomerates formed as a result of the flotation energy input, rather than high shear mixing, because agglomerates formed in either mixing stage would demonstrate very similar flotation kinetics and thermodynamics. Considering a second stage of energy input and agglomerate formation would over complicate the model. Hence, the model describing the probability of successful formation of an agglomerate, or the successful oil wetting of a single particles, during high shear mixing stage, P_{ra}, equation 12, has been somewhat empirically tempered by this assumption.

Single particles sufficient in size and oil coating, will demonstrate flotation kinetics and attachment forces similar to particles which formed agglomerates, but still require individual transport and attachment probabilities. However, carbonaceous particles that were not able to be properly oil coated, yet possessing natural hydrophobicity, would require distinctively different transport and attachment probabilities because of the lower surface hydrophobicity and the high oxidation of the test coal. However, the model will not address this later pathway because the mass of particles demonstrating natural hydrophobicity is small for this test coal and can be neglected.

Agglomerate into the Froth Phase

$$P_{ra} = P_a * P_{at} * (1 - P_{dt}) \qquad \text{eq.12}$$

In the above equation, P_{at}, is the probability of successful attachment of an air bubble to an agglomerate causing it to report to the froth phase. P_a is the probability of successful agglomeration; and P_{dt} is the probability of detachment of an air bubble, causing an agglomerate to report back to the slurry phase.

Agglomerate and Bubble Attachment

P_{at}, the probability of successful attachment of an air bubble to an agglomerate can be defined in terms of transport and attachment mechanisms.

$$\text{where, } P_{at} = P_{tr}^{f} * P_{attach}^{f} \qquad \text{eq.13}$$

where,

P_{tr}^{f} represents the predominant flotation transport forces,

and,

P_{attach}^{f} represents the predominant flotation attachment forces,

and,

$P_{tr}^{f} = (P_{i}^{f} + P_{d}^{f})$,

where,

P_{i}^{f} and P_{d}^{f} represent the probability that inertial and diffusion forces cause successful contact of air bubbles and combustible agglomerates,

and,

$P_{attach}^{f} = (P_{sur}^{f} + P_{ad}^{f} + P_{ch}^{f})$,

where,

P_{sur}^{f}, P_{ad}^{f}, and P_{ch}^{f} represent the probability that surface energy minimization, adsorption forces, and chemical bonding are the predominant attachment forces responsible for successful flotation.

Agglomerate and Bubble Detachment

The probability of agglomerate detachment, P_{dt}, depends upon the relative shear forces the particles experience, the strength of the air bubble and agglomerate attachment forces, and the time before the agglomerate reports to the product phase. P_{dt} can be defined in terms of attachment and shear forces, by equation 14 below.

$$P_{dt} = P_{sh}^{f} - P_{attach}^{f} > 0 \qquad \text{eq.14}$$

where,

P_{sh}^{f} is the probability that the shear forces exceed the attachment forces,

and,

$P_{attach}^{f'}$ is the probability that the attachment forces are weaker than the shear forces within the cell, (e.g.. $(P_{sur}^{f'} + P_{ad}^{f'} + P_{ch}^{f'})$)

Therefore, the probability of successful flotation of combustible rich agglomerates reporting to the product phase from the froth can be described by the equation 15 and 16 below.

$$P_{ra} = P_a * (P_i^f + P_d^f) * (P_{sur}^f + P_{ad}^f + P_{ch}^f) *$$

$$(1 - (P_{sh}^f - (P_{sur}^f + P_{ad}^f + P_{ch}^f))) \qquad \text{eq.15}$$

where,

$(P_{sh}^f - (P_{sur}^f + P_{ad}^f + P_{ch}^f))$ is > 0,

and,

$$P_{ra} = P_a * (P_i^f + P_d^f) * (P_{sur}^f + P_{ad}^f + P_{ch}^f) \qquad \text{eq.16}$$

where,

$(P_{sh}^f - (P_{sur}^f + P_{ad}^f + P_{ch}^f))$ is < 0

Single Particle into the Froth Phase

The probability of combustible matter reporting via single particle flotation can be described by equation 17 below.

$$P_{rw} = P_w * P_{at}^s * (1 - P_{dt}^s) \qquad \text{eq.17}$$

where,

$P_w =$ is the probability of a combustible particle reporting with the water phase,

and

$P_{at}^s =$ is the probability of the attachment of an air bubble to a single oil wetted, particle of combustible matter,

and,

$P_{dt}^s =$ is the probability of successful detachment of the same particles.

Single Particle and Bubble Attachment

The probability of successful attachment, P_{at}^s, can be related to both transport and attachment mechanisms, P_{tr}^s, and P_{attach}^s, as described in equation 18 below.

$$P_{at}^s = P_{tr}^s * P_{attach}^s, \qquad \text{eq. 18}$$

where,

P_{tr}^{s} are the transport probabilities that best describe the collision of air bubbles and single particles of combustible matter,

P_{attach}^{s} are the attachment probabilities that best describe the attachment of air bubbles to the particles,

$P_{tr}^{s} = (P_i^s + P_d^s)$, where, P_i^s, and P_d^s are the inertial and diffusion probabilities that are responsible for the transport of single particle and air bubble collision theory; and,

$P_{attach}^{s} = (P_{sur}^{s} + P_{ad}^{s} + P_{ch}^{s})$, where P_{sur}^{s}, P_{ad}^{s}, and P_{ch}^{s} represent the forces responsible for the attachment of air bubbles to single particles.

Single Particle and Bubble Detachment

The probability of detachment, P_{dt}^{s}, of single particles is related to the resolution of shear and attachment forces which exist in the flotation cell. Equations 19 and 20 below are presented for further explanation.

$$P_{rw} = P_w * (P_i^a + P_d^a) * (P_{sur}^a + P_{ad}^a + P_{ch}^a) * (1 - (P_{sh}^f - (P_{sur}^a + P_{ad}^a + P_{ch}^a))), \qquad \text{eq.19}$$

where,

$(P_{sh}^f - (P_{sur}^a + P_{ad}^a + P_{ch}^a))$ is > 0,

and,

$$P_{rw} = P_w * (P_i^a + P_d^a) * (P_{sur}^a + P_{ad}^a + P_{ch}^a) \qquad \text{eq.20}$$

where,

$(P_{sh}^f - (P_{sur}^a + P_{ad}^a + P_{ch}^a))$ is < 0.

Agglomerate Entrainment and Drainage

The high strength of the agglomeration attachment forces, and their rapid flotation kinetics and highly hydrophobic nature, indicate that the probability of an agglomerate reporting to the froth zone from entrainment from the transition zone is unlikely. Hence, P_e, which represents the probability of agglomerate recovery via entrainment from the transition zone, can be neglected and assigned a zero value.

Because of the unique design of both the flotation cell and the pyrite separator, and the high penetration wash nozzles on both cells, it is likely that some drainage of agglomerates back into the transition zone will occur, where they may either short circuit to the tailings stream, or re-attach back to the froth zone. Hence, equation 21 below can be used to describe the probability of agglomerates reporting to the product phase, P_{ca}.

$P_{ca} = P_{ra} * (1 - P_{dr}^{a}) + P_{e}^{a} * P_{t}^{a}$, eq.21

where,

P_{t}^{a} is the probability of an agglomerate reporting to the tailings zone,

P_{dr}^{a} is the probability of an agglomerate draining to the transition zone,

and,

P_{e}^{a}, represents the probability of entrainment of an agglomerate, and is assumed to be zero because of the extremely high hydrophobicity of agglomerated combustible matter. Hence, the probability of an agglomerate reporting to the product, P_{ca}, can be described by the equation 22 below.

$P_{ca} = P_{ra} * (1 - P_{dr}^{a})$ eq.22

where,

P_{ra} and P_{dr} are the probabilities as previously defined, equation 15 and 16.

Single Particle Entrainment and Drainage

The attachment forces responsible for the flotation of single particles of combustible matter are not expected to be as strong as the agglomerate bubble attachment. Hence, the washing action is expected to cause a different rate of drainage of particles from the froth zone into the tailings zone. Furthermore, some particles of combustible material, particularly if they are large in diameter, or poorly coated with oil, may exist in the transition zone for an extended period. Hence, individual probabilities of single particle drainage and entrainment to the product phase by flotation can be described by equation 23.

$P_{cw} = P_{rw} * (1 - P_{dr}^{s}) + P_{e}^{s} * (1 - P_{t}^{s})$ eq. 23

where,

P_{rw} is the probability of a single particle reporting successfully to the froth zone,

P_{dr}^{s} is the probability of a single particle draining into the transition zone and subsequently short circuiting into the tailings phase,

P_{e}^{s} is the probability of single particles being entrained in the froth phase, and,

P_{t}^{s} is the probability of single particles remaining in the tailings phase within the cell volume.

Total Combustible Recovery

Hence, the total recovery of combustible matter, P_c, via discrete oil coated combustible particles, and agglomerates, can be described by combining equations 22 and 23 to generate equation 24.

$$P_c = P_{ca} + P_{cw}$$

$$P_c = P_{ra} * (1 - P_{dr}^{a}) + P_{rw} * (1 - P_{dr}^{s}) + P_{e}^{s} * (1 - P_{t}^{s}) \qquad \text{eq.24}$$

where,

P_{dr}^{s} can be related to the impact force induced by the washing nozzles and the attachment forces within the froth zone. P_{e}^{s} and P_{t}^{s}, the probability of entrainment from the transitions zone, and the probability of a particle remaining in the tailings zone, are related to the solids percent, the particle size, and the hydrodynamic characteristics of the cell.

A1.2 Pyrite Recovery Model

A1.2.1 Agglomeration

Figure A3 summarizes the block diagram of the proposed probabilistic model describing how the pyrite rich solids report to the product phase. Similar to the combustible matter recovery model, the total pyrite removal model begins with the addition of oil, energy, and feed stock coal slurry. The probability of a pyrite particle reporting to the agglomerate phase, via either oil coating of the pyrite surface with oil and including the particle within an agglomerate, or by physically entrapping the particle within the agglomerate is given by P_{ra}^{P}. The probability of P_{ra}^{P} can be defined in terms of the probability of pyrite agglomeration and entrapment, P_{f}^{P}; and by P_{b}^{P}, the probability of pyrite detachment to the water phase. Equation 25 below describes the probabilistic relationship.

Pyrite in Agglomerate Phase

$P_{ra}^{P} = P_{f}^{P} * (1 - P_{b}^{P})$, where eq.25

P_{f}^{P} is the probability of pyrite agglomeration or entrapment, and,

P_{b}^{P} is the probability of a pyrite particle detaching and reporting back to the water phase, via re-dispersion and reworking of the agglomerate mixing.

Pyrite Attachment

The probability of pyrite agglomeration and entrapment, P_{f}^{P}, can be expressed in terms of transport, P_{trp}^{P}, and attachment, $P_{attachp}^{P}$, mechanisms. Equation 26 below describes the overall expression.

$P_{f}^{P} = P_{tr}^{P} * P_{attach}^{P}$, eq.26

where the following transport and attachment mechanisms are predominant in causing the capture of pyrite particles within the agglomerates.

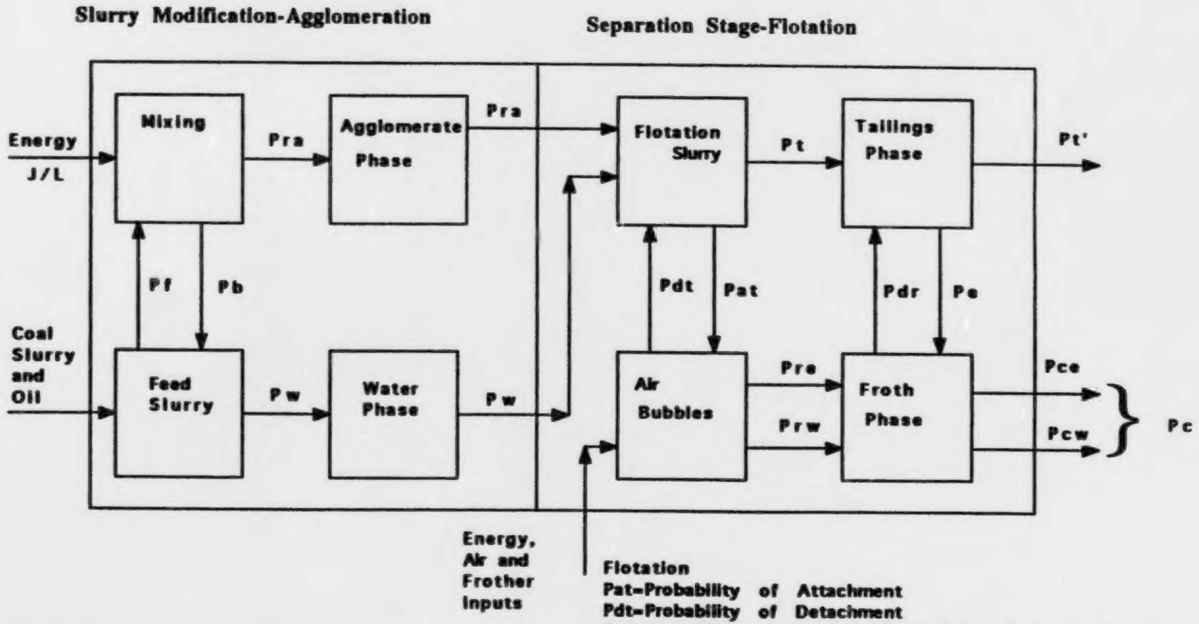

Agglomeration

Pra=Probability of Pyrite Remaining in Agglomerate Phase
Pf=Probability of Pyrite Agglomeration or Entrapment
Pb=Probability of Pyrite Detachment Back to the Water Phase
Pw=Probability of Pyrite Reporting Directly to Water Phase

Flotation

Pat=Probability of Attachment
Pdt=Probability of Detachment
Prw=Probability of Particle from Water Phase Reporting to the Froth Phase via Flotation
Pre=Probability of Entrapped Pyrite Agglomerate Reporting to Froth
Pe=Probability of Entrainment of Pyrite
Pdr=Probability of Drainage of Pyrite
Pce=Probability of Entrapped Pyrite Reporting to Product
Pcw=Probability of Pyrite From Water Phase Reporting to the Product via Flotation
Pc=Probability of Pyrite Reporting to Product
Pt and Pt'=Probability of Pyrite Reporting to Tailings

Figure A3 Total Sulphur Reduction Model

$P_{tr}^{p} = (P_{i}^{p} + P_{d}^{p})$

where P_{i}^{p} and P_{d}^{p} are defined as before, as they apply to the capture of free pyrite particles, and,

$P_{attach}^{p} = (P_{sur}^{p} + P_{ad}^{p} + P_{ch}^{p} + P_{ent}^{p})$

where P_{sur}^{p}, P_{ad}^{p}, P_{ch}^{p} and P_{ent}^{p} are as defined before, as they apply to the capture of free pyrite particles, hence, the P_{f}^{p} can be defined by equation 27 below.

$$P_{f}^{p} = (P_{i}^{p} + P_{d}^{p}) * (P_{sur}^{p} + P_{ad}^{p} + P_{ch}^{p} + P_{ent}^{p}) \qquad \text{eq.27}$$

Pyrite Detachment from an Agglomerate

The probability of pyrite detachment from the agglomerate back to the water phase, P_{b}^{p}, will depend upon the resolution of shear and attachment forces. In addition to this force resolution, the probability of detachment of the pyrite particles to the water phase, P_{b}^{p}, depends upon the resolution of the surface forces competing for the oil phase. At very low oil concentrations, combustible surfaces are expected to compete and deprive pyrite surfaces of the oil phase. Fundamental investigation describing the surface energy thermodynamics between carbonaceous and pyrite surfaces do not exist, hence, for the purposes of this study, equation 28 below is presented as a summary of the probability of pyrite particle capture within the agglomerate phase. The equation describes the process in terms of typical transport and attachment forces.

Pyrite Capture in Combustible Agglomerate

$$P_{ra}^{p} = (P_{i}^{p} + P_{d}^{p}) * (P_{sur}^{p} + P_{ad}^{p} + P_{ch}^{p} + P_{ent}^{p}) * (1 - P_{b}^{p}) \qquad \text{eq.28}$$

where,

P_{ra}^{p} is the probability of a free pyrite particle being captured within a combustible rich agglomerate.

Pyrite in Water Phase

The probability of a pyrite particle remaining in the water phase, P_w, is described by equation 29 and 30 below.

$P_w{}^p = (1 - P_f{}^p) + P_f{}^p * P_b{}^p$, eq.29

where,

$P_f{}^p$ and $P_b{}^p$, are as previously defined,

hence,

$P_w{}^p = (1 - (P_i{}^p + P_d{}^p) * (P_{sur}{}^p + P_{ad}{}^p + P_{ch}{}^p + P_{ent}{}^p)) + (P_i{}^p + P_d{}^p) *$
$(P_{sur}{}^p + P_{ad}{}^p + P_{ch}{}^p + P_{ent}{}^p) * P_b{}^p$, eq.30

where, $P_w{}^p$ is the probability a free pyrite particle remains in the water phase.

A1.2.2 Flotation

Pyrite particles have three major pathways by which they report to the product:

- pyrite particles can experience agglomeration and entrapment within the combustible agglomerates, resulting in their recovery with the combustible agglomerate into the product phase,
- Pyritic sulphur surfaces can be activated by dissolved organics from the oil phase, or by oil coating of the surfaces during high shear mixing, and
- fresh, clean pyrite surfaces which have not experience extensive oxidation, demonstrate natural hydrophobic tendencies and report via flotation.

Pyrite Particle Capture via Agglomerate Flotation

The first pathway, the probability of pyrite recovery within the agglomerate phase, $P_{re}{}^p$, is described by equation 31 below.

$P_{re}{}^p = P_{ra}{}^p * P_{at}{}^a * (1 - P_{dt}{}^a)$ eq.31

where,

$P_{ra}{}^p$ is the probability of a free pyrite being captured in an agglomerate,

$P_{at}{}^a$ is the probability of successful attachment of an agglomerate,

and,

$P_{dt}{}^a$ is the probability of detachment of an agglomerate containing free pyrite.

The probabilities of attachment and detachment of pyrite particles from the agglomerates can be defined in the same manner as presented in the combustible matter recovery model, where equations 32 and 33 summarize the possibilities.

$P_{re}^{p} = P_{ra}^{p} * (P_{i}^{a} + P_{d}^{a}) * (P_{sur}^{a} + P_{ad}^{a} + P_{ch}^{a} + P_{entrap}^{a}) *$

$(1 - (P_{sh} - (P_{sur}^{a'} + P_{ad}^{a'} + P_{ch}^{a'} + P_{entrap}^{a'})))$ eq. 32

where,

$(P_{sh} - (P_{sur}^{a'} + P_{ad}^{a'} + P_{ch}^{a'} + P_{entrap}^{a'}))$ is > 0,

and,

$P_{re}^{p} = P_{ra}^{p} * (P_{i}^{a} + P_{d}^{a}) * (P_{sur}^{a} + P_{ad}^{a} + P_{ch}^{a} + P_{entrap}^{a})$, eq. 33

where,

$(P_{sh} - (P_{sur}^{a'} + P_{ad}^{a'} + P_{ch}^{a'} + P_{entrap}^{a'}))$ is <0.

Pyrite Drainage and Entrainment from Agglomerates

The final recovery of pyrite captured in the combustible agglomerates can be described by equation 34.

$P_{ca}^{p} = P_{re}^{p} * (1 - P_{dr}^{p}) + P_{e}$ eq. 34

where,

Assuming that P_e, the probability of recovery of an combustible agglomerate by entrainment is zero, the equation can be simplified.

$P_{ca}^{p} = P_{re}^{p} * (1 - P_{dr}^{p})$ eq. 35

The nozzle washing is performed to enhance the removal of attached, and to a lesser degree, the entrapped and agglomerated pyrite. Hence, equation 35 can be considered to be the final form for the first pathway of pyrite recovery.

P_{dr}^{p}, the probability of drainage of pyrite from the agglomerate from the froth phase, can be considered to be a resolution of forces related to the strength of pyrite attachment, the force of impact exerted by the washing nozzles, and the exposure time of the washing action.

Pyrite Particle Flotation

The second pathway, by which single pyrite particles report to the product phase via flotation, may occur via three methods. The soluble components of the oil phase may serve as:

- a pyrite collector, or for surface activation, or
- oil may coat the pyrite surfaces deeming them to become hydrophobic,
- or, the process may depend on the hydrophobicity of the pyrite surfaces.

For the purposes of this model, the relative differences in the kinetics and thermodynamic of each of these pathways was not considered, and the flotation of single pyrite particles were lumped into one model. Regardless of the actual pathway responsible for pyrite particle flotation, equation 36 describes the probability of a pyrite particle reporting to the froth phase, P_{rw}.

$P_{rw}^{P} = P_{w}^{P} * P_{at}^{P} + (1 - P_{dt}^{P})$, eq. 36

where P_{w}^{P} is the probability a free pyrite particle remains in the water phase, which was described by equations 29 and 30 before,

and,

P_{at}^{P} is the probability of attachment of a pyrite particle to an air bubble, which can be related to transport, P_{tr}^{P}, and attachment, P_{attach}^{P}, mechanisms.

Pyrite Particle and Bubble Attachment

$P_{at}^{P} = P_{tr}^{P} * P_{attach,}^{P}$ eq. 37

where,

$P_{tr}^{P} = (P_{I}^{P} + P_{d}^{P})$

where,

P_{I}^{P} and P_{d}^{P} are the probabilities related to the collision of single pyrite particles and air bubbles by impact inertia and by diffusion,

and,

$P_{attach}^{P} = (P_{coll}^{P} + P_{oil}^{P} + P_{nat}^{P})$, where,

P_{coll}^{p} is the probability the oil phase imparts a dissolved component into the water which in some way serves as a collector, or for pyrite surface activation,

and,

P_{oil}^{p} is the probability that the pyrite surface becomes coated in oil, without being captured with the combustible agglomerates,

and,

P_{nat}^{p} is the probability that the pyrite surface demonstrates enough natural hydrophobicity to permit the single particles to report to the froth phase.

Pyrite Particle and Bubble Detachment

Equation 38 summarizes the probability of single pyrite particles reporting to the froth phase.

$$P_{rw}^{p} = P_{w}^{p} * (P_{i}^{p} + P_{d}^{p}) * (P_{coll}^{p} + P_{oil}^{p} + P_{nat}^{p}) * (1 - P_{dt}^{p}) \qquad \text{eq.38}$$

where,

P_{dt}^{p}, is the probability of detachment, and is related to the resolution of the shear forces present in the cell and the attachment forces typical of the single particles.

Pyrite Particle Drainage and Entrainment

When the single particles of free pyrite report to the froth phase, the washing nozzle impact may be strong enough to cause detachment of the pyrite and subsequent drainage of the particle back to the tailings phase. The probability of entrainment of pyrite does not seem likely due the particle high density. Hence, equation 39 can be presented as the probability expression relating to the recovery of single pyrite particles.

$$P_{cw}^{p} = P_{rw}^{p} * (1 - P_{dr}^{p}) \qquad \text{eq.39}$$

where,

P_{dr}^{p} is the probability of drainage of a single particle from the froth phase, and is distinctively different than the drainage from pyrite particles within the agglomerate phase. Hence, the total recovery of pyrite can be described by equation 40 below.

$P_c^p = P_{ca}^p + P_{cw}^p$ eq.40

where,

P_{ca}^p is the probability of pyrite particles reporting to the product phase via agglomerate recovery,

and,

P_{cw}^p is the probability of pyrite particles reporting to the product phase via single pyrite particle flotation.

A1.3 Total Ash Recovery Model

A1.3.1 Agglomeration

Ash Particle Capture in the Agglomerate Phase

Figure A4 summarizes the probabilistic ash recovery model for coal and oil agglomeration. Energy, oil and a coal water slurry is added to the high shear mixing system to promote the deashing of the combustible matter. The probability of an ash particle reporting to the froth phase can be given by equation 41 below.

$$P_{ra}^{ash} = P_f^{ash} * (1 - P_b^{ash}) \qquad \text{eq. 41}$$

where P_{ra}^{ash} is the probability of ash reporting to the agglomerate phase,

and,

P_f^{ash} is the probability of an ash particle being captured within an agglomerate,

and,

P_b^{ash} is the probability of ash washing free from a combustible agglomerate

Ash Attachment within Agglomerate

The probability of the capture, P_f^{ash}, of ash particles into the agglomerate can be defined in terms of transport and attachment mechanisms, P_{tr}, and P_{attach}. Equation 42 below describes the possible arrangement.

$$P_f^{ash} = P_{tr}^{ash} * P_{attach}^{ash} \qquad \text{eq. 42}$$

where,

$$P_{tr}^{ash} = (P_i^{ash} + P_d^{ash})$$

where,

P_i^{ash} and P_d^{ash} are the probabilities of transport of an ash particle by impact inertial and diffusion mechanisms, and,

$$P_{attach}^{ash} = (P_{ad}^{ash} + P_{entrap}^{ash})$$

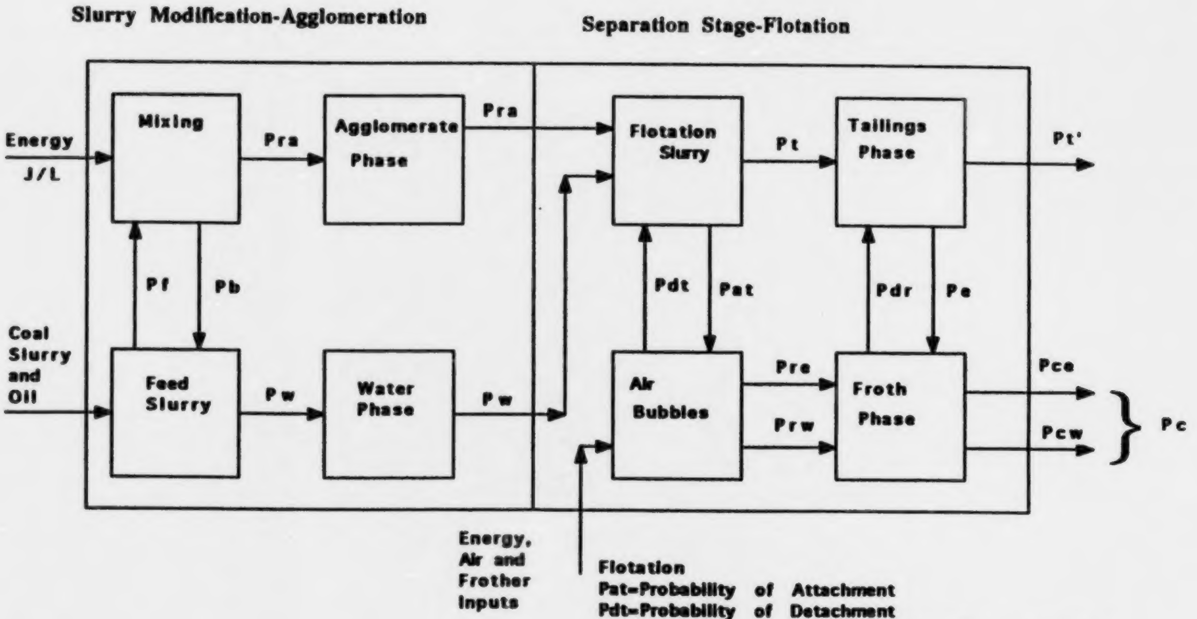

Agglomeration

Pra=Probability of Ash Remaining in Agglomerate Phase
Pf=Probability of Ash Agglomeration or Entrapment
Pb=Probability of Ash Detachment Back to the Water Phase
Pw=Probability of Ash Reporting Directly to Water Phase

Flotation

Pat=Probability of Attachment
Pdt=Probability of Detachment
Prw=Probability of Ash from Water Phase Reporting to the Froth Phase via Flotation
Pre=Probability of Entrapped Ash Reporting to Froth
Pe=Probability of Entrainment of Ash
Pdr=Probability of Drainage of Ash
Pce=Probability of Entrapped Ash Reporting to Product
Pcw=Probability of Ash From Water Phase Reporting to the Product via Flotation
Pc=Probability of Ash Reporting to Product
Pt and Pt'=Probability of Ash Reporting to Tailings

Figure A4 Total Ash Rejection Model

where,

P_{ad}^{ash} and P_{entrap}^{ash} are the probabilities of successful capture of ash within a forming combustible agglomerate by the forces of adsorption or physical entrapment of the particle within an agglomerate. Hence, the probability of capture of an ash particle within a combustible agglomerate can be defined in equation 43.

$P_f^{ash} = (P_i^{ash} + P_d^{ash}) * (P_{ad}^{ash} + P_{entrap}^{ash})$ eq. 43

Ash Particle Detachment from an Agglomerate

The probability of ash particle detachment, P_b^{ash}, is the resolution of the shear forces present within the mixing vessel and the forces holding the agglomerates together. High shear mixing systems tend to rework the agglomerates, which help release the captured ash particles because of their relatively weak adsorption forces. Equation 44 can be used to describe the process.

$P_b^{ash} = P_{sh}^{ash} - P_{attach}^{ash}$ eq. 44

where,

$P_{sh}^{ash} > P_{attach}^{ash}$

Ash Particle Capture in Combustible Agglomerate

Hence, the probability of an ash particle reporting to the combustible agglomerate phase can be described by equations 45 and 46.

$P_{ra}^{ash} = (P_i^{ash} + P_d^{ash}) * (P_{ad}^{ash} + P_{entrap}^{ash}) *$

$(1 - P_{sh} - (P_{ad}^{ash} + P_{entrap}^{ash}))$ eq. 45

where,

$(1 - P_{sh} - (P_{ad}^{ash} + P_{entrap}^{ash}))$ is > 0,

and,

$P_{ra}^{ash} = (P_i^{ash} + P_d^{ash}) * (P_{ad}^{ash} + P_{entrap}^{ash})$ eq. 46

where,

$(1 - P_{sh} - (P_{ad}^{ash} + P_{entrap}^{ash}))$ is > 0.

Ash in the Water Phase

The probability of an ash particle reporting with the water phase, P_w^{ash}, can be defined by equations 47 and 48.

$P_w^{ash} = (1 - P_f^{ash}) + P_f^{ash} * P_b^{ash}$, when $P_b^{ash} > 0$, eq. 47

where,

P_f^{ash} and P_b^{ash} are as previously defined,

and,

$P_w^{ash} = (1 - P_f^{ash})$, when $P_b^{ash} = 0$ eq. 48

A1.3.2 Flotation

Liberated particles report to the product phase via two major pathways: by capture within the combustible agglomerate and by water entrainment in the froth phase. Ash particles are typically hydrophilic in nature, and are very fine in size distribution, therefore, the flotation of ash particles is not considered to be a major pathway and was neglected in the model development.

Liberated Ash Particle Capture via Agglomerate Recovery

The ash component captured within a combustible agglomerated may be described by equation 49 below, where, the ash recovery is directly related to the probability of capture of ash within the agglomerate, P_{ra}^{ash}, and the probability of successful flotation, P_{re}^{ash}.

$P_{re}^{ash} = P_{ra}^{ash} * P_{af}^{a} * (1 - P_{dt}^{a})$ eq. 49

where,

P_{ra}^{ash} is the probability of capture of a free ash particle within a combustible agglomerate,

P_{at}^{a} is the probability of an agglomerate reporting to the froth phase by air flotation, and,

P_{dt}^{a} is the probability of agglomerate detachment back to the transition zone during air flotation.

Transport, Attachment, and Detachment of Ash Particles

The probabilities of transport and attachment of ash particles within an agglomerate can be described in equation 50.

$P_{re}^{ash} = P_{ra}^{ash} * P_{tr}^{a} * P_{attach}^{a}$ eq. 50

where,

$P_{tr}^{a} = (P_{i}^{a} + P_{d}^{a})$

and,

P_{i}^{a} and P_{d}^{a} are the transport probabilities of inertial impact and diffusion, respectively,

and,

$P_{attach}^{a} = (P_{sur}^{a} + P_{ad}^{a} + P_{ch}^{a} + P_{entra}^{a})$

where all these probabilities are as defined before, and the probabilities of detachment depends upon the shears forces which exist in the flotation cell. Equations 51 and 52 summarize the possible scenarios.

$P_{re}^{ash} = P_{ra}^{ash} * (P_{i}^{a} + P_{d}^{a}) * (P_{sur}^{a} + P_{ad}^{a} + P_{ch}^{a} + P_{entrap}^{a})$

$* (1 - P_{sh} - (P_{sur}^{a'} + P_{ad}^{a'} + P_{ch}^{a'} + P_{entrap}^{a'})$ eq. 51

where,

$(1 - P_{sh} - (P_{sur}^{a'} + P_{ad}^{a'} + P_{ch}^{a'} + P_{entrap}^{a'})$ is > 0,

and,

$P_{re}^{ash} = P_{ra}^{ash} * (P_{i}^{a} + P_{d}^{a}) * (P_{sur}^{a} + P_{ad}^{a} + P_{ch}^{a} + P_{entrap}^{a})$ eq. 52

where,

$(1 - P_{sh} - (P_{sur}a' + P_{ad}a' + P_{ch}a' + P_{entrap}a')$ is < 0.

Drainage and Entrainment of Ash Particles from an Agglomerate

The final recovery of an ash particle captured within an agglomerate can be described by equation 53.

$P_{ce}^{ash} = P_{re}^{ash} * (1 - P_{dr}^{ash}) + P_{e}$, eq. 53

where, as before, P_e, the probability of recovery of a combustible agglomerate via entrainment is assumed to be zero, hence, equation 53 can be simplified.

$$P_{ce}^{ash} = P_{re}^{ash} * (1 - P_{dr}^{ash}) \qquad \text{eq. 54}$$

The high penetration washing nozzles are used to dislodge, or wash free any attached ash particles. The probability of drainage, P_{dr}^{ash}, is considered to be a resolution of forces holding the ash particle within the agglomerate, and the impact washing exerted by the nozzles, and the washing time exposure.

Liberated Ash Particle Flotation

It may be possible that some ash surfaces could be modified into a hydrophobic state and report to the froth phase by flotation. However, considering the test coal used in this experimental program, the ash component was extremely hydrophilic in nature, and very fine in size distribution, the probability of single particles of liberated ash reporting to the froth phase, P_{rw}^{ash}, can be assumed to be zero. Hence, the only other pathway for particles of ash to report to the froth phase is via water entrainment.

Liberate Ash Particle Entrainment

The probability of free ash particles reporting to the product phase via water entrainment, P_{cw}^{ash}, can be described by equations 55 and 56.

$$P_{cw}^{ash} = P_t^{ash} * P_e^{ash} * (1 - P_{dr}^{ash}), \qquad \text{eq. 55}$$

where,

P_e^{ash}, is the probability of ash entrainment,

P_{dr}^{ash}, is the probability of ash drainage from the froth phase,

and,

P_t^{ash} is the probability of an ash particle remaining in the water phase,

where,

$$P_t^{ash} = P_w^{ash} * (1 - P_{at}^{ash}) + P_{at}^{ash} * P_{dt}^{ash},$$

however, because P_{at}^{ash} is a zero probability, the equation can simplified,

$$P_t^{ash} = P_w^{ash},$$

hence,

$$P_{cw}^{ash} = P_{w}^{ash} * P_{e}^{ash}, \qquad \text{eq. 56}$$

where the probability of entrainment is related to the water entrainment.

Total Ash Recovery in the Product Phase

The total ash recovery in the product phase can be summarized by equation 57.

$$P_{c}^{ash} = P_{ce}^{ash} + P_{cw}^{ash} \qquad \text{eq. 57}$$

where,

P_{ce}^{ash} is the probability of ash reporting to the product with the agglomerates,

and,

P_{cw}^{ash} is the probability of ash reporting to the product by water entrainment.

Appendix 2 Summary of Regression Work for Test E10

COLO2=% Soids

COLO3=Oil

COLO4=Frother

COLO5=Energy

COLO6=Temperature

Table A2.1 Regression Analysis of CMR (%) for Main Factors for Test E10

```
DEP VAR:    COL08       N:      17    MULTIPLE R:  .917   SQUARED MULTIPLE R:  .840
ADJUSTED SQUARED MULTIPLE R:   .787      STANDARD ERROR OF ESTIMATE:          7.304

  VARIABLE     COEFFICIENT     STD ERROR     STD COEF  TOLERANCE     T     P(2 TAIL)

CONSTANT          80.122         1.832        0.000        .      43.731     0.000
   COL03           7.416         1.832        0.482     0.938     4.048     0.002
   COL04           8.139         1.789        0.529     0.984     4.549     0.001
   COL05          -3.241         1.832       -0.208     0.965    -1.769     0.102
   COL06          -6.291         1.832       -0.403     0.965    -3.433     0.005


                           ANALYSIS OF VARIANCE

   SOURCE    SUM-OF-SQUARES     DF  MEAN-SQUARE      F-RATIO        P

 REGRESSION       3365.823       4      841.456       15.771       0.000
   RESIDUAL        640.242      12       53.354
```

Table A2.2 Regression Analysis of CMR (%) for Main Factors and Interactions for Test E10

```
DEP VAR:    COL08       N:        17   MULTIPLE R:  .993  SQUARED MULTIPLE R:  .986
ADJUSTED SQUARED MULTIPLE R:    .955      STANDARD ERROR OF ESTIMATE:          3.369

  VARIABLE      COEFFICIENT      STD ERROR      STD COEF TOLERANCE      T     P(2 TAIL)


CONSTANT            80.288          0.926         0.000        .      86.739     0.000
   COL03             7.249          0.926         0.471     0.782     7.832     0.001
   COL04             7.276          0.924         0.473     0.785     7.877     0.001
   COL05            -3.099          0.901        -0.199     0.849    -3.441     0.018
   COL06            -6.149          0.901        -0.394     0.849    -6.828     0.001
   COL03*
   COL04            -4.988          0.924        -0.324     0.785    -5.400     0.003
   COL03*
   COL05             0.237          0.901         0.015     0.849     0.263     0.803
   COL03*
   COL06             1.487          0.901         0.095     0.849     1.651     0.160
   COL04*
   COL05             0.988          0.895         0.064     0.837     1.105     0.320
   COL04*
   COL06             0.638          0.895         0.042     0.837     0.714     0.507
   COL03*
   COL04*
   COL06            -1.051          0.895        -0.068     0.837    -1.175     0.293
   COL03*
   COL05*
   COL06             0.124          0.926         0.008     0.782     0.134     0.899

                              ANALYSIS OF VARIANCE


  SOURCE     SUM-OF-SQUARES     DF   MEAN-SQUARE       F-RATIO          P


 REGRESSION       3949.319      11      359.029        31.635        0.001
   RESIDUAL         56.745       5       11.349
```

Table A2.3 Regression Analysis of CMR (%) for Main Factors and Interactions for Test E10

```
DEP VAR:    COL08        N:        17    MULTIPLE R:  .989  SQUARED MULTIPLE R:  .977
ADJUSTED SQUARED MULTIPLE R:     .964      STANDARD ERROR OF ESTIMATE:          3.016

  VARIABLE      COEFFICIENT      STD ERROR       STD COEF TOLERANCE      T     P(2 TAIL)

CONSTANT             79.886          0.771          0.000        .     103.608     0.000
   COL03              7.652          0.771          0.498     0.903      9.924     0.000
   COL04              7.822          0.742          0.509     0.976     10.546     0.000
   COL05             -2.806          0.759         -0.180     0.959     -3.697     0.004
   COL06             -5.856          0.759         -0.375     0.959     -7.715     0.000
   COL03*
   COL04             -5.535          0.742         -0.360     0.976     -7.462     0.000
   COL03*
   COL06              1.193          0.759          0.077     0.959      1.572     0.147


                                 ANALYSIS OF VARIANCE

   SOURCE    SUM-OF-SQUARES     DF  MEAN-SQUARE      F-RATIO        P

 REGRESSION        3915.079      6      652.513       71.716        0.000
   RESIDUAL          90.985     10        9.099
```

Table A2.4 Regression Analysis of CMR (%) for Main Factors and Interactions for Test E10

```
DEP VAR:    COL08        N:        17   MULTIPLE R:  .986  SQUARED MULTIPLE R:  .972
ADJUSTED SQUARED MULTIPLE R:   .959      STANDARD ERROR OF ESTIMATE:           3.212

  VARIABLE      COEFFICIENT     STD ERROR     STD COEF TOLERANCE      T     P(2 TAIL)

CONSTANT            79.672         0.808         0.000       .       98.594     0.000
    COL03            7.866         0.808         0.512     0.932      9.734     0.000
    COL04            7.914         0.787         0.515     0.982     10.051     0.000
    COL05           -2.790         0.808        -0.179     0.959     -3.453     0.005
    COL06           -5.840         0.808        -0.374     0.959     -7.227     0.000
    COL03*
    COL04           -5.626         0.787        -0.366     0.982     -7.146     0.000


                          ANALYSIS OF VARIANCE

    SOURCE    SUM-OF-SQUARES     DF   MEAN-SQUARE      F-RATIO        P

  REGRESSION        3892.593      5       778.519       75.470       0.000
    RESIDUAL         113.472     11        10.316
```

Table A2.5 Regression Analysis of CMR (%) for Main Factors and Interactions for Test E10

```
DEP VAR:    COL08        N:         17    MULTIPLE R:   .987   SQUARED MULTIPLE R:   .974
ADJUSTED SQUARED MULTIPLE R:   .963      STANDARD ERROR OF ESTIMATE:              3.056

 VARIABLE      COEFFICIENT      STD ERROR      STD COEF  TOLERANCE      T     P(2 TAIL)

CONSTANT            49.588          7.568         0.000        .        6.553     0.000
   COL03            47.736          4.439         1.180      0.194    10.754     0.000
   COL04          2518.029        233.123         1.425      0.134    10.801     0.000
   COL05            -0.402          0.108        -0.183      0.964    -3.721     0.003
   COL06            -0.464          0.067        -0.343      0.942    -6.898     0.000
   COL03*
   COL04         -1645.133        227.851        -1.157      0.091    -7.220     0.000


                          ANALYSIS OF VARIANCE

  SOURCE    SUM-OF-SQUARES      DF   MEAN-SQUARE       F-RATIO          P

 REGRESSION        3903.329      5       780.666        83.587        0.000
   RESIDUAL         102.735     11         9.340
```

Table A2.6 Regression Analysis of TS (% daf) for Main Factors for Test E10

```
DEP VAR:    COLO9       N:        17   MULTIPLE R:   .950  SQUARED MULTIPLE R:   .903
ADJUSTED SQUARED MULTIPLE R:   .870      STANDARD ERROR OF ESTIMATE:           0.158

 VARIABLE     COEFFICIENT     STD ERROR      STD COEF  TOLERANCE     T      P(2 TAIL)

CONSTANT            4.644         0.040         0.000       .      116.872      0.000
   COLO3            0.049         0.040         0.114     0.938      1.224      0.244
   COLO4            0.189         0.039         0.442     0.984      4.866      0.000
   COLO5           -0.130         0.040        -0.300     0.965     -3.274      0.007
   COLO6           -0.305         0.040        -0.704     0.965     -7.678      0.000


                         ANALYSIS OF VARIANCE

   SOURCE    SUM-OF-SQUARES    DF   MEAN-SQUARE      F-RATIO        P

 REGRESSION           2.789     4          0.697      27.785        0.000
   RESIDUAL           0.301    12          0.025
```

Table A2.7 Regression Analysis of TS (% daf) for Main Factors and Interactions for Test E10

```
DEP VAR:    COL09        N:        17    MULTIPLE R:   .997   SQUARED MULTIPLE R:   .993
ADJUSTED SQUARED MULTIPLE R:     .984     STANDARD ERROR OF ESTIMATE:              0.055

 VARIABLE      COEFFICIENT     STD ERROR     STD COEF TOLERANCE      T     P(2 TAIL)

CONSTANT             4.614         0.014        0.000       .      322.243     0.000
   COL03             0.078         0.014        0.183     0.862      5.471     0.001
   COL04             0.228         0.014        0.534     0.872     16.004     0.000
   COL05            -0.102         0.014       -0.235     0.887     -7.100     0.000
   COL06            -0.277         0.014       -0.639     0.887    -19.322     0.000
   COL03*
   COL04            -0.048         0.014       -0.112     0.872     -3.365     0.012
   COL03*
   COL05            -0.051         0.014       -0.117     0.887     -3.550     0.009
   COL04*
   COL06            -0.131         0.014       -0.307     0.872     -9.216     0.000
   COL03*
   COL05*
   COL06             0.043         0.014        0.101     0.862      3.026     0.019
   COL03*
   COL04*
   COL06             0.036         0.014        0.085     0.872      2.545     0.038
                               ANALYSIS OF VARIANCE

  SOURCE   SUM-OF-SQUARES    DF  MEAN-SQUARE      F-RATIO        P

REGRESSION          3.069     9        0.341      113.849      0.000
  RESIDUAL          0.021     7        0.003
```

Table A2.8 Regression Analysis of TS (% daf) for Main Factors and Interactions for Test E10

```
DEP VAR:    COL09        N:        17   MULTIPLE R:   .992  SQUARED MULTIPLE R:   .984
ADJUSTED SQUARED MULTIPLE R:     .964      STANDARD ERROR OF ESTIMATE:            0.083

 VARIABLE     COEFFICIENT    STD ERROR     STD COEF TOLERANCE     T     P(2 TAIL)

CONSTANT           4.005        0.618         0.000       .      6.480    0.000
    COL03          0.818        0.373         0.728     0.020    2.195    0.064
    COL04         79.534       19.729         1.620     0.014    4.031    0.005
    COL05         -0.004        0.008        -0.063     0.116   -0.456    0.662
    COL06          0.000        0.010         0.003     0.033    0.010    0.992
    COL03*
    COL04        -10.286       16.769        -0.261     0.012   -0.613    0.559
    COL03*
    COL05         -0.010        0.009        -0.388     0.017   -1.057    0.325
    COL04*
    COL06         -1.357        0.485        -1.161     0.013   -2.799    0.027
    COL03*
    COL05*
    COL06         -0.000        0.000        -0.085     0.021   -0.256    0.805
    COL03*
    COL04*
    COL06          0.043        0.423         0.042     0.013    0.101    0.922

                            ANALYSIS OF VARIANCE

   SOURCE    SUM-OF-SQUARES     DF  MEAN-SQUARE      F-RATIO        P

 REGRESSION           3.042      9        0.338       48.950      0.000
   RESIDUAL           0.048      7        0.007
```

Table A2.9 Regression Analysis of TS (% daf) for Main Factors and Interactions for Test E10

```
DEP VAR:    COLO9       N:        17   MULTIPLE R:  .987  SQUARED MULTIPLE R:  .974
ADJUSTED SQUARED MULTIPLE R:   .965      STANDARD ERROR OF ESTIMATE:          0.082

  /ARIABLE      COEFFICIENT     STD ERROR      STD COEF TOLERANCE     T     P(2 TAIL)

CONSTANT             4.653         0.150         0.000      .       31.044     0.000
   COLO3             0.174         0.053         0.155    0.961      3.272     0.007
   COLO4            72.665         3.786         1.480    0.363     19.192     0.000
   COLO5            -0.016         0.003        -0.257    0.963     -5.419     0.000
   COLO4*
   COLO6            -1.401         0.090        -1.199    0.362    -15.531     0.000


                             ANALYSIS OF VARIANCE

   SOURCE    SUM-OF-SQUARES     DF   MEAN-SQUARE      F-RATIO        P

 REGRESSION          3.010       4         0.752      112.622       0.000
   RESIDUAL          0.080      12         0.007
```

Table A2.10 Regression Analysis of Ash (% db) for Main Factors for Test E10

```
DEP VAR:     COLO7        N:       17    MULTIPLE R:   .977  SQUARED MULTIPLE R:   .955
ADJUSTED SQUARED MULTIPLE R:     .935      STANDARD ERROR OF ESTIMATE:             0.565

  VARIABLE      COEFFICIENT      STD ERROR      STD COEF TOLERANCE      T     P(2 TAIL)

CONSTANT             26.585          1.216         0.000     .        21.866      0.000
   COLO3              1.503          0.763         0.265    0.224      1.970      0.075
   COLO4             99.370         18.217         0.401    0.751      5.455      0.000
   COLO5             -0.080          0.028        -0.260    0.503     -2.900      0.014
   COLO6             -0.093          0.013        -0.491    0.916     -7.388      0.000
   COLO2             -0.662          0.116        -0.794    0.208     -5.686      0.000


                                ANALYSIS OF VARIANCE

   SOURCE    SUM-OF-SQUARES     DF   MEAN-SQUARE       F-RATIO        P

 REGRESSION          75.406      5        15.081        47.184        0.000
   RESIDUAL           3.516     11         0.320
```

Appendix 3 Summary of Regression Work for Tests E11

COLO2=% Soids

COLO3=Oil

COLO4=Frother

COLO5=Energy

COLO6=Temperature

Table A3.1 Regression Analysis of CMR (%) for Main Factors for Test E11

```
DEP VAR:    COL08        N:        16    MULTIPLE R:   .924   SQUARED MULTIPLE R:   .854
ADJUSTED SQUARED MULTIPLE R:    .801       STANDARD ERROR OF ESTIMATE:              6.849

  VARIABLE       COEFFICIENT       STD ERROR       STD COEF TOLERANCE       T     P(2 TAIL)

CONSTANT              78.851          1.726          0.000      .        45.674     0.000
    COL03              7.788          1.726          0.524    0.984       4.511     0.001
    COL04              9.524          1.726          0.640    0.984       5.517     0.000
    COL05              0.095          1.768          0.006    0.952       0.054     0.958
    COL06             -6.126          1.726         -0.412    0.984      -3.548     0.005


                             ANALYSIS OF VARIANCE

   SOURCE    SUM-OF-SQUARES      DF   MEAN-SQUARE       F-RATIO         P

 REGRESSION        3024.080       4       756.020        16.118        0.000
   RESIDUAL         515.957      11        46.905
```

Table A3.2 Regression Analysis of CMR (%) for Main Factors and Interactions for Test E11

```
DEP VAR:     COL08        N:         16    MULTIPLE R:   .977   SQUARED MULTIPLE R:   .955
ADJUSTED SQUARED MULTIPLE R:     .904        STANDARD ERROR OF ESTIMATE:             4.764

  VARIABLE      COEFFICIENT     STD ERROR       STD COEF  TOLERANCE     T      P(2 TAIL)

CONSTANT             79.254         1.229          0.000       .      64.476      0.000
    COL03             8.192          1.229          0.551     0.939     6.664      0.000
    COL04             9.121          1.229          0.613     0.939     7.420      0.000
    COL05            -0.828          1.266         -0.055     0.899    -0.654      0.534
    COL06            -6.529          1.229         -0.439     0.939    -5.312      0.001
    COL03*
    COL04            -4.817          1.229         -0.324     0.939    -3.919      0.006
    COL04*
    COL05             1.103          1.266          0.074     0.899     0.871      0.412
    COL04*
    COL06             0.954          1.229          0.064     0.939     0.776      0.463
    COL04*
    COL05*
    COL06            -1.203          1.266         -0.080     0.899    -0.950      0.374


                              ANALYSIS OF VARIANCE

   SOURCE    SUM-OF-SQUARES     DF   MEAN-SQUARE       F-RATIO        P

 REGRESSION        3381.174      8       422.647        18.623        0.000
   RESIDUAL         158.864      7        22.695
```

Table A3.3 Regression Analysis of CMR (%) for Main Factors and Interactions for Test E11

```
DEP VAR:    COL08        N:         16   MULTIPLE R:  .971  SQUARED MULTIPLE R:   .943
ADJUSTED SQUARED MULTIPLE R:   .922     STANDARD ERROR OF ESTIMATE:            4.294

 VARIABLE      COEFFICIENT      STD ERROR      STD COEF TOLERANCE      T      P(2 TAIL)

CONSTANT            78.863        1.073         0.000      .         73.467      0.000
   COL03             7.800        1.073         0.524     1.000       7.266      0.000
   COL04             9.513        1.073         0.640     1.000       8.862      0.000
   COL06            -6.138        1.073        -0.413     1.000      -5.718      0.000
   COL03*
   COL04            -4.425        1.073        -0.297     1.000      -4.122      0.002


                         ANALYSIS OF VARIANCE

  SOURCE    SUM-OF-SQUARES    DF  MEAN-SQUARE     F-RATIO        P

 REGRESSION        3337.235    4        834.309     45.253      0.000
   RESIDUAL         202.802   11         18.437
```

Table A3.4 Regression Analysis of CMR (%) for Main Factors and Interactions for Test E11

```
DEP VAR:    COL08        N:        16   MULTIPLE R:   .971  SQUARED MULTIPLE R:   .943
ADJUSTED SQUARED MULTIPLE R:    .923      STANDARD ERROR OF ESTIMATE:            4.276

 VARIABLE      COEFFICIENT       STD ERROR       STD COEF TOLERANCE        T     P(2 TAIL)

CONSTANT            34.306           7.394          0.000       .         4.639      0.001
   COL03            42.149           6.260          1.091     0.197      6.733      0.000
   COL04          2514.113         359.539          1.386     0.131      6.993      0.000
   COL06            -0.496           0.091         -0.390     0.999     -5.431      0.000
   COL03*
   COL04         -1345.301         338.699         -0.979     0.085     -3.972      0.002


                           ANALYSIS OF VARIANCE

   SOURCE    SUM-OF-SQUARES       DF  MEAN-SQUARE       F-RATIO          P

 REGRESSION        3338.927        4      834.732        45.657        0.000
   RESIDUAL         201.111       11       18.283
```

Table A3.5 Regression Analysis of TS (% daf) for Main Factors for Test E11

```
DEP VAR:    COL09       N:        16    MULTIPLE R:   .929  SQUARED MULTIPLE R:   .862
ADJUSTED SQUARED MULTIPLE R:    .812       STANDARD ERROR OF ESTIMATE:           0.201

 VARIABLE      COEFFICIENT      STD ERROR      STD COEF  TOLERANCE     T      P(2 TAIL)


CONSTANT             4.812          0.051         0.000          .    94.968      0.000
   COL03             0.130          0.051         0.289      0.984     2.560      0.027
   COL04             0.293          0.051         0.652      0.984     5.778      0.000
   COL05             0.032          0.052         0.071      0.952     0.620      0.548
   COL06            -0.263          0.051        -0.587      0.984    -5.200      0.000



                             ANALYSIS OF VARIANCE

   SOURCE    SUM-OF-SQUARES     DF   MEAN-SQUARE       F-RATIO         P


  REGRESSION          2.781     4          0.695       17.203          0.000
    RESIDUAL          0.445    11          0.040
```

Table A3.6 Regression Analysis of TS (% daf) for Main Factors and Interactions for Test E11

```
DEP VAR:    COLO9       N:        16    MULTIPLE R:   .983  SQUARED MULTIPLE R:   .967
ADJUSTED SQUARED MULTIPLE R:     .950      STANDARD ERROR OF ESTIMATE:          0.103

 VARIABLE     COEFFICIENT     STD ERROR      STD COEF TOLERANCE      T     P(2 TAIL)

CONSTANT            4.810         0.026         0.000       .      184.429     0.000
    COLO3           0.127         0.026         0.284     0.983      4.881     0.001
    COLO4           0.295         0.026         0.658     0.983     11.320     0.000
    COLO5           0.052         0.027         0.114     0.937      1.919     0.084
    COLO6          -0.261         0.026        -0.581     0.983    -10.009     0.000
    COLO4*
    COLO6          -0.146         0.026        -0.326     0.983     -5.616     0.000


                          ANALYSIS OF VARIANCE

   SOURCE    SUM-OF-SQUARES    DF  MEAN-SQUARE      F-RATIO         P

 REGRESSION          3.118      5        0.624       58.279         0.000
   RESIDUAL          0.107     10        0.011
```

Table A3.7 Regression Analysis of TS (% daf) for Main Factors and Interactions for Test E11

```
DEP VAR:    COLO9       N:        16   MULTIPLE R:  .977  SQUARED MULTIPLE R:  .955
ADJUSTED SQUARED MULTIPLE R:    .938      STANDARD ERROR OF ESTIMATE:          0.115

 VARIABLE     COEFFICIENT     STD ERROR      STD COEF TOLERANCE     T     P(2 TAIL)

CONSTANT           4.816         0.029         0.000       .     166.977    0.000
   COL03           0.134         0.029         0.298    1.000      4.637    0.001
   COL04           0.289         0.029         0.643    1.000     10.011    0.000
   COL06          -0.268         0.029        -0.596    1.000     -9.274    0.000
   COL04*
   COL06          -0.140         0.029        -0.312    1.000     -4.854    0.001


                          ANALYSIS OF VARIANCE

  SOURCE    SUM-OF-SQUARES     DF  MEAN-SQUARE      F-RATIO        P

REGRESSION           3.079      4        0.770       57.822      0.000
  RESIDUAL           0.146     11        0.013
```

Table A3.8 Regression Analysis of TS (% daf) for Main Factors and Interactions for Test E1

```
DEP VAR:    COLO9       N:        16   MULTIPLE R:  .978  SQUARED MULTIPLE R:  .956
ADJUSTED SQUARED MULTIPLE R:   .940      STANDARD ERROR OF ESTIMATE:          0.113

 VARIABLE     COEFFICIENT     STD ERROR      STD COEF TOLERANCE      T     P(2 TAIL)

CONSTANT            3.764         0.211         0.000        .      17.809     0.000
   COL03            0.340         0.074         0.292     0.999      4.621     0.001
   COL04           88.883        10.764         1.623     0.103      8.258     0.000
   COL06            0.003         0.005         0.085     0.200      0.602     0.560
   COL06*
   COL04           -1.548         0.296        -1.218     0.074     -5.232     0.000


                           ANALYSIS OF VARIANCE

  SOURCE    SUM-OF-SQUARES     DF   MEAN-SQUARE      F-RATIO          P

 REGRESSION          3.084     4          0.771      60.045         0.000
   RESIDUAL          0.141    11          0.013
```

Table A3.9 Regression Analysis of TS (% daf) for Main Factors and Interactions for Test E11

```
DEP VAR:     COL09        N:          16   MULTIPLE R:   .977   SQUARED MULTIPLE R:   .955
ADJUSTED SQUARED MULTIPLE R:        .943     STANDARD ERROR OF ESTIMATE:             0.110

 VARIABLE      COEFFICIENT      STD ERROR      STD COEF TOLERANCE      T      P(2 TAIL)

CONSTANT             3.877          0.094         0.000         .     41.152      0.000
   COL03             0.339          0.072         0.291     1.000      4.736      0.000
   COL04            83.389          5.547         1.523     0.367     15.032      0.000
    COL04*
   COL06            -1.389          0.129        -1.092     0.367    -10.781      0.000


                          ANALYSIS OF VARIANCE

  SOURCE    SUM-OF-SQUARES     DF   MEAN-SQUARE      F-RATIO         P

 REGRESSION          3.079      3         1.026       84.428      0.000
   RESIDUAL          0.146     12         0.012
```

Table A3.10 Regression Analysis of Ash (% db) for Main Factors and Interactions for Test E11

```
DEP VAR:    COL07       N:       16   MULTIPLE R:   .982  SQUARED MULTIPLE R:   .965
ADJUSTED SQUARED MULTIPLE R:   .948      STANDARD ERROR OF ESTIMATE:            0.626

  VARIABLE     COEFFICIENT      STD ERROR      STD COEF TOLERANCE     T     P(2 TAIL)

CONSTANT           28.440          2.117          0.000       .      13.432     0.000
    COL02          -0.780          0.061         -0.962     0.610  -12.752     0.000
    COL03           2.355          0.444          0.341     0.840    5.308     0.000
    COL04          77.983         21.008          0.241     0.826    3.712     0.004
    COL05          -0.058          0.033         -0.117     0.800   -1.776     0.106
    COL06          -0.112          0.015         -0.494     0.827   -7.619     0.000


                             ANALYSIS OF VARIANCE

    SOURCE   SUM-OF-SQUARES     DF  MEAN-SQUARE      F-RATIO        P

 REGRESSION        109.001       5        21.800       55.571        0.000
   RESIDUAL          3.923      10         0.392
```

Table A3.11 Regression Analysis of Ash (% db) for Main Factors and Interactions for Test E11

```
DEP VAR:    COLO7       N:        16    MULTIPLE R:   .977  SQUARED MULTIPLE R:   .954
ADJUSTED SQUARED MULTIPLE R:   .938       STANDARD ERROR OF ESTIMATE:           0.685

  VARIABLE     COEFFICIENT     STD ERROR      STD COEF TOLERANCE     T     P(2 TAIL)


CONSTANT            25.261         1.238         0.000       .      20.407     0.000
   COLO2            -0.735         0.061        -0.908     0.732  -12.048     0.000
   COLO3             2.148         0.468         0.311     0.903    4.588     0.001
   COLO4            87.199        22.263         0.269     0.880    3.917     0.002
   COLO6            -0.105         0.015        -0.463     0.890   -6.780     0.000


                          ANALYSIS OF VARIANCE

   SOURCE    SUM-OF-SQUARES     DF   MEAN-SQUARE      F-RATIO         P


  REGRESSION          107.763     4         26.941       57.422       0.000
    RESIDUAL            5.161    11          0.469
```

Appendix 4 Summary of Regression Work for Tests E10 and E11

COLO2=Oil

COLO3=Frother

COLO4=Energy

COLO5=Temperature

COLO6=Size

COLO7=% Solids

COLO8=Age

Table A4.1 Regression Analysis of CMR (%) for Main Factors and Interactions for Test E10 and E11

```
DEP VAR:   COLO10        N:        35    MULTIPLE R:   .966   SQUARED MULTIPLE R:   .933
ADJUSTED SQUARED MULTIPLE R:   .922       STANDARD ERROR OF ESTIMATE:            4.170

  VARIABLE      COEFFICIENT      STD ERROR       STD COEF TOLERANCE      T     P(2 TAIL)


CONSTANT            45.608          7.278          0.000         .       6.266      0.000
   COLO2            43.067          4.192          1.120      0.193     10.274      0.000
   COLO3          2310.136        232.192          1.329      0.129      9.949      0.000
   COLO5            -0.432          0.062         -0.339      0.968     -6.968      0.000
   COLO2*
   COLO3         -1306.552        222.836         -0.936      0.090     -5.863      0.000
   COLO4            -0.292          0.114         -0.125      0.966     -2.561      0.016


                            ANALYSIS OF VARIANCE

   SOURCE    SUM-OF-SQUARES      DF   MEAN-SQUARE       F-RATIO         P


 REGRESSION        7073.887       5       1414.777       81.372         0.000
   RESIDUAL         504.208      29         17.386
```

Table A4.2 Regression Analysis of TS (% daf) for Main Factors and Interactions for Test E10 and E11

```
DEP VAR:   COL011        N:          35    MULTIPLE R:   .979   SQUARED MULTIPLE R:   .958
ADJUSTED SQUARED MULTIPLE R:     .950        STANDARD ERROR OF ESTIMATE:              0.103

 VARIABLE      COEFFICIENT      STD ERROR      STD COEF TOLERANCE      T     P(2 TAIL)

CONSTANT             6.083          0.416          0.000         .     14.632      0.000
   COL02             0.275          0.046          0.231     0.993      6.020      0.000
   COL03            78.288          3.354          1.451     0.378     23.345      0.000
   COL03*
   COL05            -1.390          0.080         -1.081     0.376    -17.348      0.000
   COL06            -0.027          0.005         -0.985     0.047     -5.608      0.000
   COL08            -0.083          0.019         -0.748     0.047     -4.266      0.000


                              ANALYSIS OF VARIANCE

  SOURCE    SUM-OF-SQUARES     DF   MEAN-SQUARE       F-RATIO         P

 REGRESSION          6.985      5         1.397      131.245       0.000
   RESIDUAL          0.309     29         0.011
```

Table A4.3 Regression Analysis of CMR (%) for Main Factors and Interactions for Test E10 and E11

```
DEP VAR:    COL09        N:         35    MULTIPLE R:   .974   SQUARED MULTIPLE R:   .950
ADJUSTED SQUARED MULTIPLE R:      .939       STANDARD ERROR OF ESTIMATE:             0.606

  VARIABLE     COEFFICIENT      STD ERROR      STD COEF TOLERANCE       T      P(2 TAIL)

CONSTANT          28.950          1.041          0.000        .      27.809      0.000
   COL02           2.247          0.314          0.356     0.727      7.156      0.000
   COL03          89.082         12.346          0.312     0.961      7.216      0.000
   COL04          -0.068          0.017         -0.177     0.965     -4.098      0.000
   COL05          -0.097          0.009         -0.463     0.932    -10.530      0.000
   COL06          -0.034          0.007         -0.230     0.854     -4.998      0.000
   COL07          -0.717          0.039         -0.987     0.612    -18.199      0.000


                              ANALYSIS OF VARIANCE

   SOURCE    SUM-OF-SQUARES     DF   MEAN-SQUARE       F-RATIO         P

  REGRESSION        193.645      6        32.274       87.932        0.000
    RESIDUAL         10.277     28         0.367
```

Appendix 5 Summary of Regression Work for Tests E10, E11, and E12

COLO2=Oil

COLO3=Frother

COLO4=Energy

COLO5=Temperature

COLO6=Size

COLO7=% Solids

COLO8=Age

Table A5.1 Regression Analysis of CMR (%) for Main Factors and Interactions for Test E10, E11, and E12

```
DEP VAR:   COLO10        N:        55    MULTIPLE R:  .934  SQUARED MULTIPLE R:   .873
ADJUSTED SQUARED MULTIPLE R:    .860       STANDARD ERROR OF ESTIMATE:           4.946

  VARIABLE      COEFFICIENT      STD ERROR       STD COEF TOLERANCE      T     P(2 TAIL)

CONSTANT             34.031          5.950          0.000        .        5.720     0.000
    COLO2            44.257          4.703          1.144      0.175      9.411     0.000
    COLO3          2578.811        257.689          1.462      0.121     10.007     0.000
    COLO5            -0.478          0.072         -0.398      0.725     -6.662     0.000
    COLO8            -0.213          0.044         -0.284      0.739     -4.792     0.000
    COLO2*
    COLO3         -1520.466        249.974         -1.065      0.085     -6.082     0.000


                            ANALYSIS OF VARIANCE

    SOURCE     SUM-OF-SQUARES     DF   MEAN-SQUARE      F-RATIO        P

  REGRESSION        8248.361      5      1649.672        67.436       0.000
    RESIDUAL        1198.672     49        24.463
```

Table A5.2 Regression Analysis of CMR (%) for Main Factors and Interactions for Test E10, E11, and E12

```
DEP VAR:   COLO10        N:         55    MULTIPLE R:   .942  SQUARED MULTIPLE R:   .888
ADJUSTED SQUARED MULTIPLE R:       .877       STANDARD ERROR OF ESTIMATE:           4.642

  VARIABLE     COEFFICIENT      STD ERROR       STD COEF  TOLERANCE      T     P(2 TAIL)

CONSTANT            31.964          5.389          0.000        .        5.931     0.000
    COLO2           46.743          4.403          1.208      0.176     10.617     0.000
    COLO3         2555.122        242.019          1.448      0.121     10.558     0.000
    COLO5           -0.480          0.066         -0.400      0.761     -7.306     0.000
    COLO8*
    COLO2           -0.232          0.041         -0.317      0.743     -5.718     0.000
    COLO2*
    COLO3        -1500.577        234.740         -1.051      0.084     -6.392     0.000


                            ANALYSIS OF VARIANCE

    SOURCE    SUM-OF-SQUARES    DF   MEAN-SQUARE      F-RATIO        P

  REGRESSION       8391.144      5      1678.229       77.881       0.000
    RESIDUAL       1055.889     49        21.549
```

Table A5.3 Regression Analysis of TS (% daf) for Main Factors and Interactions for Test E10, E11, and E12

```
DEP VAR:   COLO11        N:       55   MULTIPLE R:  .966  SQUARED MULTIPLE R:   .934
ADJUSTED SQUARED MULTIPLE R:    .927       STANDARD ERROR OF ESTIMATE:          0.120

 VARIABLE      COEFFICIENT      STD ERROR      STD COEF TOLERANCE      T     P(2 TAIL)

CONSTANT             4.801          0.101         0.000     .        47.659     0.000
    COLO2            0.230          0.048         0.177    0.991      4.797     0.000
    COLO3           75.205          3.492         1.269    0.388     21.538     0.000
    COLO3*
    COLO5           -1.375          0.089        -0.945    0.363    -15.490     0.000
    COLO6           -0.011          0.001        -0.357    0.970     -9.586     0.000
    COLO8           -0.017          0.001        -0.687    0.771    -16.418     0.000


                              ANALYSIS OF VARIANCE

   SOURCE    SUM-OF-SQUARES     DF  MEAN-SQUARE      F-RATIO         P

 REGRESSION          9.949       5        1.990      138.543        0.000
   RESIDUAL          0.704      49        0.014
```

Table A5.4 Regression Analysis of TS (% daf) for Main Factors and Interactions for Test E10, E11, and E12

```
DEP VAR:   COLO11        N:        55    MULTIPLE R:   .977   SQUARED MULTIPLE R:   .955
ADJUSTED SQUARED MULTIPLE R:      .948      STANDARD ERROR OF ESTIMATE:            0.101

  VARIABLE      COEFFICIENT     STD ERROR      STD COEF  TOLERANCE      T     P(2 TAIL)

CONSTANT             3.871         0.055         0.000       .       70.972      0.000
    COLO2            0.659         0.115         0.507     0.121      5.708      0.000
    COLO3          106.901         6.974         1.804     0.069     15.328      0.000
    COLO3*
    COLO5           -1.415         0.076        -0.972     0.346    -18.502      0.000
    COLO2*
    COLO6           -0.005         0.002        -0.286     0.100     -2.927      0.005
    COLO2*
    COLO8           -0.010         0.002        -0.388     0.185     -5.393      0.000
    COLO3*
    COLO6           -0.388         0.093        -0.497     0.067     -4.175      0.000
    COLO3*
    COLO8           -0.458         0.099        -0.355     0.162     -4.626      0.000


                                ANALYSIS OF VARIANCE

   SOURCE    SUM-OF-SQUARES     DF  MEAN-SQUARE      F-RATIO        P

 REGRESSION         10.175       7        1.454     142.903        0.000
   RESIDUAL          0.478      47        0.010
```

Table A5.5 Regression Analysis of Ash (% db) for Main Factors and Interactions for Test E10, E11, and E12

```
DEP VAR:    COL09       N:        55   MULTIPLE R:  .913  SQUARED MULTIPLE R:  .834
ADJUSTED SQUARED MULTIPLE R:    .810      STANDARD ERROR OF ESTIMATE:         1.160

  VARIABLE     COEFFICIENT     STD ERROR     STD COEF TOLERANCE     T     P(2 TAIL)

CONSTANT            23.864         1.598        0.000       .      14.932     0.000
   COL02             1.123         0.519        0.144     0.793     2.166     0.035
   COL03           123.381        21.487        0.348     0.961     5.742     0.000
   COL04            -0.041         0.026       -0.102     0.846    -1.581     0.121
   COL05            -0.088         0.017       -0.363     0.730    -5.225     0.000
   COL06            -0.024         0.012       -0.127     0.934    -2.059     0.045
   COL07            -0.418         0.042       -0.783     0.575    -9.998     0.000
   COL08            -0.026         0.012       -0.171     0.517    -2.069     0.044


                           ANALYSIS OF VARIANCE

   SOURCE   SUM-OF-SQUARES    DF  MEAN-SQUARE      F-RATIO        P

 REGRESSION        318.625     7        45.518      33.803       0.000
   RESIDUAL         63.288    47         1.347
```

Table A5.6 Regression Analysis of Ash (% db) for Main Factors and Interactions for Test E10, E11, and E12

```
DEP VAR:    COL09       N:        55   MULTIPLE R:  .936  SQUARED MULTIPLE R:   .876
ADJUSTED SQUARED MULTIPLE R:   .851       STANDARD ERROR OF ESTIMATE:          1.027

 VARIABLE     COEFFICIENT     STD ERROR      STD COEF TOLERANCE      T     P(2 TAIL)


CONSTANT          33.942          3.483         0.000       .        9.744    0.000
   COL02           1.037          0.460         0.133     0.792     2.257    0.029
   COL03          63.513         25.354         0.179     0.540     2.505    0.016
   COL04          -0.059          0.023        -0.147     0.809    -2.517    0.015
   COL05          -0.098          0.015        -0.408     0.690    -6.444    0.000
   COL06          -0.138          0.040        -0.736     0.061    -3.446    0.001
   COL07          -1.017          0.210        -1.902     0.018    -4.844    0.000
   COL08          -0.108          0.028        -0.714     0.082    -3.884    0.000
   COL03*
   COL08           3.962          1.362         0.514     0.088     2.909    0.006
   COL06*
   COL07           0.009          0.003         1.335     0.014     2.963    0.005



                           ANALYSIS OF VARIANCE


  SOURCE    SUM-OF-SQUARES     DF  MEAN-SQUARE      F-RATIO        P


 REGRESSION        334.472     9        37.164       35.251        0.000
   RESIDUAL         47.441    45         1.054
```

Appendix 6 Summary of Regression Work for Tests E10, E11, E12 and E13

COLO2=Oil

COLO3=Frother

COLO4=Energy

COLO5=Temperature

COLO6=Size

COLO7=% Solids

COLO8=Age

Table A6.1 Regression Analysis of CMR (%) for Main Factors and Interactions for Test E10, E11, E12, and E13

```
DEP VAR:   COLO10        N:        60    MULTIPLE R:   .904   SQUARED MULTIPLE R:   .817
ADJUSTED SQUARED MULTIPLE R:   .800       STANDARD ERROR OF ESTIMATE:            5.777

  VARIABLE      COEFFICIENT     STD ERROR      STD COEF TOLERANCE      T     P(2 TAIL)


CONSTANT           41.514         6.632          0.000        .       6.260     0.000
   COLO2           38.418         5.204          1.012      0.181     7.382     0.000
   COLO3         2131.797       271.557          1.319      0.120     7.850     0.000
   COLO5           -0.473         0.084         -0.402      0.673    -5.664     0.000
   COLO8           -0.265         0.050         -0.376      0.683    -5.340     0.000
   COLO2*
   COLO3        -1153.951       266.409         -0.850      0.088    -4.331     0.000



                              ANALYSIS OF VARIANCE

   SOURCE    SUM-OF-SQUARES    DF   MEAN-SQUARE      F-RATIO        P


 REGRESSION        8042.983     5      1608.597       48.198        0.000
   RESIDUAL        1802.237    54        33.375
```

Table A6.2 Regression Analysis of CMR (%) for Main Factors and Interactions for Test E10, E11, E12, and E13

```
DEP VAR:  COLO10        N:         60   MULTIPLE R:   .908  SQUARED MULTIPLE R:   .825
ADJUSTED SQUARED MULTIPLE R:     .808      STANDARD ERROR OF ESTIMATE:           5.654

  VARIABLE     COEFFICIENT      STD ERROR      STD COEF TOLERANCE      T     P(2 TAIL)


CONSTANT           38.809         6.302          0.000       .       6.158     0.000
   COL02           40.871         5.089          1.076     0.181     8.031     0.000
   COL03         2039.275       266.358          1.262     0.120     7.656     0.000
   COL05           -0.460         0.080         -0.391     0.709    -5.773     0.000
   COL02*
   COL03        -1073.667       261.614         -0.791     0.087    -4.104     0.000
   COL02*
   COL08           -0.264         0.047         -0.390     0.686    -5.670     0.000



                             ANALYSIS OF VARIANCE

   SOURCE    SUM-OF-SQUARES     DF   MEAN-SQUARE      F-RATIO         P


 REGRESSION        8118.990      5      1623.798       50.796         0.000
   RESIDUAL        1726.229     54        31.967
```

Table A6.3 Regression Analysis of TS (% daf) for Main Factors and Interactions for Test E10, E11, E12, and E13

```
DEP VAR:   COL011         N:        60   MULTIPLE R:   .961   SQUARED MULTIPLE R:   .924
ADJUSTED SQUARED MULTIPLE R:      .917       STANDARD ERROR OF ESTIMATE:            0.126

 VARIABLE      COEFFICIENT      STD ERROR      STD COEF TOLERANCE     T     P(2 TAIL)

CONSTANT             4.844          0.102         0.000                47.573     0.000
   COL02             0.247          0.049         0.192      0.986      5.078     0.000
   COL03            71.599          3.319         1.307      0.383     21.573     0.000
   COL03*
   COL05            -1.322          0.091        -0.894      0.374    -14.566     0.000
   COL06            -0.012          0.001        -0.373      0.928     -9.573     0.000
   COL08            -0.018          0.001        -0.738      0.688    -16.330     0.000


                               ANALYSIS OF VARIANCE

 SOURCE   SUM-OF-SQUARES     DF  MEAN-SQUARE      F-RATIO        P

REGRESSION       10.446       5        2.089      131.451       0.000
  RESIDUAL        0.858      54        0.016
```

Table A6.4 Regression Analysis of TS (% daf) for Main Factors and Interactions for Test E10, E11, E12, and E13

```
DEP VAR:   COLO11        N:       60   MULTIPLE R:  .970  SQUARED MULTIPLE R:  .941
ADJUSTED SQUARED MULTIPLE R:    .933      STANDARD ERROR OF ESTIMATE:          0.114

 VARIABLE      COEFFICIENT      STD ERROR      STD COEF TOLERANCE      T     P(2 TAIL)

CONSTANT            3.823         0.059         0.000        .       64.560     0.000
   COLO2            0.659         0.124         0.512      0.123      5.321     0.000
   COLO3          108.799         7.545         1.987      0.060     14.420     0.000
   COLO3*
   COLO5           -1.418         0.086        -0.958      0.338    -16.478     0.000
   COLO2*
   COLO6           -0.004         0.002        -0.271      0.096     -2.484     0.016
   COLO2*
   COLO8           -0.009         0.002        -0.383      0.226     -5.386     0.000
   COLO3*
   COLO6           -0.399         0.100        -0.579      0.054     -3.975     0.000
   COLO3*
   COLO8           -0.482         0.089        -0.458      0.160     -5.423     0.000


                           ANALYSIS OF VARIANCE

  SOURCE    SUM-OF-SQUARES     DF  MEAN-SQUARE      F-RATIO          P

REGRESSION         10.632      7         1.519     117.546       0.000
  RESIDUAL          0.672     52         0.013
```

Table A6.5 Regression Analysis of Ash (% db) for Main Factors and Interactions for Test E10, E11, E12, and E13

```
DEP VAR:    COL09        N:          60   MULTIPLE R:   .917  SQUARED MULTIPLE R:   .842
ADJUSTED SQUARED MULTIPLE R:   .820       STANDARD ERROR OF ESTIMATE:              1.131

 'ARIABLE     COEFFICIENT      STD ERROR      STD COEF TOLERANCE      T      P(2 TAIL)

CONSTANT           23.675          1.478         0.000        .      16.020      0.000
    COL02           1.097          0.480         0.140     0.814      2.286      0.026
    COL03         130.275         19.027         0.390     0.937      6.847      0.000
    COL04          -0.041          0.025        -0.102     0.786     -1.645      0.106
    COL05          -0.087          0.016        -0.359     0.675     -5.343      0.000
    COL06          -0.024          0.011        -0.124     0.889     -2.117      0.039
    COL07          -0.413          0.038        -0.802     0.549    -10.769      0.000
    COL08          -0.026          0.012        -0.180     0.445     -2.173      0.034


                            ANALYSIS OF VARIANCE

  SOURCE    SUM-OF-SQUARES     DF  MEAN-SQUARE      F-RATIO        P

 REGRESSION       353.215       7       50.459       39.463       0.000
   RESIDUAL        66.489      52        1.279
```

Table A6.6 Regression Analysis of Ash (% db) for Main Factors and Interactions for Test E10, E11, E12, and E13

```
DEP VAR:    COL09        N:          60   MULTIPLE R:   .934  SQUARED MULTIPLE R:   .873
ADJUSTED SQUARED MULTIPLE R:   .850       STANDARD ERROR OF ESTIMATE:              1.034

 VARIABLE     COEFFICIENT     STD ERROR     STD COEF  TOLERANCE     T      P(2 TAIL)

CONSTANT          32.531         3.388         0.000      .        9.603     0.000
   COL02           1.161         0.440         0.148     0.809     2.638     0.011
   COL03          74.600        24.786         0.224     0.462     3.010     0.004
   COL04          -0.061         0.023        -0.155     0.732    -2.625     0.011
   COL05          -0.096         0.015        -0.393     0.646    -6.255     0.000
   COL06          -0.119         0.038        -0.624     0.063    -3.097     0.003
   COL07          -0.920         0.201        -1.786     0.017    -4.578     0.000
   COL08          -0.079         0.021        -0.543     0.120    -3.721     0.001
   COL03*
   COL08           2.466         0.976         0.385     0.110     2.528     0.015
   COL06*
   COL07           0.007         0.003         1.180     0.012     2.548     0.014


                         ANALYSIS OF VARIANCE

   SOURCE    SUM-OF-SQUARES     DF   MEAN-SQUARE     F-RATIO        P

 REGRESSION        366.210       9       40.690       38.032      0.000
   RESIDUAL         53.494      50        1.070
```

Appendix 7 Summary of Computer Data used in Regression for Appendices 1-6

Table A7.1 Coded Regression Data for Test E10

Interval	x1	x2	x3	x4	x6	R1	R2	R3
1	-1	-1	-1	-1	12.2	13.7	64.6	4.28
2	1	1	-1	-1	12.6	17.9	99.6	5.47
3	1	-1	-1	-1	9.3	18.8	93.2	4.91
4	-1	1	-1	-1	8.5	20.3	95.9	5.23
5	1	-1	-1	1	11.9	14.4	83.8	4.36
6	-1	1	-1	1	8.1	17.4	78.2	4.47
7	-1	-1	-1	1	7.5	16.7	57.1	4.27
8	1	1	-1	1	15.3	14.0	85.0	4.64
9	-1	-1	1	1	9.1	14.2	46.6	4.07
10	-1	-1	1	1	8.9	14.3	46.2	4.06
11	1	1	1	1	15.6	12.7	84.5	4.32
12	1	-1	1	1	14.4	12.5	78.2	4.26
13	-1	1	1	1	10.8	14.7	79.7	4.31
14	-1	1	1	1	10.4	15.0	77.7	4.27
15	1	-1	1	-1	15.5	13.7	85.8	4.52
16	-1	1	1	-1	11.7	17.2	86.6	5.24
17	-1	-1	1	-1	11	13.9	65.9	4.32
18	1	1	1	-1	12.5	16.6	90.2	5.06

Table A7.2 Raw Regression Data for Test E10

Run	Interval	x1 oil	x2 frother	x3 energy	x4 temp.	x6 % solids	ash %db	cmr %	ts % daf
e10	1	0.61	0.008	33.9	20.8	12.2	13.7	64.6	4.28
e10	2	1.37	0.025	33.9	20.8	12.6	17.9	99.6	5.47
e10	3	1.37	0.009	33.9	20.8	9.3	18.8	93.2	4.91
e10	4	0.61	0.025	33.9	20.8	8.5	20.3	95.9	5.23
e10	5	1.37	0.008	33.9	44.8	11.9	14.4	83.8	4.36
e10	6	0.61	0.025	33.9	44.8	8.1	17.4	78.2	4.47
e10	7	0.61	0.007	33.9	44.8	7.5	16.7	57.1	4.27
e10	8	1.37	0.026	33.9	44.8	15.3	14	85	4.64
e10	9	0.61	0.007	48.1	44.8	9.1	14.2	46.6	4.07
e10	10	1.37	0.025	48.1	44.8	15.6	12.7	84.5	4.32
e10	11	1.37	0.008	48.1	44.8	14.4	12.5	78.2	4.26
e10	12	0.61	0.025	48.1	44.8	10.8	14.7	79.7	4.31
e10	13	1.37	0.009	48.1	22.5	15.5	13.7	85.8	4.52
e10	14	0.61	0.027	48.1	22.5	11.7	17.2	86.6	5.24
e10	15	0.61	0.009	48.1	22.5	11	13.9	65.9	4.32
e10	16	1.37	0.025	48.1	22.5	12.5	16.6	90.2	5.06
e10	17	0.61	0.007	48.1	44.8	8.9	14.3	46.2	4.06
e10	18	0.61	0.025	48.1	44.8	10.4	15	77.7	4.27

Table A7.3 Coded Regression Data for Test E11

Interval	x1	x2	x3	x4	x6	R1	R2	R3
1	1	-1	-1	-1	20.6	12.9	84.3	4.72
2	-1	-1	1	-1	15.8	12.5	62.8	4.41
3	-1	1	-1	-1	12.2	17.6	96	5.37
4	1	1	1	-1	6.7	23.6	99.5	5.8
5	-1	-1	-1	1	9.8	15.6	50	4.36
6	1	-1	1	1	11.3	14.9	75.8	4.51
7	1	1	-1	1	16.2	14.4	92.4	4.84
8	-1	1	1	1	10	15.9	77.5	4.6
9	1	-1	-1	1	16.7	12.8	76.8	4.38
10	-1	-1	1	1	8.8	16.3	48	4.35
11	-1	1	-1	1	12.9	14.6	75.1	4.52
12	1	1	1	1	13.4	14.9	86.2	4.83
13	-1	-1	-1	-1	17.2	12.4	67.7	4.43
14	1	-1	1	-1	17.5	13.8	86.8	4.86
15	1	-1	1	-1	17.6	14	86.9	4.92
16	1	1	-1	-1	14.2	17.1	88.9	5.46
17	-1	1	1	-1	12.1	17.9	91.4	5.42

Table A7.4 Raw Regression Data for Test E11

Run	Interval	x1 oil	x2 frother	x3 energy	x4 temp.	x6 % solids	ash %db	cmr %	ts % daf
e11	1	1.38	0.008	35.4	23.8	20.6	12.9	84.3	4.72
e11	2	0.61	0.009	46.2	23.8	15.8	12.5	62.8	4.41
e11	3	0.61	0.025	35.4	23.8	12.2	17.6	96	5.37
e11	4	1.38	0.025	46.2	23.8	6.7	23.6	99.5	5.8
e11	5	0.61	0.008	35.4	45.6	9.8	15.6	50	4.36
e11	6	1.38	0.008	46.2	45.6	11.3	14.9	75.8	4.51
e11	7	1.38	0.025	35.4	45.6	16.2	14.4	92.4	4.84
e11	8	0.61	0.025	46.2	45.6	10	15.9	77.5	4.6
e11	9	1.38	0.008	35.4	45.6	16.7	12.8	76.8	4.38
e11	10	0.61	0.008	46.2	45.6	8.8	16.3	48	4.35
e11	11	0.61	0.024	35.4	45.6	12.9	14.6	75.1	4.52
e11	12	1.38	0.025	46.2	45.6	13.4	14.9	86.2	4.83
e11	13	0.61	0.008	35.4	21.3	17.2	12.4	67.7	4.43
e11	14a	1.38	0.009	46.2	21.3	17.5	13.8	86.8	4.86
e11	14b	1.38	0.009	35.4	21.3	17.6	14	86.9	4.92
e11	15	1.38	0.024	46.2	21.3	14.2	17.1	88.9	5.46
e11	16a	0.61	0.025	35.4	21.3	10.6	17.8	78.8	5.41
e11	16b	0.61	0.025	35.4	21.3	12.1	17.9	91.4	5.42

Table A7.5 Raw Regression Data for Test E10 & E11

Run	Interval	x1 oil	x2 frother	x3 energy	x4 temp.	x5 size	% solids	age	ash %db	cmr %	ts % daf
e10	1	0.61	0.008	33.9	20.8	80	12.2	0	13.7	64.6	4.28
e10	2	1.37	0.025	33.9	20.8	80	12.6	0	17.9	99.6	5.47
e10	3	1.37	0.009	33.9	20.8	80	9.3	0	18.8	93.2	4.91
e10	4	0.61	0.025	33.9	20.8	80	8.5	0	20.3	95.9	5.23
e10	5	1.37	0.008	33.9	44.8	80	11.9	0	14.4	83.8	4.36
e10	6	0.61	0.025	33.9	44.8	80	8.1	0	17.4	78.2	4.47
e10	7	0.61	0.007	33.9	44.8	80	7.5	0	16.7	57.1	4.27
e10	8	1.37	0.026	33.9	44.8	80	15.3	0	14.0	85.0	4.64
e10	9	0.61	0.007	48.1	44.8	80	9.1	2	14.2	46.6	4.07
e10	10	1.37	0.025	48.1	44.8	80	15.6	3	12.7	84.5	4.32
e10	11	1.37	0.008	48.1	44.8	80	14.4	2	12.5	78.2	4.26
e10	12	0.61	0.025	48.1	44.8	80	10.8	2	14.7	79.7	4.31
e10	13	1.37	0.009	48.1	22.5	80	15.5	3	13.7	85.8	4.52
e10	14	0.61	0.027	48.1	22.5	80	11.7	3	17.2	86.6	5.24
e10	15	0.61	0.009	48.1	22.5	80	11.0	2	13.9	65.9	4.32
e10	16	1.37	0.025	48.1	22.5	80	12.5	2	16.6	90.2	5.06
e10	17	0.61	0.007	48.1	44.8	80	8.9	2	14.3	46.2	4.06
e10	18	0.61	0.025	48.1	44.8	80	10.4	2	15.0	77.7	4.27
e11	1	1.38	0.008	35.4	23.8	47	20.6	10	12.9	84.3	4.72
e11	2	0.61	0.009	46.2	23.8	47	15.8	9	12.5	62.8	4.41
e11	3	0.61	0.025	35.4	23.8	47	12.2	10	17.6	96.0	5.37
e11	4	1.38	0.025	46.2	23.8	47	6.7	9	23.6	99.5	5.8
e11	5	0.61	0.008	35.4	45.6	47	9.8	9	15.6	50.0	4.36
e11	6	1.38	0.008	46.2	45.6	47	11.3	9	14.9	75.8	4.51
e11	7	1.38	0.025	35.4	45.6	47	16.2	10	14.4	92.4	4.84
e11	8	0.61	0.025	46.2	45.6	47	10.0	9	15.9	77.5	4.6
e11	9	1.38	0.008	35.4	45.6	47	16.7	10	12.8	76.8	4.38
e11	10	0.61	0.008	46.2	45.6	47	8.8	9	16.3	48.0	4.35
e11	11	0.61	0.024	35.4	45.6	47	12.9	10	14.6	75.1	4.52
e11	12	1.38	0.025	46.2	45.6	47	13.4	9	14.9	86.2	4.83
e11	13	0.61	0.008	35.4	21.3	47	17.2	10	12.4	67.7	4.43
e11	14	1.38	0.009	46.2	21.3	47	17.5	9	13.8	86.8	4.86
e11	15	1.38	0.009	35.4	21.3	47	17.6	9	14.0	86.9	4.92
e11	16	1.38	0.024	46.2	21.3	47	14.2	10	17.1	88.9	5.46
e11	17	0.61	0.025	35.4	21.3	47	10.6	9	17.8	78.8	5.41
e11	18	0.61	0.025	35.4	21.3	47	12.1	9	17.9	91.4	5.42

Table A7.6 Raw Regression Data for Tests E10, E11 and E12

Run	Interval	x1 oil	x2 frother	x3 energy	x4 temp.	x5 size	x6 % solids	x7 age	ash %db	cmr %	ts % daf
e10	1	0.61	0.008	33.9	20.8	80	12.2	0	13.7	64.6	4.28
e10	2	1.37	0.025	33.9	20.8	80	12.6	0	17.9	99.6	5.47
e10	3	1.37	0.009	33.9	20.8	80	9.3	0	18.8	93.2	4.91
e10	4	0.61	0.025	33.9	20.8	80	8.5	0	20.3	95.9	5.23
e10	5	1.37	0.008	33.9	44.8	80	11.9	0	14.4	83.8	4.36
e10	6	0.61	0.025	33.9	44.8	80	8.1	0	17.4	78.2	4.47
e10	7	0.61	0.007	33.9	44.8	80	7.5	0	16.7	57.1	4.27
e10	8	1.37	0.026	33.9	44.8	80	15.3	0	14	85	4.64
e10	9	0.61	0.007	48.1	44.8	80	9.1	2	14.2	46.6	4.07
e10	10	1.37	0.025	48.1	44.8	80	15.6	3	12.7	84.5	4.32
e10	11	1.37	0.008	48.1	44.8	80	14.4	2	12.5	78.2	4.26
e10	12	0.61	0.025	48.1	44.8	80	10.8	2	14.7	79.7	4.31
e10	13	1.37	0.009	48.1	22.5	80	15.5	3	13.7	85.8	4.52
e10	14	0.61	0.027	48.1	22.5	80	11.7	3	17.2	86.6	5.24
e10	15	0.61	0.009	48.1	22.5	80	11	2	13.9	65.9	4.32
e10	16	1.37	0.025	48.1	22.5	80	12.5	2	16.6	90.2	5.06
e10	17	0.61	0.007	48.1	44.8	80	8.9	2	14.3	46.2	4.06
e10	18	0.61	0.025	48.1	44.8	80	10.4	2	15	77.7	4.27
e11	1	1.38	0.008	35.4	23.8	47	20.6	10	12.9	84.3	4.72
e11	2	0.61	0.009	46.2	23.8	47	15.8	9	12.5	62.8	4.41
e11	3	0.61	0.025	35.4	23.8	47	12.2	10	17.6	96	5.37
e11	4	1.38	0.025	46.2	23.8	47	6.7	9	23.6	99.5	5.8
e11	5	0.61	0.008	35.4	45.6	47	9.8	9	15.6	50	4.36
e11	6	1.38	0.008	46.2	45.6	47	11.3	9	14.9	75.8	4.51
e11	7	1.38	0.025	35.4	45.6	47	16.2	10	14.4	92.4	4.84
e11	8	0.61	0.025	46.2	45.6	47	10	9	15.9	77.5	4.6
e11	9	1.38	0.008	35.4	45.6	47	16.7	10	12.8	76.8	4.38
e11	10	0.61	0.008	46.2	45.6	47	8.8	9	16.3	48	4.35
e11	11	0.61	0.024	35.4	45.6	47	12.9	10	14.6	75.1	4.52
e11	12	1.38	0.025	46.2	45.6	47	13.4	9	14.9	86.2	4.83
e11	13	0.61	0.008	35.4	21.3	47	17.2	10	12.4	67.7	4.43

Table A7.6..... Continued

e11	14	1.38	0.009	46.2	21.3	47	17.5	9	13.8	86.8	4.86
e11	15	1.38	0.009	35.4	21.3	47	17.6	9	14	86.9	4.92
e11	16	1.38	0.024	46.2	21.3	47	14.2	10	17.1	88.9	5.46
e11	17	0.61	0.025	35.4	21.3	47	10.6	9	17.8	78.8	5.41
e11	18	0.61	0.025	35.4	21.3	47	12.1	9	17.9	91.4	5.42
e12	1	1	0.017	32	31	73	17.3	40	12.3	70	4.06
e12	2	0.98	0.017	33	31	73	17.8	40	12	72.8	4.1
e12	3	1	0.017	32	31	73	17.9	40	12	70.3	4.02
e12	4	0.72	0.012	44	25	73	23.8	40	9.8	53.2	3.96
e12	5	1.16	0.011	40	25	73	28.6	40	10.4	69.8	4.04
e12	6	0.72	0.022	44	24	73	15.1	40	13.7	80.9	4.29
e12	7	1.26	0.022	43	24	73	15	40	14.6	84.4	4.45
e12	8	0.72	0.01	48	23	73	15.3	41	12	59.4	4
e12	9	1.26	0.012	49	20	73	19.8	41	11.8	72.8	4.12
e12	10	0.72	0.022	49	20	73	18.4	41	13.3	83.5	4.43
e12	11	1.26	0.022	49	21	73	25.5	41	12.8	85.1	4.4
e12	12	0.98	0.022	48	21	73	14.4	41	14.7	82.3	4.47
e12	13	1	0.026	50	21	73	12.4	41	16.4	79	4.61
e12	14	1.26	0.017	50	21	73	20.7	41	12.5	80	4.22
e12	15	0.61	0.025	49	19	73	7.9	42	19.2	90.3	4.72
e12	16	0.61	0.021	50	20	73	7.3	42	18.9	88.5	4.6
e12	17	0.71	0.011	50	19	73	8.3	43	13.4	68.8	4.18
e12	18	1.26	0.01	50	20	73	13.6	43	12	76.8	4.18
e12	19	0.72	0.021	51	20	73	21.9	43	12	87.8	4.33
e12	20	1.26	0.02	50	20	73	24.4	43	12	84.6	4.41

Table A7.7 Raw Regression Data for Tests E10, E11, E12 and E13

Run	Interval	x1	x2	x3	x4	x5	x6	x7	R1	R2	R3
e10	1	0.61	0.008	33.9	20.8	80	12.2	0	13.7	64.6	4.28
e10	2	1.37	0.025	33.9	20.8	80	12.6	0	17.9	99.6	5.47
e10	3	1.37	0.009	33.9	20.8	80	9.3	0	18.8	93.2	4.91
e10	4	0.61	0.025	33.9	20.8	80	8.5	0	20.3	95.9	5.23
e10	5	1.37	0.008	33.9	44.8	80	11.9	0	14.4	83.8	4.36
e10	6	0.61	0.025	33.9	44.8	80	8.1	0	17.4	78.2	4.47
e10	7	0.61	0.007	33.9	44.8	80	7.5	0	16.7	57.1	4.27
e10	8	1.37	0.026	33.9	44.8	80	15.3	0	14	85	4.64
e10	9	0.61	0.007	48.1	44.8	80	9.1	2	14.2	46.6	4.07
e10	10	1.37	0.025	48.1	44.8	80	15.6	3	12.7	84.5	4.32
e10	11	1.37	0.008	48.1	44.8	80	14.4	2	12.5	78.2	4.26
e10	12	0.61	0.025	48.1	44.8	80	10.8	2	14.7	79.7	4.31
e10	13	1.37	0.009	48.1	22.5	80	15.5	3	13.7	85.8	4.52
e10	14	0.61	0.027	48.1	22.5	80	11.7	3	17.2	86.6	5.24
e10	15	0.61	0.009	48.1	22.5	80	11	2	13.9	65.9	4.32
e10	16	1.37	0.025	48.1	22.5	80	12.5	2	16.6	90.2	5.06
e10	17	0.61	0.007	48.1	44.8	80	8.9	2	14.3	46.2	4.06
e10	18	0.61	0.025	48.1	44.8	80	10.4	2	15	77.7	4.27
e11	1	1.38	0.008	35.4	23.8	47	20.6	10	12.9	84.3	4.72
e11	2	0.61	0.009	46.2	23.8	47	15.8	9	12.5	62.8	4.41
e11	3	0.61	0.025	35.4	23.8	47	12.2	10	17.6	96	5.37
e11	4	1.38	0.025	46.2	23.8	47	6.7	9	23.6	99.5	5.8
e11	5	0.61	0.008	35.4	45.6	47	9.8	9	15.6	50	4.36
e11	6	1.38	0.008	46.2	45.6	47	11.3	9	14.9	75.8	4.51
e11	7	1.38	0.025	35.4	45.6	47	16.2	10	14.4	92.4	4.84
e11	8	0.61	0.025	46.2	45.6	47	10	9	15.9	77.5	4.6
e11	9	1.38	0.008	35.4	45.6	47	16.7	10	12.8	76.8	4.38
e11	10	0.61	0.008	46.2	45.6	47	8.8	9	16.3	48	4.35
e11	11	0.61	0.024	35.4	45.6	47	12.9	10	14.6	75.1	4.52
e11	12	1.38	0.025	46.2	45.6	47	13.4	9	14.9	86.2	4.83
e11	13	0.61	0.008	35.4	21.3	47	17.2	10	12.4	67.7	4.43
e11	14	1.38	0.009	46.2	21.3	47	17.5	9	13.8	86.8	4.86

Table A7.7... Continued

e11	15	1.38	0.009	35.4	21.3	47	17.6	9	14	86.9	4.92
e11	16	1.38	0.024	46.2	21.3	47	14.2	10	17.1	88.9	5.46
e11	17	0.61	0.025	35.4	21.3	47	10.6	9	17.8	78.8	5.41
e11	18	0.61	0.025	35.4	21.3	47	12.1	9	17.9	91.4	5.42
e12	1	1	0.017	32	31	73	17.3	40	12.3	70	4.06
e12	2	0.98	0.017	33	31	73	17.8	40	12	72.8	4.1
e12	3	1	0.017	32	31	73	17.9	40	12	70.3	4.02
e12	4	0.72	0.012	44	25	73	23.8	40	9.8	53.2	3.96
e12	5	1.16	0.011	40	25	73	28.6	40	10.4	69.8	4.04
e12	6	0.72	0.022	44	24	73	15.1	40	13.7	80.9	4.29
e12	7	1.26	0.022	43	24	73	15	40	14.6	84.4	4.45
e12	8	0.72	0.01	48	23	73	15.3	41	12	59.4	4
e12	9	1.26	0.012	49	20	73	19.8	41	11.8	72.8	4.12
e12	10	0.72	0.022	49	20	73	18.4	41	13.3	83.5	4.43
e12	11	1.26	0.022	49	21	73	25.5	41	12.8	85.1	4.4
e12	12	0.98	0.022	48	21	73	14.4	41	14.7	82.3	4.47
e12	13	1	0.026	50	21	73	12.4	41	16.4	79	4.61
e12	14	1.26	0.017	50	21	73	20.7	41	12.5	80	4.22
e12	15	0.61	0.025	49	19	73	7.9	42	19.2	90.3	4.72
e12	16	0.61	0.021	50	20	73	7.3	42	18.9	88.5	4.6
e12	17	0.71	0.011	50	19	73	8.3	43	13.4	68.8	4.18
e12	18	1.26	0.01	50	20	73	13.6	43	12	76.8	4.18
e12	19	0.72	0.021	51	20	73	21.9	43	12	87.8	4.33
e12	20	1.26	0.02	50	20	73	24.4	43	12	84.6	4.41
e13	1	0.61	0.023	52	19	80	20.5	44	10.9	70.4	4.14
e13	2	1.38	0.013	50	19	80	21.8	44	11.1	69.9	4.2
e13	3	1	0.023	49	19	80	24.6	44	11.3	75.7	4.26
e13	4	1.27	0.033	50	19	80	19	44	14.7	93.6	4.9
e13	5	0.61	0.038	51	19	80	20.5	44	15.3	83.2	4.94

Appendix 8 Graphic Evaluation of Main Factors

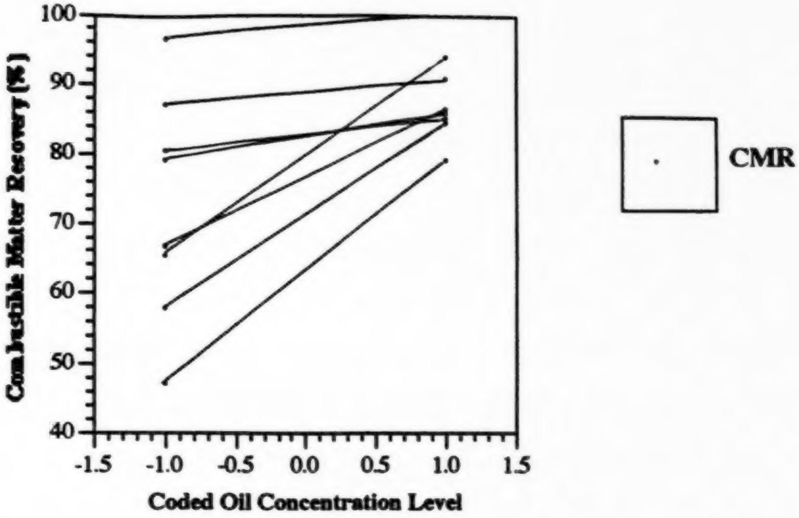

Figure A8.1 % Combustible Matter Recovery versus Coded Oil Concentration for Test E10

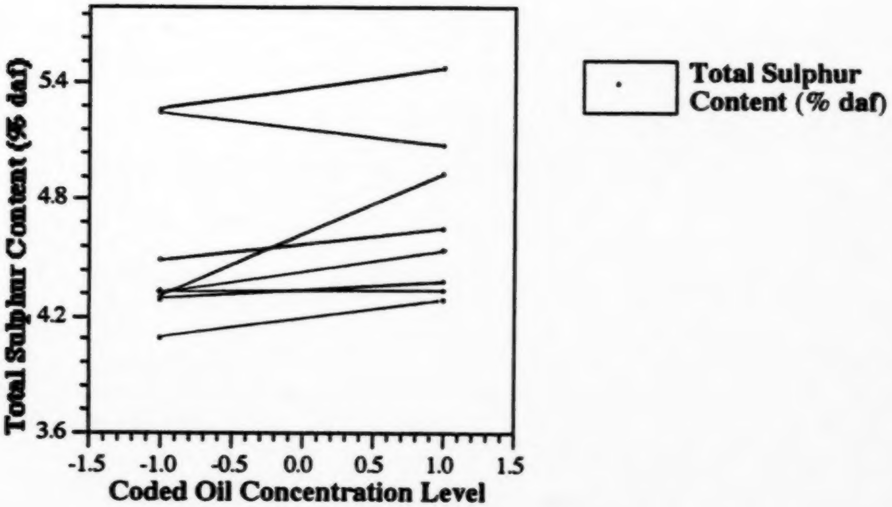

Figure A8.2 Total Sulphur Content (% daf) versus Coded Oil Concentration for Test E10

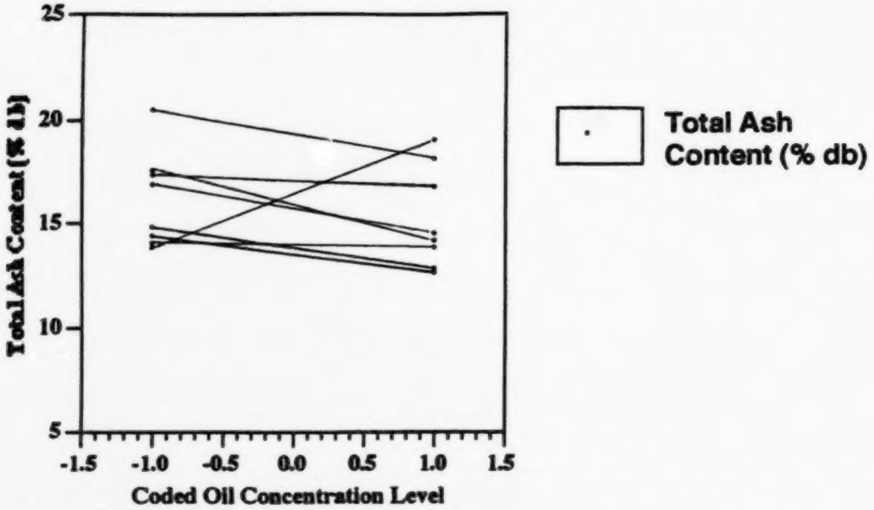

Figure A8.3 Total Ash Content (% db) versus Coded Oil Concentration for Test E10

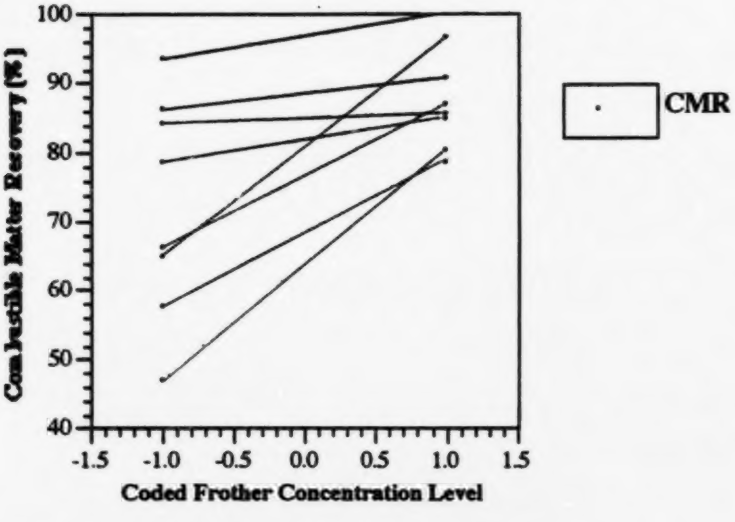

Figure A8.4 % Combustible Matter Recovery versus Coded Frother Concentration for Test E10

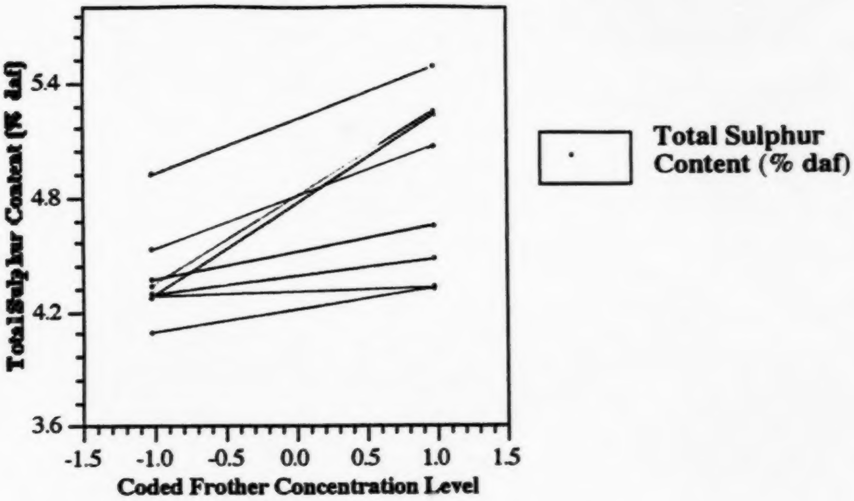

Figure A8.5 Total Sulphur Content (% daf) versus Coded Frother Concentration for Test E10

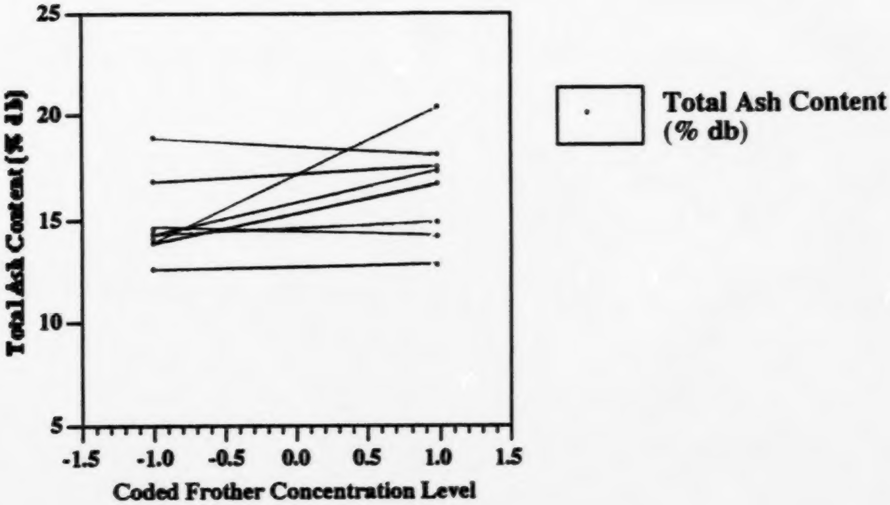

Figure A8.6 Total Ash Content (% db) versus Coded Frother Concentration for Test E10

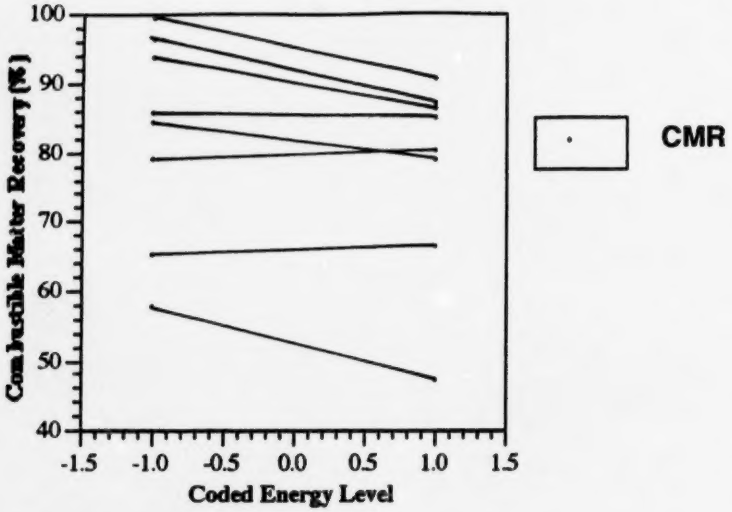

Figure A8.7 % Combustible Matter Recovery versus Coded Energy Input for Test E10

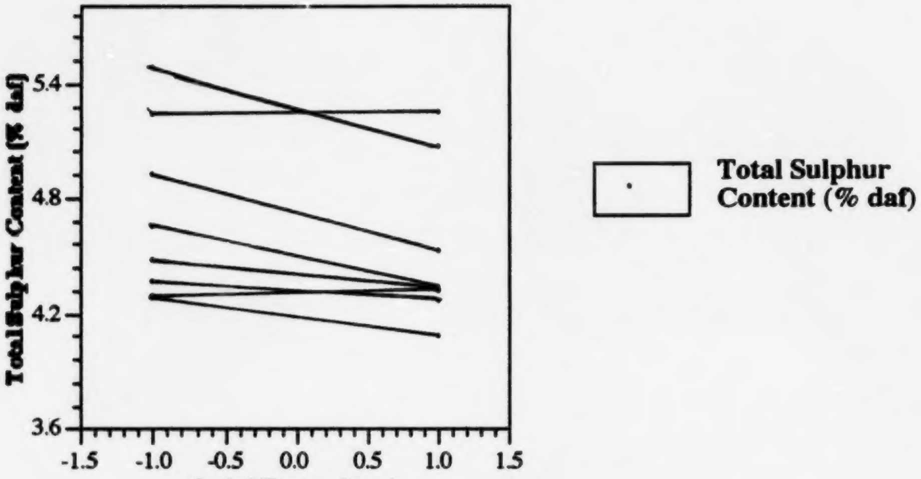

Figure A8.8 Total Sulphur Content (% daf) versus Coded Energy Input for Test E10

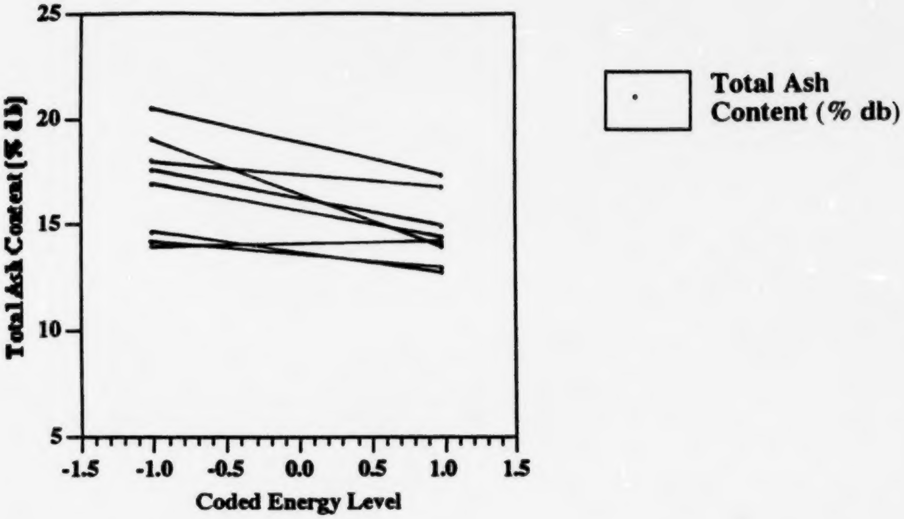

Figure A8.9 Total Ash Content (% db) versus Coded Energy Input for Test E10

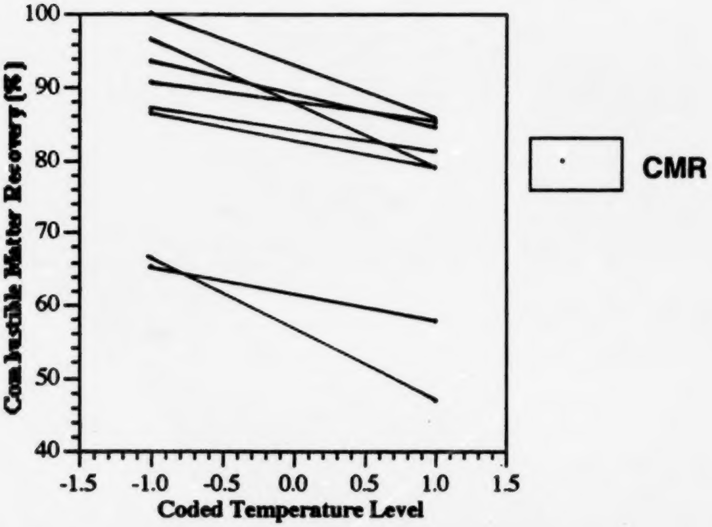

Figure A8.10 % Combustible Matter Recovery versus Coded Temperature for Test E10

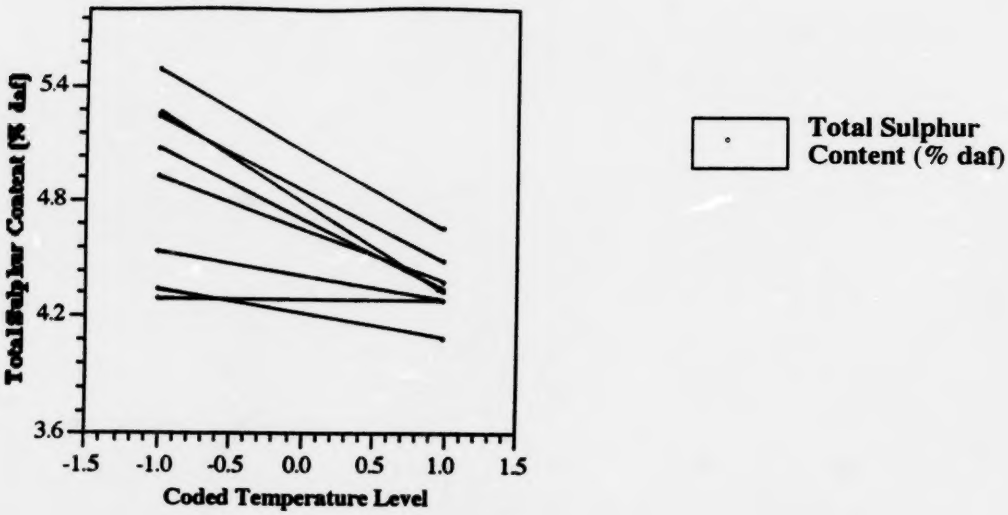

Figure A8.11 Total Sulphur Content (% daf) versus Coded Temperature for Test E10

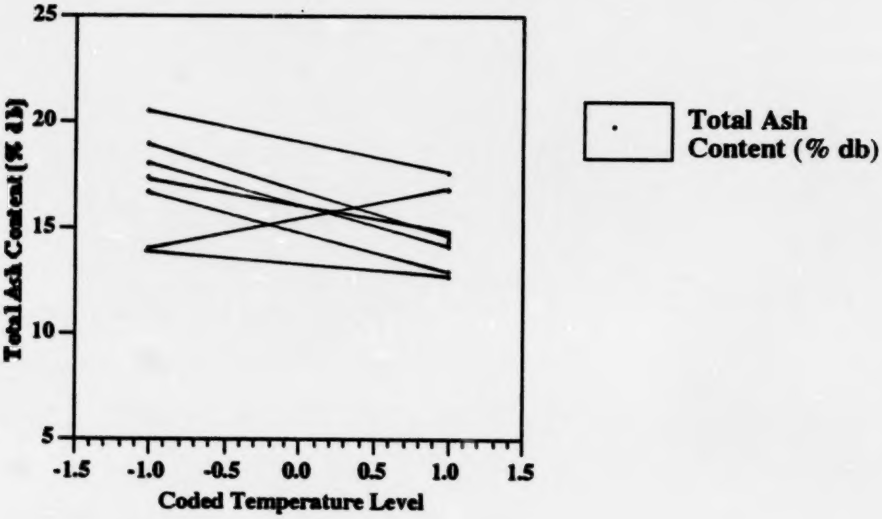

Figure A8.12 Total Ash Content (% db) versus Coded Temperature for Test E10

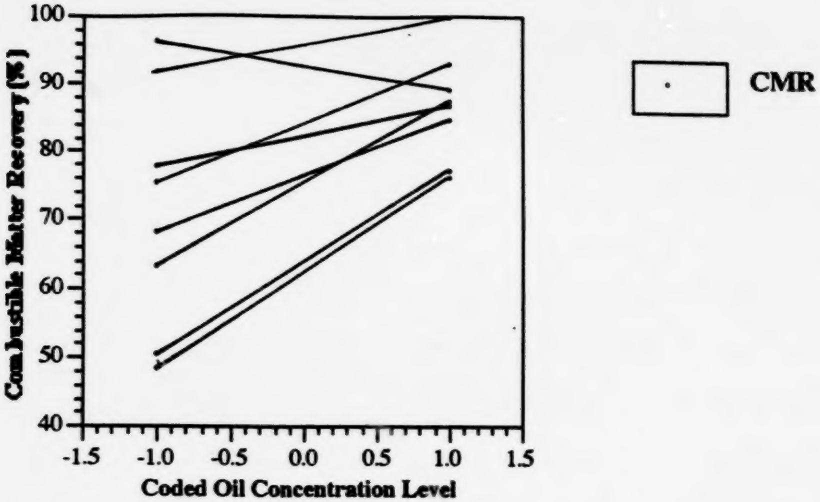

Figure A8.13 % Combustible Matter Recovery versus Coded Oil Concentration for Test E11

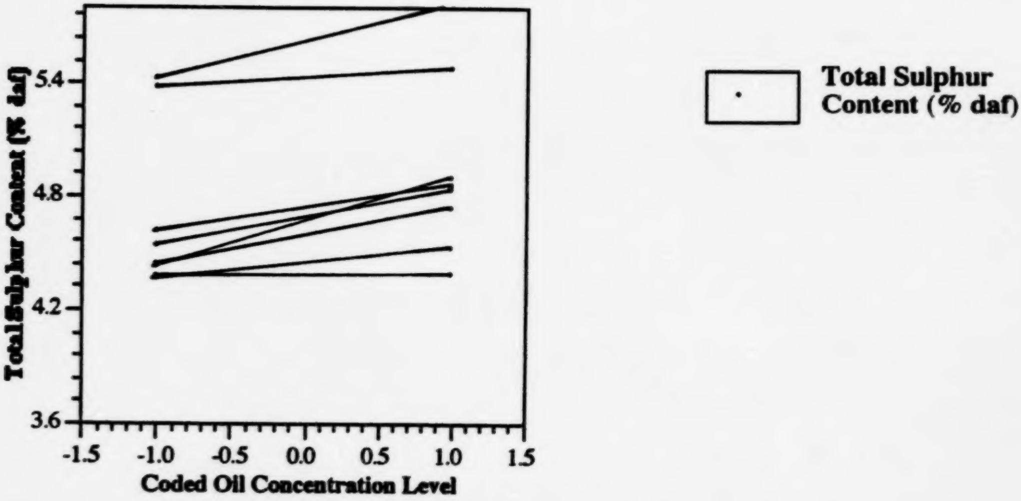

Figure A8.14 Total Sulphur Content (% daf) versus Coded Oil Concentration for Test E11

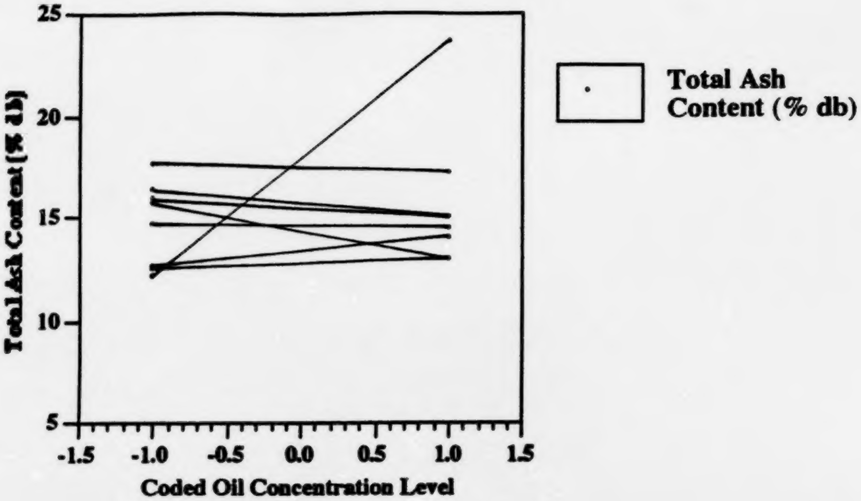

Figure A8.15 Total Ash Content (% db) versus Coded Oil Concentration for Test E11

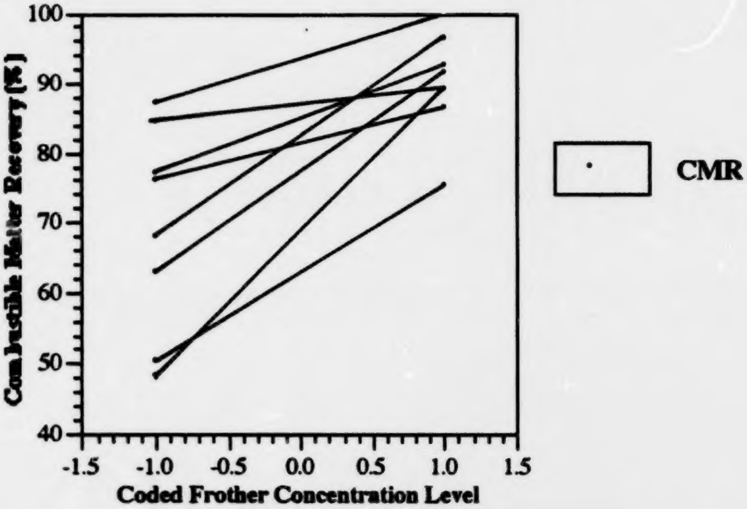

Figure A8.16 % Combustible Matter Recovery versus Coded Frother Concentration for Test E11

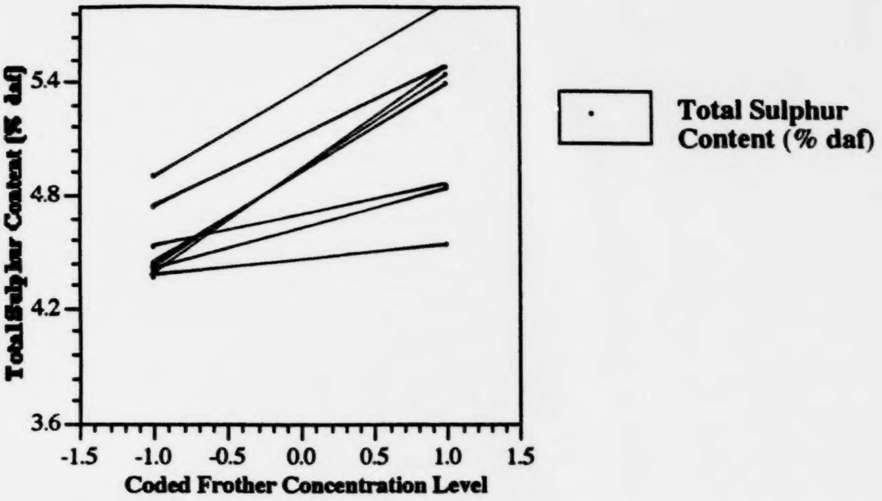

Figure A8.17 Total Sulphur Content (% daf) versus Coded Frother Concentration for Test E11

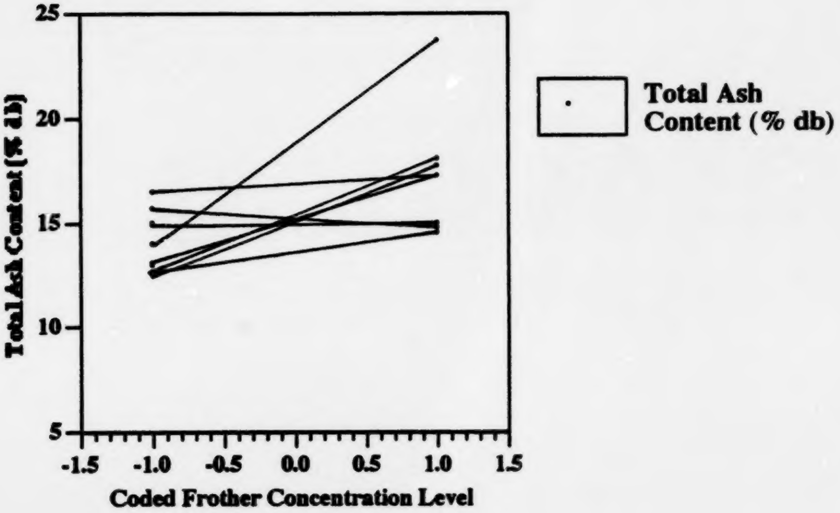

Figure A8.18 Total Ash Content (% db) versus Coded Frother Concentration for Test E11

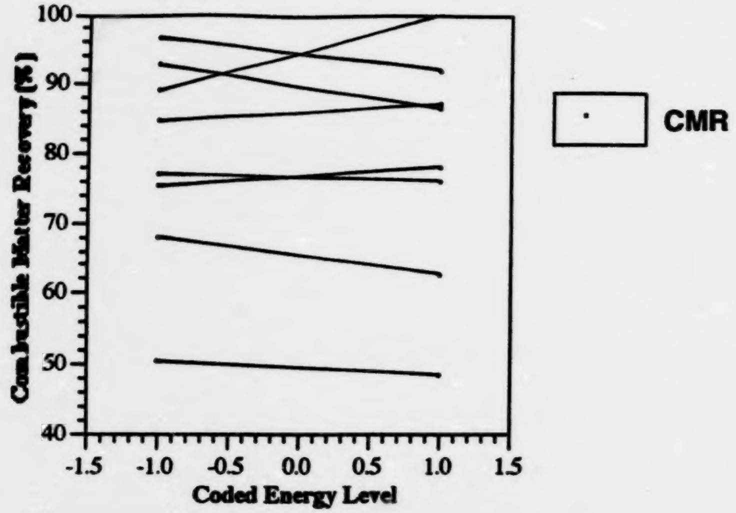

Figure A8.19 % Combustible Matter Recovery versus Coded Energy Input for Test E11

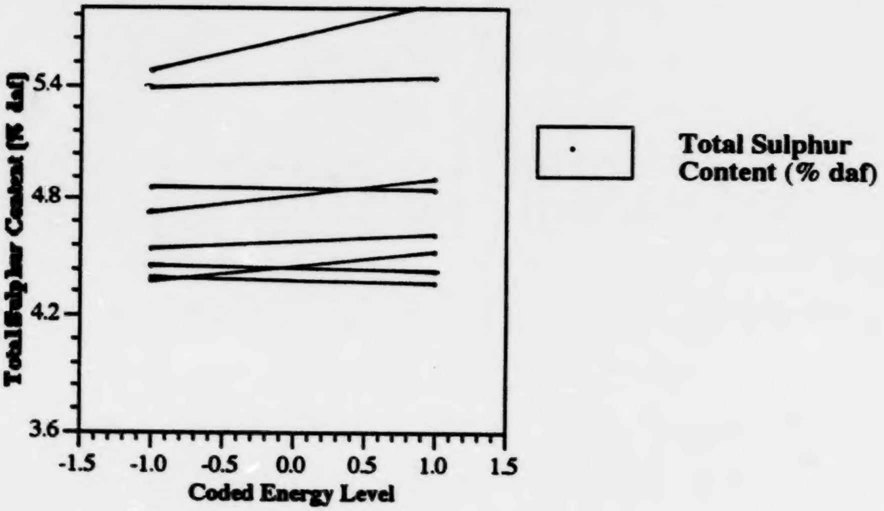

Figure A8.20 Total Sulphur Content (% daf) versus Coded Energy Input for Test E11

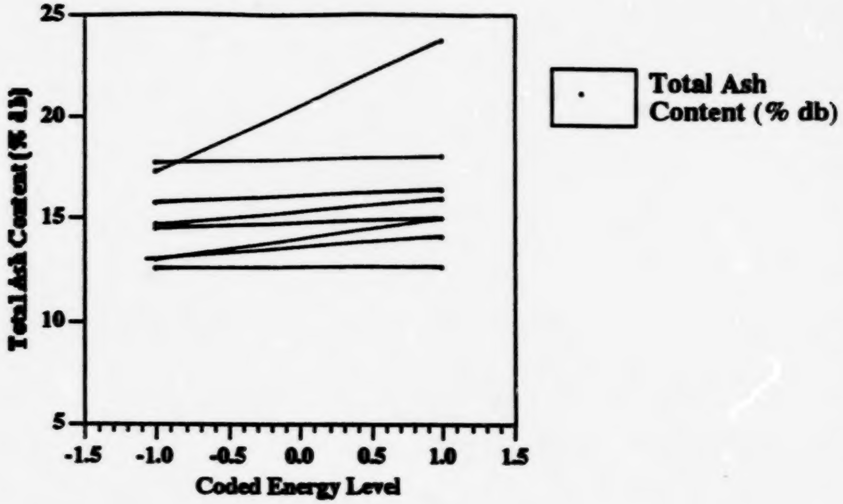

Figure A8.21 Total Ash Content (% db) versus Coded Energy Input for Test E11

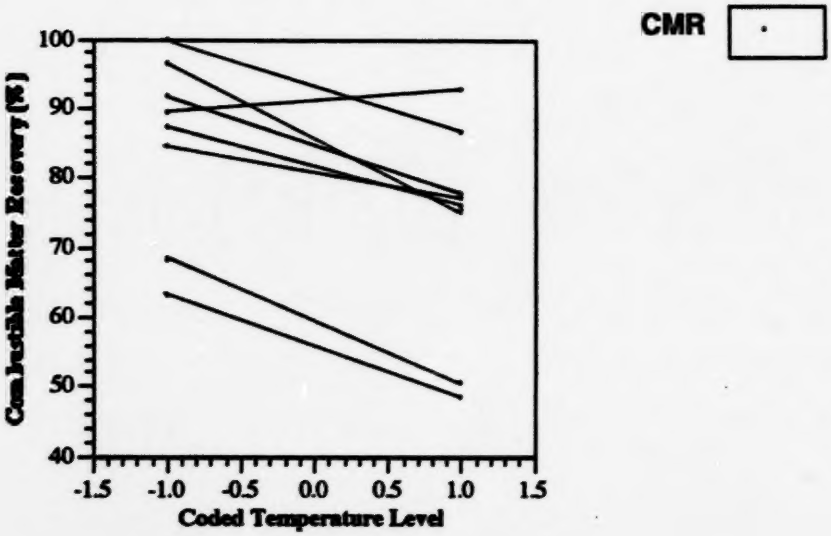

Figure A8.22 % Combustible Matter Recovery versus Coded Temperature for Test E11

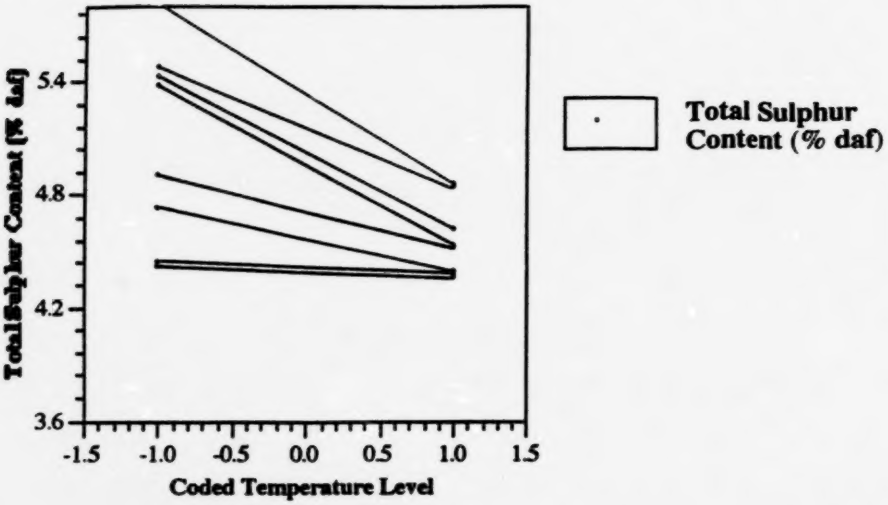

Figure A8.23 Total Sulphur Content (% daf) versus Coded Temperature for Test E11

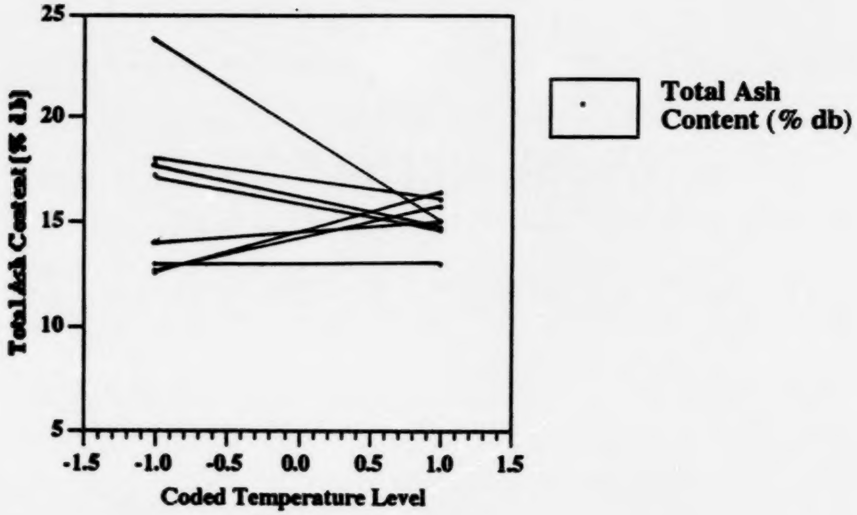

Figure A8.24 Total Ash Content (% db) versus Coded Temperature for Test E11

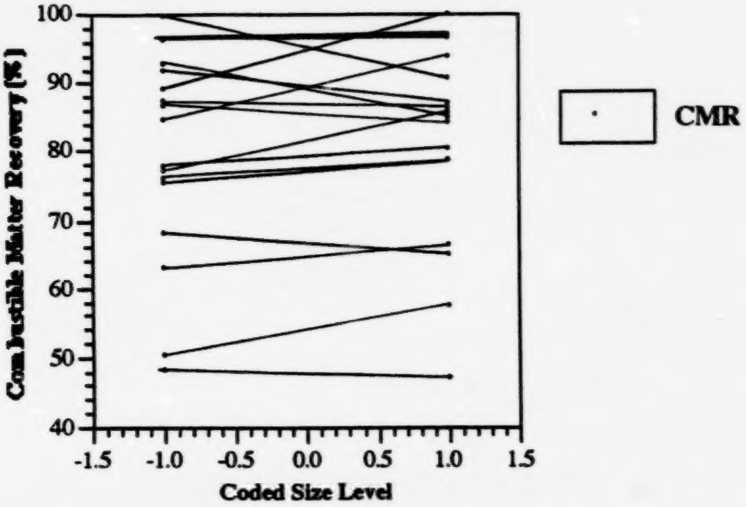

Figure A8.25 % Combustible Matter Recovery versus Coded Size for Tests E10 and E11

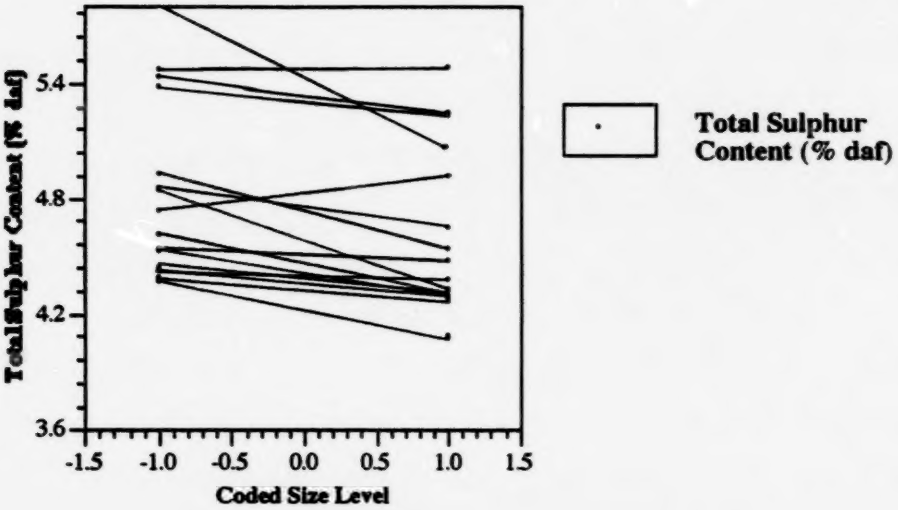

Figure A8.26 Total Sulphur Content (% daf) versus Coded Size for Tests E10 and E11

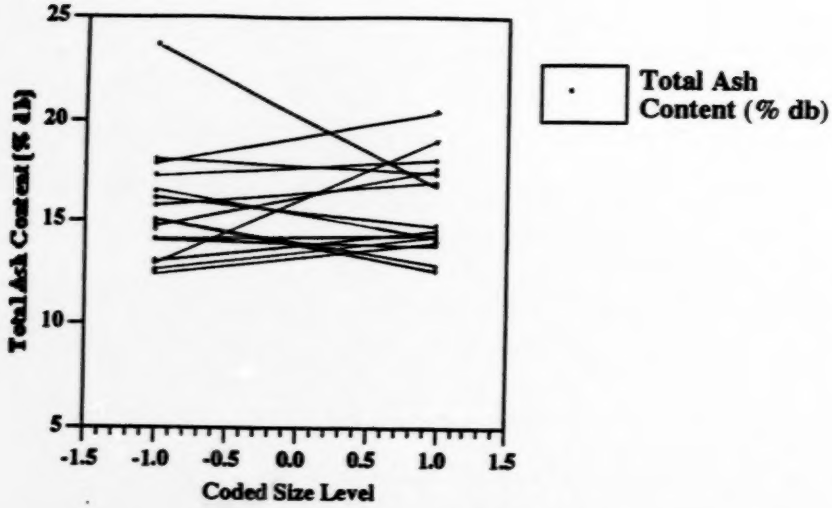

Figure A8.27 Total Ash Content (% db) versus Coded Size for Tests E10 and E11

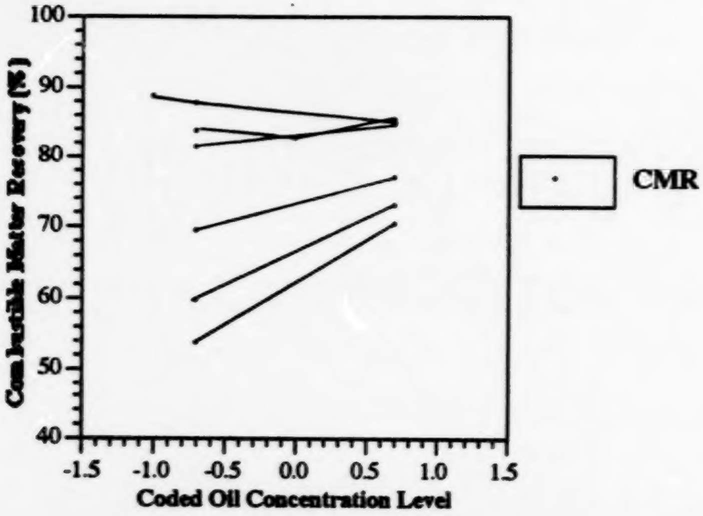

Figure A8.28 % Combustible Matter Recovery versus Coded Oil Concentration for Test E12

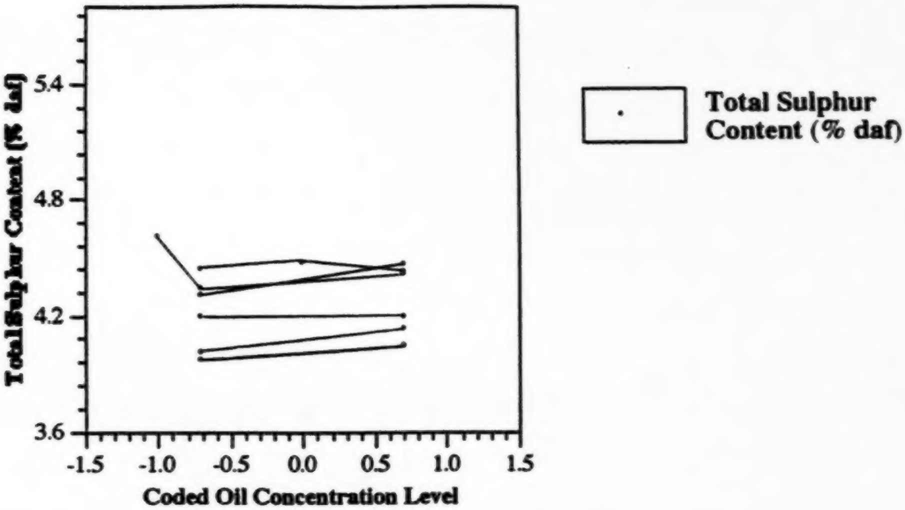

Figure A8.29 Total Sulphur Content (% daf) versus Coded Oil Concentration for Test E12

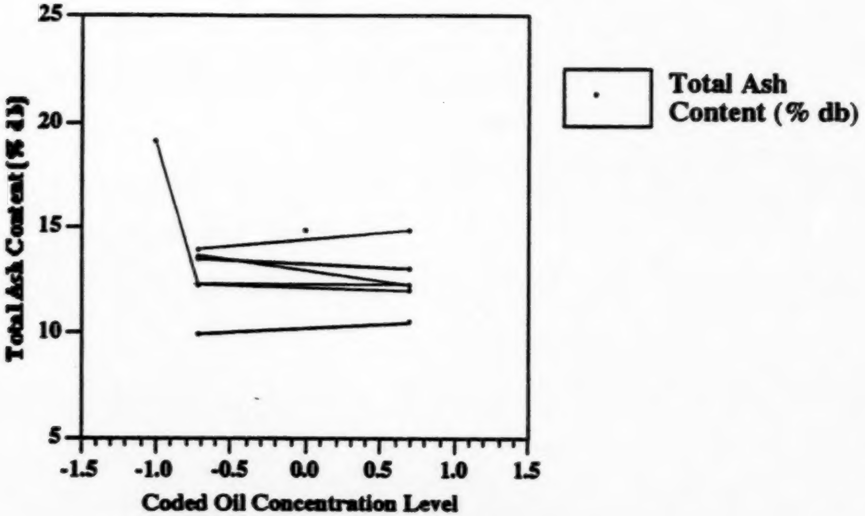

Figure A8.30 Total Ash Content (% db) versus Coded Oil Concentration for Test E12

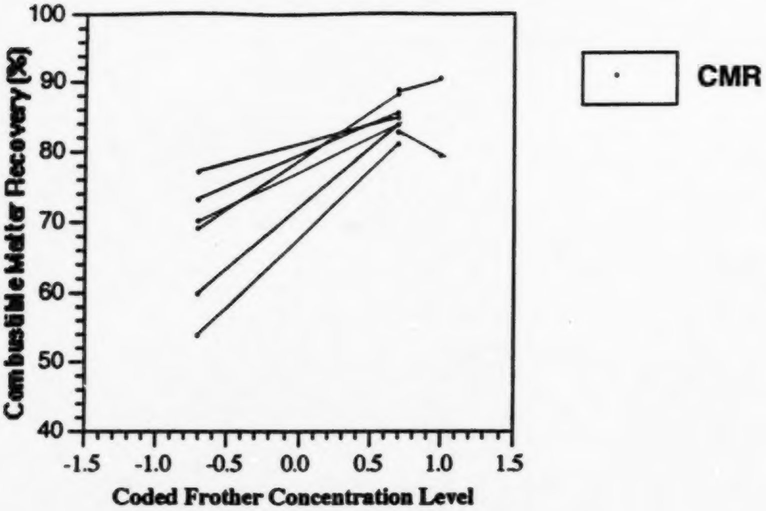

Figure A8.31 % Combustible Matter Recovery versus Coded Frother Concentration for Test E12

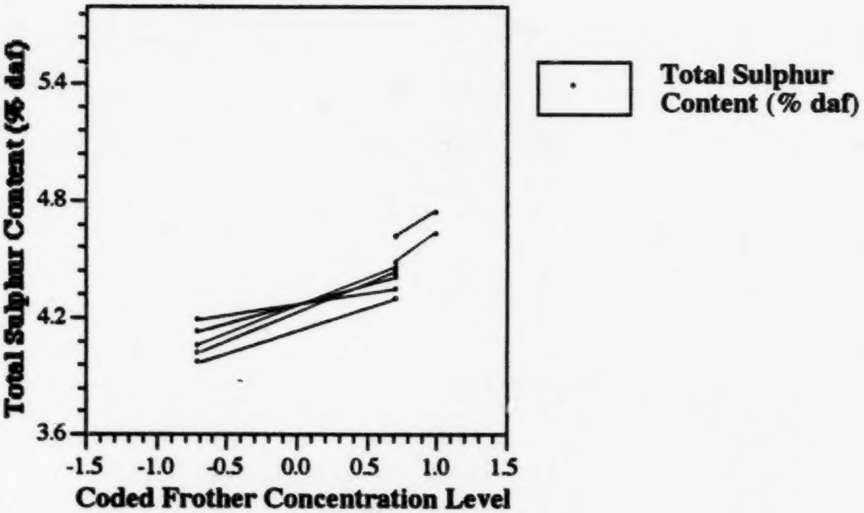

Figure A8.32 Total Sulphur Content (% daf) versus Coded Frother Concentration for Test E12

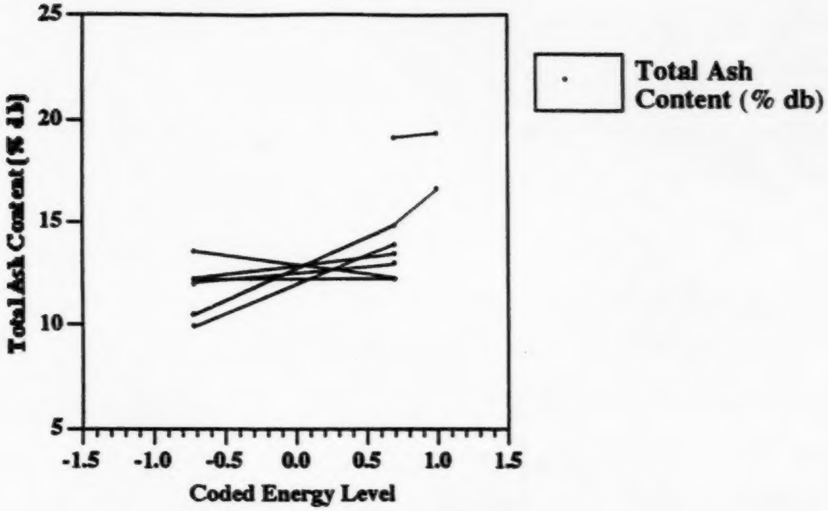

Figure A8.33 Total Ash Content (% db) versus Coded Frother Concentration for Test E12

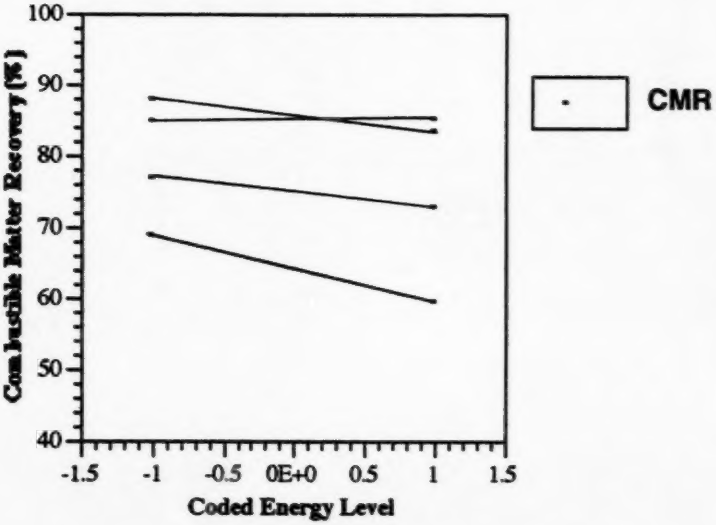

Figure A8.34 % Combustible Matter Recovery versus Coded Energy Input for Test E12

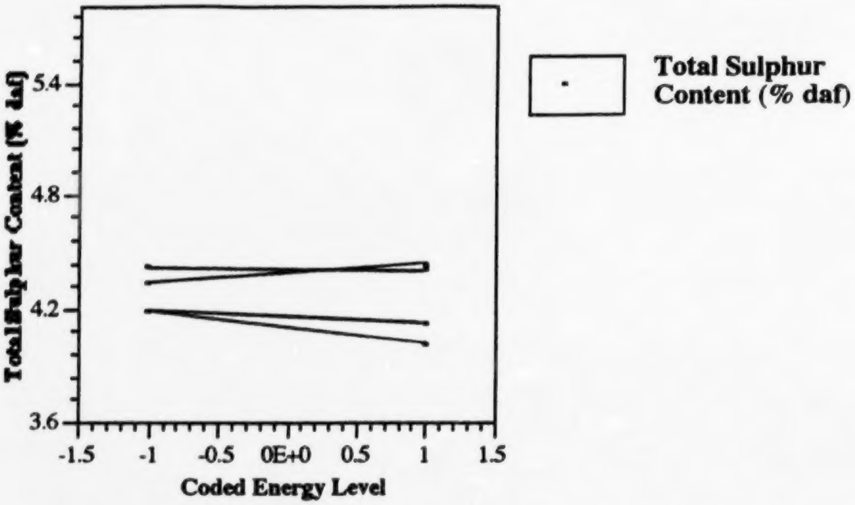

Figure A8.35 Total Sulphur Content (% daf) versus Coded Energy Input for Test E10

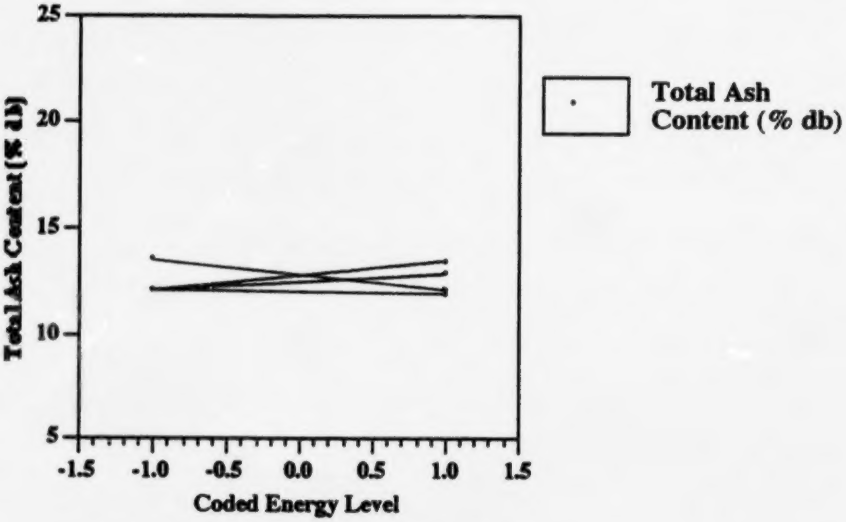

Figure A8.36 Total Ash Content (% db) versus Coded Energy Input for Test E12

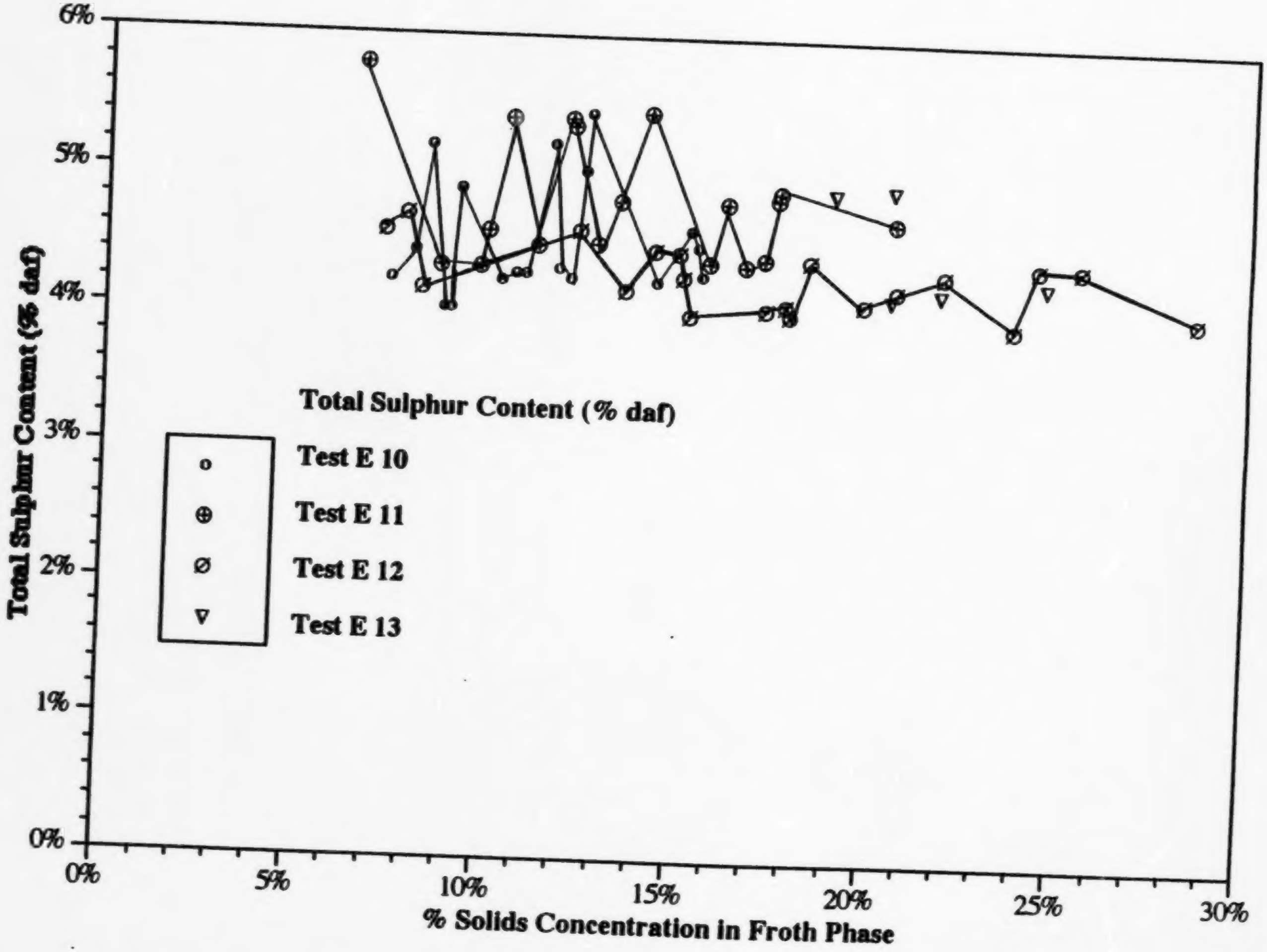

Figure A8.37 Total Sulphur Content (% daf) versus % Solids Concentration in the Froth Phase for Tests E10, E11, E12 and E13

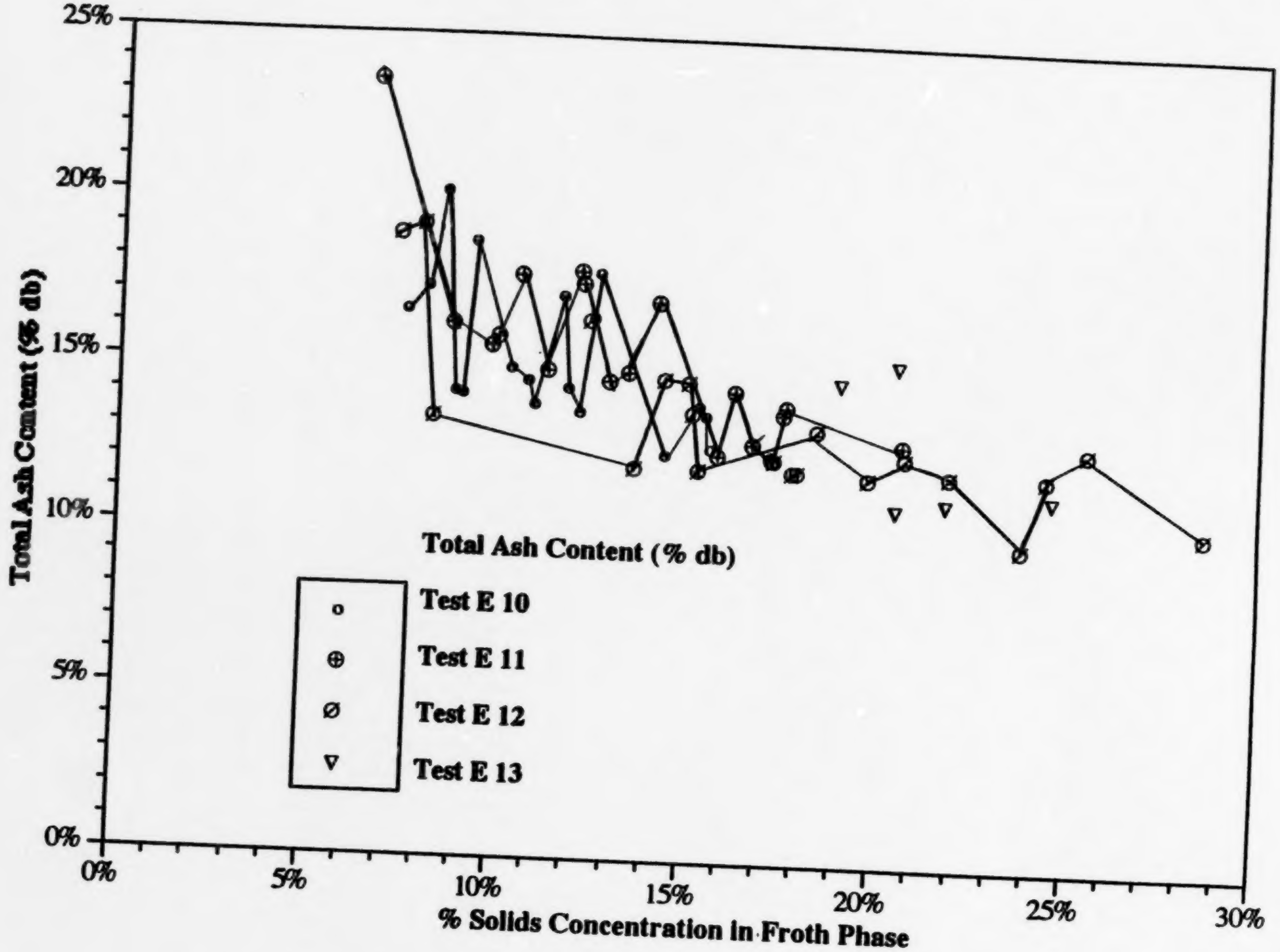

Figure A8.38 Total Ash Content (% db) versus % Solids Concentration in the Froth Phase for Tests E10, E11, E12 and E13

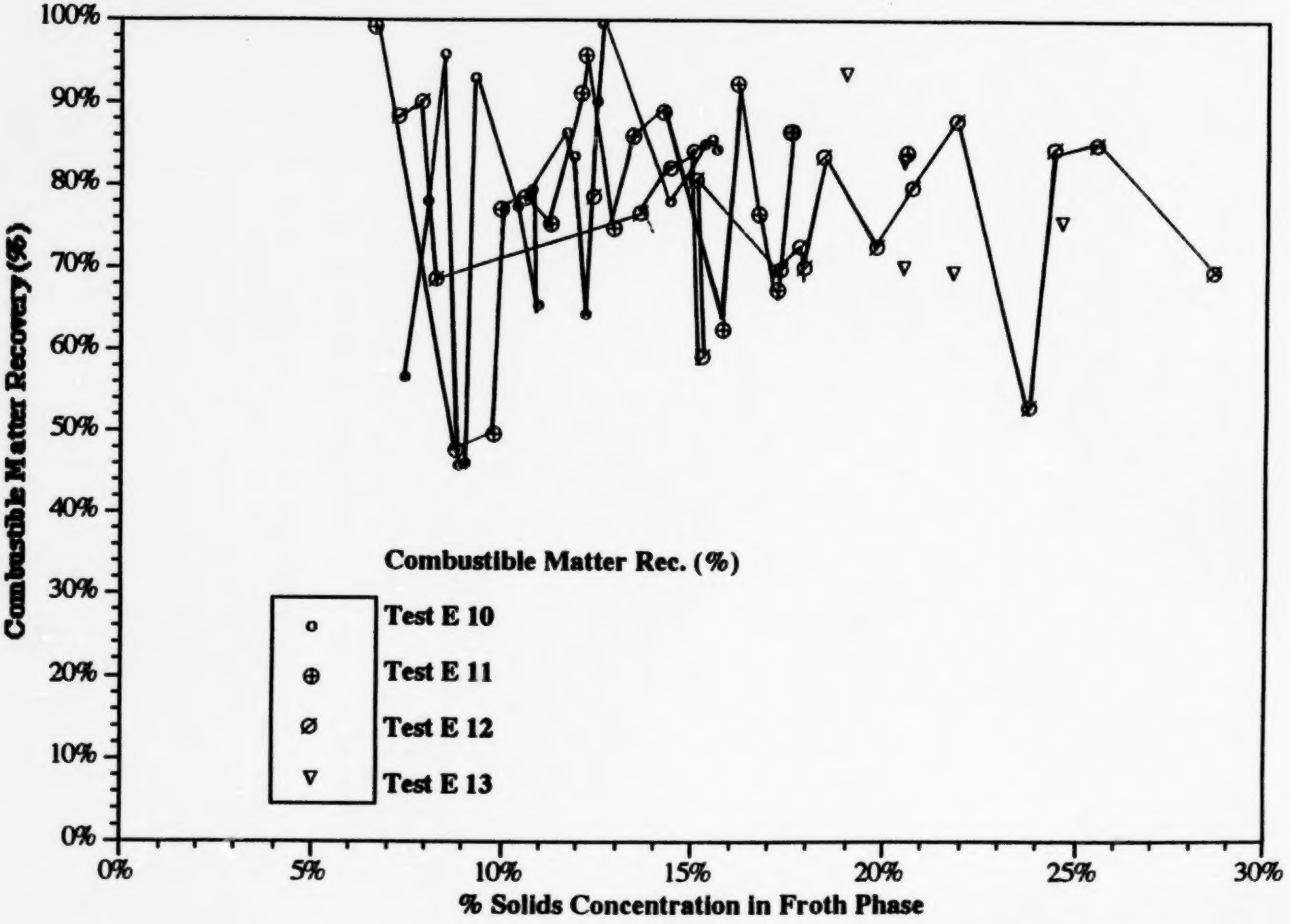

Figure A8.39 Combustible Matter Recovery (%) versus % Solids Concentration in the Froth Phase for Tests E10, E11, E12 and E13